Title of Grant / Cooperative Agreement:		
Type of Report:		
Name of Principal Investigator:		
Period Covered by Report:		
Name and Address of recipient's institution:		
NASA Grant / Cooperative Agreement Number:		
Reference 14 CFR § 1260.28 Patent Rights (abbreviated below) The Recipient shall include a list of any Subject Inventions required report, technical report, or renewal proposal. A complete list (or a nathe summary of research. Subject inventions include any new process, machine, manufacture, or new applications of, existing processes, machines, manufactures	egative statement) for the entire aw or composition of matter, including	ard period shall be included in software, and improvements to,
Have any Subject Inventions / New Technology Items resulted from work performed under this Grant / Cooperative Agreement?	No	Yes
If yes a complete listing should be provided here: Details can be provided in the body of the Summary of Research report.		
Reference 14 CFR § 1260.27 Equipment and Other Property (ab A Final Inventory Report of Federally Owned Property, including equ by the Recipient no later than 60 days after the expiration date of the required.	uipment where title was taken by the	
Is there any Federally Owned Property, either Government Furnished or Grantee Acquired, in the custody of the Recipient?	No	Yes
If yes please attach a complete listing including information as set forth at § 1260.134(f)(1).		

Attach the Summary of Research text behind this cover sheet.

Reference 14 CFR § 1260.22 Technical publications and reports (December 2003)

Reports shall be in the English language, informal in nature, and ordinarily not exceed three pages (not counting bibliographies, abstracts, and lists of other media).

A Summary of Research (or Educational Activity Report in the case of Education Grants) is due within 120 days after the expiration date of the grant, regardless of whether or not support is continued under another grant. This report shall be a comprehensive summary of significant accomplishments during the duration of the grant.

BioBot: Innovative Offloading of Astronauts for More Effective Exploration 80NSSC20K1029 NIAC Phase 2 Final Report

Charles P. Hanner *, Nicolas U. Bolatto, Daniil Gribok [†], Rahul Vishnoi [‡], Nicholas M. Limparis*, Meredith A. Embrey, Justin M. Rhoads, Adam B. Youssef [§], and David L. Akin [¶] *University of Maryland, College Park, Maryland, 20742*



Fig. 1 From foreground left to right: Spencer Quizon, Meredith Embrey, Rahul Vishnoi, Daniil Gribok, Charlie Hanner, Nicolas Bolatto, David Akin. Suited Subject: Romeo Perlstein

^{*}Doctoral Candidate, Department of Aerospace Engineering.

[†]Doctoral Student, Department of Aerospace Engineering.

[‡]Masters Student, Department of Computer Science.

[§]Undergraduate Student, Department of Aerospace Engineering.

[¶]Space Systems Laboratory Director and Professor of Aerospace Engineering.

Nomenclature

AF	RMLiS	SS =	Active Rover Mounted Life Support System (umbilical-tending arm)	
CL	LPS	=	Commercial Lunar Payload Services	
CC	OTS	=	Commercial Off The Shelf	
DC	OF	=	Degree Of Freedom	
EV		=	Extravehicular Activity	
LC	CG	=	Liquid Cooling Garment	
LR	^{2}V	=	Lunar Roving Vehicle	
PL	LSS	=	Portable Life Support System	
	ILS	=	Suit Mounted Life Support	
SS	L	=	Space Systems Laboratory	
UN	MD	=	University of Maryland	
VE	ERTE	X =	Vehicle for Extraterrestrial Research, Transportation, and EXploration (rover)	
C	onte	nts		
I	Int	roducti	on	5
II	The	e BioBo	ot Concept	5
	II.A		e 1 Findings	5
		II.A.1	Rover Configuration	6
		II.A.2		6
		II.A.3		7
		II.A.4	Umbilical Disconnect	7
	II.B		ous Rover Experience	8
	II.C		nating the concept: Lunar vs. Earth Analogue	8
III	Duo		ry Lunar Designs	9
111	rie	:111111111a	Lunai Designs	
IV	Bio	Bot Ea	rth-Analogue System Overview	9
V	Um		8	10
	V.A	•		10
	V.B			11
	V.C		ϵ	11
		V.C.1		14
		V.C.2		16
		V.C.3	1	16
	V.D		,	17
	V.E	Mou	nting ARMLiSS	18
VI	Ext	reme-A	Access Rover Design: VERTEX	19

VI.B

19

	VI.C	Mobilit	у				 	 	 		 •		 20
	V	/I.C.1	Wheels				 	 	 				 20
	V	/I.C.2	Drive Actuators				 	 	 				 20
	V	/I.C.3	Drive Structural	l Support			 	 	 				 21
	VI.D	Suspens	sion				 	 	 				 22
	V	-	Preliminary Des										22
			First Iteration Is	·									23
			Final Design .										24
	VI.E		g										25
			Requirements .										25
		/I.E.1 /I.E.2	Design Overvie										26
			•										
	VI.F		re										27
		/I.F.1	Chassis										27
		/I.F.2	Swingarms										29
		/I.F.3	Over-Wheel Ste										30
	VI.G	Wheel-	Angle Adjustme	nt			 	 	 	•	 •	 •	 31
X 7 T	r D	TN4-	•										22
VI		er Electi											33
		•	Emergency Stop										
	VII.B	Battery					 	 	 	•	 •	 •	 34
V/T	II Soft	WORO											35
V I			LVEDTEV Cyrote										35
			I VERTEX Syste										
			High Level Ove										35
			User Controller										35
			Intermediate Co										35
			Low Level Con										36
			ut Following Su	-									36
			General System										36
	V	/III.B.2	Onboard Camer	a Turret.			 	 	 				 37
	V	/III.B.3	Tip Camera wit	h Gimbal			 	 	 				 37
IX		nan Inte											38
	IX.A		ut Seat										38
	IX.B	Control	Panel				 	 	 				 39
. .	2 5 5 7	a											40
X			uit Simulators										40
	X.A												40
	X.B	Interact	ion With Systen	1			 	 	 	•	 •	 •	 41
vi	Tr4*	lna.											11
ΧI			C1 1 .										41
	XI.A	-	em Checkouts .										41
	XI.B	•	stem Checkouts										43
	XI.C		est 1 - UMD Car	-									44
	XLD	Improve	ements to the Se	cond Field	1 Tria	1.		 	 				48

XI.E Field Test 2 - NASA Goddard	49
XI.F Lessons Learned	53
XII Study Conclusions	54
XIII Future Work, Research Extensions	55
XIII.A Near-Term System Improvements	55
XIII.B Field Testing Locations	55
XIV Student Involvement and Acknowledgements	56
XV BioBot Publications, Presentations, and Awards	58
ICES 2019, BioBot: Investigating an Alternative Paradigm for Planetary EVA	58
ICES 2021, Design and Development of an EVA Assistance Roving Vehicle for Artemis	
and Beyond	73
ICES 2022, Development and Testing of the BioBot EVA Support System	85
ICES 2022, Development of an Autonomous Umbilical Tending System for Rover-	
Supported Surface EVAs	101
ICES 2023, Development and Testing of Crew Interfaces for an Advanced Unpressurized	
Exploration Rover	114
AIAA ASCEND 2023, Earth-Analogue Roving System Development and Testing for	
Lunar Surface Exploration	130
ICES 2024, Initial Testing and Evaluation of the BioBot EVA Support System	

I. Introduction

Human exploration of the Moon and, eventually, Mars is primarily driven by the capabilities and limitations of the spacesuit and portable life support system (PLSS). Apollo astronauts were limited by the A7L-series pressure garments to using long-handled tools to interact with the lunar surface, as the suits were not flexible enough to allow them to reach their hands directly to the surface without significant effort. While theory indicates an unencumbered human should be able to leap five meters or higher on the Moon, the Apollo astronauts were limited to short shuffling or loping gaits by the weight of the pressure garment and PLSS.

At the time of the original proposal to NIAC, the situation with suit weight for Artemis appeared to be even worse than Apollo. Proposers to the Human Landing System competition were directed to assume that each extravehicular suit would have a mass of 187 kg, which broke down into 83 kg for the pressure garment and 103 kg for the PLSS. This means the typical astronaut would find their body mass tripled for lunar surface activities, with the majority of the extra mass in the life support system carried on their back.

The first extravehicular activities were performed with an umbilical supplying consumables to the suit. For the U.S. program, this included the Gemini and Skylab programs. There was some consideration of using umbilicals for Apollo lunar exploration, which would have limited the crew to the immediate vicinity of the lunar module. Umbilicals are difficult to handle and stow, and would run the risk of dragging and snagging on the surface if untended. In the end, the backpack-based portable life support system was developed, which freed the suits from the vicinity of the lunar module and enabled the extensive EVA exploration of the Apollo program.

The genesis of the BioBot project was a reflection of the projected weight for the Artemis pressure garment and PLSS, with the accompanying impact on the astronaut's mobility, workload, and safety. The J-series Apollo missions (15, 16, and 17) clearly demonstrated the utility of the lunar roving vehicle to provide greater surface mobility, which expanded the feasible exploration area by more than an order of magnitude. At the same time, in the half century since Apollo, robotic capabilities have grown exponentially, and it seemed likely that robotic manipulators could provide the necessary dexterity for autonomously handling the umbilical in support of lunar surface EVAs. Similarly, robot mobility has grown to the point that autonomous control algorithms should allow a rover to closely follow the astronaut on the surface to stay within reach of the umbilical handling system. The last piece to fall into place was the capability to design and develop a rover which is capable of safely traversing any surface which an astronaut would be able to traverse walking in a spacesuit. Given a system which meets those capabilities, the resulting system could relieve the lunar explorer of the weight and bulk of the PLSS, reducing workload and enhancing mobility. This, then, was the birth of the BioBot concept.

II. The BioBot Concept

A. Phase 1 Findings

The NIAC Phase 1 research for BioBot validated the basic concept, and taught the team a number of important lessons that drove much of the Phase 2 activities. The Phase 1 final report covers this in much greater detail, but there were a few notable findings that drove Phase 2 development.

Much of the activity of Phase 1 focused on critical trade studies for the concept. Beyond "the

rover carries the life support for the EVA crew", there were myriad possible combinations of design choices; the goal of our Phase 1 activities were to resolve as many top-level trade studies as possible.

1. Rover Configuration

The rover component of BioBot conceptually could range from a small dedicated system to installing the life support and umbilical handling systems on a pressurized rover. Some simple tests were performed with existing hardware in the Space Systems Laboratory to assess the potential of the specific concepts, which were:

- (a) Minimally-sized rover transporting only the life support system
- (b) Small rover with life support and umbilical handling systen, but also capable of carrying tools and collected samples
- (c) Rover designed to carry a single EVA crew along with their life support and umbilical handling systems
- (d) Rover designed to nominally transport a single EVA crew and their life support/umbilical handling, and capable of transporting a second crew in a contingency and sharing life support with them while on the rover
- (e) Two-person rover with dual life support and umbilical tending systems
- (f) Pressurized rover with dual life support and umbilical tending systems

The two small rover options (a) and (b) were rejected because they could not follow the crew into all regions which could be safely traversed in EVA. They were also found to be more susceptible to overturning due to the high center of gravity created by the umbilical tending system. There was also a general consensus that if the astronaut is tied to a rover, it would be suboptimal to make the crew walk everywhere instead of providing transportation. The two largest concepts, (e) and (f), were dropped because of the potential for the dual umbilical systems to interfere with each other and to become entangled.

The concepts remaining were the two single-person rovers, (c) and (d). Lunar EVAs with the Apollo Lunar Roving Vehicle were dominated by the "walk-back criteria", which prohibited the crew from being farther away from the Lunar Module than, following a rover failure, they could walk back well within the remaining consumables in their backpack-mounted portable life support systems (PLSSs). A probabilistic risk analysis showed that two single-person rovers with the capacity to transport both crew in a contingency was the best solution, and could arguably eliminate the need for the walk-back criteria. For this reason, option (d) was selected as the best design concept for a BioBot rover.

2. Umbilical Handling

It was clear from the original conceptualization of BioBot that the umbilical handling would be the essential enabling technology. The umbilical had to be kept off of the surface to prevent regolith coating the cover and snagging on rocks; the entire system from the rover to the umbilical handling also had to be transparent to the user to minimize the impact on EVA operations. The initial assumption was that the umbilical handling had to be automated; it was not clear what the best approach would be.

During the Phase 1 NIAC study, two approaches to umbilical handling were developed and evaluated. The most straightforward concept was a robotic manipulator to hold the umbilical above the surface and maintain the distal end above the EVA crew. It was judged to be important to provide

the EVA crew with a free-range area in the vicinity of the rover to minimize the need to continueally servo the rover position to the astronaut's every motion The design exercise showed that a 10 m umbilical tending manipulator would be feasible in lunar gravity, but that a 5 m arm would be the limit for an Earth analogue system. This approach would require active control of the manipulator position, increasing the demand on control systems and mass on the rover.

The other approach considered was a passive pantograph-type design that was extended and retracted by the crew's motion, and would tend the umbilical without a need for actuators or computation. A prototype of this system was developed and tested in simulated EVAs. This concept proved feasible in terms of deployed operations, but is could not be compacted enough at full retraction to clear the crew's driving position on the rover, and it did not move after the user disconnected from it, requiring the crew to potentially circle the rover to reach the place where the connection was dropped to reconnect before rover ingress for driving to the next site. The decision was made to baseline a fully robotic umbilical tendiing manipulator despite the addition impact on the design and development process.

3. Suit-Mounted Life Support System

While the life support system on the BioBot rover was expected to provide the bulk of consumables over an EVA sortie, there was never a time when there was not a requirement for some form of PLSS worn by the EVA crew, if only to cover the time from airlock egress to hookup and checkout of the BioBot life support system. Eventually it was realized that the greatest unknown question was the best choice of duration and life support technologies for this suit-mounted life support system, designated SMLS to differentiate it from the traditional PLSS.

During Phase 1, the BioBot team developed 10 SMLS concepts, ranging in capacity from a 20 minute duration to allow transition from the airlock to BioBot and back again, to an 8 hour duration backpack larger and heavier than the Apollo PLSS. Short duration designs used open-loop oxygen supply for both breathing and gas cooling, as they were designed only for airlock transits. longer duration units were designed with water cooling and CO₂ scrubbing for high physiological workloads, with the intention to allow the user to disconnect from BioBot and have some capacity for independent EVA operations, such as accessing sample regions not accessible by the rover and out of reach of the umbilical system. A further design decision rested on the issue of whether or not the SMLS system should be designed to be recharged when attached to the umbilical, effectively eliminating both duration limits and constraints on the number of independent intervals that could be performing on any given EVA sortie. While these issues were considered conceptually, it was determined that the only valid method of determining the best design decision was to obtain data from Earth analogue testing, ideally performing realistic EVA simulations such as geological exploration.

4. Umbilical Disconnect

The concept of operations which evolved in Phase 1 was to have the BioBot user disconnect from the umbilical for periods of independent mobility, then reconnect to go back on rover-mounted life support and to recharge the SMLS system. This gave rise to the concept of a simpler BioBot sytem, in which the rover life support was only connected while driving, and the SMLS was used for all phases of the EVA off of the rover. In any case, the need to connect and disconnect the life support umbilical during an EVA gave rise to the need for an umbilical connection with EVA-compatible

release interfaces. Critical to this study was the need to have the umbilical operations be easily performed unaided, which eliminated connections on the back of the suit. The interface was designed adherent to the principle of three independent actions to release, which further led to the decision to limit it to the two-handed work volume of the suit, with a further requirement to be in the line of sight of the EVA crew.

The final decision was to place the umbilical interface on the upper chest of the suit, right below the helmet ring. Two simultaneous lateral motions were required to release the latches, with a pulling motion to separate the umbilical sealing plate from the suit chest plate. To prevent interference with arm motion and minimize impact on range of vision, the umbilical was designed to terminate with a rigid section shaped to run along the chest and over the wearer's left shoulder, then transition to the flexible umbilical once behind the shoulder. The suit handling umbilical would hold the umbilical end approximately at shoulder height above the local surface to keep it accessible to the user and clear of surface regolith to the extent feasible.

B. Previous Rover Experience

The design of VERTEX was strongly affected by the experience of the Space Systems Laboratory with the Robotic Assist Vehicle for Extraterrestrial Navigation, or RAVEN vehicle. Based on a Senior capstone design class in 2010, RAVEN was dewsigned to serve as a single-person EVA transport vehicle for lunar exploration, with the capability for assisting the EVA crew through crew-directed robotic sampling or teleoperated geological exploration and sampling. RAVEN was originally developed as a differential-drive system with two powered front wheels and a fully swiveling solo rear wheel. In this configuration, it was used in a series of analogue field tests in collaboration with Arizona State University from 2010-2013. After that time, it was converted to a four-wheel skid-steer vehicle, and is still used by the SSL today in that configuration. Experience with RAVEN's shortcomings, particularly issues with limited slope capabilities and difficulties of extended skid-steer operations, drove many of the design decisions on VERTEX for capabilities such as the adaptive suspension and crab driving.

C. Evaluating the concept: Lunar vs. Earth Analogue

At the outset of creating a roving vehicle to adequately test the BioBot concept, an overall approach for Earth testing needed to be selected. At a very high level, the rover needed to be able to nominally support the test subject along with an umbilical arm in full Earth gravity field tests. Full concept evaluation is hinged on more than empirical evidence, benefiting from the ability to generate and convey human experiences. The Earth tests need to evaluate the concept more than the particular details of the mechanisms created so long as they adequately function. Supporting a human test subject during field trials ultimately means no overall scaling of the vehicle dimensions beyond normal iterative design updates.

There are three main ways to design a test vehicle based on an anticipated flight rover. First is dubbed "The Similarity Law" and attempts to create a test vehicle to match a rover's performance through considerations of vehicle weight, inertia, weight on wheels and other parameters [1]. Ultimately this results in the creation of a rover proportionally scaled between the gravitational levels of the two bodies in consideration, a non-starter for BioBot testing requirements. The second method is to maintain rover scale but with less mass to preserve the center of gravity [2]. This generates fidelity benefits in testing terramechanics under the assumption that soil parameters are

gravitationally independent, stability, and suspension mechanisms aboard a rover. For BioBot this would be at the expense of payload capacity and likely create a system without onboard power, control, and drive systems and significantly increased manufacturing complexity. The third approach is what the SSL calls "capability-matched" in which the rover is allowed to increase in mass and use additional mechanisms as long as the final product achieves the same performance in climbing slopes, suspension leveling, and payload on Earth. In the specific case for BioBot, this allowed the main structures of VERTEX and ARMLiSS to be fabricated from MIG welded mild steel, trading ease in fabrication and modification at the expense of added weight.

III. Preliminary Lunar Designs

The core set of requirements for the lunar design were as follows:

- Operating speed of 4 m/sec on level, flat terrain
- Accommodate a 0.3 m obstacle at minimal velocity
- Accommodate a 0.1 m obstacle at 2.5 m/sec
- Safely accommodate a 20° slope at any direction and a speed of at least 1 m/sec
- Nominal sortie range of 54 km at an average speed of 2.5 m/sec with at least 8 hour duration capability
- Capable of carrying one 250kg EVA crew member (modified from original paper after xEMU details released), and 80kg if assorted payload
- Capable of carrying a second crew member in a contingency scenario
- Incorporate roll-over protection for crew and all required ingress/egress aids and crew restraints
- Capable of two landers launching on a CLPS lander (Single rover mass ≤250 kg)
- Developed in time for the first Artemis mission
- Capable of indefinite operation without crew including being controlled directly, remotely, or in automated fashions
- Capable of following an astronaut, an astronaut's path, or autonomously path planning between waypoints
- Capable of operating during any portion of the lunar day/night cycle and at any latitude

Four lunar concepts were created by students in an ENAE788X Planetary Surface Robotics design class, featured in Figure 2. These designs were approached from a mechanical, structural, and kinematics focus, with some consideration for power systems. The final VERTEX roving vehicle combined some of the best features from these designs such as articulated suspension and 360° over-wheel steering.

IV. BioBot Earth-Analogue System Overview

An overview of the BioBot system can be seen in Figure 4, with a Figure of the built system found in Figure 3. As built, VERTEX is a 12-DOF roving vehicle featuring independently articulated suspension, 360° over-wheel steering on all four wheels, and independently driven traction actuators. The vehicle weighs ≈ 1000 kg, and is able to level the chassis on slopes (40° cross slope and 28.5° on slope). Atop the rover sits a 5 meter, planar, umbilical tending robotic manipulator named ARMLiSS.

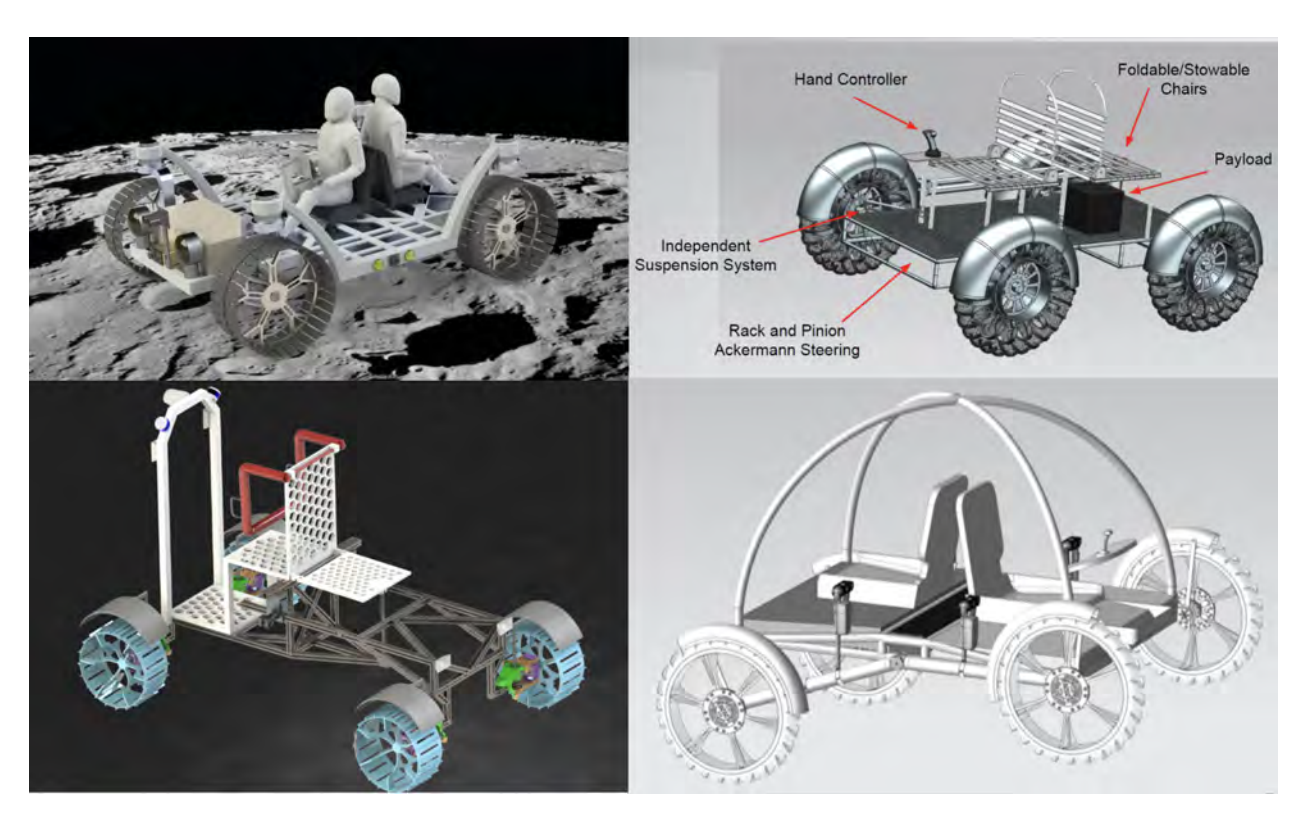


Fig. 2 Initial lunar concepts from ENAE788X

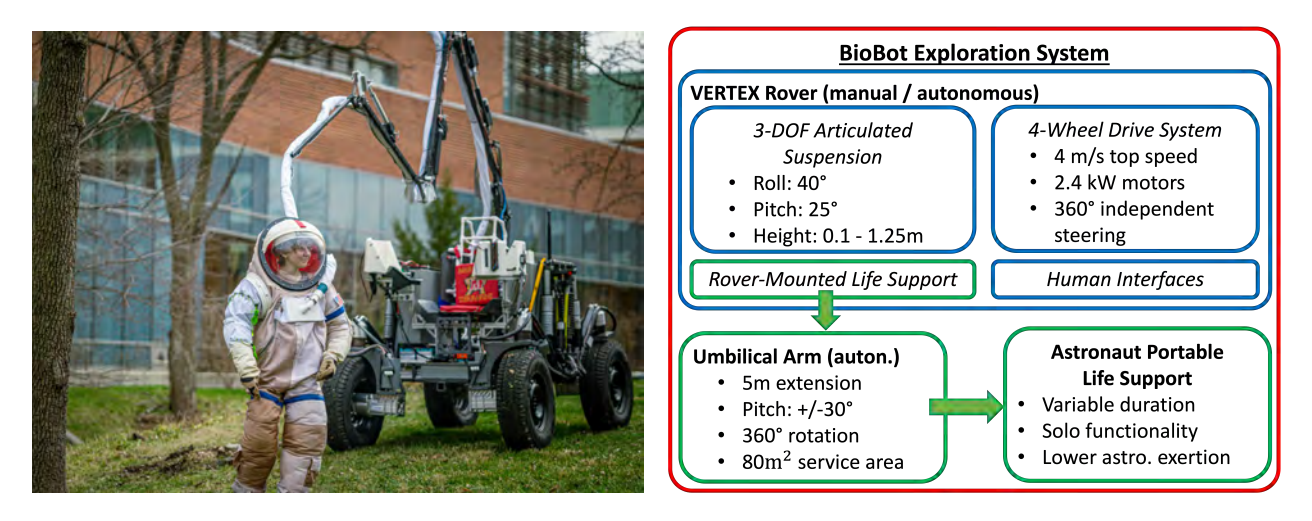


Fig. 3 BioBot concept deployment

Fig. 4 BioBot overview block diagram

V. Umbilical Tending Robot Design: ARMLiSS

Active Rover Mounted Life Support System

A. System Overview

The final arm design when mounted on VERTEX is capable of umbilical tending on 30° slopes. The umbilical line reaches up to 4 m above the base of the arm or down to 1 m below - in either case the arm can reach up to 4.4 m away or up to 5.08 m when the arm is straight out with no

inclination. The umbilical reaches 0.5m from the arm base at minimum extension with the arm fully above the rover seat. This leaves enough space to service an astronaut while entering the rover seat, driving, or walking anywhere around the rover (Fig. 10). The arm's yaw joint pivots a full 360°, providing a total service area of 80 m² around the rover (Fig. 5). Taking into account only linear tip extension $\pm 30^{\circ}$ from the base, the umbilical arm's workspace is ≈ 270 m³. Although it would require a sophisticated tracking system, it is mechanically possible for the arm to reach much higher or lower if it operates joints unevenly to increase its workspace. For example, the arm in Fig. 8 could halve the angle of J3 in order to raise J4 and the tip directly overhead.

In order to maintain ample clearance as the astronaut dismounts from the driver's seat, the arm will be programmed to pitch the first joint upwards 30° from its stowed position (Fig. 10). The second joint will then be used to follow the astronaut as they step off of the seat and onto the ground in front of the rover. From there, the arm is free to actuate joints 2-4 to extend at maximum velocity while joint 1 exclusively adjusts for extension angle, and the yaw joint rotates the arm with respect to the rover. The arm generates a tip speed of 0.55 m/s while joints 1-4 actuate together in this fashion after the astronaut dismounts.

B. Life Support System and Umbilical Design

The BioBot life support system could be nothing more than a marginally repackaged portable life support system from current suits. Improvements planned for the Artemis PLSS, such as the rapid amine system for CO₂ removal, would provide an essential life support service without the need for physical replacement units between sorties, unlike the lithium hydroxide or METOX canisters in the current PLSS. The rover-mounted life support system could have larger storage capacity for consumables, including oxygen and water, than is practical in a SMLS system. Power for life support could come from the rover's main energy storage system or a dedicated battery. Redundant systems could be incorporated for greater crew safety and mission assurance, as both mass and volume limits are far more relaxed on a rover than in a crew-carried backpack unit. The only operational requirement would be to ensure the rover can be plugged in to recharge batteries and replenish consumable fluids; the details of this are not included in this study, but it could range from crew-actuated umbilical connections to the use of automated robotic manipulation of recharging connectors.

For the actual space application, the umbilical to the spacesuit must convey oxygen, cooling water, and electrical power and data to and from the astronaut. The oxygen would essentially be at suit pressure, necessitating larger diameter lines that would be the case for a higher pressure supply. The umbilical would then have to contain two oxygen lines, two water lines, and a wiring bundle for power, voice communications, and digital data. This would be packaged in an outer envelope made of ortho fabric or similar soft goods to maintain the minimal cross-section of the umbilical. A similar system would be used for Earth analogue testing if a full pressure suit were worn by the test subject.

C. Manipulator Design

The purpose of the umbilical arm design presented in the following sections is to demonstrate the BioBot concept's capabilities on Earth, where field testing can show the merits of the unique system before implementation on the Moon or Mars. In other words, the goal is to show the effectiveness of an umbilical handling arm that can offload the life support equipment for an EVA astronaut up to 5

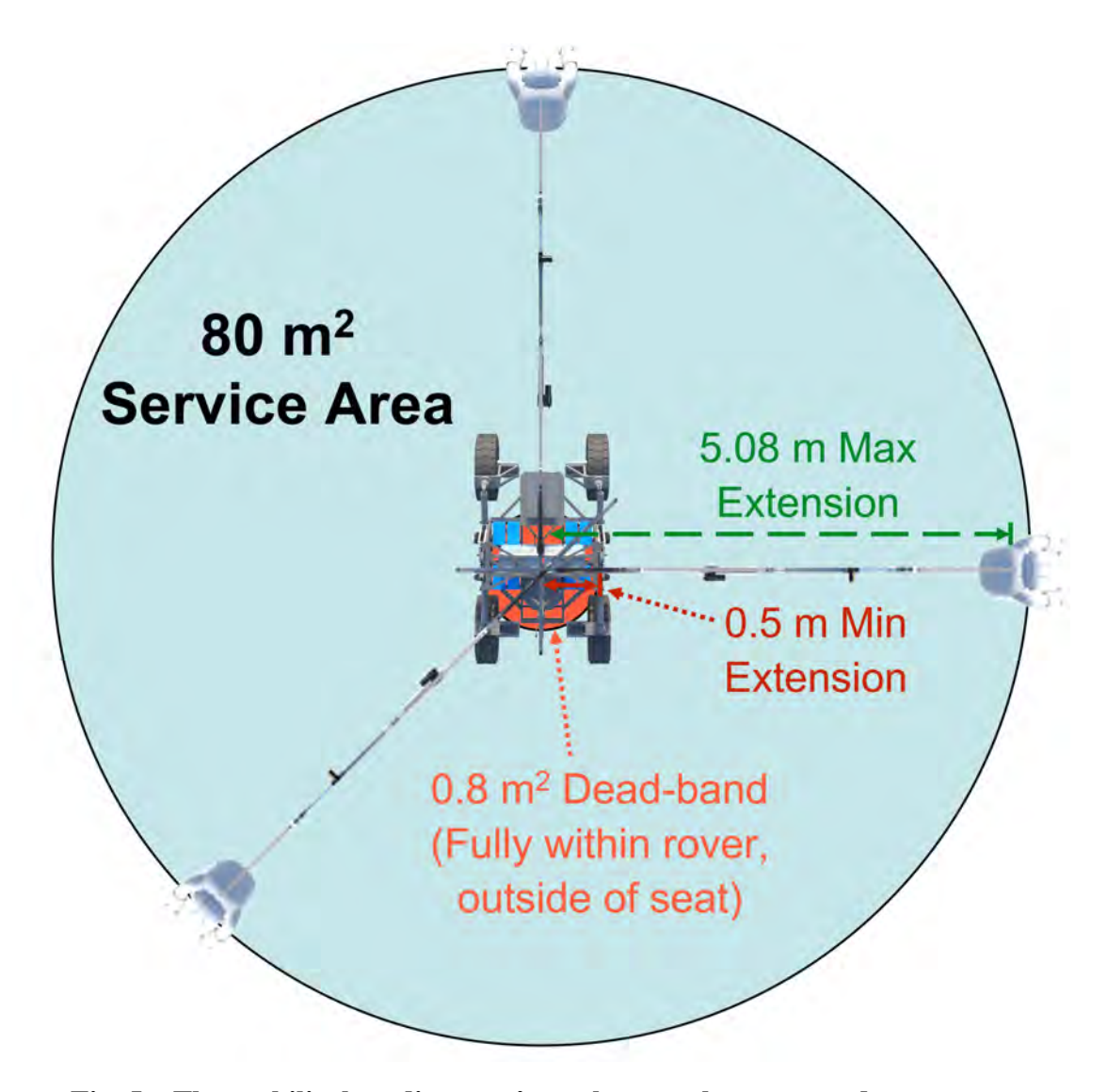


Fig. 5 The umbilical tending arm's work area when mounted on a rover.

m away and on 30° slopes. This design however cannot be directly compared to what a true "flight" version of the umbilical tending system would be in terms of mass, power, and volume. Designing an Earth-analogue robot with the same capabilities as a lunar version comes at a significant cost to structural and actuator mass due to gravity being approximately 6 times greater as shown in the design of the VERTEX rover. This additional mass does not necessarily scale at the same rate as the change in gravity environment due to compounding factors (such as increases in structural mass driving increases in actuator mass and power which drive further increases in structural mass) [3]. This relationship also is expected to hold for the martian gravity case, albeit to a lesser degree due to the gravity levels of the Earth and Mars being closer than that of the Earth and Moon. As a result of these factors and limitations, the design of ARMLiSS is expected to be less capable in extension speed and more massive than a flight equivalent because of the actuator gearing required for Earth gravity. As such, if this concept is shown to improve EVA performance and comfort through field testing compared to a traditional PLSS, a flight equivalent (without the limitations of weight and

speed) is thought to be only more effective. A future goal of this study is to design a version to lunar specifications and compare the lunar and Earth-analogue designs.

With the intention of creating a design that is as conducive to implementation on the Moon or Mars as possible, the ability to compactly package the arm was key. To be suitable for field-testing transportation and for use atop a mobile platform, the umbilical arm must be able to retract while driving for greater stability while still maintaining a connection to the astronaut. These requirements originally removed telescopic-boom-style arms from consideration, and SSL's NIAC Phase 1 study showed that a pantograph design would be costly in terms of mass and volume to scale upwards in length. A tension-cable design like NASA's Lightweight Surface Manipulation System could be more mass-efficient, although it would be difficult to modify for stowage and would require significant on-site assembly by astronauts. Based on these requirements, preliminary designs from phase 1, and space limitations on the rover, a redundantly-actuated arm was chosen. This requires more resources in terms of power, computation, and sensing; but these costs are necessary to achieve the desired performance while keeping the arm relatively transparent to the astronaut. Considering the footprint of the rover and the desired workspace, an arm of five serial links was decided upon. Other initial design ideas explored were single-actuator pantographs, deemed too bulky yet flexible in NIAC Phase 1, as well as telescopic booms which were too high-mass for the necessary stiffness and had too great of a storage volume when retracted.

The SSL has conducted significant field testing on the impacts of using rovers to aid in suit-simulated EVA as part of Desert Field Lessons in Engineering And Science (D-FLEAS) with suited geologists traveling and collecting samples with and without a transportation rover [4]. These studies demonstrated that subjects would often be interested in locations that were accessible on foot but not for a wheeled rover: "Test subjects routinely traversed slopes of up to 30° in the approach to the vertical faces of the test sites, and climbed slopes in excess of 60° in cases where the footing was acceptable." [5] To enable the exploration of difficult terrain that may be beyond the rover's capa-

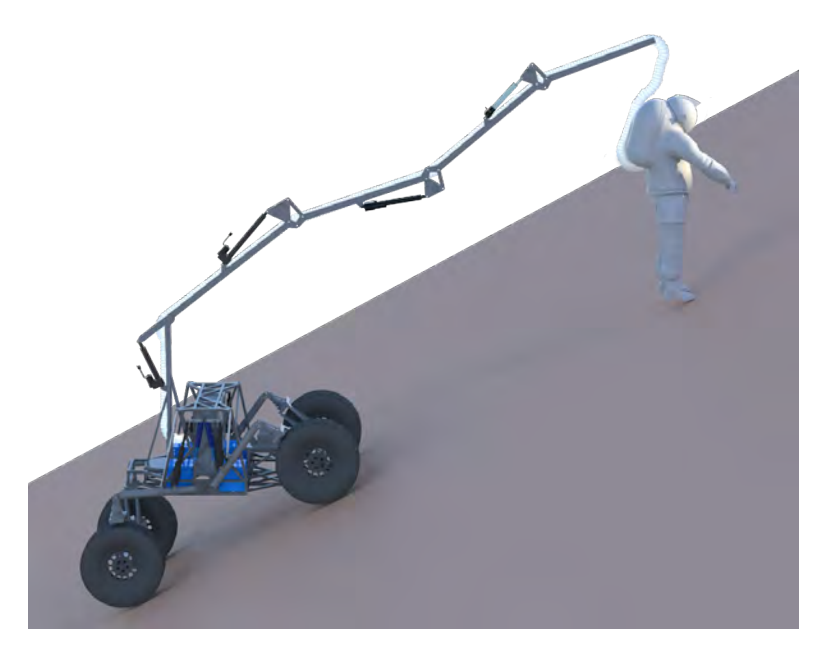


Fig. 6 Rover-mounted arm providing umbilical tending on up to 30° slopes while the VERTEX rover maintains a level deck for stability.

bilities, such as rocky areas, crater rims, and other steep faces, the arm's workspace was maximized. At the same time, the umbilical arm must retract far enough for an astronaut to drive in the front seat of the rover or to access the rover exterior where scientific payloads may be stored. This way, the number of umbilical disconnect and reconnect operations and potential for dust impingement is minimized.

As such, ARMLiSS was made to access a wide radius around the rover to not disturb walking exploration of regions that the rover cannot enter, such as sheer rock faces or areas with a high concentration of rock scatter. Additionally, ARMLiSS is able to support astronaut life-support delivery while the astronaut is walking on a slope of up to 30° in any direction with respect to the rover. In other words, the umbilical tending system can support the astronaut exploring on foot around the rover for all conceivable terrains the rover may enter. To truly benefit surface



Fig. 7 Hardware deployment of BioBot at full umbilical arm extension

operations, the umbilical arm must be operationally transparent to astronauts and easy to set up for use. Therefore, ARMLiSS must also allow for typical movements astronauts may make during exploration of these areas. The arm positions the flexible portion of the astronaut's umbilical above and behind the astronaut's head, with enough umbilical "slack" to connect to the suit without restricting high-frequency motions such as bobbing while walking or kneeling to collect samples.

1. Pitch Joints



Fig. 8 Diagram of arm joint locations, corresponding to torques in Fig. 9. Structural links are numbered by their proximal joint, with the vertical mast being link 0 and the tip being link 4.

A parametric model of the arm was created in MATLAB, containing the measurements and mass of each link bar, joint lever assembly, and linear actuator. The additional mass of the umbilical itself was modelled as a 2 kg/m linear density across the full length of the arm, with a further 1.5 m of umbilical leading from the tip of the arm to the astronaut. Margin for the mass of an umbilical quick-disconnect at the tip was also factored in. By inputting a trajectory of joint angles from the stowed configuration to full extension, an accurate model of the torques experienced by each joint was created (Fig. 9). The maximum torques required for each joint are summarized in Table 1.

Joints 2 through 4 of the arm need to to actuate about 160 degrees and also require a large

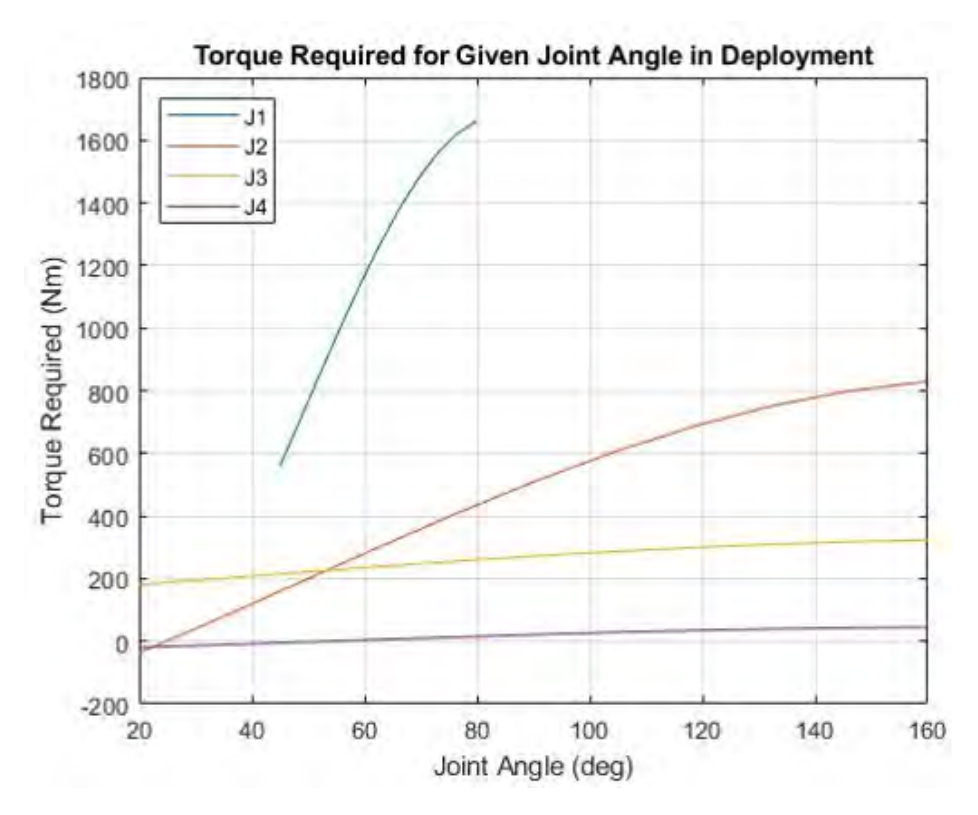


Fig. 9 Torque required for each joint from the stowed configuration to full extension, color-coded to Fig. 8.

amount of torque. Due to the high torque requirements, the joints were designed to take advantage of a lever arm, rather then generating the torque at the pivot with a direct drive solution. Initial design inspiration was taken from concrete pump trucks. They have long arms which fold compactly onto the back of a truck. In many ways, this is similar to ARMLiSS, except it supplies water, power, and data as opposed to concrete. Initial designs of the arm considered two types of joints driven by linear motion, ones driven from the outside and ones driven from the inside. By alternating these two types, the folded volume can be minimized. However, as design efforts progressed, the interior style joints were abandoned. This design decision cost a few inches of vertical space when the arm is folded, but cut development time in half by discarding the need for an additional lever design. For this Earth-analogue system, the trade-off was considered acceptable as there is more interest in the overall concept than the detailed design of the arm itself. Following this decision, extensive optimization of a generic design was carried out for joints 2 through 4.

Using MATLAB to create surface plots, the distances between each pivot point were optimized to produce the required torque. At the same time, the design also tried to minimize the lever arm to keep the speed up and volume and mass minimal. The optimized dimensions were then verified for a safety factor of at least 1.6 and optimally 2. As iterations were made, the CAD models were updated and verified with FEA, and various linear actuators were considered. This produced more accurate mass estimations, allowing for further refinement of the parameters. Joint 1 differs from the other joints in that it is a simpler first-class lever. It serves mostly to keep the arm clear of the astronaut's head and contributes very little to extending the arm and folding compactly, unlike the other joints. Because of this, joint 1 does not need the range of motion that the other joints do and is

not as space constrained. Like the other joints, the design was optimized for torque and speed, and it was analyzed to ensure that it could actuate sufficiently throughout its entire range.

2. Yaw Joint

Controllability of the yaw joint was always a concern during the design process of ARMLiSS. Effectively cantilevering a 5 meter, $\approx \! 100$ kg manipulator off a slew bearing was estimated to require approximately 450 Nm to keep the arm pointed at a 10° chassis angle. While technically possible, with the VERTEX suspension system capable of leveling the chassis on 30° slopes, it was decided that a manually actuated pin system would be simpler and more cost effective for the testing requirements. The trade study to find the motor and gearbox combination to actuate the arm ended with significant implications to available footprint on the rover. Pinning the arm to a set angle during transit and unpinning once the astronaut disembarks from the rover simplified the system greatly for Earth testing.

3. Arm Speed and Position Determination

The target tip speed was about $0.6\,\text{m/s}$, the average walking speed of the later Apollo missions [6]. Tips speeds of up to $2\,\text{m/s}$, the average walking speed on Earth, were considered but quickly found to be impractical and the objective was set to $1\,\text{m/s}$ at most. Additionally there were safety concerns about having the arm tip move at significant speeds near the astronaut's head. The final design has a maximum linear extension speed of $0.55\,\text{m/s}$. In the event that the astronaut outruns the arm, there will be slack in the umbilical and the rover can translate to accommodate. In the final design, to reach the desired tip speed most of the linear actuators selected are overrated for the application as they move faster at lower loads. Additionally, for joint 2, two linear actuators were put in series to double the actuation speed.

All arm joints are directly instrumented with 12-bit absolute encoders. Higher bit count encoders were considered, but the added resolution would have little benefit as tip deflection at full extension would have been greater than the pointing accuracy, rendering the additional accuracy useless without extensive and complicated control software that could account for arm deflection based on pose. Such advanced software may prove useful for a lunar model, but for demonstrating the concept on Earth, this capability is outside the scope of the project for now.

Joint	Torque Required (Nm)	Linear Force Required (N)	Actuator Capability
0	452	N/A	484 Nm
1	1650	4400	5338 N
2	830	6600	8896 N
3	320	3520	5338 N
4	45	660	890 N

Table 1 Joint summary table. Joint 0 is actuated by a revolute motor, joints 1-4 use a linear actuator and lever arm.



Fig. 10 Umbilical arm in its retracted "stowed" pose, mounted on a cross-section of the VERTEX rover.



Fig. 11 Retracted ARMLiSS integrated with the kneeling VERTEX rover, clear of the driver for ingress.

D. Umbilical Arm Safety

With BioBot being a human system, there were several design choices made for increasing operator safety. The rover base itself, VERTEX, was designed considering the large umbilical arm as a possible payload. The rover is able to actively control the vertical position of all wheels in order to maintain the chassis horizontal on slopes up to 30°. This has been shown to increase stability on slopes, especially when the combined center of gravity of the vehicle is raised by large robotic arm payloads [7]. The rover design also increases dynamic stability by pitching into the local gravity vector tracked by onboard accelerometers, which is also expected to provide stabilizing responses to forces on the umbilical arm. All of these capabilities reduce the probability of vehicle rollover while umbilical tending.

Despite the benefits provided by mounting the umbilical arm to VERTEX, additional safeguards are of course necessary in the design of both the umbilical and the arm. Further discussed in Section VIII.B, an astronaut tracking system is still being developed to allow the umbilical arm to follow an astronaut on foot. Tracking will be used to maintain the umbilical arm close enough to the astronaut to prevent any pulling by the umbilical while still maintaining a safe position above and behind the astronaut at all times. Umbilical slack between the arm tip and astronaut has also been provided to account for motions of higher bandwidth than the arm's response, the necessary length of which will be determined through further field testing. The effects of umbilical torsion on the astronaut are unknown but will also need to be analyzed during further testing, however, initial testing with an unpressurized umbilical resulted in no astronaut test subject discomfort, and the slack given was adequate. Sufficient slack in the umbilical combined with arm and rover control schemes should prevent pulling on the astronaut in nominal-use cases, but low breakaway-force mounting points between the arm and umbilical as well as a breakaway disconnect analogue in the umbilical itself will protect the astronaut from being significantly affected in off-nominal situations

once implemented. For the first tests, the umbilical was secured to the test subject through a low-tech connection and series of suit-mounted parts that would breakaway in case of umbilical pulling. This solution worked well for preliminary testing.

In all cases, emergency stops are present on the rover and on multiple testing observers to halt all robot motions should they become unsafe. Integration of an emergency stop on the suit for test subject use is also being worked on, however, the test subject was kept out-of plane of all arm motions during testing thus far (effectively outside the workspace with a pinned yaw joint). Additionally, the arm actuators were chosen such that, even in the event of a power loss (or emergency stop), the arm seizes but does not collapse. The selected linear actuators operate with an ACME screw and nut rather than a ball screw, providing superior backdriving resistance. The weight of the arm is not sufficient to backdrive any of the joints by over 50%.

E. Mounting ARMLiSS



Fig. 12 Adjustable ARMLiSS mounting

The original mounting plan for ARMLiSS was to weld the steel plate that the yaw joint bolts to onto VERTEX, and then mount/unmount the bearing each time the arm is put on or taken off. This caused two concerns in the initial design that weren't remedied until production had started. First, the arm is not balanced about the yaw point, so a custom stand would have had to have been designed to hold the arm when off the rover. Secondly, the absolute encoder for the yaw joint was originally mounted under the yaw joint, and would require careful positioning through the welded rover plate and on the test stand. Both of these were remedied during the arm fabrication process. First, the absolute encoder was rotated 180° and hidden within the first link of the arm, protecting from damage. Secondly the plate originally intended to be welded to the chassis was drilled into and a series of weld studs were placed at consistent intervals on the chassis allowing the plate to be bolted on, as shown in Figure 12. The holes drilled in the plate are clearance for a 5/16-18 bolt, the standard for 15-series 8020TM allowing for long extrusions to be bolted to this plate to make a space-efficient and cheap stand. Not welding the plate to the chassis allows many different payloads

to be added to the rover later without having to consider the specific bolt pattern required for the yaw bearing, and the many weld studs mean the arms position can be adjusted forwards or backwards depending on a desired configuration.

VI. Extreme-Access Rover Design: VERTEX

Vehicle for Extraterrestrial Research, Transportation, and EXploration

A. Roving Requirements

The lunar requirements were down selected to a reasonable set to start from for the Earth design. First the first four requirements pertaining to vehicle performance were maintained as-is. This drove sizing and terramechanics requirements for wheels and traction motors. Examining the expected testing regimen while being mindful of cost and added mas,s the range and duration requirements were removed as a hard bound in lieu of requiring on-board batteries support a day of testing. The mass requirements for carrying humans was relaxed to the ability to carry test subjects in the SSL's MX-series spacesuit simulators. Requirements regarding the downmass and other lunar-specific development and operations were relaxed under the knowledge of "capability-matched" tradeoffs as discussed in section II.C. An autonomous feature set was included in the design process and progression towards that is still underway.

Various feature sets from the ENAE788X design effort were taken from each of the designs. Most notably over-wheel steering and independently articulated suspension were prioritized. The over-wheel steering, specifically the 360° system implemented, allows the rover to very quickly change direction to adapt and follow an astronaut's movements around the rover, crater, or testing site. It also allows for a multitude of steering modes to be evaluated by the operator. The independently articulated suspension allows for the chassis to intentionally adjust height, pitch, and/or roll whether for slope compensation or to act as mobility aid such as kneeling. Slope compensation greatly increases a rover's static stability regions and provides a greater sense of stability to an astronaut by remaining more aligned with the gravity vector. Leveling the rover chassis also reduces the torque requirements to hold the base yaw joint of ARMLiSS to a level that the astronaut can easily impart as they walk around the rover.

B. System Overview

VERTEX is a 12 DOF rover featuring independently articulated suspension, 360° over-wheel steering, and high-torque capable traction motors. The vehicle has 32" consumer-grade off-road tires, eight brushless DC motors, and four linear actuators. The vehicle weighs approximately 2,250 lbs (\approx 1,000 kg) without ARMLiSS (an additional 220 lbs or 100 kg).

The primary structures for the rover were welded from mild steel include the main chassis, swingarms, and over wheel steering.

Each swingarm is capable of rotating 45° above, and 13.8° below the level point with the chassis. One end of the swingarm is mounted to the chassis via a pair of tapered roller bearings and the other attaches to the top of the steering stackup. This generates a capability of leveling the chassis 40° in roll and 28.5° in pitch. Each swingarm is actuated via a linear actuators placed in series with a spring damper to create a series-elastic actuator. Additional weight-offset mechanisms were added to aid in alleviating actuator requirements and this process is further discussed in section VI.D.



Fig. 13 VERTEX built photo

C. Mobility

1. Wheels

Once terramechanics had determined the optimal wheel size was 0.8m diameter and 0.2m width a commercial tire was sought. Pneumatic tires were desired for their ease of repair/replacement during a field test and low cost compared to custom piano wire mesh or airless tire limited availability. Medium aggression off-road tires were selected as a balance between grip and respectfulness in not tearing up grasses or soils too badly in testing locations. Tire Rack was able to provide a recommendation and confirmation that the OD of GENERAL Grabber APT "E" 235/85R16 tires measures at 31.7" diameter when installed on a 16x6.5" 5x100 wheel.

2. Drive Actuators

Previous terramechanics studies showed that VERTEX was likely to need 200 Nm of torque at each wheel to drive continuously over relatively flat terrains off-road, and it simultaneously needed to maintain the speed requirement of 4 m/s. The rover was also projected to need up to 400 Nm at peak during hill-climbs. Several AC electric motors were found capable of these torque outputs, but their bus voltages of 480+ Vac were deemed unsafe for a student research platform. A wide variety of hydraulic motors and pumps were also analyzed for use, however the high-pressure fluid line requirement was also considered potentially dangerous.

Achieving 400 Nm torques with DC electric motors proved difficult, especially with the requirement that the motors also be capable of 95 RPM at 200 Nm to achieve a top speed of 4 m/s with 0.8 m wheels. High gear ratios with strain-wave gears and two-speed transmissions were considered for some motors that could not achieve the speed range at load. However, research into other large rover analogues like Chariot found that the Magmotor company made extremely high-torque DC motors that met torque requirements - as long as a suitable gearbox could be found.

Again, most readily-available gearboxes in this size range were not capable of achieving both the required maximum velocity and the maximum expected torque. Tabulating best-fit Magmotor products showed that a gear ratio in the 30-40 range would be required, which is lower than harmonic gearing and higher than many planetary and worm-gear systems could provide at load. Custom two-stage gears consisting of a strain-wave speed reducer and a low-ratio spur gear speed increaser were considered, but finally a planetary gear system from Harmonic Drive LLC was found.

The final drive system consists of a 90Vdc Magmotor BFA42-2E-300 motor coupled to a 33:1 Harmonic Drive LLC HPG-50A-33 planetary gearbox (figure 14). The motor can sustain a 12 Nm output (400 Nm after the gear reduction) for 15 minutes. In fact, the torque/speed curves are such that the required hill-climbing torque can be sustained at nearly no-load speeds of 3300 RPM, or 100 RPM after the gear reduction. With forced-air cooling, this temperature-limited duration could be doubled in the future. The actuator also has an integrated incremental encoder, as well as a 5.7 Nm dynamic brake (resulting in 186 Nm at the wheel).



Fig. 14 Traction actuator stackup



Fig. 15 Traction gearbox bearing support housing and wheel hub

3. Drive Structural Support

To support the drive actuators and transfer torque to the wheels a series of four pieces were designed and milled. Existing grooves in the Magmotor housing were modeled and milled into the aluminum motor holder. A pinned and bolted rear cap was bolted to both the motor holder and the rear of the motor through holes milled into the rear motor plate.

The motor holder is then connected to the aluminum gearbox holder via three pins allowing these pieces to be snugged up to their respective pieces without causing interference and unnecessary tension. The gearbox holder was milled to contour closely to the planetary's structural housing and use as much surface area as possible. To affix this piece to the front, long shoulder bolts tie into an

aluminum front bearing support.

On the output plate of the planetary gearset a wheel interface piece was milled in stainless featuring pins and counterbored holes for bolts to affix into the plate and tapped holes for lug nuts. 303 stainless was used as a higher strength option for affixing the wheels via threads over aluminum and allows for helicoils to be inserted if the threads are ever damaged in-lieu of starting with helicoils. The outer diameter of the wheel interface piece was milled and turned to a slip bearing fit and features a 5" radial bearing that the front bearing support holds the OD of and seals with an x-ring. The wheel is then bolted to this piece with standard lug nuts.

D. Suspension

The ability to articulate the chassis in roll and pitch allows for the CG of the rover's sprung mass to be articulated and leveled and kept within the stability region of the wheels across a larger magnitude of slopes. ARMLiSS requires significantly less torque to rotate the umbilical arm around its yaw joint if the chassis is kept at a maintained level with the horizon.

The main complicating requirement of the suspension system was in combining both articulated and passive suspension to maximize adjustability and comfort. Passive suspension systems are designed to manage and reduce displacements, and the VERTEX suspension goal is to have independent, intentional, large displacements of each wheel to balance the chassis but also to have compliance for the wheel to displace up or down just as a car for dealing with rocks, potholes, etc. The optimization is highly non-trivial, especially when factoring cost, especially for VERTEX which has a very large range of articulation, the root cause of the difficulty.

1. Preliminary Design

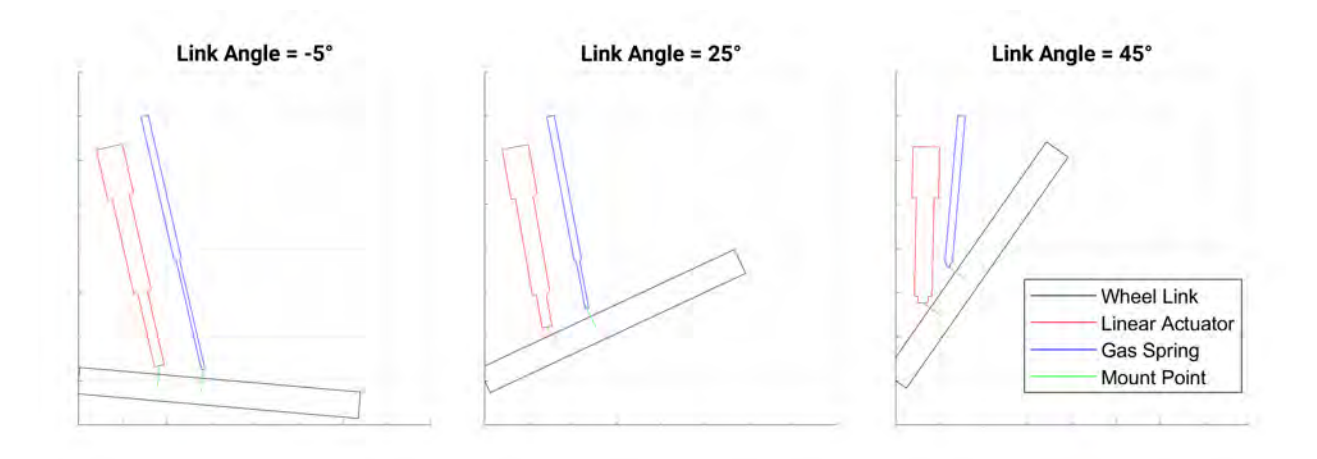


Fig. 16 Positioning optimization overview of the first suspension design iteration

A trade study was performed comparing requirements for rotational and linear actuators balancing cost, form factor, and structural implications for the vehicle. Rotational actuators required too much power in 1G at this scale, and linearly adjusting the wheel position up and down along linear rails was deemed structurally impractical for a vehicle this size. Linear actuators were available at high force ratings for a low cost but require an optimization to be completed between the intercorrelated

factors of placement, required force, and actuation range. However, affordable linear actuators meant sufficient force and actuation speed were mutually exclusive. As such, a 2000 lb linear actuator was selected with added offloading from pairs of 250 lb gas struts while balancing force requirements and individual component stroke and mounting positions, all while achieving the desired 60° of swingarm motion. The full trade study was explained in a previous publication [3], and because this design has been modified since, the explanation will not be repeated here again. In summary, the placement analysis resulted in a configuration shown in Figure 16, where the articulated suspension was able to adjust between -5° and +55° to level the chassis on 30° slopes. This design was assembled and underwent preliminary testing (figure 17, during which some issues were discovered, described in the following section (VI.D.2).



Fig. 17 Early testing with the first suspension design iteration

2. First Iteration Issues

This initial actuator placement was performed under the assumption that the chassis mount for the linear actuators was highly stable. Effectively meaning the upper mounting point was assumed to be unmoving, whereas in the fabricated system there needed to be an elastic element included to allow for the compression and rebound of the passive suspension requirements.

The series elastic element was physically sized to fit between the mounting points of the linear actuators. The design progression first minimized the distance between the pivot points of the swingarms, and since the suspension optimization was completed with respect to the swingarm

pivots, the actuator and strut mounting points were already set and as a result defined the volumes allotted to any series elastic element. A compact placement for a set of spring-dampers was found and a pivot was used to translate the force to them from the linear actuators. Based on initial estimates for the sprung mass, and volume available a pivot ratio of 2.625:5.75 was used here, which contributed to the seen issues.

The actuator placement and series-elastic elements were designed in parallel with each other concurrently before manufacturing and the assumption was not recognized or rectified in the short time jump between design and manufacturing efforts. Ultimately what resulted was a system capable of lifting itself and demonstrating the chassis leveling techniques, but once payloads were added above 200 lbs and/or the suspension was at high swingarm angles, the rover suspension began to lose its ability to rebound.

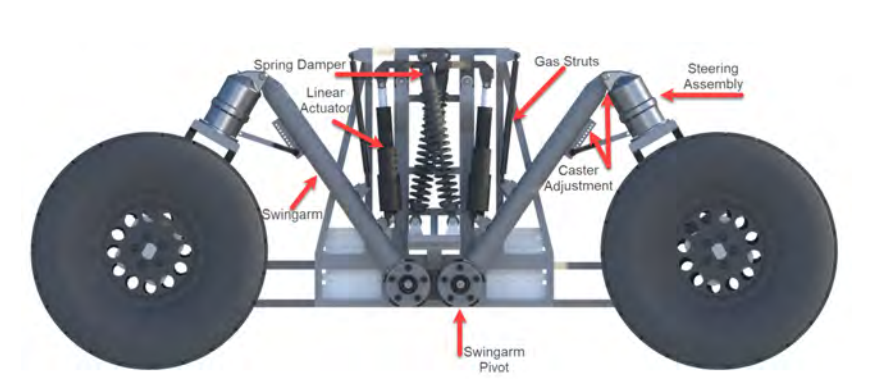




Fig. 18 VERTEX suspension 1 overview diagram

Fig. 19 VERTEX suspension 2

3. Final Design

Retrofitting a new suspension system needed to be low cost, and modifications needed to be as minimal as possible as the chassis was already nearly complete and beginning preparations for integration. The benefit at this point in time of the advanced progression of individual subsystems such as traction, steering, and electronics was that a new model could be created factoring more accurate to the built design. This model was verified by generating estimated points of rebound loss of the first generation suspension and comparing to the actual points. The iterative designer code attempted to minimize changes to the suspension system, only adjusting the placement and/or replacing a component of one of the two passive members. Each change that needed to be made consequently increased cost and delayed the project further. Additionally the code varied the amount of sprung, unsprung, and payload masses on the vehicle in an attempt to create robustness in the system due to modeling errors. The code attempted to guarantee stability across a series of discretized points in the swingarm range of motion while balancing linear actuator force limitations. The compactness of the two linear actuator connected series elastic systems gave very little room for component movement or replacement, and the code ultimately found replacing the gas struts with a set of dual-rate adjustable coilovers.

These coilovers, as seen in figure 19, are 32" in length with 14" of stroke and a pair of 14" springs stacked one atop the other with 150 and 200 lb/in rates. These dampers were originally created for long-length travel truck suspension, commonly found in the off-road and Baja racing

communities and use a standardized 2.5" spring diameter allowing the rates to be adjusted at a low cost in the future should alternate suspension response characteristics be desired. These coilovers feature adjustability in three main ways: damping, preload, and breakover. Nitrogen gas can be added to the internal cylinder to increase the damping coefficient. It is not yet fully understood how beneficial greater damping in this system will be and the initial hypothesis is that it will have minimal impact due to the relatively low deflection rates of the swingarms but future experimentation is expected. Increasing or decreasing preload is achieved via threaded rings that compress the dual spring stackup, increasing the starting amount of force the coilovers exert on the swingarms by the combined spring rate. The breakover point is the point where the interconnect piece between each of the springs contacts a 'breakover ring' and any further deflection of the springs causes deflection only in the lower spring, in this case 200 lb/in. The analysis code suggests this breakover point should occur very early in the deflection process and is currently set at the earliest possible position.

This adjustability has been very beneficial for the integration and operations of the rover. As the electronics integration proceeded, the total sum mass of all of the different components was significantly greater than initially estimated. Having the ability to increase the preload by an inch on each corner after this integration gave the rover a much more responsive articulation system, as did adjusting the preload differentially front and rear to compensate for the mounting location of ARMLiSS. Further research into suspension configurations is underway and may reveal a more optimal configuration that VERTEX may be perfect to test on.

E. Steering

1. Requirements

Due to its unique design for controlling chassis level through independent wheel positioning, VERTEX demanded an independent steering system - traditional steering racks across wheel pairs was not possible. Independent 360° steering was also required for precise and omnidirectional motions for umbilical tending an astronaut on foot. While the umbilical tending arm accounts for astronaut motions within a 5 m radius of the vehicle, further exploration on foot would require simultaneous arm-and-rover motions, and a holonomic drive system would be ideal for user transparency.

An over-wheel steering axis was favored over an off-axis system to minimize wheel-ground scrubbing friction, and so that the wheels could be actively steered while the drive system brakes were engaged for superior vehicle safety on slopes. While an over-wheel steering system minimizes on-axis steering torque, immense loads must nevertheless be reacted by the steering actuator due to the ≈ 1 m lever arm between it and the wheel contact patch - especially at large caster angles. As shown in Fig. 20, the combination of caster/camber angle with over-wheel steering on such large wheels requires extreme bearing strength to sustain full vehicle roll-overs. In nominal driving cases the caster/camber angle can still be in the 0° - 40° range, where the rover will still regularly enter 2 or 3 contact-point states that generate $\approx 10,000$ lb bearing loads. Simple oil-lubricated composite bushings surrounding the harmonic flexspline cup were selected over larger cylindrical or needle bearings to minimize the overall assembly size, which is over 5.5" in diameter and 8.5" tall. Additional length would have proportionally multiplied loads on both the steering and caster structure. The specifics of the caster adjustment structure are discussed in a later section (VI.G).

2. Design Overview

Each of the four VERTEX steering actuators has over 160 parts with 16 of them being custom machined and a total weight of 26 lbs. Steering system design was complicated by the high torque requirements, the need for both incremental and absolute encoding, and the massive potential loads due to its over-wheel position far from the wheel contact patch and the chassis structure.

An interior cross-section of the steering actuator can be seen in figure 21, where black, gray, and brown defines COTS parts and the various shades of blue, green, and red colors define custom parts. The most important COTS parts are the absolute encoder, incremental encoder, electric motor, and gearbox (labelled A-D respectively). The wiring for all the

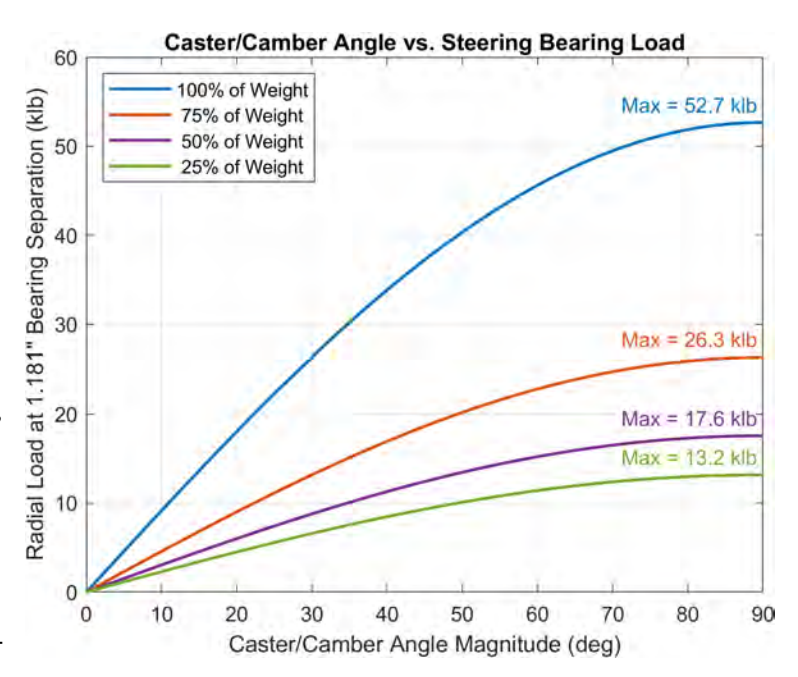


Fig. 20 Radial bearing load on the steering assembly in various loading cases. Full weight at 90° would indicate a complete rollover onto one wheel. The 50%-25% load cases at angles of $0^{\circ}-40^{\circ}$ show nominal loads in 2-4 point contact scenarios.

internal electronics exit the actuator housings through a conduit (E) in the top conical housing. These steering system wires run along the swingarms to the chassis, while the wheel drive motor wiring runs external to the steering actuator with sufficient slack to allow +/- 180° of rotation. The SSL used existing motor and gearbox spares from the Ranger Telerobotic Shuttle Experiment manipulator to cut down on costs and COVID supply chain delays. The BLDC motor (C) is a Kollmorgen RBE-02112-A with 2.4 Nm stall torque, and the connected gearbox is a Harmonic Drive LLC HDC-032-100, which results in 240 Nm of continuous steering torque.

The non-COTS parts in the figure 21 assembly are divided into color/label groups with respect to their unified rotation. The green group (F-H) are interconnected and rotate with the gear output and rotate the wheels when they are steered. The blue group (K-N) are the structural housings which serve as non-rotating mounting points for the motor stator, gear circular spline, and encoder sensors. The red group (I-J) are hollow parts which turn at the motor rotor speed and serve as the input to the gear assembly (D). The three parts denoted by J form an Oldham coupling, which accounts for potential driveshaft (I) misalignment as it transfers torque into the gear. Part F is a small diameter shaft that passes through the hollow driveshaft and Oldham coupling (I-J) so that the absolute encoder (A) may read the steering output rotation angle.

Parts G and H are mild steel parts which transfer all the loads described in the previous section from the wheel assembly to housings M and N through radial POM composite bushings and a pair of Oilite thrust bushings. Housings M and N are also steel for this reason. A series of ring seals between the housings (L-N) and actuator output (G-H) as well as sealing bolts in part H allow oil to

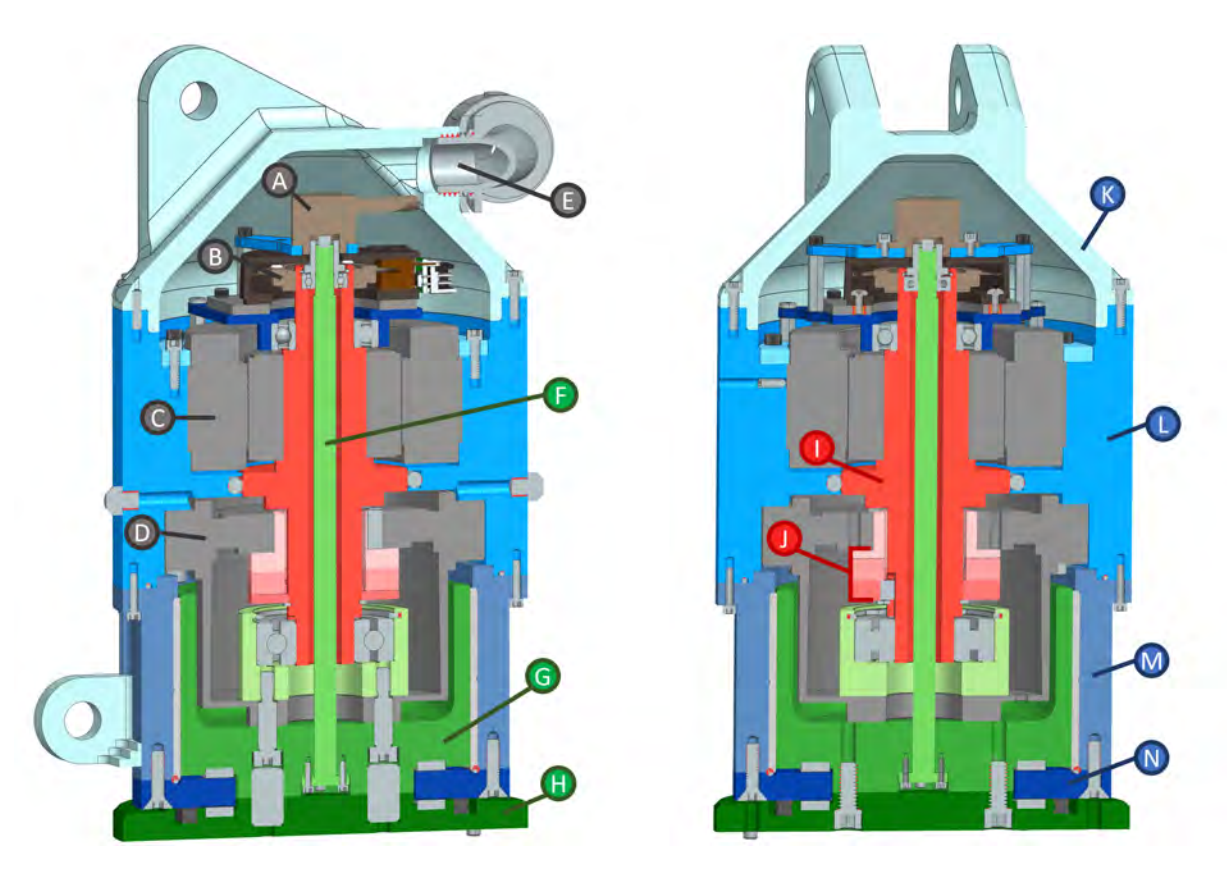


Fig. 21 Steering actuator cross-section views at 90° rotation. Black/gray/brown parts are COTS while other colors denote custom parts. Like color shades indicate parts that are fastened and rotate together: green parts rotate with the gearbox output and steer the wheels (F-H), red parts rotate with the motor rotor and the gearbox input (I-J), blue parts are proximal and stationary with respect to the caster and swingarm structure (K-N).

be contained in the lower half of the actuator to lubricate the bushings, bearings, and gearbox.

F. Structure

1. Chassis

The original design of the chassis was covered mostly in the first BioBot-related publication [7] and the large structural layout has remained generally the same. The chassis is a cross between a spaceframe and compartmentalized chassis, made from 1" square tubing and MIG welded. The chassis dimensions were created by a balance of component size requirements like with the batteries, and estimated volumes required for astronauts and ARMLiSS, which had not been designed yet. The final configuration for the chassis can be seen in Figure 24 with coloring scheme:

- Teal area for main driver
- Purple payload
- Yellow batteries
- Red wiring and auxiliary batteries

The chassis was also subsectioned into three main assembly parts that were then assembled



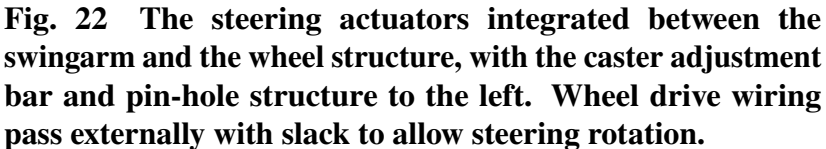




Fig. 23 Steering electronics are routed through the conical cap and back towards the swingarm and chassis.

together for ease of manufacturing and maintenance of tolerances. Shown in Figure 27 the chassis walls with the various suspension mounts were completed before welding to the main chassis structure as shown in the initial mockups in Figure 26. These chassis walls were intentionally not connected at the top resulting in an overall "U" shape to the chassis giving lots of unrestricted room for crew and payloads between such walls. To accomplish this without plastic deformation thicker tubes were used as the main structural members in these walls, and additional diagonal structure was added tying the lower part of the wall into the central longitudinal runners of the chassis.

The chassis also features a mild steel underbody welded to the bottom most structure. The main purpose of these panels is to prevent large debris intrusion and provide some form of a floor for items to be mounted to.

Once the chassis had been structurally designed and manufacturing had begun, it slowly was becoming more clear that permanently affixing structures like payloads and seats was going to, at some point, become a hinderance to either testing or future testing endeavors. Items like a removable roll cage, seat, and electronics had not been fully designed yet and as a result a series of 1/4-20 weld studs were added in strategic locations around the rover. 1/4-20 was used first as it is the most common thread choice in photography and videography and allows for cameras and lights to be mounted with little to no modification, and was strong enough to mount seat rails and ultimately ARMLiSS for much easier installation and removal during various rebuilds and integration efforts. Various 1/4-20 weldnuts were also included in locations for mounting electronics boxes and a retention mechanism for the LiFePO4 batteries.



Chassis isometric with labeling



Chassis underbody Fig. 25



with chassis



Chassis wall preliminary assembly Fig. 27 Finished chassis walls with suspension 1 configuration

2. Swingarms

The swingarm tubes themselves were relatively simple to design once expected loads were determined. Bending calculations and FEA completed, tube was ordered with a significantly thicker wall than the initial static analysis to deal with dynamic and any other non-considered forces. This was beneficial because the thicker tube provided good margin once the second suspension system was designed and had much larger forces exerted upon it.

Mounting the swingarm tubes to the chassis was an opportunity to employ a cheaper commercial option over custom bearing fitted housings. An original design effort was completed for a multi-part assembly requiring bearing fits, but a lateral option was found once a first draft of the system was completed. 3,500 lb rated trailer hub bearings and axles were a low-cost, widely available solution that simplified the design process greatly. These purchasable assemblies featured a pair of tapered roller bearings, grease fittings, and simple bolted attachment fixtures for both ends of the mechanism. A two piece adapter was milled and welded from mild steel between the 5-spoke trailer hub and the swingarm, with an absolute encoder mounted to track the rotational position of this axis. In-field



Fig. 28 Weld studs added atop the suspension



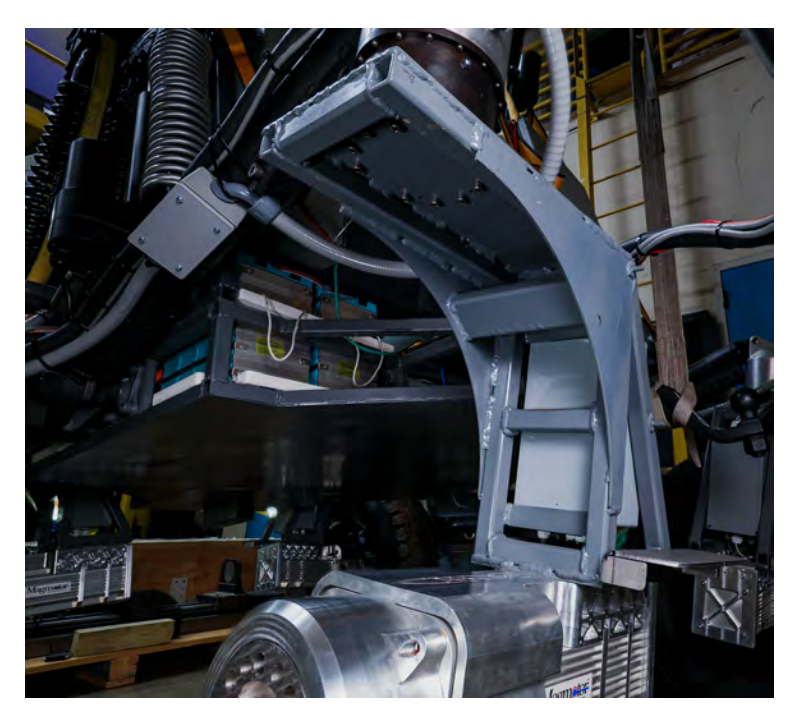
Fig. 29 Swingarm attachment point

Fig. 30 Swingarm attachment encoder cap

replacements of the trailer hub components will be easy to find anywhere within the US and reduces custom documentation required internally.

3. Over-Wheel Steering

Requirements definition for designing the connection between the output of the steering mechanism and the traction motor was not trivial. Steering loads, especially at high caster angles, are not yet modeled well in the state-of-the-art. A series of static load cases were used, specifically focused on situations where the rover is momentarily on less than four wheels of contact to ensure the over-wheel steering bracket is not a source of failure during nominal operations. Shear pins and bolts were used to affix this structure to the steering actuator, and a series of six shoulder bolts were used in the connection to the traction actuators. What resulted was a combination tube structure with four lasercut steel panels providing strength and mounting for both sides of this piece. Additional 1/4-20 mounts were added to mount lights, steps, and any other accessories desired.



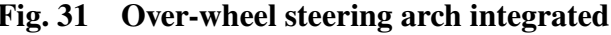




Fig. 32 Over-wheel steering arch with headlight, integrated

G. Wheel-Angle Adjustment

With such a large range of articulation present in the suspension system, 58.5° in the final configuration, depending at what the nominal chassis height is desired to be different angles between the swingarm and the steering axis are required. Joint effort required for steering is minimized when the caster and camber angles are as close to 0° as possible. Figure 33 illustrates adjustability in caster in the top row, and camber in the bottom row (with the steering actuators turned 90°).

A few mechanisms were considered to address the desire to vary this angle. Ultimately a rigidly bolted bar between the swingarm and the steering was implemented as the strongest and simplest mechanism. A linear rail combined with a linear actuator was investigated in an attempt to actively actuate this angle, but was set aside due to a large added cost. A four bar linkage was also considered but the number of added joints, added weight, and complexity in manufacturing became too large of a detractor.

During testing, it became most convenient to set the caster adjustment system to be as close to 0° as possible with the chassis set at a desired nominal height above the ground. Once this is set, as the rover attempts to level the chassis on a hill the resulting required motion of the swingarms naturally kept the caster angles close to 0° as long as the average height of the chassis above the ground was maintained.

The caster and camber of the vehicle became an area of concern as testing continued. Steadily, as the vehicle was tested more and more, it was noticed that the wheels were tending to gain undesired camber in and out depending on deltas between commanded and actual steering angles. Any amount that a wheel was pointing either left or right when attempting to go straight caused the wheels to want to splay in or out in that direction.

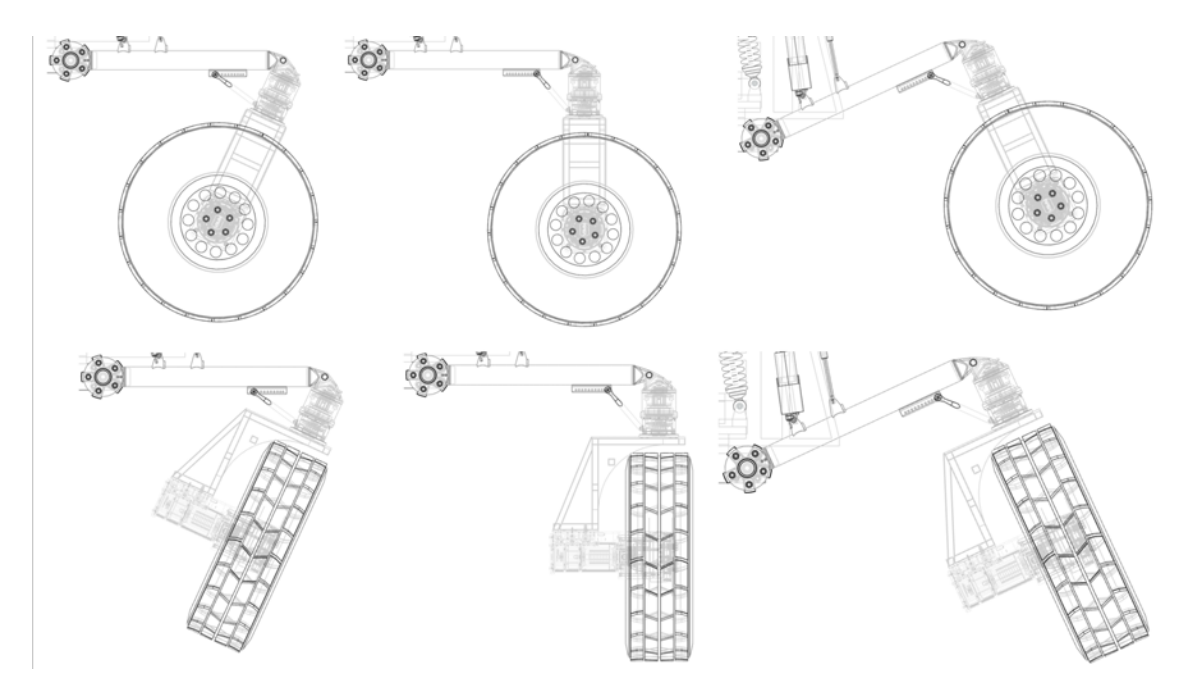


Fig. 33 Caster and camber adjustability diagram

When the wheels lose traction, even momentarily such as driving over ice, the wheels wanted to self correct back to straight up and down. The ultimate source of this was tracked down to angular backlash in the out-of-plane axis of the triangle formed by the steering attachment point and the two connection points on the caster angle adjustment system. The root cause of this angular backlash is ultimately a series of fits that were slightly too loose in a few places. First the shoulder bolts that attach the bar between the steering housing and the swingarm tube were slightly too large in diameter and were simply acting as pins. A revised design uses a pair of



Fig. 35 Camber differential shown on front two wheels during a test

short-thread shoulder bolts into very close fitting counterbores on either end. This allows the bar to be pulled tightly against one side of the assembly and placed in tension by the force applied by the second bolt. This significantly reduced felt backlash in the assembly, but did not entirely eliminate the problem. Further investigation into the problem showed the bushing pair that connects the top of the steering actuator to the swingarm had cracked and the hole they were fit into had become ovular. A new steel sleeve is being designed alongside a weldable clevis system to be affixed and significantly increase the surface area that the shoulder bolt has available to counteract these camber forces. In theory, slight amounts of negative camber (bottoms of wheels further outside the tops of the wheels), positive caster (steering axis slightly behind the normal), and toe in (wheels pointed slightly inwards along the normal axis) would be expected to increase stability, but at the speeds VERTEX is expected to endure these effects will be negligible. However, it is recognized that this



Fig. 34 Caster adjustment mechanism side profile

vehicle will never be able to achieve perfectly 0° on each of these angles, as would be the goal for minimum steering effort, and intentionally being conscious of this and operating with slight amounts of angle in each of these three directions may improve handling.

VII. Power Electronics

A. Safety/Emergency Stops

The VERTEX high-voltage power management system was designed to handle a variety of fault/stop conditions, as well as providing graceful startup and shutdown sequences. Figure 36 provides a top level overview of how battery power is managed by the 3 safety systems: hardwired protection, Battery Management System (BMS) protection, and user e-stop protection. Each of these systems handles a specific type of fault, with systems earlier in the chain having progressively more authority to shut off of power to various parts of the vehicle.

The hardwired protection system is composed of two elements: a 500 Amp, High Rupture Capacity (HRC) fuse, and a manually operated master power switch. The fuse is designed to protect the entire system against shorts between the high voltage supply line, and the vehicle ground bus. Due to the high current capacity and voltage available to the system, a specialized fuse is required. The aforementioned HRC fuse is chosen specifically to ensure that it can reliably interrupt the circuit in a short condition, and contain the resulting arc and energy dump when opening. Following the fuse, a manually operated battery disconnect switch is installed. This is a user-actuated 1/4 turn switch, designed to allow the user to connect/disconnect the battery from all components of the vehicle. The switch features a lock lug, allowing it to be padlocked in the open position, disabling all power to the vehicle. This features is used when maintenance is performed on the vehicle, and it must be ensured that nobody energizes the high voltage bus while the maintenance is ongoing.

The next cutoff system is the Battery Management System (BMS) disconnect relays. Two relays are installed in series, and are independently controlled by the BMS controller. The controller continuously monitors the state of every battery cell, including voltage, temperature, and overall

current, and can open the relays if a fault or abnormal condition is detected. One relay is typically used to disconnect the battery if any one cell drops below the minimum voltage, while the other relay will disconnect the pack if any cell rises above the maximum voltage. Other faults, such as over/under temperature and overcurrent may trigger both relays. The placement of the relays is important: overvoltage relay is earlier in the chain than the undervoltage relay, and the battery charger is connected between the two. This configuration allows for easy recovery if the battery undervoltage alarm is tripped. While in that condition, the relay arrangement will cut power to the vehicle, but leave the charger connected to the battery. This will allows the charger to recharge the pack, without having to manually close nay relays. However, the pack is still protected by the overvoltage relay, so that when the pack finishes charging, the BMS can stop charging by opening the overvoltage relay. In the event that the BMS looses power, the relays will open ,as they all are 'normally open' relays, ensuring failsafe operation.

The last protection system us the user emergency stop system. This system is designed to only cut power to the actuators of the vehicle, while leaving the control system power connected.

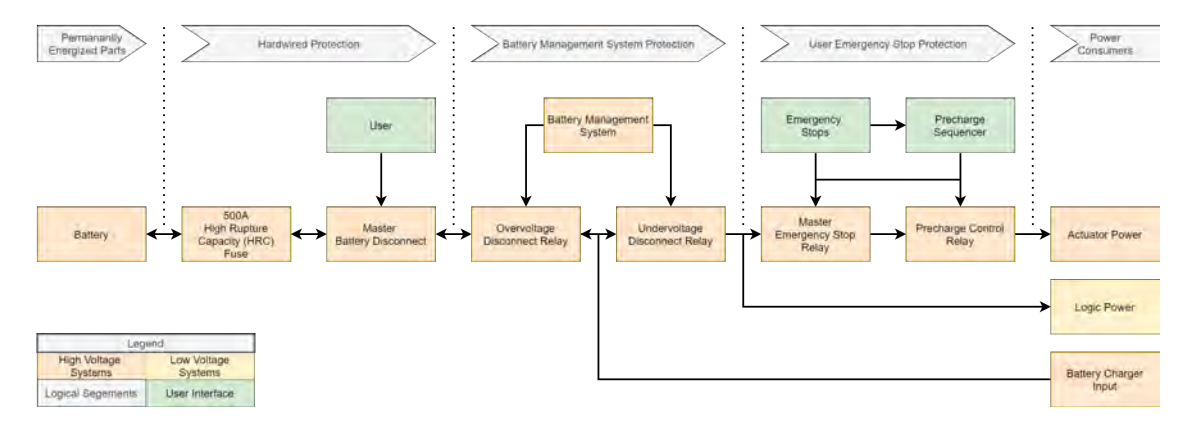


Fig. 36 VERTEX high voltage disconnect system

B. Battery

Due to their high power requirements, battery selection was largely based on the demands of the wheel drive motors. The design requirement was for a maximum delivery of 200 amps at 100 VDC, leading to the use of 32 LiFePO4 cells arranged in series, each with a 300A maximum. It should be noted that while the pack is capable of discharging at 100KW for short times, it is limited to 500 amp surges by the battery management and protections systems. The choice of LiFe batteries was made to minimize concerns with battery events during charging, discharging, and storage. The total energy storage capability of 10kWh should allow at least 0.5 hours of maximum power of operation starting from a fully charged state, although typical usage results in runtimes between 4 and 6 hours. The pack is protected from overvoltage, undervoltage, overcurrent, and overtemperature events by a manufacturer-provided battery management system, which also provides the charger interface.

VIII. Software

A. General VERTEX System

1. High Level Overview

Our software stack is built entirely upon the ROS noetic and the lab's custom software. From ROS, VERTEX utilizes: the ROS middle ware bus to manage messages; ROS nodes, services, publishers and subscribers; and utility libraries such as the Joy package which manages the user input. From the custom general lab software, VERTEX utilizes: the lab's custom server to manage all of the nodes and all the safety features for VERTEX; and the lab's custom ROS control wrapper that is used to ensure VERTEX's safety protocols are utilized and prioritized. The software stack itself is comprised of 3 layers: user controller interface, intermediate controllers, low level controllers and hardware interfaces.

2. User Controller Interface

Starting of at the very top of the software stack, there is the user controller interface. Currently this interface is latched to the a joystick node that spits out data from a farm simulator controller to command and drive the suspension system and the steering. There are some human factor issues with this controller since the buttons are a bit sticky and some of the buttons are too close together which makes the system some what challenging to control.

3. Intermediate Controllers

The next layer of the general software are the intermediate controllers. These controllers are separated in 4 groups: debugging, suspension, steering and arm. For safety purposes, these controllers can only be switched between once the rover is halted and has motion disabled. Once those 2 conditions are met, the driver can click through the controllers until they want to activate the one they want to use. Note these 2 conditions effectively require for the rover to not be in motion to change its controller modes.

The debugging group consist of just one controller that basically only drives one joint at a time. It is a reliable controller that lets us move joints on the robots to ensure that the hardware works without having to run the coordinated controllers which can put the hardware at risk. Also lets the operate gain signal joint control in situations where it is required.

The suspension group consists of 5 controllers that sit on a virtual dial. The default suspension controller is the proportional controller which makes sure that the chassis is balanced via input from an inertial measurement unit(IMU), but still lets the operator temporarily adjust the roll and pitch. The next controller on the dial is the zero auto controller which uses the IMU to keep the chassis's roll and pitch at 0 degrees always. This controller will let the driver lift and lower the chassis but will try and keep the roll and pitch at 0 degrees. The next controller is the on the dial is the vertex suspension controller which lets the driver manually adjust the chassis height, roll and pitch. Then there is the locked suspension controller that will try its best to hold the current height, roll and pitch of the chassis. Finally there is the kneel suspension controller that lowers the chassis to aid astronauts who are getting on the rover.

The steering group consists of 5 controllers that sit on a virtual dial as well. The default steering

controller is the forward ackermann controller which basically fixes the back wheels and lets the driver control the front ones. The next controller on the dial is the reverse ackermann controller which basically does the opposite of the forward one. The next controller is the double ackermann controller which moves both the forward and rear wheels. Then there is the in place steering controller which moves the wheels inwards to make the rover rotate in place. Finally, there is the crab steering controller with moves all the wheels to the same angle to let the rover move sideways.

The final controller group is the arm controller group. At the moment this group only consists of the inverse kinematics controller. This controller moves the arm forwards and backwards to keep the tip over the astronauts head through the use of inverse kinematics. This controller for the most part is utilized when the rover into its astronaut tracking mode.

4. Low Level Controller

The final piece of the general software is the low level controllers and hardware interfaces. This section of the software is focused on making sure that the joints are moved to the location that the intermediate controllers expect them to be. There are 3 low level controllers in this system. The first one is the general suspension controller which manages the suspension system for the rover. This controller tries its best to make sure that the hardware is exactly where the intermediate controller expects it to be. Much like the general suspension controller, there is also a general arm controller and a general steering controller that manage their respective subsystems.

For the hardware interface itself, VERTEX utilizes the Galil programming interface to communicate instructions to the Galil cards. Since VERTEX has multiple cards, its interface needs to be extremely generalized and organized to ensure that the right commands are being sent to the right cards. Unlike other interfaces, thanks to the simplicity of Galil's programming interface, sending the actual commands down to the cards is extremely simple and intuitive. Instead of sending a complex byte array or integer embedded with different bit encoding, the Galil programming interface expects strings which consist of a command, an axis to control and a value or list of values.

B. Astronaut Following Subsystem

1. General System Overview

The Biobot subsystem that is in charge of managing the Astronaut trailing ability of VERTEX consists of several components. The system was architected as a plugin in for the main VERTEX source code. To trigger the autonomous features, the driver simply has to press one button on the controller which lets the User Controller Interface yield partial control to the Autonomy interface in the Biobot subsystem plugin. As such, rather than listening for motion input from the controller, it changes its subscribers to listen to the autonomy nodes to get motion instructions. Do note that the User Controller Interface does not yield control of all the safety features on the vehicle, such as halt and enable motion.

The system itself works by breaking the arm's range into 3 concentric rings. The rough radii for these rings are 1.5 meters, 3 meters and 4.5 meters. Since the hardware has a bit of backlash, for the sake of safety the software currently limits the full service area a bit, requiring the rover to move more than it would on a lunar version. If the astronaut is in the inner most ring sets the rover to in-place mode and limits the motion of the arm. This way the rover can change its heading to track the astronaut while not putting the astronaut in significant danger in the case of a runaway.

If the astronaut is in the middle ring, the rover keeps its steering as in-place and solely uses the inverse kinematics controller for the arm to keep the tip over the head of the astronaut. Finally, if the astronaut is in the final ring, the rover will change its steering from in-place to double Ackermann and move to try and get the astronaut back into the middle circle. The arm will also retract while the rover moves closer via the inverse kinematics controller. By only letting the rover catch up to the astronaut once they are in the out most ring, the potential harm to the astronaut that may occur due to a mishap on the rover is significantly mitigated.

To ensure that the astronaut can be tracked within these rings, the system utilizes two independent camera systems to create an idea of where the astronaut is relative to the rover itself. Through communicating to both systems, the rover is able to gather the x,y and z positions of the astronaut. The camera on the onboard camera turret is in charge of tracking the astronauts x and y positions to adjust the height of the arm and the steering, while the camera at the tip is solely in charge of the z position which is found by maintaining the tip near the astronaut and using forward kinematics to solve for the z distance.

2. Onboard Camera Turret

The camera turret subsystem is build almost entirely on its own stack and sits on the VERTEX stack as a stand alone peripheral which is driven via serial commands to an Arduino that manages a 2 degree of freedom turret with a camera. The hardware itself is for the most part quite trivial and exists only to move the camera to face the center of the astronaut at all times.

The way the turret knows where to look is through the use of computer vision. Earlier iterations of the model utilized April tags. The issue with this iteration of the camera turret implementation is that the model does not work well when the tags are in a non-lab environment. As a result, new iterations of the camera turret's computer vision model are being trained to identify the suit itself, rather than the tags. By doing so, VERTEX will have a far better and robust understanding of where the astronaut is in reference to where the turret is looking.

Once the turret has identified the astronaut, it will do its best to move such that the center of the image is at the center of the astronaut. Additionally it will pipe the commands that is uses to correct the turret to the rover so that the rover can reposition as well. Note that the rover will only reposition if the astronaut is near the very end of the frame when the camera turret can no longer continue to track the astronaut. Once detected, the rover will rotate so that the astronaut is easier to track for the system.

For the most part, all the computer vision aspects of the turret are offloaded to the Nvidia Jetson that is onboard connected to the main VERTEX network. Data is piped through ROS nodes over the network between the Jetson and the Latte Panda(the computer in charge of running the core software).

3. Tip Camera with Gimbal

In support of the astronaut tracking capabilities of the VERTEX lunar-rover, a two-axis gimbal was designed to utilize a closed-loop, PID controlled feedback system to ensure continuous ground-pointed camera orientation, remaining stable amidst rapidly changing and unpredictable BioBot movement. Fundamentally, the concept utilizes two 12V, brushed DC motors with quadrature encoders for both axes of rotation, a 12A dual-channel motor driver, a 9 DOF IMU with internal sensor-fusion capabilities, a standard Logitech HD camera, and a programmable Arduino micro



Fig. 37 Tip Gimbal Render - Front

Fig. 38 Tip Gimbal Render - Rear

controller board. An estimated torque requirement of 0.75 N-m for both DC motors was calculated using static loading conditions, and a safety factor of 1.5.

A comprehensive electrical diagram was created for all components using KiCad, ensuring that necessary digital interrupt pins were available for use within the encoders. All electrical components within this system are under the control of the programmable Arduino board. An initial model of the mechanical design was created using Siemens NX. To allow the gimbal to have as few moving parts as possible, the model was created with the goal of simplicity. The mechanical design incorporates two main components, coinciding with two DOFs. The first component connects with the end of the BioBot arm and houses the first DC motor. This component also includes an electronics bay housing the motor driver, Arduino, and IMU. The second component, whose orientation is controlled by this first motor, houses the second motor which is attached to a camera mounting bracket, for a flush connection with the camera. Under this system the camera can rotate about the actuator's orthogonal axes.

A test circuit, containing all electrical components, is currently being utilized for preliminary electrical and software testing. Once finalized, the circuitry will be ready for integration into the mechanical assembly, which will be 3D printed. The Arduino micro controller will be programmed in Arduino C.

IX. Human Interfaces

A. Astronaut Seat

Two different astronaut seats are available to be installed on the vehicle depending on the desired tasks to be performed: the shirt-sleeved seat and the EVA seat. The shirt-sleeved seat is a more traditional padded seat with a suspension system similar to that seen in busses and construction equipment. This seat was used during early testing of control panels and seating positions. The

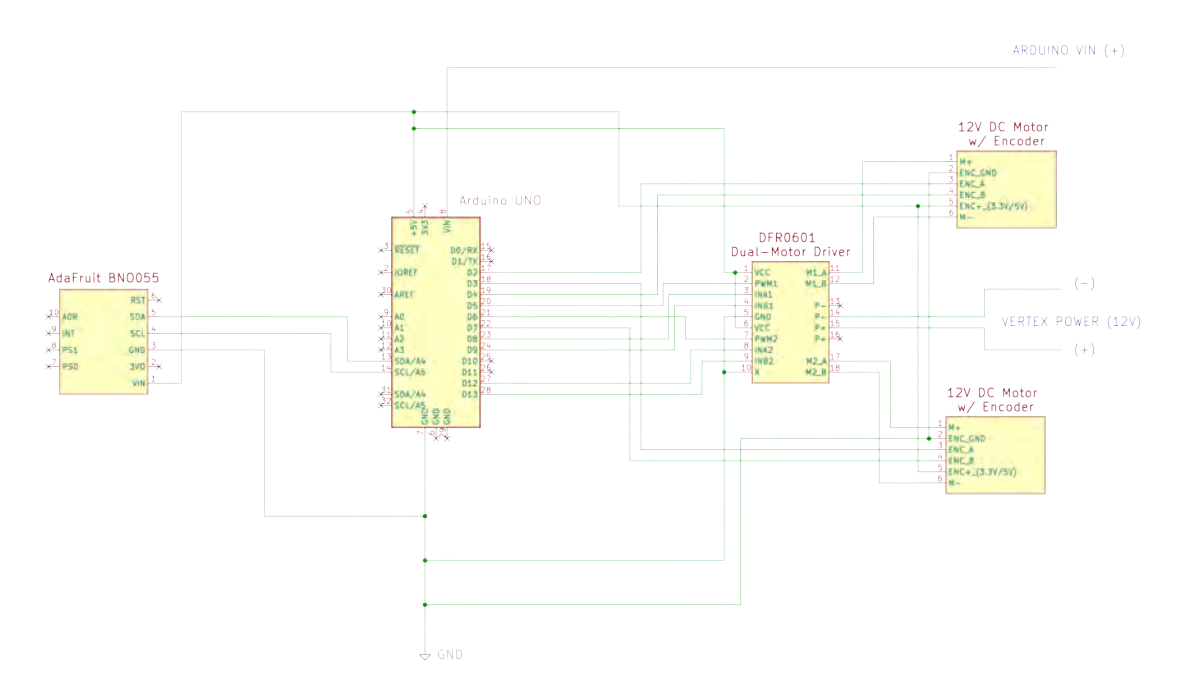


Fig. 39 Tip Gimbal Circuit Diagram

EVA seat was designed to accommodate the MX-series of spacesuit simulators the SSL has been designing across the multiple PLSS sizes. This seat uses a 4-point harness for restraint of the astronaut. It is recognized that this type of restraint is not very conducive to the physical restrictions present in pressurized spacesuit gloves, and larger handle features could be added to increase the ability to affix oneself, but the goal during testing efforts was to simply restrain the test subject safely with the ability to quickly disembark if needed. This restraint provides that though a very large, spring loaded lever that the suited person can twist and disconnect the restraint straps from the central hub.

The seats are mounted on commercial seat rails that allow the whole assembly to be translated forward and aft, giving both customization to the seating position and allowing access to both electronics boxed tucked underneath the seat path. This is another example of prioritizing customizability and future compatibility in lieu of the structural strength and simplicity gained in directly welding structures together.

B. Control Panel

The original development process of the control panel has been documented in an attached publication [8]. From initial concepts to early mockups, interative simulators, and eye-tracking trials the control panel evolution may have been the longest continuous effort of the entire project. The final result, as shown in figure 42, features a battery management screen, 'carputer' (car-computer) monitor screen, three indicator lights, one button, an e-stop, turn switch, and rocker button, and room for further expansion. The housings were 3D printed for verification of placement, size, mounting, and cable accommodation features and once finalized these will likely evolve into weather-resistant boxes. The 3D printing of various front panel configurations has been exceptionally convenient to rapid-prototype with. A commercial joystick with button board was procured for ease of integration





Fig. 40 IVA seat on rover

Fig. 41 EVA seat on rover

with the software stack written for the rover and will slowly be phased out in favor of larger control joysticks and custom button configurations.



Fig. 42 Control panel as used in full testing

X. MX-Series Suit Simulators

A. MX-C+

The newest design of the MX-Series suit simulator. This design enables the suit to be modular for different tests and different sized test subjects to wear it. With a bearing at the shoulder of the suit, the arm can be removed in the field and replaced with other designs. The bearing design also grants a larger range of motion for the person wearing the suit compared to the normal seam at the shoulder of the suit, as the bearing rotates with the wearer's natural arm movement. The new design

also enables length changes while being worn. An upper and lower section of the arm are sewn with loops that chord runs through them. Both sections can be altered independently of one another, by simply pulling the chord and using the elastic lock to keep position. This ability to change lengths of the arm can be done by the person wearing the suit simulator. Although the method used will be upgraded in the future to reduce the use of string that may dangle during field testing, it works well in its current state for modular field testing.

This design also allows the test astronaut to don the suit by themselves. A single zipper has replaced the previous pair of zippers in the midsection of the suit simulator, connecting the top to the overalls-style pants. This single zipper makes it easier for the test astronaut to hold the zipper pull instead of attempting to find the second zipper behind their back. This process previously needed a second person to help zip up the suit.

B. Interaction With System

The MX-C+ suit also piloted a front mounted umbilical to interface with the arm. The Umbilical sits above the head of the astronaut during most testing, an angle for front mount at an angle allows for it to not obstruct vision during operation. The umbilical is kept on the left side of the astronaut ideally, but can be moved to accommodate different preferences during testing.

This front mount is a rigid connection to the flexible umbilical, and is attached in the upper center of the chest, covering the seam between the upper and lower pieces of the suit simulator. The plate is large enough that it covers the seam regardless of who wears the suit simulator. The plate itself did not hinder mobility or functionality, and stays attached to the chest using a hook and loop closure.

XI. Testing

A. Subsystem Checkouts

Each of the individual actuator subsystems were checked out independently and before slowly integrating with eachother. At the time of writing, the suspension and steering systems are controlled digitally, and the traction motors are controlled via an analogue joystick. Circuit boards for digital control of the traction drivers are underway, but analogue control was sufficient for all testing to date and simplified the demand from the software and control electronics.

Suspension testing has been the longest running set of tests to date. The earliest tests of the suspension system included a set of switches and a 12V battery mostly used to verify the mechanism kinematics and ranges of motion, but eventually progressed to closed loop control of the swingarm angles via the Galil system. This closed loop control was only achieved after absolute encoders had been mounted to the axis of rotation and became an important for the software autonomy later that was sending position and not velocity commands. As the vehicle became heavier and heavier with the progressive integration of electronics and ARMLiSS, the suspension response characteristics were trending more sluggishly with more weight. Each significant increase in mass required a corresponding increase of preload in all four corners, and at the moment the preload setting on the springs is at its maximum, indicating the electronics weighed more than expected and stiffer springs may want to be swapped in for future testing.

Steering actuators, once assembled, were checked out for nominal performance and encoder

verification on the lab bench. After all alignments were verified to be acceptable, the steering motors were mounted to the rover and validation testing could begin. As this occurred before the batteries and drive electronics were integrated, a test setup was created using lab power supplies and the to-be-integrated drivers. Steering was tested progressively, first with no load, then progressively more load at zero caster until the full vehicle weight was on its wheels, and then the vehicle was lowered and caster slowly increased to the maximum available at the caster setting. On the laboratory floor, which has a much lower coefficient of friction when compared to asphalt, the steering actuators were easily able to turn the wheel even at high caster angles. Figure 43 was taken on the first testing day. Some of the wheels that day were turned by hand to avoid moving the electrical hookups and power supplies to each corner, but the ability to turn the wheels at high caster angles, even manually, was an accomplishment for the team.

Testing the robot software with the vehicle suspended from the crane was agreed to be the safest approach until confidence was built. The steering actuators required, logically, significantly lower proportional gains to be used to prevent instability. With the vehicle weight on the wheels, at the higher gain setting, the vehicle was regularly able to return from a step response to within one or two encoder values. Every wheeled vehicle needs some form of an alignment to drive straight and reduce off-axis steering forces to acceptable levels. Alignments in the steering actua-



Fig. 43 First full steering attempt

tors are set in the software by an absolute encoder position, and at 12-bit precision each increment corresponds to $\approx 0.08^{\circ}$. Even with the vehicle traveling short distances slowly, at one or two encoder counts off from goal position resulted in significant amounts of camber to be added, thus re-stating the importance of strengthening the connection between the swingarms and the steering actuators. On asphalt, the steering actuators predictably required higher efforts to steer, and were quicker to respond and converge to the desired angles when the vehicle was slowly moving.

The traction system was a particularly interesting system to test. Integration of the traction drivers is set to progress starting with an analog control scheme and then transition to digital control. The analog controls were seen as a reasonable first step to get the vehicle moving as the commercial motor drivers have out-of-the-box support for potentiometer signals and a suite of in-built control customization features. These features, helpful as they may be in more traditional vehicles, plagued the vehicle with odd drive characteristics such as individual drivers suddendly stopping, locking the motors, and spinning up to high speeds for brief moments before returning to a zero position. After a few days of experimentation during the full system checkouts, as the available documentation did not cover a large number of the available featureset, these drivers were tuned and found to be reliable enough for the first field trials.

B. Full System Checkouts

Once all systems had been individual verified to be functional and validated to perform in nominal, slow, flat ground conditions in the laboratory, the vehicle was rolled out the high-bay door to a small road with a hill. This hill was used to validate and stress test the systems, as well as to checkout and approve incremental changes in autonomous systems such as the auto-leveling of the chassis. Figure 44 shows the first time the rover went to climb the hill, and Figure 45 shows the first time the hill was climbed with ARMLiSS attached as the payload.





Fig. 44 21° hill

First full integration tests climbing a Fig. 45 Complete VERTEX with ARMLiSS climbing the 21° hill

The vehicle performed very well when climbing the hill, even in snowy conditions. Overall vehicle currents were seen in the 50-70 A range at the crux of the climb, well under the batteries' rated 300 A capacity. Operationally, driving on a hill was difficult for the operator due to the analog control of the motor drivers. The operator in effect had to hold the joystick slightly forward to maintain position on the hill, and when rolling back down the hill had to hold the joystick slightly less forward and control the rate of descent with forward commanded speed. This will be remedied with the digital control of the traction motor drivers very soon, and did not impact overall testing, just an operational note.

Steering tests required extra room to test beyond the first hill, so the rover was driven back and forth on the road just outside the robotics assembly laboratory, and occasionally mounted the curbs on that road to access small patches of grass. During this testing, each steering mode was validated to turn the selected steering motors to the correct position based on current steering mode, and verified the vehicle was able to move as expected. All steering modes except turn-in-place were able to be validated except for turn-in-place which requires the wheels to move differentially. This is another improvement that digital control of the traction motors will bring to the rover.

VERTEX's capabilities were tested both with and without ARMLiSS onboard, beginning with just VERTEX and an operator. Once ARMLiSS was loaded onto the vehicle, and the suspension was set to automatically level itself, an interesting control harmonic was found. ARMLiSS weighs \approx 10% of VERTEX, and while its center of gravity isn't able to drastically change the rover's CG, it is enough to cause slight compression in the suspension on whichever side it was leaning towards. The automatic leveling features of the suspension then naturally want to fight this compression,

resulting in a commanded raise of that side, forcing the arm to then lean the other way and the cycle continues. Partially, this is the fault of ARMLiSS' yaw joint and its ability to be pinned. The ability to lock the arm to face a specific direction has been beneficial during transport, and has helped prevent the arm from swinging accidentally in the laboratory during suspension testing. This locking feature is achieved through a quick-release pin and a series of holes, and unfortunately these holes were specified to be too large and while the pin is easy to insert, $\approx 15^{\circ}$ of backlash exists at the joint. Backlash in ARMLiSS is a general problem that affects software efforts and ways to address and other ways around these issues are being attempted, but has not prevented or delayed testing. Increasing the spring rates and preload in the suspension may remove some of the resonance seen between the arm and the leveling software.

C. Field Test 1 - UMD Campus

Full system field testing of BioBot aimed to provide an evaluation for the concept in various conditions that an astronaut may experience. Images from the first field test are dictated below in this section, and future testing that combines more hands-on operation of the rover by the test subject with greater rover autonomy are planned. As this was the first test of the entire roving system and the autonomous stowage and unstowage of ARMLiSS as an astronaut boards/disembarks the rover has not been fully completed yet, the tests progressed in stages. Transporting the vehicle between different testing areas and then disembarking while deploying the arm manually, having the astronaut walk and explore around the rover area, and then moving to a different testing scenario was the test mode for the day. Two test subjects wore the suit simulator and tested the system concept.

Testing began with BioBot in nominal driving position, at the chosen caster setting this was with a chassis height above the ground of ≈ 20 in, and ARMLiSS fully retracted. VERTEX drove from the robotics assembly lab to the selected testing site in this state, transitioning from asphalt to grass. The testing site chosen was a relatively narrow strip of grass (≈ 20 ft. wide)



Fig. 46 Test subject aboard BioBot

that started flat and then became wider and hilly towards the far-end with slopes approaching 30° and 40° .

The first disembarkation aimed as a simplified first attempt at validating the concept. The rover was on flat ground, with the arm at a medium extension length. The test subject found the arm overall easy to rotate around the base and unobtrusive when picking up rocks or interfacing with





Fig. 47 Test subject disembarked and ARM- Fig. 48 Test subject with deployed umbilical LiSS beginning to unfold

arm

the rover displays while standing. One mechanical issue became apparent during this early testing. To reinforce the thin plate that ARMLiSS is mounted on and reduce deflections, steel tubes were welded to the plate. One of these tubes was welded slightly too closely to the gears on the yaw bearing, and depending on how the arm was position caused some dragging. Simple fix as this may be, it does show that the current state of the system is still being worn in and the issues being discovered were minor and not worthy of ending the test.



Testing with ARMLiSS extended Fig. 49



Fig. 50 Test subject moving umbilical arm as they explore

The next configuration aimed to test deployment while compensating for a slope. Starting at the base of the first hill in the testing area, the arm was deployed with the chassis compensating for a very slight slope. At the full five meter extension length, the test subject was able to walk significantly further up the hill than the rover position. Once the test subject had circled the rover and tested various poses, the rover then climbed the hill while the BioBot arm was deployed. Since this was the first hill climb with ARMLiSS fully deployed, the arm was pinned to point in the up-hill direction and the test subject disconnected from the umbilical temporarily.

The next test aimed to have VERTEX positioned higher than the astronaut. The slope between VERTEX and the test subject in Figure 56 was approximately 40° and technically if VERTEX's auto



extended



Slope testing with ARMLiSS fully Fig. 52 Additional angle of slope testing with arm fully extended



Fig. 53 on slope



BioBot with ARMLiSS fully extended Fig. 54 Additional angle of BioBot with ARMLiSS fully extended on slope

zero suspension controller was engaged and the rover slowly crept over the edge the vehicle should be able to descend that slope. However, with only analog control of the traction motor drivers and no computer overseeing the wheel and descent rates, effectively no hill descent or traction control beyond a single, and sensitive, analog joystick the team decided to not descend the hill from the approach angle in Figure 56. Instead this situation would be analogous to an astronaut descending into a small crater while the vehicle remained around the crater rim, while attached to the life support system.

After the test subject climbed up the slope and returned to the vehicle, VERTEX was driven into the lower area via a shallower slope and all of the steering methods were demonstrated on grass. During most of the testing efforts combinations of front-ackermann and double-ackermann were used to position the vehicle. Rear-ackermann will become an easier steering mode to use once cameras are placed around the rover or a graphical user interface is implemented in the robot software as the operator's line of sight to the rear wheels is interrupted by the electronics boxes hanging on the chassis walls. As an interesting operational note, since the traction drivers were being controlled in torque mode via the analog joystick, sometimes not all wheels started moving at the same exact time. This was less noticeable when VERTEX was traversing straight, but when



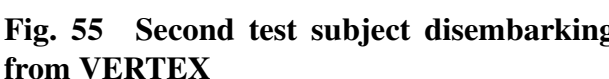




Fig. 55 Second test subject disembarking Fig. 56 Astronaut investigating within a depression with VERTEX above the area rim

steered heavily it was interesting to see one wheel move slightly before the rest of the rover followed. This is another minor observation that did not affect operations during testing, and won't be an issue once the traction motors are hooked up digitally.



Fig. 57 steering



Double Ackermann Fig. 58 Double Ackermann Fig. 59 steering - rear view



Turn in place steering

The SSL considers the first field trial to be a resounding success. Even with some operational bugs, VERTEX and ARMLiSS proved themselves to be a highly functional pairing. The rover was operated at relatively low speeds, and had not yet climbed sharp obstacles taller than a curb as we continue to build confidence in the system. Wattage required for climbing steep hills was in the 6kW range, and the batteries are capable of 30kW sustained so there is still a lot of margin left for tackling much more challenging terrain.







Fig. 60 Crab steering

Fig. 61 steering

Rear Ackermann Fig. 62 Front Ackermann steering

D. Improvements to the Second Field Trial

Three areas of system improvements were deemed necessary before field trial 2, starting with ARMLiSS. The connecting plate between the arm and VERTEX was the main source of arm deflections and a low resonance frequency, and did not allow the arm to be pinned straight along the vehicle's centerline. A new, thicker plate needed to be designed, manufactured, and integrated that solved these issues. Next, the suspension system was nearly maxed out in preload and still felt too soft to each of the operators. This means the gravity offset springs had no ability to put any more force into the swingarms, and caused the rover to sway left and right a little too much. This problem was solved before the second field trial by integrating a stiffer spring combination and re-analyzing the suspension dynamics considering a heavier vehicle than estimated when the present. Third, as field trial 1 continued the team noticed the connection between the steering actuators and the swingarms to have an excess amount of play. The caster and camber forces transferred into this connection from the wheels had cracked a series of bushings that maintained the alignment, and a milled stiffening clevis had to be machined and welded on before the next adventure. Finally, the team agreed that the vehicle was hard to climb into at the nominal operating height without either lowering the chassis or using the traction motor as an intermediate step. A physical step was added to the structure that holds the traction motor for the Goddard test.

BioBot-specific modifications include a chest plate interface for the umbilical, which initially is a mechanical interface only, with the suit continuing to supply ventilation and cooling for field testing. Two versions of the chest connection have so far been tested, the first of which can be seen in Figure 63. Upgrades between the first and second field trails, as shown in Figure 64, included a magnetically-actauted mechanical connection, umbilical port, and a power connector for batteries. The electrical connector distributes power to the ventilation and LCG (Liquid Cooling Garment) system and provides an easy, field-replaceable battery for field trials. Ultimately, a higher fidelity umbilical cable carrying water, power, and air lines will be included but for the moment the umbilical

provides a mechanical representation of the concept and the suit provides these operations.





Fig. 63 Closeup of MX-C+ suit with umbilical attach- Fig. 64 Version 2 MX-C+ umbilical ment and FDM printed bearing arm interface device

The other primary BioBot modification is in the reconfigurable PLSS mockup. One of the major test objectives of BioBot is the better understand the operational implications of the umbilicalsupplied primary life support system, supplemented with a smaller backpack-based portable system to allow the crew to release the umbilical for surface operations incompatible with the umbilical and/or accompanying rover. These operations could include transition from the habitat to the vehicle, activities on slopes or ledges, or emergencies in transitioning life support to the second rover on EVA. The size and mass of backpack required is directly proportional to the allowable disconnect time; the new backpack consists of a small base module incorporating a UMD-developed solid state cooling system and suit-mounted ventilation fans, along with the ability to attach different sized PLSS outer mold lines to represent longer-duration suit life support systems. Figures 65 and 66 show the cooling and ventilation in the lower unit, with a small unit added atop that represents a 20-30 minute life support duration. Larger volumetric modules with appropriate ballast are presently being created to allow for in-field adjustment of PLSS duration. Field tests with experienced field geologist test subjects will examine the role of untethered intervals on data collection, with the aim of obtaining a better understanding of the trade-offs between umbilical and onboard life support systems. BioBot aims to optimize for minimum PLSS mass, and therefore untethered duration, without interfering with the exploration desires of field geologists and test subjects.

E. Field Test 2 - NASA Goddard

The first testing location outside UMD was hosted on the NASA Goddard campus. A 15 minute drive from campus, Goddard is familiar with a lot of the projects happening at UMD and has a perimeter trail with varying slopes including an extended 15° gravel track, surface conditions, and off-road trails that branch from the main path. Due to badging requirements, testing dates for April 18th and 19th 2024 were set in mid March in case of any forecasted rain, and provided the team with a set deadline for improvements to be complete from the UMD campus testing.

Tests at Goddard required additional transportation to the test site as seen in Figure 69. The



Fig. 65 Reconfigurable PLSS with outer pro- Fig. 66 tective fabric covering ture

Fig. 66 Reconfigurable PLSS internal structure



Fig. 67 NASA Goddard off-road path



Fig. 68 NASA Goddard gravel trail

test was hosted across two days, with the primary test configuration occurring on day 2. Day 1 focused on resolving logistical challenges, vehicle checkouts of improved electrical systems, and software validation of recent patches. While digital control of the traction system was attempted, the implementation within the physical electronics did not produce a smooth and responsive control scheme and the team chose to revert to the same control scheme as the first field trial. The traction motor drivers were capped at 25% of full speed, approximately 3 m/s, to reduce oversensitivity in the joystick. Figure 70 shows the test subject operating VERTEX without the BioBot arm as a comparative operational mode.

Testing trials on day 1 were brief as multiple components in the electronics, software, and suit simulators were still in preparatory phases for more rigorous testing on day 2. Figure 71 shows the test subject operating VERTEX without a visor attached due to ventilation repairs that were underway. Figure 72 shows the VERTEX vehicle being driven during checkout, testing driving in multiple modalities including reverse. The newly added structural clevises appeared to significantly



Fig. 69 VERTEX transportation method



Fig. 70 EVA with test subject, VERTEX, no umbilical arm

stiffen the connection between the swingarms and the steering actuators, effectively removing any back and forth camber motions as seen in the first field trial. The new suspension configuration provided a much stiffer vehicle and removed the unsettling side-to-side motion felt by operators in the first field trial.



Fig. 71 Test subject operating vehicle



Fig. 72 VERTEX capability checkouts

The second testing day was unfortunately shortened due to a combination of intermittent rain and on-scene code upgrades, but still provided a highly valuable experience for both the UMD BioBot team, but also the students visting from the University of Maryland Eastern Shore (UMES). Challenges with the electrical and software systems minimized the deployment of ARMLiSS throughout the testing, and as a result day 2's goals shifted to prioritizing the loose gravel surface available and evaluating VERTEX's performance driving, turning, and slope climbing. This loose surface is very valuable to the team as UMD tends to only have grassy hills to test on. While this may work fine for testing ARMLiSS, the suspension, traction, and steering performance varies greatly when compared to a loose rocky surface.

Figures 73 and 74 show the vehicle being checked out after unloading and the team pausing during one of the tests. Figure 75 presents a test subject just after ingress to the vehicle, with the umbilical attached via the improved suitport connector. Figure 76 shows the test subject operating



Fig. 73 Day 2 unloading



Fig. 74 UMD and UMES team with a test subject

VERTEX for the first time, which after some jerkyness in learning the throttle sensitivity, provided a smooth and largely uneventful drive. VERTEX continued to have no issues accelerating to approximately 3 m/s, consuming roughly 2.5 kW of power during normal driving.



Fig. 75 Day 2 test subject Fig. 76 after vehicle ingress above



Fig. 76 Test subject operating vehicle with ARMLiSS stowed above

Figures 77 and 78 show the team testing the vehicle post rain shower. Once the rains had passed, approximately one hour of testing window remained before our agreed upon departure time from Goddard, and with still needing to load everything back onto the trailers and pack up the team decided to have everyone operate the vehicle to generate their own opinions and operational evaluations. This included two team members, as shown in these figures, operating in a pseudo-contingency case where two astronauts must use one rover to return to base camp during an anomaly with a rover on EVA. Including ARMLiSS mounted on top (which in a contingency may be jettisoned onto the lunar surface to provide a more stable seating configuration), the vehicle carried approximately

325 kg of payload up an extended 15° gravel slope with seemingly zero hesitation. The vehicle's speed remained constant the entire climb, and power consumption raised to 5 kW, but with the limit of 30 kW of continuous power available a much steeper slope is going to be needed to challenge VERTEX. Additionally, the suspension was set to automatically maintain chassis on the slope which was another huge success.





Fig. 77 Day 2 team operations/evaluations

Fig. 78 Day 2 team operations/evaluations

F. Lessons Learned

Direct sightlines to the rear wheels were essentially non-existent due to the large electronics boxes, and suit mobility restrictions not allowing test subjects to turn their heads as far as shown in Figure 72 means a high information bandwidth set of sensors and cameras will be required for reverse operations if needed in the future. A second suit-mobility improvement to be made focus on the added steps on the traction motor structure. The new steps require the test subject's knees and hips to bend too sharply when climbing into the rover at nominal operating height. However, when egressing from the seat the hardware is adequate as a first step to get down, but then requires the operator to hop down onto the surface. A second, intermediate step could reduce this strain.

When the test subject is sitting in the seat with the umbilical attached, as seen in Figure 75, the current angle that the umbilical naturally rests at does block vision in the left-most quadrant of an operator's vision. Further consideration of the departure angle of the umbilical attachment may be necessary to minimize this intrusion. Additionally, the current control panel prototypes provide good line of sight to the front wheels and the road ahead, but the current suspension and steering mode indicators available on the terminal screen are are too small alongside the joysticks. These are improvements to be addressed in the next generation prototype. The improvements made to the suspension provided a highly stable and controllable articulation mechanism, and the stiffness of ARMLiSS was significantly increased with the new thicker baseplate added. Currently, backlash tolerant algorithms and mechanisms are being investigated to improve the performance of ARMLiSS before the next field trails alongside progressive steps in motion automation.

XII. Study Conclusions

BioBot presents a promising avenue for future lunar explorer teams to consider during preparation and collaboration between NASA and both the commercial suit and LTV providers. Testing so far at UMD has gone well, and from what has been seen so far the SSL is confident that a vehicle of some form like BioBot could be beneficial to extended exploration efforts of the Artemis program. Removing or minimizing the requirement for an astronaut to carry the full duration of their life support during an EVA may lead to lower fatigue and greater mobility during the exploratory efforts. Using an umbilical is the only way to provide extended amounts of life support in a scenario like this, and the astronaut would still require a small amount of life support as well as the air circulation and liquid cooling to still be present in a reduced size to the full backpack on their lower back.

Suspension systems with very large ranges of articulation but also passive damping, at this scale, are highly non-trivial and hard to design. However, they may be worth their weight in gold (on Earth) in controlling large, difficult payloads like ARMLiSS and essentially guarantee stability when climbing or crossing slopes within the order of magnitude that safety standards would allow.

Long manipulators are, unsurprisingly, prone to large deflections and low resonant frequencies. While this may not be a huge problem on the moon with reduced gravity, it is still worth considering the response characteristics of a 5 or 10 meter arm as well as the logistics for mounting, unmounting, or deploying the arm from the landed configuration. Making ARMLiSS from epoxied carbon fiber tubes would have significantly helped the resonance and backlash at a much greater cost, but may have allowed for the full original 10 meter goal to be achieved. Stowage of the arm requires an interesting set of considerations. On VERTEX the arm is stowed above the astronauts head, and in theory with a large enough bounce may cause contact between the astronaut and the arm. This hasn't yet occurred and every effort was made in the stowage position to avoid this. While pinning the arm to be facing out the left or right sides of the vehicle provides a non obtrusive solution, it may create uneven suspension responses from both sides, and motorizing the yaw joint is estimated from a preliminary trade study to consume great amounts of mass and power. Pinning the arm to face the rear of the vehicle may alleviate all of these issues during transport, but has additional steps to then board or disembark the rover.

Having adjustable caster on the moon is likely not necessary. Once you have a caster setting that gives you the proper chassis height you want the caster to be 0 at, you could arrange the kinematics of the rover around this setting. The length of the steering stackup with the wheel will not change, so you must adjust caster angle and correspondingly swingarm angle to set this point. Once set, having articulation range up and down from this point appears to cause the wheels on slopes to remain steerable as the chassis levels itself as seen in the VERTEX testing efforts so far. The articulation systems present on rovers such as VIPER actuate on the transverse axis to the vehicle midline similar to a traditional car suspension with axle lift system. Double wishbone suspension systems allows for a smaller amount of articulation while maintaining a constant caster angle, whereas VERTEX actuates longitudinally requiring less actuation volume within the centerline of the chassis and greater articulation range, but has higher sine and cosine losses across said range.

BioBot appears from these field trials to be a highly-capable roving vehicle that has yet to have its true limits stress tested. As testing reveals individual components that may need upgrades, the form factor of the vehicle has been compact and appropriate over time and the actuators and chassis have proven to perform as well as or better than expected. One very important lesson learned by the team in the creation of an evolving Earth-analogue system is maintaining elements of modularity

in the design. As systems are upgraded, new research ideas spawn, and overall improvements are drafted, a series of 1/4-20 threaded studs, 80/20 TMcompatible hole patterns, and a pair of 2" trailer hitch receivers provide limitless potential for upgrades without heavy modifications. From camera mounts to steps, lights, and payload adjustments these features have lowered the barrier for fast-paced iteration.

While further testing may reveal through additional testing that energy expenditure on EVA decreases with the BioBot system, the added system complexity cannot be overlooked in the comparison. Carrying a large (5 to 10 meter) manipulator arm atop a roving vehicle, while not impossible, may be a costly proposition, sensitive to lunar challenges like regolith abrasion over time. Similarly, the high range of motion articulating suspension system may have similar sensitivity challenges on the lunar surface, but provides advantages in significantly increased stability margins and controllability of otherwise unwieldy payloads. On a similar note cycling of the umbilical connector, responsible for transferring water, power, and air to the astronaut, in the unpressurized surface environment while using dirty EVA gloves may bring challenges. These considerations will obviously need focused and intense study for this and any other similar system for the lunar case, but do not present as issues in testing on Earth.

XIII. Future Work, Research Extensions

A. Near-Term System Improvements

The foremost improvement before the third field trial will be identifying and addressing backlash and lack of dampening in ARMIiSS that will significantly help the control software efforts. The thicker baseplate significantly reduced bending and increased the low resonance frequency of the arm, which will help computer vision efforts and be safer for humans to operate around. Additionally, a lack of dampening and a fair amount of backlash is present and is most noticeable in the last powered joint which has a tendency to go unstable when operating in certain regimes. The backlash is caused from keeping the arm manufacturing process simple by welding lasercut plates and using pins. While this method is cost effective and strong, backlash compensation in some form must now happen.

As before mentioned, conversion of the traction driver system from analog to digital control will greatly improve ease of operation and allow for more sophisticated control such as hill-hold assist and finer coordination of wheel motions via their incremental encoders. Additionally from a human interface perspective, larger joysticks are being installed to improve comfort and controllability especially with gloved hands. Both joysticks present on the vehicle were chosen as the easiest first integration path, and now that the subsystems they control have been checked out they can be incrementally improved.

B. Field Testing Locations

Local and appropriate field testing locations are still being pursued. At the highest level, an area with loose soil and slopes could provide value in the testing operations. Ideally, more closely representative environments like beaches and quarries with finer grains and rocky objects. Maryland offers Off-Road Vehicle (ORV) permits for driving on Assateague island, just not on the sloped dunes could would be beneficial for testing. Collaboration with the University of Maryland Eastern

Shore may reveal some additional sandy testing locations as well and those talks are underway. There are also private off-road trails in the Maryland area that are being coordinated now that the vehicle has been proven to have functionality. Testing BioBot in field trial events such as GEODES (Geophysical Exploration of the Dynamics and Evolution of the Solar System) at test locations further away may provide a higher fidelity analogue at the expense of a greater overhead and distance from the home base. The vehicle fits within a commercial boxtruck so traveling to test sites should be relatively simple, and testing efforts are expected to progress further and further away from the UMD campus as confidence is built in the system.

XIV. Student Involvement and Acknowledgements

This NIAC project has not only supported the authors' work, but it has also supported numerous student volunteers and undergraduate research mentorships, many of whom co-authored attached publications. Robert Fink conducted the detailed ARMLiSS mechanical design, as did Chandler Sheatzley with VERTEX's over-wheel steering support structure and caster adjustment bars. Spencer Quizon, Rowan Quintero, and Ian Welfeld conducted design and testing of the control panel interfaces aboard VERTEX. Tarun Batchu and Adam Ben Youssef contribute to astronaut tracking hardware and camera vision software. Sam Heintz's work in progressing the development of the solid-state spacesuit cooling and modular PLSS simulators has made for higher fidelity field testing in the future. Field testing and hardware build support from Ryan Mahon, Brent Barbee, and Melissa Buys is deeply appreciated.

Last but not least, several 5-7 member student groups also contributed preliminary studies to BioBot as part of the introductory course for aerospace engineering laboratory research, ENAE100. These groups worked on prototypes and conducted semester-long studies, gathering quantitative or human-factors data for design improvement in various parts of BioBot. Freshman groups investigated: button and switch placement for the control panels, adjustable vehicle seating for use with PLSS-simulating backpacks, on-suit lighting placement for exploration in darkness, and rover sensor experimentation for detecting wheel-ground contact.

References

- [1] Kuroda, Y., Teshima, T., Sato, Y., and Kubota, T., "Mobility performance evaluation of planetary rover with similarity model experiment," *IEEE International Conference on Robotics and Automation, 2004. Proceedings. ICRA '04. 2004*, Vol. 2, ????, pp. 2098–2103 Vol.2. https://doi.org/10.1109/ROBOT.2004. 1308133, ISSN: 1050-4729.
- [2] Liu, Y., Qi, Y., Pan, D., Chen, Z., Yuan, B., and Zou, M., "Gradeability of 'Zhu Rong' Mars rover based on the simulated Martian terrain," Vol. 106, ????, pp. 57–73. https://doi.org/10.1016/j.jterra.2023.01.002, URL https://www.sciencedirect.com/science/article/pii/S0022489823000022.
- [3] Hanner, C., Bolatto, N., Martin, J., Gribok, D., and Akin, D., "Development and Testing of the BioBot EVA Support System," 51st International Conference on Environmental Systems, 2022, p. 16. URL https://ttu-ir.tdl.org/handle/2346/89836, accepted: 2022-06-21T13:56:19Z Publisher: 51st International Conference on Environmental Systems.
- [4] Akin, D. L., Saripalli, S., Hodges, K., Young, K., and Davis, K. P., "Desert FLEAS IV: Results from Field Tests of EVA/Robotic Collaborative Planetary Geological Exploration," *43rd International Conference on Environmental Systems*, American Institute of Aeronautics and Astronautics, 2013. https://doi.org/10.2514/6.2013-3429.
- [5] Akin, D., Saripalli, S., Hodges, K., Young, K., Capua, M. D., Davis, K., and D'Amore, N., "Results from Desert FLEAS III: Field Tests of EVA/Robotic Collaboration for Planetary Exploration," *42nd International Conference on Environmental Systems*, American Institute of Aeronautics and Astronautics, 2012. https://doi.org/10.2514/6.2012-3464.
- [6] Jones, E. M., and Glover, K., "Lunar Gaits,", 2001. URL https://www.hq.nasa.gov/alsj/a11/a11.gaits.html.
- [7] Akin, D., Hanner, C., Bolatto, N., Gribok, D., and Lachance, Z., "Design and Development of an EVA Assistance Roving Vehicle for Artemis and Beyond," 50th International Conference on Environmental Systems, 2021, p. 12. URL https://ttu-ir.tdl.org/handle/2346/87097, accepted: 2021-06-23T23:02:42Z Publisher: 50th International Conference on Environmental Systems.
- [8] Hanner, C., Bolatto, N., Gribok, D., Quizon, S., Quintero, R., Welfeld, I., and Akin, D., "Development and Testing of Crew Interfaces for an Advanced Unpressurized Exploration Rover," *52nd International Conference on Environmental Systems*, 2023. URL https://ttu-ir.tdl.org/handle/2346/94805, accepted: 2023-06-21T14:21:28Z Publisher: 2023 International Conference on Environmental Systems.

XV. BioBot Publications, Presentations, and Awards

The BioBot project has succeeded in disseminating the years of NIAC research effort with publications and presentations on a wide variety of subsystems. The following six paper titles have been published since NIAC Phase 1, and they are attached to the end of this report as a supplement:

- 1) BioBot: Investigating an Alternative Paradigm for Planetary EVA (ICES 2019, pre-Phase 2)
- 2) Design and Development of an EVA Assistance Roving Vehicle for Artemis and Beyond (ICES 2021)
- 3) Development and Testing of the BioBot EVA Support System (ICES 2022)
- 4) Development of an Autonomous Umbilical Tending System for Rover-Supported Surface EVAs (ICES 2022)
- 5) Development and Testing of Crew Interfaces for an Advanced Unpressurized Exploration Rover (ICES 2023)
- 6) Earth-Analogue Roving System Development and Testing for Lunar Surface Exploration (AIAA ASCEND 2023)
- 7) Initial Testing and Evaluation of the BioBot EVA Support System (ICES 2024)

Two more VERTEX-related manuscripts are being prepared for ICES 2024 and AIAA ASCEND 2024. A manuscript about the MX-D suit simulator which interfaces with the BioBot umbilical is also being prepared for ICES 2024 and the draft final report is attached below.

Each of the publications also consisted of an oral presentation at their respective conferences. Four other presentations and student posters were made for the AIAA Young Professionals, Students, and Educators Conference, the Maryland Robotics Center Symposium, and the Space & Satellite Professionals International conference, where the "SSPI Best Presentation Award" was won for a VERTEX presentation in 2021.

BioBot: Investigating an Alternative Paradigm for Planetary EVA

David L. Akin*, Kate Melone †, Brady Sack ‡, and Jeffrey Zhu § *University Of Maryland, College Park, MD, 20742, USA*

One of the biggest burdens on an astronaut when conducting planetary surface operations is the need to carry a portable life support system (PLSS). This unit is typically comparable in weight to the astronaut themselves, and disturbs mobility by displacing the center of gravity of the human in the spacesuit aft and upwards. The additional weight leads to increased energy expenditures, as well as overall reductions in performance and duration. The motivation to minimize the loads on EVA crew served as the inspiration for the BioBot concept: an EVA-companion rover which carries life support for the spacesuit, and supplies the user via self-tending umbilicals. This paper outlines the design requirements for BioBot, and documents the results of a variety of trade studies, including providing self-contained suit life support for various periods of time for safety and local independence, and designs for BioBot configurations ranging from minimal rovers to incorporation into pressurized rovers. In addition to BioBot systems analyses and trade studies, a prototype BioBot has been developed at the University of Maryland using a Segway RMP440LE robotic vehicle and tested with MX-C suit simulators. Results of this testing are discussed as well. The benefits of BioBot go beyond just reducing the mass that an astronaut would be required to carry, as it opens the possibility for using alternative suit components that could enhance mobility, extend range and endurance, and support exploration operations. In addition, BioBot could also allow for the use of potentially larger and heavier, but more efficient life support systems that normally would not fit in a PLSS, but could be mounted on a rover. Conclusions and future work will also be presented in this paper.

Nomenclature

AEMU	Advanced extravehicular mobility unit
ATCL	Auxiliary thermal control loop
EMU	Extravehicular mobility unit
EVA	Extravehicular activity
NASA	National Aeronautics and Space Administration
NIAC	NASA Innovative Advanced Concepts
OPS	Oxygen purge system
PLSS	Portable life support system
PRA	Probabilistic risk assessment
ROS	Robot Operating System
SMLS	Suit-mounted life support
SSL	Space Systems Laboratory
UHS	Umbilical Handling System
UMd	University of Maryland

^{*}Director, Space Systems Laboratory. Associate Professor, Department of Aerospace Engineering

[†]Graduate Research Assistant, Space Systems Laboratory

[‡]Undergraduate Research Assistant, Space Systems Laboratory

[§]Undergraduate Research Assistant, Space Systems Laboratory

I. Introduction

No parameter in the design of spacesuits for planetary exploration is more important than "weight on the back": the weight of the suit system which must be supported by the wearer under the gravity of the Moon or Mars. The added weight of the spacesuit garment and portable life support system (PLSS) drives the required exertion level of the wearer, and ultimately sets limitations on EVA duration, distance traveled on foot, and productivity of the exploration mission.

As an example, the A7L-B suits worn on the later Apollo lunar missions had a mass of 96 kg, composed of 34 kg for the garment assembly and 61 kg for the PLSS. A 73 kg astronaut found their weight increased by 130% due to the suit, with the PLSS weight alone almost equal to their body weight. This system was capable of supporting a 6-hour nominal surface EVA, but strongly impacted the gaits, transport speeds, and energy expenditures of the astronauts. The PLSS weight was particularly burdensome, as it moved the astronaut's overall center of mass upwards and backwards. This could be seen in the convoluted motions of the crew when trying to bend over and pick up items, work with the long-handled sampling tools, or just maintain balance, especially when changing direction or starting and stopping.

Short-distance, short duration EVAs in microgravity have used umbilicals rather than PLSS units. This relieved the crew from the bulk and mass of the PLSS, at the cost of needing to control the motion of the flexible umbilical. For the deep-space EVAs of the J-class Apollo missions, one crewman would translate aft on the service module to retrieve film canisters, while another would be stationed in the command module hatch to handle the umbilical. Although umbilicals were briefly considered for the first Apollo surface missions, they were rejected due to the operational limitation of being tethered to the spacecraft, and the overhead burden of handling umbilical motions.

It is clear that planetary surface exploration activities would be greatly improved if the astronauts did not have to carry a PLSS to maintain life support functions. At the same time, additional restrictions on crew mobility or operational capabilities would be unacceptable. The concept for this study is to accomplish these two seemingly conflicting requirements through the application of advanced robotic systems to deal with biological requirements (i.e., life support) for the astronauts: the "BioBot".

The BioBot concept consists of a robotic rover which is capable of traversing the same terrain at the same speed as a spacesuited human. It carries the primary life support system for the astronaut, including consumables, atmosphere revitalization systems (e.g., CO₂ scrubbing, humidity and temperature management, ventilation fan), power system (e.g., battery, power management and distribution), and thermal control system (e.g., water sublimator, cooling water pump), along with umbilical lines to connect to the supported astronaut. Although not technically part of life support, it would be logical for the BioBot to also provide long-range communications, video monitoring, tool and sample transport, and other functions to enable and enhance EVA productivity in planetary surface exploration.

The design reference scenario for this concept is that astronauts involved in future lunar or Mars exploration will be on the surface for weeks or months rather than days, and will be involved in regular EVA operations. It is not unreasonable to think of geologists spending several days in EVA exploration each week over a prolonged mission duration, with far more ambitious operational objectives than were typical of Apollo. In this scenario, each astronaut will be accompanied by a BioBot, which will transport their life support system and consumables, an extended umbilical, and robotic systems capable of controlling the position and motion of the umbilical (Figure 1). The astronaut will be connected to the robot via the umbilical, carrying only a small contingency open-loop life support system similar to those contained in every PLSS. The robotic mobility base will be designed to be capable of traveling anywhere the astronaut can walk at the same speed as its user; it will also be useful as a transport for the EVA tools, science instrumentation, and collected samples. In addition, the BioBot can potentially carry the astronaut on traverses as well. Such a system will also be a significant enhancement to public engagement in these future exploration missions, as the robotic vehicles can also support high-resolution cameras and high-bandwidth communications gear to provide high-definition video coverage of each crew throughout each EVA.

There are also architecture-level benefits to this concept. For example, in the drive to reduce suit weight to the absolute minimum due to the load of the PLSS, design elements which would enhance suit mobility (such as low-friction rotary bearings) are frequently deleted, resulting in a lighter but less flexible suit enclosure. By offloading the life support system, electrical power, and consumables, the relatively meager increase in garment mass to incorporate these mobility features would be easily accommodated. This would result in a lighter, more flexible spacesuit system with an overall center of gravity very close to that of the wearer's body. Since the PLSS weight restrictions would be negated by placing the system and its consumables on an accompanying robot, the overall EVA system could easily adapt to longer durations, higher capacity astronaut cooling systems, and/or higher levels of redundancy to enhance crew safety and minimize the possibility of a loss-of-crew event. When no longer constrained to fit within the mass and volume constraints of a spacesuit backpack, portable life support designers can consider technology alternatives better suited to extended exploration, such as radiators for cooling, solar panels to extend electrical power, or regenerable



Figure 1. Artist's concept of BioBot in operation

CO₂ scrubbing systems.

This paper details research performed on the BioBot concept as a result of a Phase I award under the NASA Innovative Advanced Concepts (NIAC) program. This activity was performed over nine months in 2018-2019, and will be continued at some level based on future funding availability.

II. Systems Design Trade Studies

An initial priority for the BioBot team was to explore the widest possible design space for the system. Since the BioBot represents a new category of system in an EVA surface exploration scenario, it was important to conceptualize as many different types of systems as possible, and to compare them to select the most favorable design concept for further development.

As a way to better understand the design space, the BioBot team worked with different teams from a University of Maryland graduate course in Planetary Surface Robotics to produce detailed designs for six configurations of BioBot, based on size and functionality:

- (a) Minimum possible robot, capable of carrying only astronaut life support system and umbilical tending system (Figure 2)
- (b) Similar to (a) but also capable of transporting geological tools and samples (Figure 3)
- (c) Similar to (b) but including the capacity to nominally transport one EVA crew as well (Figure 4)
- (d) Similar to (c) but also including the capability to transport a second EVA crew as a contingency (Figure 5)
- (e) Two-person roving vehicle with dual EVA life support systems and umbilical handling systems (Figure 6)
- (f) Two-person pressurized rover (e.g., NASA Space Exploration Vehicle) with dual EVA life support systems and umbilical handling systems (Figure 7)

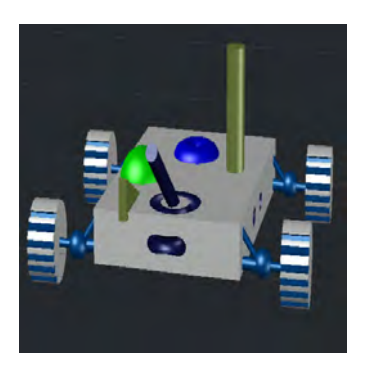


Figure 2. Type (a) BioBot: Life support hardware transport only



Figure 3. Type (b) BioBot: Life support and EVA support transport

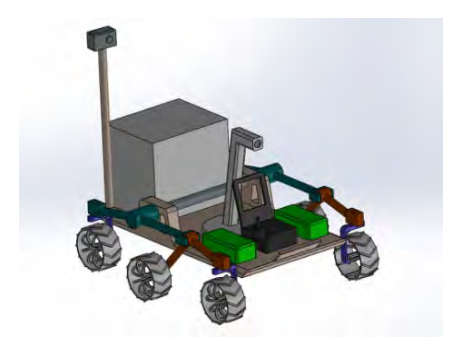


Figure 4. Type (c) BioBot: Single EVA crew transport



Figure 5. Type (d) BioBot: One EVA crew nominally; two in contingency



Figure 6. Type (e) BioBot: Two nominal EVA crew



Figure 7. Type (f) BioBot: Two crew with pressurized cabin

It should be noted that, as the umbilical handling technology development was being performed in parallel, these vehicle studies focused on trafficability, using a common requirements document based on assumed operational limits for regions accessible by walking EVA crew: slopes up to 30°, obstacles up to 30cm in height, and soil bearing parameters based on data from both lunar and Mars exploration missions. Vehicle speeds were required to meet or exceed 3 m/sec on level, flat terrain; 1.75 m/sec in the presence of obstacles up to 10 cm in height; and 1 m/es on slopes up to 30°. Top-level mass and volume requirements were given to the design teams to accommodate the design of mounting locations for life support and umbilical handling systems.

The parallel design efforts showed clearly that the BioBot concept could be implemented successfully across the entire spectrum of mobility system sizes and mission applications. The larger configurations – (e) and (f) – presented additional concerns in terms of multiple umbilical handling systems on the same vehicle. Handling two independent umbilical systems could give rise to interference issues if the crew traverses were not carefully monitored to prevent umbilical entanglement with each other or with large elements of the rover, such as the pressurized cabin in (f).

At the same time, a probabilistic risk assessment (PRA) was performed for the BioBot concept, looking at all major categories of failures in the life support system, umbilicals, and the mobility platform. As a result of all of this activity, it became clear that, based on crew safety, the best configuration for an initial BioBot prototype would be (d): a single-person rover capable of carrying two crew in a contingency mode. This would allow the widest range of possible responses to one or more failures, including having both crew return to base on a single rover, sharing a life support system for the traverse.

III. Portable Life Support Trade Studies

The basic concept of the BioBot is to offload the weight of the portable life support system from the EVA crew and transfer it to the accompanying robot. It is clear, however, that it is neither practical nor desirable to eliminate all life support capability from the pressure suit. On Skylab, where the A7L-B suits were entirely supplied with life support via umbilicals, an emergency oxygen pack was designed and mounted on the suit in case of umbilical failure. It is probably impractical to have BioBot routinely ingress and egress the airlock with the crew, so they will need to have

independent life support capability for ingress and egress at least. BioBot is being designed for redundancy and the ability to support two crew on one system ("buddy breathing") in a contingency, while maintaining suit pressure and ventilation during those contingencies.

It was also realized during Phase I studies that there could be a benefit to having nominal operations independent of BioBot for some defined periods of time. If the EVA crew needed to access a site outside of the "reach" of the BioBot umbilicals and difficult for the mobility base to transit, the astronaut could unplug from BioBot and have an independent PLSS take over life support functions for a short period of time. This capacity for independent operations would permit the successful completion of that task and enhance the overall utility of the concept.

To that end, an extensive trade study was undertaken to create a number of suit-mounted life support (SMLS) designs of varying duration and capabilities, in order to understand the relationship between SMLS usage and installed weight on the suit. While a nominal life support system would be based on a closed-loop design to minimize oxygen usage, short-duration suit-mounted systems (such as the Apollo and EMU secondary oxygen systems) were designed for open-loop use of oxygen for both breathing and gas cooling of the crew. The simplicity of an open-loop system minimizes mass on the suit, and the independent oxygen supply can be designed to be replenished during the time the crew is tethered to BioBot, eliminating restrictions on the number of times or cumulative duration of usage of the independent system. However, in longer durations it is more effective to return to a closed-loop system; if independent duration is long enough to allow substantial distances from the EVA crew to BioBot, it would even make sense to run a split system with a closed loop primary life support and a secondary open-loop system for contingencies. At this point the weight of the SMLS becomes similar to that of the current PLSS concepts, and use of the BioBot would have to be based on considerations other than reduction of total suit weight.

To better understand the design and operational implications of the suit-mounted life support system design, a series of candidate designs for the SMLS were developed in this study. Two of the key objectives were to design a minimum mass SMLS system, and to design multiple configurations that could accommodate a variety of EVAs (short duration, long duration, tethered to BioBot, untethered from BioBot, etc.). The minimum mass goal was accomplished by first determining the necessary components that could be used for the SMLS. The modular design objective was accomplished by building upon the baseline minimum mass design, and adding components/features (cooling, CO₂ scrubbing, etc.) as appropriate to optimize between untethered capability and additional weight on the suit. The amount of additional life support that the astronaut will have is dependent on the type of EVA they will be performing, as well as the capabilities of that specific system. Shorter range operations such as routine maintenance on BioBot or the habitat, installation of other equipment within close proximity of the habitat, etc. would require less additional life support for the astronaut, since the amount of untethered time from the crew member's BioBot would be brief, if at all. However, for surface exploration missions, the astronaut may require additional life support for extended planned untethered time from BioBot if the areas to be explored are not directly accessible by BioBot. The purpose of having a modular SMLS design is so that the astronaut will not have to be burdened with the mass of additional life support that would remain unused. The options presented allow for flexibility in terms of overall PLSS structure mass, volume, and life support duration, all of which can be customized. A summary of each of the additional life support configurations can be seen in Table 1 below.

The width and depth dimensions for all of the SMLS backpack configurations are 50 cm and 22 cm respectively; different designs resulted in different backpack heights as shown in Table 1. All of these are smaller than the current PLSS design on the extravehicular mobility unit (EMU). It should be emphasized that these are presented as *feasible* SMLS backpack sizes; a detailed design process would almost certainly reduce these sizes somewhat. Design choices listed in Table 1 were based on mass optimization, as shown in Figure 8.

The C1 configurations have the same components as the Apollo Oxygen Purge System (OPS), which include a heater for controlling the oxygen temperature, battery for the heater, pressure regulator, and oxygen tank(s). The C1.1 (Figure 9) and C2.2 (Figure 10) concepts do not have a cooling system, so the oxygen flow rate for both of them is 3.7 kg/hr, which was determined to be an acceptable value for both suit pressurization and cooling. The C2 configurations (Figures 11 and 12) have the same components as the C1 configurations, but each sub-configuration also has the addition of a thermal loop, allowing for a reduced oxygen flow rate of 1.9 kg/hr, as well as extended life support duration. The thermal loop design used for these configurations is based on the Auxiliary Thermal Control Loop (ATCL) for the Advanced Extravehicular Mobility Unit (AEMU).⁴ The primary components in the ATCL are a pump, stepper motor, sensors, relief valves, water tank/water, and tubing to circulate the water; the version used for this design can provide up to 120 minutes of cooling. Both the C1 and C2 series options operate in an open loop mode.

The C3 configuration introduces a closed loop operating mode. The reason for doing so is due to mass (and volume) constraints. It can be seen from the plot in Figure 8 that a closed loop system is more mass efficient than an open loop system once a certain design duration is reached. The C3 configuration, shown in Figure 13, utilizes aspects from

Table 1. Suit-mounted life support (SMLS) system reference configurations

Configuration	Mass [kg]	Backpack	O_2	O ₂ Flow	Life Support	Standard
		Height (cm)	Available [kg]	Rate [kg/hr]*	Duration [min]	Operating Mode
C1.1	18	22	1.2	3.7	20	Open Loop
C1.2	21	22	2.4	3.7	40	Open Loop
C2.1	28	30	1.2	1.9	80	Open Loop
C2.2	31	30	2.4	1.9	120	Open Loop
C3	44	43	1.0	1.2	240	Closed Loop
C4.1	55	60	2.2	1.2/1.9	280	Closed/Open
C4.2	58	60	3.4	1.2/1.9	320	Closed/Open
C5.1	61	60	2.2	1.2/1.9	400	Closed/Open
C5.2	65	60	3.4	1.2/1.9	440	Closed/Open
C5.3	68	60	4.6	1.2/1.9	480	Closed/Open

^{*}Values based on standard operating pressures from references.^{2,3}

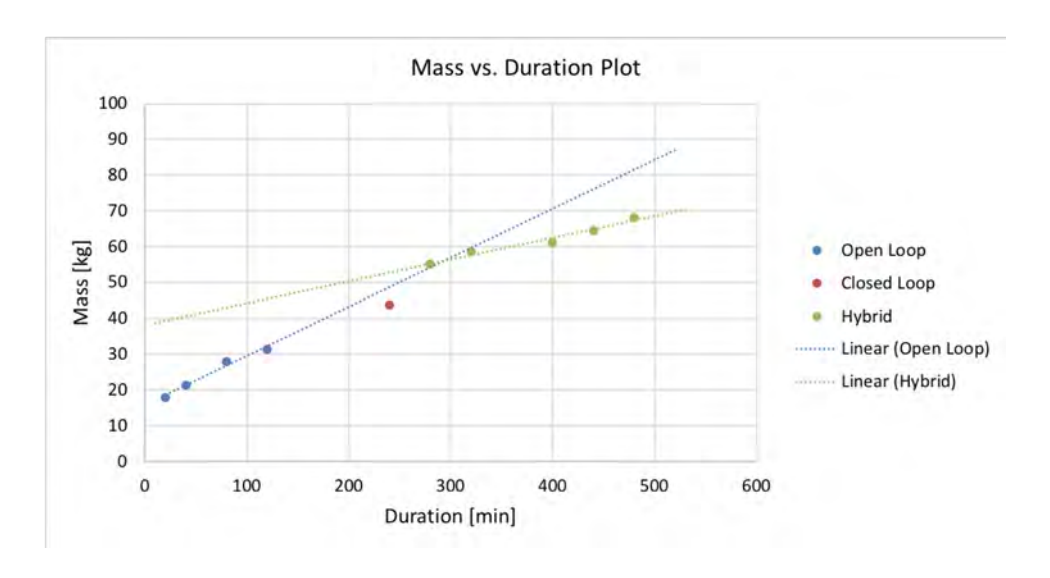


Figure 8. Suit-mounted life support system mass vs. operational use time

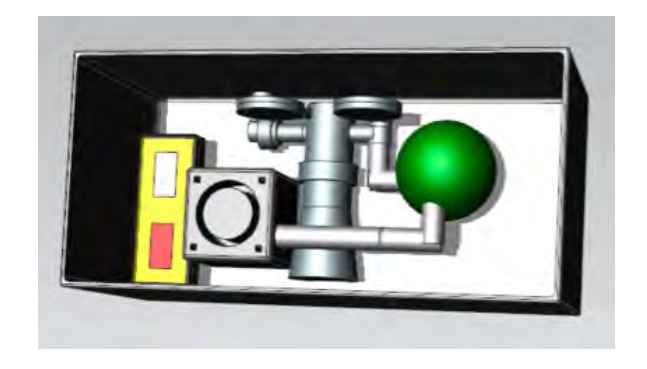


Figure 9. PLSS configuration 1.1 – open loop O_2 system for breathing and cooling, 20 minute duration

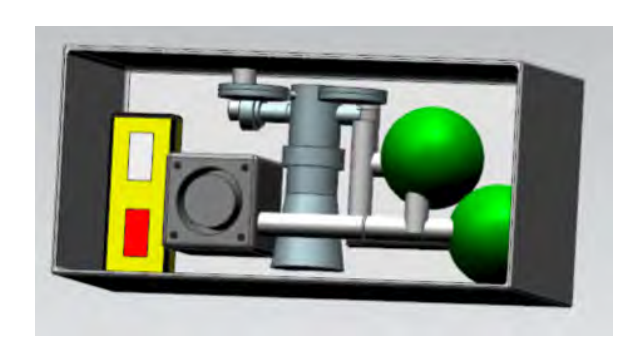


Figure 10. PLSS configuration 1.2 – additional O_2 tank in PLSS 1.1 configuration increases duration to 40 minutes



Figure 11. PLSS configuration 2.1 – open-loop O_2 breathing system with thermal cooling loop, 80 minute duration

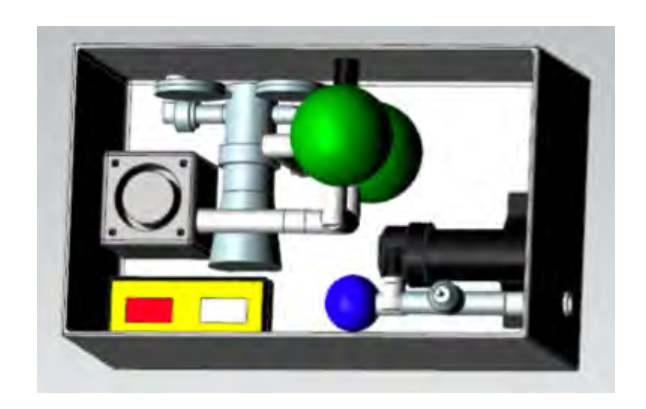


Figure 12. PLSS configuration 2.2 – additional O_2 tank in PLSS 2.1 configuration increases duration to 120 minutes

the AEMU design, including a primary oxygen loop, thermal loop, and oxygen ventilation loop. The primary oxygen loop consists of several components including pressure regulating valves, pressure vessel, pressure transducers, and the necessary tubing for the loop.⁴ These components were determined by looking at the AEMU schematics, and its main functions include providing breathable oxygen and suit pressurization.³ The primary components of the oxygen ventilation loop include the rapid cycle amine CO₂ scrubber, centrifugal fan, check valves, a controller to regulate airflow for monitoring CO₂ levels, relief valves, motor, heat exchanger, and necessary tubing for the loop,⁴ and is used for CO₂ washout and humidity control.³ The thermal loop has essentially the same components as the ATCL but is sized to accommodate up to a maximum of 360 minutes of liquid cooling for the astronaut. However, the C3 configuration is only intended to be used for up to 240 minutes of additional life support, as there is no redundant/secondary oxygen assembly (or OPS) for the primary oxygen loop in this configuration.

The C4 configuration is a combination of the C2 and C3 configurations. The C4 series options have a primary oxygen loop, thermal loop, oxygen ventilation loop, and an oxygen purge system similar to the AEMU, except the OPS replaces the secondary oxygen assembly that is used in the AEMU.⁴ In the C4 series configurations (Figures 14 and 15), the OPS is used as a back-up to the primary oxygen loop as opposed to the primary source of oxygen/suit pressurization as it was in the C1 and C2 configurations. The primary oxygen loop, thermal loop, and oxygen ventilation loop all operate in a closed loop mode, and can support a minimum of an additional 240 minutes of life support on its own, as it is equivalent to the C3 configuration. Once the space suit pressure drops below a certain value (3.8 psi),³ the redundant life support system will be activated and operated in an open loop mode, allowing for an additional 40 minutes and 80 minutes of life support, respectively, for the C4.1 and C4.2 configurations. The C5 configurations are the same as the C4 configurations, except there is the addition of the auxiliary thermal control loop, which was used in the C2 series configurations. The addition of the auxiliary thermal control loop extends the cooling capacity, allowing for longer EVAs. The C5.1 configuration (Figure 16) will provide 360 minutes of life support from the primary oxygen loop, plus an additional 40 minutes of life support from the OPS configuration; the OPS used for the C5.2 and C5.3

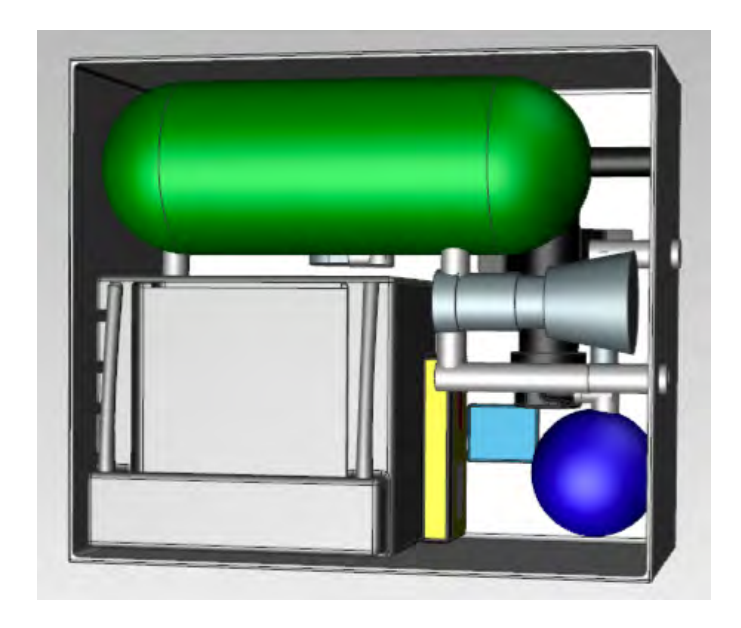


Figure 13. PLSS configuration 3 – closed-loop O_2 breathing system with thermal cooling loop but no secondary system, 240 minutes duration

configurations (Figures 17 and 18) will provide an additional 80 minutes and 120 minutes of additional life support, respectively.

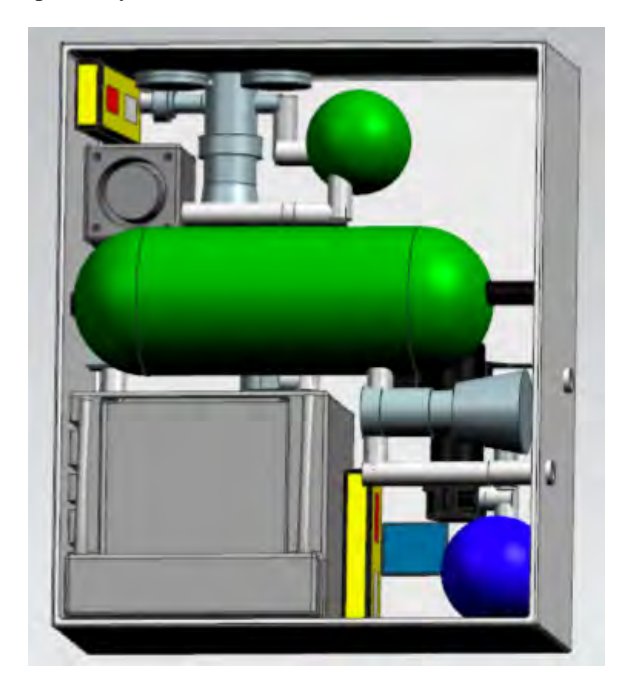


Figure 14. PLSS configuration 4.1 – closed-loop O_2 breathing system with thermal cooling loop for 240 minutes of nominal EVA; secondary open-loop O_2 system for additional 40 minutes

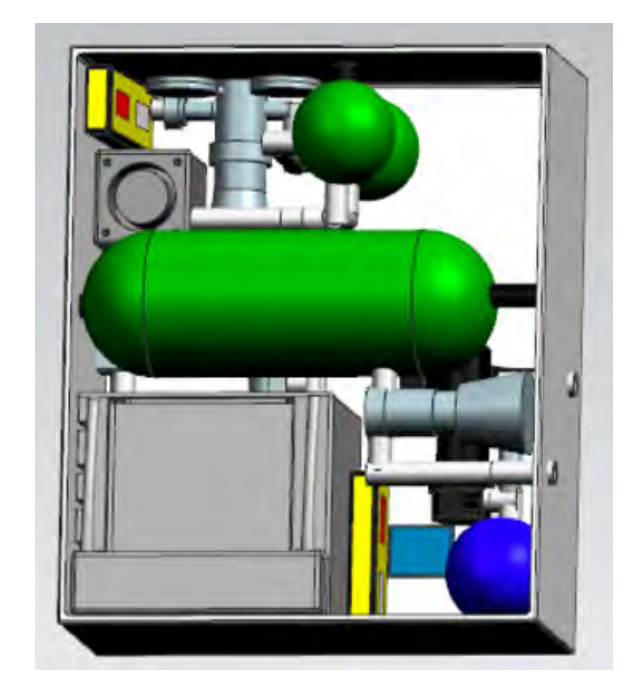


Figure 15. PLSS configuration 4.2 – second secondary O_2 tank in PLSS 4.1 configuration increases secondary open-loop supply to 80 minutes

While the astronauts will nominally be tethered to BioBot via an umbilical for life support, as mentioned previously, there are cases in which the crew may want to detach from BioBot. Untethered operations could provide advantages over tethered operations in situations in which it may be difficult or impossible for BioBot to traverse a certain terrain. Table 2 shows the amount of untethered time a crew member may have from BioBot, as well as

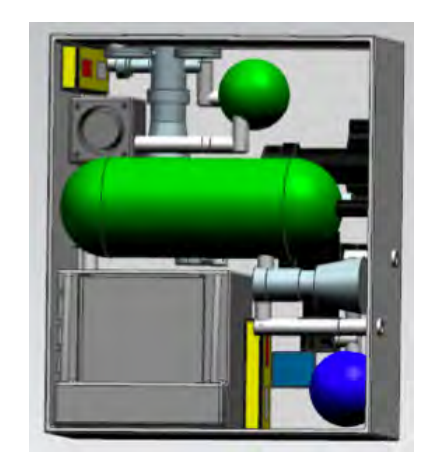


Figure 16. PLSS configuration 5.1 – closed-loop O_2 breathing system with thermal cooling loop for 360 minutes of nominal EVA; secondary open-loop O_2 breathing system with secondary thermal cooling loop for additional 40 minutes

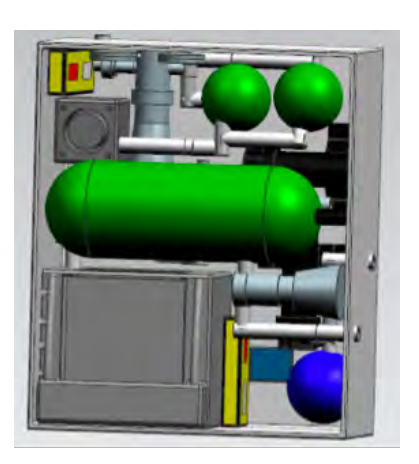


Figure 17. PLSS configuration 5.2 – second secondary O_2 tank in PLSS 5.1 configuration increases secondary open-loop operations to 80 minutes

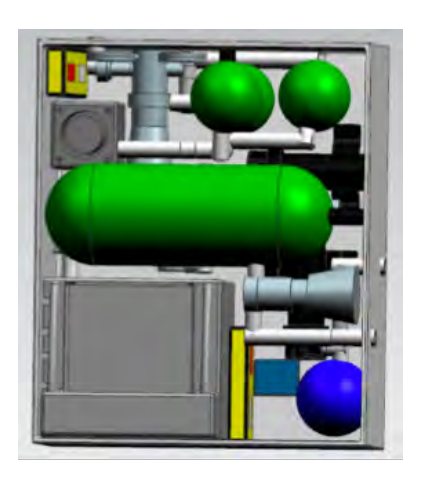


Figure 18. PLSS configuration 5.3 – third secondary O_2 tank in PLSS 5.1 configuration increases secondary open-loop operations to 80 minutes

the maximum distance that a crew member may travel away from BioBot from untethered. All configurations allow for untethered time, except for the C1.1 configuration. The reason for this is the underlying requirement that the crew member shall always have a minimum of 20 minutes of additional life support in reserve when untethered from BioBot, and this reserve life support should only be used in an untethered scenario if there is an emergency. The maximum allowable distance values are based off of assuming an average walking speed of 0.5 m/s, so the distance values provided are conservative estimates.

Table 2. Allowable straight-line traverse distances for suit-mounted life support system configurations

Configuration	Mass	Life Support	Un-tethered Operations	Maximum Allowed Un-Tethered
	[kg]	Duration [min]	Duration [min]	Distance from BioBot [km]
C1.1	18	20	N/A	N/A
C1.2	21	40	20	0.6
C2.1	28	80	60	1.8
C2.2	31	120	100	3.0
C3	44	240	220	6.6
C4.1	55	280	260	7.8
C4.2	58	320	300	9.0
C5.1	61	400	380	11.4
C5.2	65	440	420	12.6
C5.3	68	480	460	13.8

IV. Initial Prototype Development and Testing

Although hardware development is not traditionally a large part of a Phase I NIAC effort, it was felt that the BioBot concept could only be adequately evaluated on the basis of a realistic implementation of the system to allow meaningful user evaluations. To that end, the BioBot team adapted an existing Segway RMP440LE mobility base for use in BioBot testing through the addition of an external framework for payload mounting, fenders to protect humans and payloads from adjacent wheels, and the implementation of a control system using the Robotic Operating Systems (ROS), an open-source platform for robot control. A radio controlled E-stop was added to remotely command the

robot to stop/brake. The RMP440LE is suboptimal for realistic testing of the concept largely because of its lack of a suspension system, which limits its ability to overcome obstacles in field testing. It did prove to be an excellent development platform for the Phase I studies, however, and has been used extensively for laboratory and light field testing of various BioBot concepts and candidate system designs.

The BioBot concept is clearly predicated on the development of robotic technologies to autonomously tend the umbilicals attaching the EVA crew to BioBot, ensuring the continual supply of life support to the suit without snagging the local terrain or interfering with crew mobility. The original concept was to provide single or double lifting points to the umbilical, to keep the catenaries far enough above the ground to prevent contact. This was mocked up and tested with materials on hand, mounted on the Segway robotic mobility base (Figure 19). As an early proof of concept, a student researcher manually actuated the "robotic manipulator" for controlling the umbilical while another student acted as the test subject.

This initial mockup was used to test different umbilical lengths, supports on the umbilical, and feasible areas of operation for the astronaut tethered to BioBot. A retractable umbilical on a reel was mounted to the back side of the rails, and a person seated on the Segway controlled the umbilical support structure. The initial assessment goal was to see how much assistance the umbilical needed to allow the EVA crew free movement around obstructions, and to keep the umbilical from touching the ground or elevated obstacles. While these tests were promising from the standpoint of avoiding snag hazards, the physics of an umbilical forming a catenary between two end supports meant the simulated EVA crew had to support half of the umbilical weight; this reduced the effectiveness of the overall concept in terms of offsetting loads on the astronaut. There were also some concerns about lateral swinging of the umbilical catenary, which would induce cyclic side-to-side loads on the astronaut. This testing indicated more complete support and control of the umbilical were needed to minimize the physical and cognitive loads on the BioBot user.



Figure 19. Initial test of umbilical management

V. Umbilical Handling Technology Development

Subsequent development focused on manipulators with extended kinematics to keep the umbilical elevated, connect to the EVA suit in its immediate vicinity to minimize weight load, and track crew motions within a 5-10m radius of the mobility base. Two approaches were implemented in this stage of development: an actively-controlled manipulator, and a pantograph-type passive kinematic chain for automatic umbilical handling. The powered manipulator (Figure 20) was implemented using engineering prototyping extrusions and electromechanical linear actuators for high torque. While this worked satisfactorily, the computational complexity of performing inverse kinematics as the EVA crew moved about presented an interesting control challenge beyond the scope of this initial proof-of-concept testing. This test apparatus did demonstrate the ability to easily rotate the umbilical handling system on a passive base yaw

joint, eliminating the need for actuation and control in that axis.

The ease of passive actuation in base yaw led to a focused effort to produce an entirely passive umbilical handling system (UHS). An isokinetic structure inspired by Hoberman Sphere kinematics was prototyped in quarter-scale in laser-cut acrylic to validate the design. The full-scale prototype was then fabricated using a computer numerically controlled router from 3/16in plywood, with 3D printed internal spacers and routing blocks for the umbilical. This system was then integrated onto the RMP440LE motion platform for testing (Figure 21), which included the use of the University of Maryland MX-C suit simulator for the first time. The passive system was also found to be feasible, and offered functionality without control or power requirements, but needs to be redesigned to increase torsional stiffness and to suppress an over-center "latching" behavior.





Figure 20. Actively controlled robotic umbilical handling mechanism

Figure 21. Passive pantographic umbilical handling mechanism

At this point, development of the umbilical handling system is proceeding on both the active and passive concepts. The active system appears to be lighter and more easily stowed, but is more complex and requires continual autonomous control inputs. The passive system has more rotational joints and is kinematically complex, but had lower reaction forces at the spacesuit than the current active system, and does not add power or control requirements to the BioBot. Both systems will be further refined and tested before settling on the best design for a protoflight unit.

VI. Autonomy Technology Development

Since the aim of the BioBot is to increase crew mobility without imposing new restrictions or requiring additional crew resources, it is critical that the rover be able to navigate without need of human intervention. While current Mars rovers operate autonomously over a distance of tens of meters, the BioBot mission requires that the vehicle travel at human traverse speeds, which are an order of magnitude faster than the Mars rovers. The BioBot's navigation system must also be able to autonomously follow its user, avoid unknown obstacles, and maintain a safe and consistent following distance so as to prevent collisions with its crew member. Autonomous following and obstacle avoidance is accomplished through the Robotic Operating System (ROS) and the integration of the ROS navigation stack with the AprilTags visual fiducial system.

The software operates in the following sequence. A camera on board BioBot streams video data to the AprilTags software, which detects the fiducial tags (Figure 22) worn by the astronaut, and outputs data concerning the tags' position and orientation to the navigation stack. While the astronaut is only required to wear one tag for the system to operate, multiple tags provide robustness in the system in the event that one of the tags is obstructed from the view of the camera.



Figure 22. Examples of AprilTag markers

The navigation stack then uses the position data sent from the AprilTags software to set a new navigation goal. To prevent the rover from colliding with crew members, the goal is offset from the astronaut by one meter while maintaining the original orientation and polar coordinate angle of the tag. In the event that the astronaut comes within one meter of the robot, the software sends zero velocity commands to stop BioBot motion. The adjusted goal is combined with data published from a visual depth sensor, which sends information to the navigation stack about obstacles in the robot's path. Since the navigation stack requires a laser scanner (rather than a depth sensor), an intermediate ROS node converts the depth sensor data to laser-scan data in the current system. Finally, the stack combines the navigation goal with the laser-scan data to plan paths around the detected obstacles. The flow chart in Figure 23 summarizes this process.

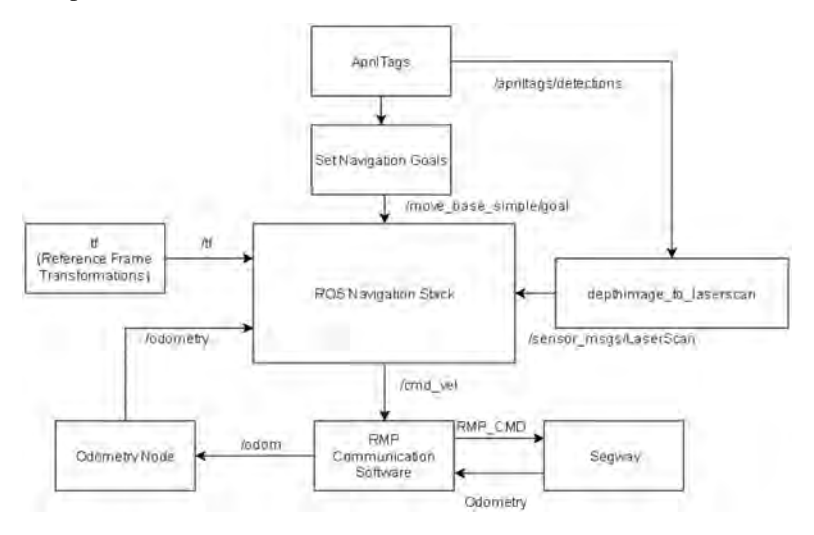


Figure 23. Software architecture - boxes represent ROS nodes, arrows are topics

Each component – the camera, depth-sensor, AprilTags, and navigation stack – uses ROS to send and receive messages. Since the components are independent of one another from a software perspective, ROS allows for extended modularity; thus, the software package can easily accommodate new laser scanners and cameras, or even be implemented directly on a robotic platform other than the Segway RMP.

Testing hardware includes an Xbox 360 Kinect, which houses a visual depth sensor and camera and is powered by the Segway RMP's auxiliary battery (12V, 1.2A). Both the Kinect and Segway are connected to a laptop running Linux Ubuntu 16.04 with ROS Kinetic. For future iterations, the laptop will be replaced by an on-board computer dedicated solely to BioBot, and the Kinect will be replaced by a more robust laser scanner that can operate in brighter, outdoor environments.

The process is illustrated (Figure 24) with RVIZ, a ROS visualization software package. As shown, the software sets its goal (shown as a purple arrow) a meter ahead of the AprilTag marker, which is represented by a purple box. The base of the arrow indicates the position of the goal in the world map, and its direction indicates the orientation of the goal. The software uses data sent from the depth sensor and laser scan node, depicted as white lines, to construct a cost map which identifies low cost areas as light gray and high cost areas as black. Any object within the inflation radius is considered an obstacle and assigned a high cost. The navigation stack then uses Dijkstra's algorithm to operate over the cost map and identify the lowest cost path from the robot to the goal pose, shown as a green line. On the right, the real-world image is also displayed as a reference. The marker is placed on the gray bin in the center of the image.

VII. Additional Innovations Enabled by BioBot System

As the design process proceeded and the various BioBot configurations emerged, it became clear that the BioBot concept would enable a number of other capabilities to enhance future planetary surface research. Obviously, a rover accompanying an EVA crew would be a logical place to locate communications, video cameras, and science systems such as sampling robotics or core drills. Beyond those "mundane" augmentations, relieving the mass limitations on the suit and crew simultaneously eases logistics-based constraints such as distance and duration. At minimal impact to the user, a BioBot could carry oxygen, cooling water, CO₂ scrubbing, and power far beyond the current six-hour

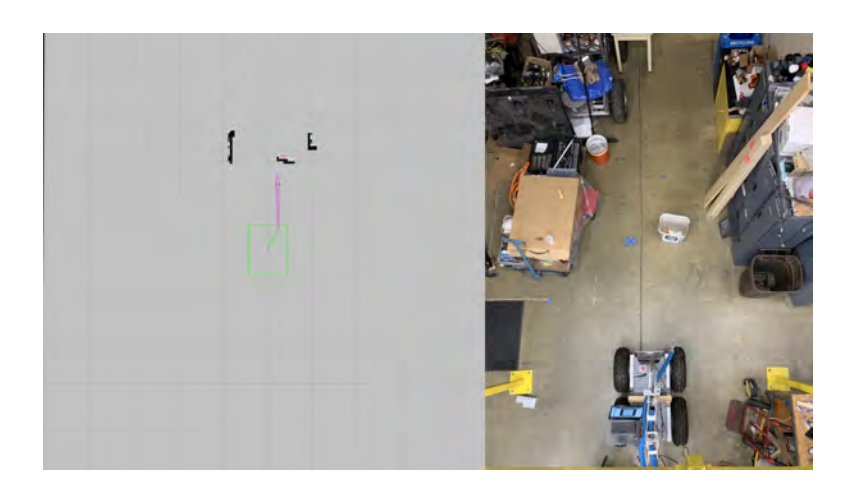


Figure 24. (Left) RVIZ representation of navigation software. (Right) Corresponding real-world environment

nominal limitation. The endurance of the EVA system would be limited only by the crew's physiological limits of wearing and operating in a pressure suit.

One of the concerns for Mars exploration is that the density of the Martian atmosphere is too great to allow the use of sublimation cooling, which has been the standard practice in all PLSS designs to date. A BioBot system would allow the use of "low-tech" solutions such as an ice reservoir to dissipate waste heat via water phase change and specific heat. On the other hand, eliminating the volumetric and surface area limitations of a backpack-mounted PLSS would make the use of radiators feasible, particularly with innovative concepts such as the use of Peltier junctions to increase the temperature of the radiators. Similarly, EVA duration could be augmented by photovoltaic arrays on the BioBot for real-time power generation. Alternatives to canister-based CO₂ scrubbing could minimize resupplies between EVA sorties, and further reduce limitations on EVA duration. Innovative logistics concepts such as the use of hydrogen peroxide as a single source of oxygen, power, and cooling water (a previous NIAC study) would become a viable candidate for consideration.

VIII. Conclusions and Future Plans

At the end of the nine-month NIAC Phase 1 program, the University of Maryland team has shown that the BioBot concept is definitely feasible. All of the critical elements of the concept – autonomous tracking of a suited subject, provision and tendering of life support umbilicals, and reduction of PLSS weight – have been demonstrated on a prototype system. Trade studies have examined the ability of the user to adopt various suit-mounted life support systems to allow various periods of independent activity ranging from 20 minutes to a nominal six hours. A probabilistic risk assessment has shown that the BioBot concept can meet a loss of crew reliability requirement below 0.1%, and that the ideal architecture for a two-person EVA using BioBots would be two individual units with the ability to provide life support to and carry both crew in the event of a life support or mobility unit failure.

While future developments are dependent on the availability of funding, one of the advantages of the university environment is that some research can and will proceed using volunteer student effort even in the event of a hiatus in sponsored research funding. At this point, the most critical task remaining is that of proving trafficability of the BioBot vehicle into regions capable of EVA traverse. The logical next step would focus on the development of a BioBot end-to-end prototype for analog field trials, including a highly capable mobility chassis, an optimized umbilical handling system, and a vehicle-mounted life support system (ventilation air, cooling water, communications, and monitoring electronics) compatible with a next-generation spacesuit simulator: the MX-D, currently under development at the University of Maryland. The current focus for this program phase will be to perform field testing at the NASA Johnson Space Center "Rockyard" planetary surface simulation facility, to elicit feedback and evaluations from the EVA and robotics branches of NASA.

Subsequent follow-on activities would be to assess the end-to-end BioBot prototype at extended-duration analog test sites, such as the Mars Desert Research Station or HI-SEAS facility. This would allow the collection of user data during extended operations, again using an MX-D or equivalent spacesuit simulator. In parallel, it would be ideal to

develop a BioBot system capable of supporting a full pressure suit in analog field trials such as the NASA Desert RATS tests, to assess the effect of the robot-transported life support system based on a previously-developed system such as the Oceaneering liquid-air backpack.

Work done to date has met the letter and spirit of the NIAC program: taken a "blue-sky" concept, demonstrated basic feasibility, and identified both the benefits of a successful implementation for future space missions and a path forward for further development. More detailed design, fabrication, and testing will be necessary to bring the BioBot concept to the technology readiness level where it would become a viable candidate for use in a future exploration surface architecture.

Acknowledgements

The authors would express our appreciation to like to thank the Jason Derleth and the NASA Innovative Advanced Concepts (NIAC) Program for sponsoring the BioBot Phase I research program. We would also like to like to thank Erik Bryson and the Maryland Space Grant Consortium, which sponsored him for a summer internship with the BioBot team. Erik did much of the work designing and prototyping the active robot arm for the umbilical handling system. Great appreciation to Justin Kanga, who drew the highly useful and informative graphic in Figure 1.

References

¹William C. Stone, "Design of Extended Range EVA PLSS Systems: Lessons From Terrestrial Exploration Missions" Space Studies Institute 12th Conference on Space Manufacturing, Princeton, NJ, May 8-11, 1997.

²"Portable Life Support System" NASA.gov, www.hq.nasa.gov/alsj/LM15_Portable_Life_Support_System_ppP1-5.pdf. Accessed 27 Feb. 2019.

³Campbell, Colin. "Advanced EMU Portable Life Support System (PLSS) and Shuttle/ISS EMU Schematics, a Comparison" American Institute of Aeronautics and Astronautics.

⁴Schematics and Behavioral Description for the Advanced EMU (AEMU) Portable Life Support Subsystem (PLSS). NTRS.NASA.gov, ntrs.nasa.gov/archive/nasa/casi.ntrs.nasa.gov/20170009505.pdf. Accessed 27 Feb. 2019.

⁵Christopher Carlsen and David L. Akin, "Investigation of a Solid-State Cooling System for Analog EVA Life Support" ICES-2018-256, 48th International Conference on Environmental Systems, Albuquerque, New Mexico, 8-12 July 2018

⁶Craig M. Lewandowski and David L. Akin, "Development of a Single-Fluid Consumable Infrastructure for Portable Life Support Systems" SAE 2007-01-3246, 37th International Conference on Environmental Systems, Chicago, IL, July 2007

Design and Development of an EVA Assistance Roving Vehicle for Artemis and Beyond

David L. Akin¹, Charles Hanner², Nicolas Bolatto³, Daniil Gribok², and Zachary Lachance² *University Of Maryland, College Park, MD, 20742, USA*

It seems logical that the Artemis program to return humans to the Moon should begin with capabilities at least equivalent to the last Apollo missions: specifically, a roving vehicle for crew transport. Given the intervening half-century, such a vehicle should also have advanced robotic capabilities to enhance and extend human exploration activities. Under support from the NASA Moon-to-Mars X-Hab program, the University of Maryland is developing such a robotic roving vehicle concept for Earth analog testing and evaluation. The approach taken is to design a vehicle for lunar use, then prototype the most similar vehicle possible for testing on Earth. Rather than a single vehicle for two EVA crew, probabilistic risk assessments indicated a greater utility for two vehicles designed for nominal single-person use, but each capable of carrying a second EVA crew in the event of a vehicle failure. This mitigates the Apollo-era stringent "walk-back" criteria, which limited both overall traverse distance and allowable exploration time at remote sites. Since human lunar landing systems are in preliminary design at this time, the UMd rover design was constrained to permit launching a pair on a single Commercial Lunar Payload Services (CLPS) landing mission, allowing the rovers to be pre-emplaced at the Artemis landing site before the arrival of the crew. The mobility system for the rover is designed to transport a 170 kg suited crew with 80 kg of exploration payload in nominal circumstances, and to additionally transport a second 170 kg crew as a contingency. The rover is designed for a top speed of 4 m/sec, "cruising" speed of 2.5 m/sec, with a 54 km range and peak slope capability of 20°. The paper covers design trades, prototype fabrication, and plans for initial testing results in analog conditions with EVA simulation.

I. Introduction

Nothing made a larger impact on the science and exploration functions of the Apollo lunar missions than the addition of the Lunar Roving Vehicle (LRV) for Apollos 15, 16, and 17. These vehicles were made feasible by performance increases in the lunar module (LM), and had an empty mass of 210 kg with a design payload of 490 kg. The primary (non-rechargeable) batteries provided a theoretical maximum traverse distance of 92 km, although the actual data from the three missions using the LRV are listed in Table 1. This data can be compared to that of Apollo 14, which was the last mission limited to walking for crew surface mobility. While the Apollo 14 mission only included two EVAs compared to three for each LRV-equipped mission, the total estimated traverse distance of 5.3 km was only 15-20% that of the later missions. A more direct comparison would be the longest Apollo 14 traverse of 2.4 km in total, which represents only 12-20% the distance of the longest single traverse for each mission using the LRV. Each of the LRV missions also more than doubled the mass of lunar samples taken compared to Apollo 14.

With Project Artemis, NASA has announced its intention to send "the first woman and the next man" to the Moon as expeditiously as possible. While discussions until recently had focused on a first landing in calendar year 2024, recent budget allocations and the change of administrations have refocused efforts on arguably more viable targets between 2026 and 2028 for that mission. Given the very tight budget constraints and short development lead time, it seems likely that the first human lunar exploration mission in almost 60 years will be more like Apollo 14 or earlier landing missions than the later "J-class" Apollo missions with LRVs.

¹Director, Space Systems Laboratory. Associate Professor, Department of Aerospace Engineering

²Graduate Research Assistant, Space Systems Laboratory

³Undergraduate Research Assistant, Space Systems Laboratory

Table 1. Performance of Apollo Lunar Roving Vehicles (adapted from Morea¹)

	Apollo 15	Apollo 16	Apollo 17
Surface distance traveled (km)	27.9	26.7	35.9
Longest single-EVA traverse (km)	12.5	11.6	20.1
Max distance from LM (km)	5.0	4.5	7.6
Average speed (m/sec)	2.54	2.15	2.24
Fraction of EVA time driving	16.3%	16.3%	20.6%

II. Providing Rovers for Early Artemis Missions

So what is to prevent having an LRV-type rover on the first Artemis landing mission? The obvious culprit is the cost, but the \$32M cost for the LRV program (including four flight vehicles) in 1970 would convert to \$297M in 2021, less than 15% the expected cost of a single SLS launch vehicle. A more likely issue is the present uncertainty about the human landing system (HLS) currently in the early stages of development. At the time of writing, three corporate entities have initial contracts to develop an HLS vehicle design, with the expectation of downselect to one or two systems in the coming months. The early stage of design precludes any reliable knowledge on the allowable mass or volume for landed payload as part of a human mission. Combining cost constraints and the uncertainty over HLS performance drives towards the assumption that LRV-type unpressurized rovers would come on a later Artemis mission. Given NASA enthusiasm for pressurized rovers, it might be suspected that LRV-type systems will not be needed at all in the Artemis program architecture.

This, however, would be a mistake. A pressurized rover would mass 4-6 metric tons, requiring a dedicated mission to deliver a rover with a mass of the same order of magnitude as a human cabin, assuming the use of an HLS lander for the large mass. Use of a top-level cost estimating algorithm³ predicts a cost of approximately \$3B for the development and production of a single unit for a pressurized rover. Given the tight cost constraints of the Artemis program, it is clear that a pressurized rover would not be available until well into the sequence of human landings. Until that time, Artemis crews would be restricted to explorations within safe walking range of their landers.

Nor is it clear that a pressurized rover is superior to an unpressurized rover in all circumstances. The benefit of a pressurized rover, other than its ability to greatly extend the exploration range by supporting multi-day sorties, is that the crew need not spend the day in a pressurized suit, but can "pop out" via a suitport for a brief surface excursion whenever it seems useful. This concept was checked via an examination of Apollo experience with the LRV, summarized in Figure 1. For the purpose of this brief analysis, it was assumed that egress or ingress via a suitport would take 5-10 minutes, so it would be inefficient to egress if the planned surface interval was less than twice that time (20 minutes), or to ingress to travel to the next site if the traverse time were likewise less than 20 minutes. As shown in this figure, only a small fraction of the Apollo surface stops would have met this criteria for egress from a pressurized rover. Indeed, NASA field tests with the Space Exploration Vehicle (SEV) prototypes evolved to provide an external driving station to allow short traverses with the crew in their suits but docked to the suitports, thereby using the SEV somewhat like an unpressurized rover for extended periods.

The Apollo LRV represents an existence proof for a small, lightweight rover carried with the crew to the lunar surface. However, it is difficult to make intelligent plans for such a vehicle in the absence of any information on the potential cargo mass and volume limits for the as-yet-unselected human landing system. However, there is another alternative: the Commercial Lunar Payload Services (CLPS) program and its planned set of small cargo transports for lunar surface delivery. One of the larger planned systems, the Astrobotics Griffin lander, is designed for a landed payload mass of 475 kg,⁴ more than enough for the 210 kg Apollo LRV.

While it is conceptually possible to rebuild an Apollo LRV and use it for early Artemis missions, it would be a mistake to do so. The LRV was designed solely as a human-operated vehicle, and would require astronauts on site to unload and drive it. This would miss valuable new opportunities, such as using the rover to survey the planned landing site to select a specific landing target location, or to allow science teams to more accurately map out the highest priority exploration targets for the Artemis crew. A rover with autonomy and/or Earth control modes would also allow extended exploration after the completion of the human mission.

Once we have committed to the concept of developing a new unpressurized rover, another augmentation of capabilities is reached with a simple concept: don't send one rover, send two. Specifically, replace the two-person design

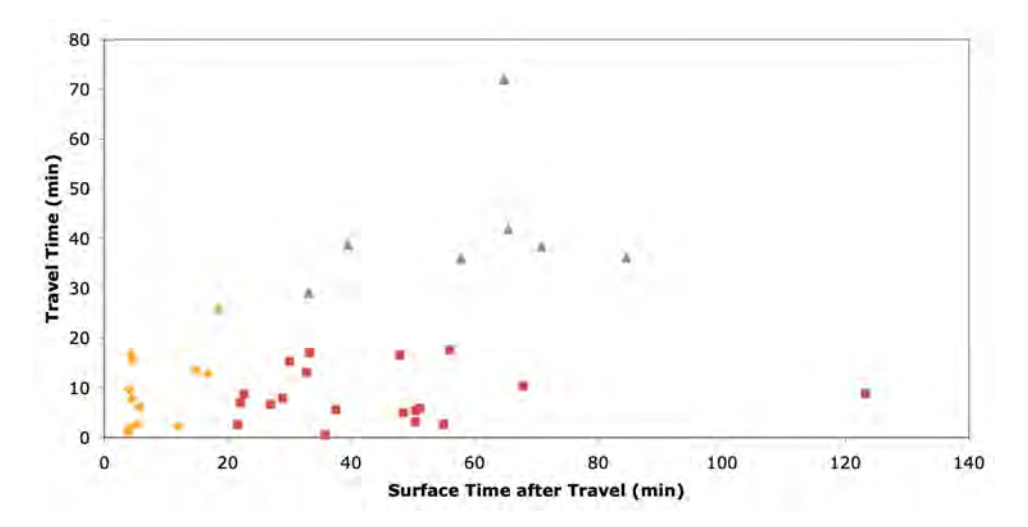


Figure 1. Apollo LRV EVA correlation of duration of LRV traverse plotted against subsequent duration of surface activities. Red: travel duration less than 20 minutes; yellow: surface duration less than 20 minutes; green: travel greater than 20 minutes followed by surface duration greater than 20 minutes. It is argued that only the green cases would be well served by a pressurized rover.

of the LRV with two single-person rovers. While LRV increased the range of human exploration five-fold, all EVA planning was based on the imperative of the *walkback criterion*: the crew would never be allowed to be farther away from the lander than they had sufficient consumables in their portable life support systems to allow them to walk back and ingress with a safety margin. This mandated sortie plans which started with the longest traverse at the beginning of the EVA, and continual driving back towards the lander as the sortie progressed. As life support consumables were expended, the allowable distance from the lander decreased steadily. This caused several instances on Apollo where the crew was ordered to leave scientifically interesting sites to head closer to the LM to stay within walkback constraints. It also limited the maximum distance the crew would be allowed to travel from the lander to the 7.6 km from Apollo 17, although more recent testing has indicated that 10 km would probably be a feasible limit for walkback.⁵

The walkback limitation would be reduced or eliminated with the provision of two rovers, each intended for one rider nominally but capable of carrying two crew in a contingency. In this case, failure of a rover would result in both EVA crew riding the functional unit back to the lander or habitat, allowing travel times 1/2-1/4 those of walking depending on the specific terrain, with much lower physiological workloads (and required life support consumables). The capability for autonomy or ground control would further increase crew safety, allowing an incapacitated EVA crew to ride a functional rover back to the lander without actively controlling the vehicle locally.

Based on this argument, the University of Maryland started a program to examine the feasibility of a single-person lunar rover design capable of being delivered as a pair on a single CLPS lander prior to the first Artemis human landing, and available to the initial crew throughout their surface stay, while operating under a combination of autonomy and ground control before and after the human mission. This formed the basis of a successful proposal to the NASA Moon-to-Mars X-Hab program, which has supported the project to date.

III. Requirements Development

To begin the design process, a set of Level 1 requirements for the rover was established. Like all good academic projects, this one was designed to satisfy more than one requirement. The Level 1 requirements were established for a lunar rover that meets the goal of two functional rovers on a CLPS lander. However, there was always the intent to develop a physical version of the design for Earth analog testing, with necessary modifications to the lunar design to make it functional on Earth. Initial design efforts would form the core of the Fall 2020 graduate class in Planetary Surface Robotics in the University of Maryland Department of Aerospace Engineering, which would also provide a series of point designs to lead into the Earth analog rover development process. Bearing all of that in mind, the following set of Level 1 requirements was created for the lunar rover designs.

1. Rover shall have a maximum operating speed of at least 4 m/sec on level, flat terrain – This corresponds to 14.4 kph, based on the published LRV top speed of 13 kph, although the LRV Operations Handbook⁶ states that the

- LRV is "uncontrollable" above 10 kph (2.8 m/sec).
- 2. Rover shall be designed to accommodate a 0.3 m obstacle at minimal velocity This sets a minimum ground clearance of 30 cm, comparable to the 35 cm ground clearance for the LRV.
- 3. Rover shall be designed to accommodate a 0.1 m obstacle at a velocity of 2.5 m/sec This was deemed a reasonable value for an obstacle which could be safely driven over at a nominal cruise speed.
- 4. Rover shall be designed to safely accommodate a 20° slope in any direction at a speed of at least 1 m/sec and including the ability to start and stop The Lunar Exploration Science Working Group study of 1995 found that, for general access to anywhere on the moon, rovers should be capable of ascending and descending a 25° slope. This did not look at the dynamics of locomotion, including the interactions of slopes with turning and acceleration limits, or the increasing difficulty of specifying motors and gearing for peak slopes while accommodating desired maximum velocities. Since even younger craters with steeper wall slopes usually have one or more ingress/egress routes with more limited slopes, the decision was made to adopt 20° as the maximum slope including a worst-case turn and/or acceleration profile.
- 5. The rover shall have a nominal sortic range of 54 km at an average speed of 2.5 m/sec This is six hours of constant driving on level terrain at 2.5 m/sec. On the basis of kinetic energy, it also equals 2.4 hours of driving at the peak speed of 4 m/sec, with a total traverse distance of 34 km. This provides a significant energy margin for sorties involving maximal slopes over extended distances.
- 6. Rover shall be capable of carrying one 170 kg EVA crew and 80 kg of assorted payload in nominal conditions—
 The nominal mass of the EVA crew was based on an 80 kg astronaut and a 90 kg spacesuit/life support system.
 The 80 kg of additional payload was allocated for tools, science instruments, and samples.
- 7. Payload may be modeled as a 0.25 m³ box This was a minimal constraint to ensure that there was some space on the rover deck for payload other than the crew.
- 8. Rover shall be capable of also carrying a second 170 kg EVA crew in a contingency situation. Payload may be jettisoned if design permits Required for the redundancy element of the twin-rover architecture. Jettisoning the nominal payload was left as an additional accommodation for the designers.
- 9. Rover design shall incorporate roll-over protection for the crew and all required ingress/egress aids and crew restraints This was not present on the Apollo LRV nor on most Earth analog rover systems. It would seem to be a good precaution for crew safety, and the presence of a second rover should provide options for righting an overturned rover not feasible based on crew strength alone.
- 10. A nominal sortie shall be at least eight hours long This is based on the fact that later Apollo surface EVAs were six hours or slightly more, and that the HLS requirement document⁷ cites a standard EVA duration of "6±2" hours. The intent was to ensure that the rover would not be the critical item in allowable sortie duration.
- 11. Two rovers must be launched on a single CLPS lander Fundamental to the concept, assuming that the additional capabilities of a more massive rover would not be sufficient to justify doubling the cost by delivering two rovers to the surface via individual CLPS missions.
- 12. A single rover shall mass ≤250 kg This was based on the understanding that the Astrobotics Griffin rover had a 500 kg payload limit, although no specific information was available at the time. Since the creation of these requirements Astrobotics has announced that the Griffin payload limit is 475 kg,⁴ so the actual mass limit should be 237 kg, or 166 kg to leave a 30% mass margin for this preliminary design.
- 13. Rovers shall be developed in time to be used on the first Artemis landing mission This is an unknowable constraint at present, but an assumption of 2026 would probably be appropriate.
- 14. Rover shall be capable of operating indefinitely without crew present Due to the desire to operate extensively in the Artemis exploration site both before and after the crewed mission, the rovers must have the capability to recharge *in situ*.
- 15. Rover shall be be capable of being controlled directly, remotely, or automated This is fundamental to the utility of the rover outside of the crewed mission. It is expected that a combination of teleoperation and ground-supervised autonomy will be the standard operating procedure for uncrewed activities.

- 16. Rover shall be capable of following an astronaut, following an astronaut's path, or autonomous path planning between waypoints Given the nominal operation as a dedicated transport for an individual EVA crew, it makes sense that it may be beneficial to have the rover safely follow the user on an extended traverse on foot to be available for tool exchange or sample curation, as well as eliminating the need for the crew to retrace steps to return to the original parking spot.
- 17. Rover shall be capable of operating during any portion of the lunar day/night cycle and at any latitude This was intended to not preclude the use of the rovers on any particular Artemis mission, regardless of landing site or duration. It should be emphasized that this refers to actual operations; for example, the rover shall be equipped with lighting for driving in lunar night, but is not expected to recharge in the absence of dedicated power supplies during the nighttime.

IV. ENAE788X Point Designs

The Fall 2020 graduate class in Planetary Surface Robotics was given the set of requirements above for a term design project. Four teams of from 2-4 students independently developed designs to meet the requirements, using the analytical tools taught in the class throughout the term. The designs were directed to focus on the mobility aspects, including terramechanics (wheel/soil interactions), weight transfer over obstacles, static and dynamic stability, steering, suspension design, motor and gearbox specification, and related trade studies. The teams also examined placement of the EVA crew and payload and instrumentation for autonomous navigation.

The final designs of the four teams are shown in Figure 2. As a result of trade studies, largely driven by the tight constraint on system mass, all four team chose a four-wheel design over alternatives with larger numbers of wheels. All of the designs used hub-mounted motors and gearboxes in each wheel, and some form of independent suspension. All four designs used a tandem arrangement for carrying two EVA crew in a contingency, with the second crew sitting back-to-back with the driver. Two used independent active wheel steering; one used independent front and rear rack-and-pinion Ackermann steering; and one used skid-steering. Protogonus incorporated the ability to extend the rear wheels and articulate them vertically to increase the stability margin when climbing or descending slopes, and to increase rear deck area to allow carriage of the second EVA crew. SCAMP independently articulated each wheel on a rotating link to allow control of deck angle in both pitch and roll, which both increased stability margins in both axes on slopes and allowed the rover deck to remain horizontal (and the crew upright) throughout all specified terrains.

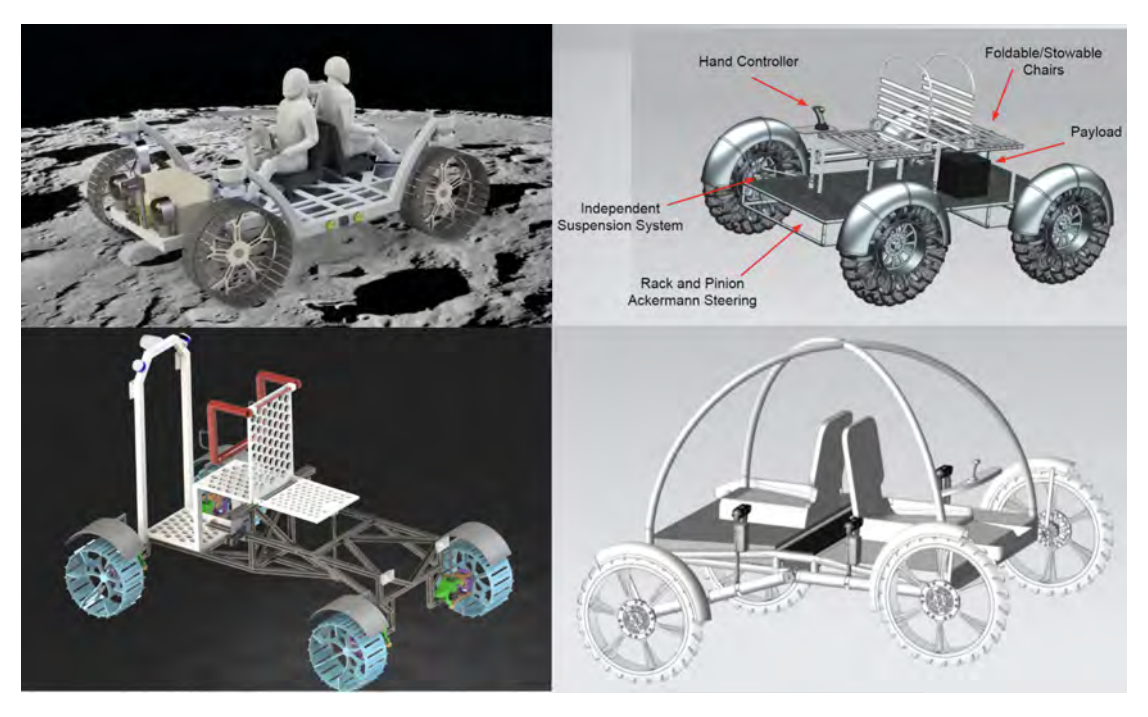


Figure 2. Design studies from ENAE 788X - upper left: ROCI; upper right: Courage; lower left: Protogonus; lower right: SCAMP

V. VERTEX

A. Design Overview

With the completion of the ENAE 788X point designs, the UMd Space Systems Laboratory (SSL) team started the detail design for a rover capable of supporting the first Artemis crewed lunar landing mission with two single-person rovers predeployed using a single CLPS lander. To denote this phase of the development effort, this system was named the Vehicle for Extraterrestrial Research, Transport, and EXploration, or VERTEX. Although the VERTEX design was drawn from the previous lunar designs, VERTEX was to be developed for Earth analog field tests, and was modified as necessary for that environment and mission.

The VERTEX development process started with the detailed examination of the four ENAE 788X point designs and the extraction of design concepts for synthesis into a next-generation design. In addition, a number of requirements were modified or added, as will be discussed in this section. The first added requirement was that in operating mode, VERTEX must have a maximum width less than 150 cm and a maximum length less than 240 cm. In field operations, the rover needs to be easily transported with minimal reconfiguration. Keeping the outer dimensions to less than 5 ft by 8 ft allows it to be driven into a rental panel truck for transport or safekeeping overnight. As it turns out, these dimensional constraints also work well to keep the rover sized such that two can fit on a Griffin CLPS lander deck.

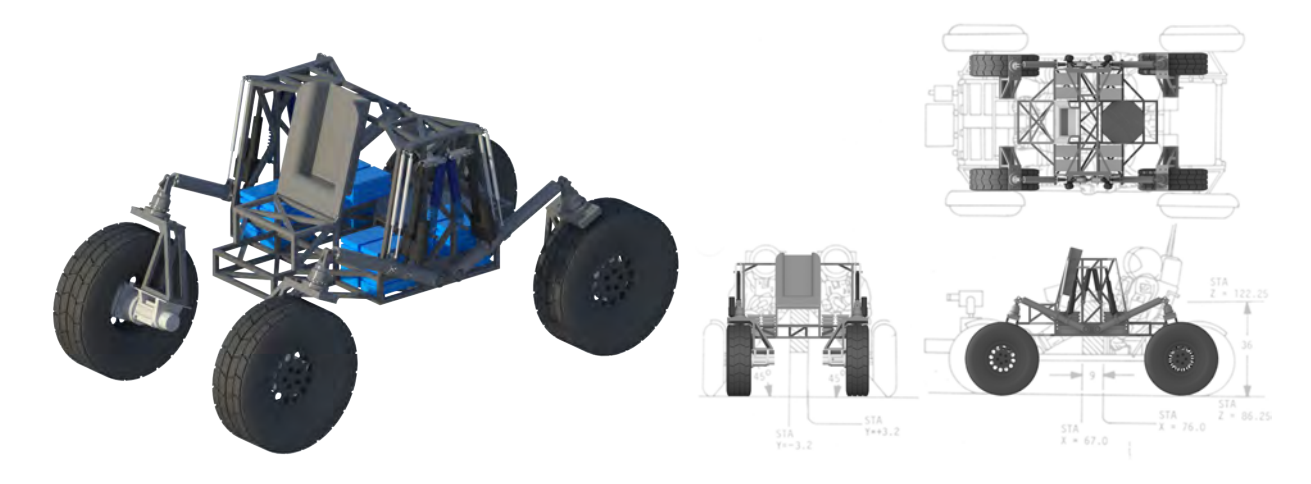


Figure 3. VERTEX design in perspective

Figure 4. Three-view of VERTEX (Apollo LRV in background for scale)

Based on reviews of the four point designs, a number of design decisions were made by the team. In order to keep the rover as small and lightweight as possible, a four-wheeled design would be maintained. The wheels would be

independently suspended and steered to maximize mobility and minimize the effects of unimproved surfaces on ride quality. To enhance stability, the independent articulation via wheel linkages originated on the SCAMP design would be adopted, allowing the deck to remain level in most terrains and especially increasing stability when the center of gravity is high.

The final design of VERTEX is shown in Figure 3. The rover as shown is equipped with commercial off-road pneumatic tires for Earth analog operations; while a design and scale prototype exists for lightweight spring-steel wheels with grousers for flight applications, those wheels would be too destructive of the terrain to use them in sensitive Earth environments. Figure 4 presents a three-view diagram of VERTEX superimposed on the Apollo LRV for scale. While the overall wheelbase and vehicle width are driven by the stability requirements, the Earth analog prototype of VERTEX is also driven by the requirement to fit into rental panel trucks in its operating configuration for ease of field testing. As detailed below, VERTEX has

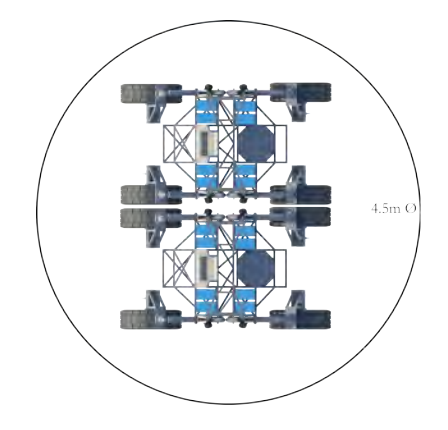


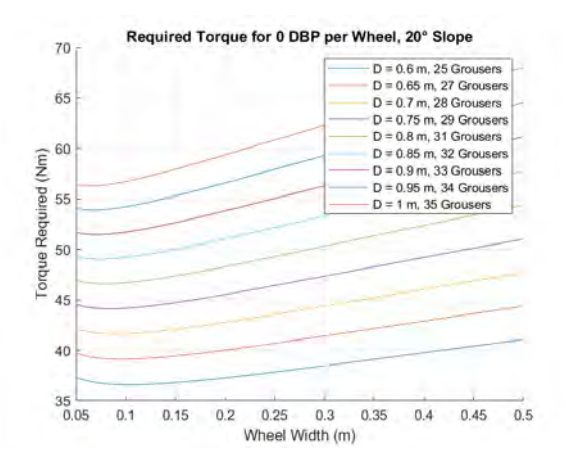
Figure 5. Two VERTEX vehicles on outline of Astrobotics Griffin lander payload deck

independently controlled positioning of the rotational link holding each wheel, allowing the maintenance of a level deck angle on slopes up to its 20° design limit. The wheel links also connect to tuned spring-damper systems for passive ride smoothing for the driver and payloads.

While Astrobotics has not yet published a user's guide to the Griffin CLPS lander, their current website lists a maximum payload diameter of 4.5 m and mass of 475 kg. Figure 5 shows a notional configuration of two VERTEX landers in a ready-to-drive configuration on the Griffin payload deck with room to spare. The ability to launch the VERTEX landers without the need to deploy or assemble after landing greatly simplifies their initial operational availability, and ensures they can be unloaded from the lander without crew aid and are thereby available for landing site surveys and preliminary science exploration prior to the arrival of the Artemis crew.

B. Terramechanics

Wheel-soil interaction analyses based on Bekker's terramechanics model for both a lunar rover and an Earth analog system were the primary contributor to the selection of the wheel diameter and width. The main metrics that were compared were the drawbar pull (DBP), required motor torque, and required drive power, with these properties varying as a function of wheel diameter, wheel width, number of wheels, slip ratio, and grouser height. The number of grousers was determined for each combination of wheel diameter and grouser length such that each grouser enters into undisturbed soil. The final wheel design from the analysis was then selected by a trade-off between motor torque/power requirements and available DBP. Torque graphs from a subspace of the full tradespace focusing on a 4-wheel design on a 20 degree slope are shown in Figures 6-7. The wheels in these graphs all have 0.06 meter grousers, and a slip ratio of 0.5 was used. Additionally, as can be seen in Figure 8, the wheel sizing on the Moon has much less impact on the required torque compared to driving on Earth, thus the Earth-based terramechanics analysis formed the main wheel sizing requirements in order to meet the system requirements. For the power, the highest required continuous power occurs on flat terrain due to the higher velocity requirement, thus this portion of the tradespace showing the power on flat terrain can be seen in Figure 9, and it displays the same trend as in Figure 8 with regard to the impact of gravity level.

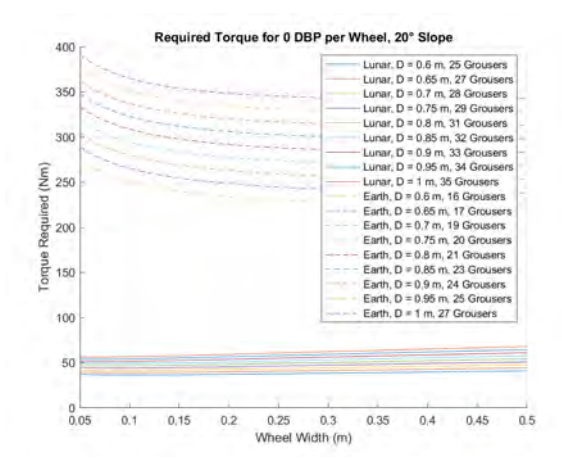


Required Torque for 0 DBP per Wheel, 20° Slope 400 380 D = 0.65 m, 17 Grouser D = 0.7 m, 19 Grousers D = 0.75 m, 20 Grousen 360 D = 0.8 m, 21 Grousers D = 0.85 m, 23 Grousers (NA) 340 D = 0.9 m. 24 Grousers D = 0.95 m, 25 Grous D = 1 m, 27 Grousers Required 320 300 280 240 0.2 0.25 0.3 0.35

Figure 6. Required torques for various wheel sizes in Lunar conditions

Figure 7. Required torques for various wheel sizes in Earth conditions

Based on the Earth terramechanics analysis, a 32" 215/85R16 tire (\approx 0.8 m diameter and \approx 0.2 m width) was selected for the Earth analog rover, as these dimensions result in both positive DBP under all operational conditions and also are commercially available without additional manufacturing requirements. As a result, the required continuous torque on Earth is \approx 160 Nm per wheel for flat terrain, with a torque requirement of 290 Nm per wheel for navigating 20 degree slopes. Additionally, the analysis indicates that peak torques of up to 500 Nm may be encountered for short durations. The minimum motor power requirement per wheel is \approx 1.6 kW, or 2 kW with 25% margin. By comparison, for this size wheel on a Lunar rover, the minimum torque requirement is \approx 48 Nm and the minimum power requirement is \approx 260 W. However, since the soil properties, and thus the terramechanics analysis, for an Earth system have an extreme degree of variation in the types of soils encountered, the Earth analog analysis shown uses worst-case soil properties and is thus highly conservative. It is also important to note that, in general, Bekker's model is also conservative and tends to under-predict DBP and thus over-predict required torque and power. Thus, it is anticipated that the rover will require lower torque and power than this analysis indicates under most use cases.



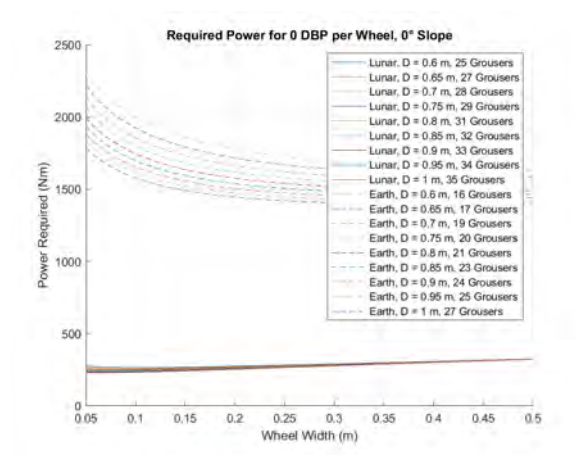


Figure 8. Required torques for various wheel sizes in both Lunar and Earth conditions on 20 degree slopes

Figure 9. Required power for various wheel sizes in both Lunar and Earth conditions on flat terrain

Testing of the wheel/motor/gearing system prior to vehicle assembly is planned to validate the numbers calculated by the terramechanics model.

C. Drive Systems

To be capable of a maximum speed of 4 m/sec over open terrain, the terramechanics calculations show that the rover would require a constant torque of 160 Nm at each wheel, and 290 Nm at each wheel is required in order to scale 20° slopes at 1 m/s. Additionally, the rover will require 500 Nm of peak torque momentarily. With the 0.8 m diameter wheels chosen above, 4 m/sec travel speed requires ≈95 RPM and a minimum motor power output of about 2 kW continuous per wheel (with the 25% margin). A wide variety of motors were considered, but few were able to meet the drive and programmatic requirements. Most DC motors were not able to produce the required power continuously while having a high enough RPM to al-

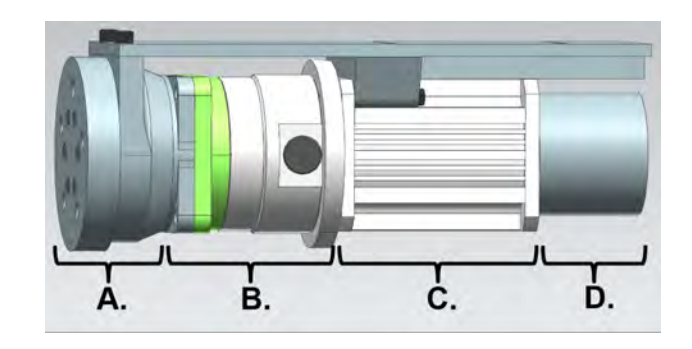


Figure 10. Wheel-Motor Stack Diagram. A) Wheel attachment via tapered roller bearing, B) Gearbox, C) Motor, D) Brake and encoder housing

low for 4 m/sec travel without being prohibitively massive. AC motors required high voltage (400 Vac+) and were considered unsafe for student use while also requiring the added mass of an on-board inverter. Hydraulic motors were considered for their high torque output, but they were decided against due to safety considerations regarding the necessary high-pressure fluid lines (1200-3000 psi).

Furthermore, drive system selection was complicated by the structural strength of typical gearboxes: most could not continuously output 290 Nm and 95 RPM without exceeding 25 kg each. Ultimately Magmotor's 90V BFA42-2E-300FBE paired with Harmonic Drive's highly efficient HPG-32A-33-BL3-D-F0 33:1 planetary gearbox were selected as the final system, providing acceptable drive characteristics including 3.8 m/s travel speed, and repeated torque capacity of 330 Nm and momentary peak up to 600 Nm (Figure 10). The speed reduction of 0.2 m/s was deemed acceptable as other system designs severely increased mass (≥ 80 kg) and volumetric properties. The motors were also specified to include an encoder and dynamic braking systems.

D. Suspension and Steering

The ability of VERTEX to independently adjust the articulation of each wheel in reference to the body manifests itself in three independent systems connected in series. The most obvious of these controls the angle of each tubular link connecting the wheel assembly to the chassis body via a pinned linear actuator. This system allows for the arm

links to pivot upwards from body level 50° and downwards 10° to allow for a total displacement of 60° accommodating up to 30° slopes. The greater biasing of the adjustment arc in the "upwards" direction helps compensate for the overwheel steering system displacing the attachment point vertically from the wheel spin axis, and the flat terrain driving position of the rover such that the wheel center is in-line with mid-chassis requires roughly 35° of upward travel.

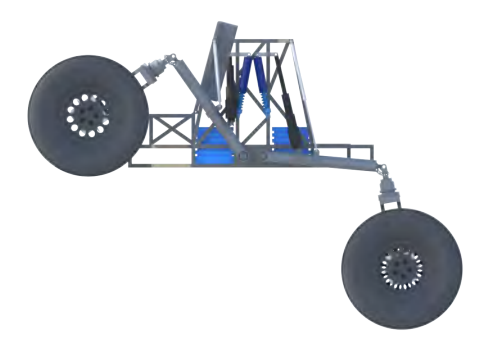




Figure 11. Side view of VERTEX with wheels configured for traveling up/down slopes

Figure 12. Front view of VERTEX with wheels configured for traveling cross slopes

The over-wheel steering system was implemented due to its historical reliability in projects like Chariot, Centaur, and Curiosity. Determining required torque values for the steering actuator became a less concrete study than desired, and simply utilizing an excessively sized manipulator caused too great concern in both mass and power draw. Thus, a set of nominal design guidelines needed to be created, and field testing for verification and adjustment of these parameters is planned. Major contributing factors to the steering moment included friction scrubbing of the wheel contact patch, bulldozing efforts from the sides of each wheel, and any offset of the steering axis from the wheel patch centroid. This analysis assumes the steering axis is directly in line, and further study of the caster and camber angle adjustments will be performed in testing. In Equations 1-4, the calculations of the required steering torques are shown. Here, P is the pressure under the wheel, A is the contact patch area, W_w is the weight of the rover on an individual wheel, b is the width of the wheel and assumed to be the contact patch diameter, μ is the friction coefficient, and τ is the steering torque.

$$P = \frac{W_w}{A} = \frac{W_w}{\pi (\frac{b}{2})^2} = \frac{4W_w}{\pi b^2} \tag{1}$$

$$d\tau = rP\mu rdrd\theta \tag{2}$$

$$\tau = P\mu \int_0^{\frac{b}{2}} \int_0^{2\pi} r^2 dr d\theta \tag{3}$$

$$\tau = \mu \frac{W_w b}{3} \tag{4}$$

Nominal steering torques required for each wheel are estimated to be approximately 100Nm or 75ft-lbs fully loaded and with some margin on Earth sand or other loose soils. Current designs for steering system follow a traditional brushless DC motor and Harmonic Drive pairing with an expected torque capacity in excess of 300 Nm for short duration, and closer to 200 Nm during nominal operating conditions. Future testing is planned to verify and, if necessary, adjust these parameters, and design alteration paths are being planned to better adjust to these results.

The large positional changes of each wheel during pitch and roll control motions create a non-constant caster angle issue. Most vehicles are designed to maintain a positive caster angle for inherent straight-line stability, especially at higher speeds, but VERTEX's over-wheel design dictates the steering axis moves with the caster angle. Climbing large slopes can see changes in excess of $\pm 20^{\circ}$ of inadvertent caster adjustment depending on the initial caster angle setting, consequently creating a large inefficiency in the steering system. Two approaches were considered in minimizing these effects, the first of which integrated a four-bar linkage replacement for the singular wheel linkages. This solution reduced the maximum caster angle generated to +/-6° while simultaneously increasing stowed volume by $\approx 25\%$, an inappropriate opportunity cost for a lunar-analogue payload. Therefore, an adjustment pivot mechanism to compensate for the caster effects was designed and coincidentally directly adjusts wheel camber when all steering motors turned

90° in a crab-driving configuration. This effort provides future research opportunities to gain detailed insight into the steering and driving characteristic variances across these two variables, and future improvements to the system could include motorization and integration of a closed loop system to automatically maintain stability in any configuration.

Attached to the linear actuator is a pivot transferring motion into a spring damper system, effectively creating an elastic linear actuator. The rover mass by requirement definition is subject to increasing by 420 kg from empty, having the potential to drastically adjust optimal spring and damping rates for testing situations. To relieve the compromise in choosing singular spring and damping values, adjustable automotive coil-over suspension was chosen for its ability to change pertinent values such as rebound, compression, and spring rates during



Figure 13. VERTEX's manual caster adjustment mechanism

field testing with only hand tools and the common availability of design recommendations from previous off-road testing.

E. Chassis Design

The VERTEX chassis design requirements mainly focused in the areas of strength, system support, and ease of field repair. The balance between strength and mass of the chassis led the design path away from SSL's history of 80/20 structures and ultimately to a combination ladder and space-frame style 4130 Chrome-Moly welded assembly. This hollow square tubing is of the most commonly available across the United States, aiding contingency remote repair operations, and traditional chassis design strategies provide helpful design guidelines for this Earth analog system. The chassis additionally has the capability of easily including steel mounting plates or other hardware mounting systems (e.g. rivets) for any systems integration needs. The nominal chassis is shown in Figure 14, and examples of the FEA analysis completed for each iteration is shown in Figure 15.



Figure 14. VERTEX Chassis design isometric

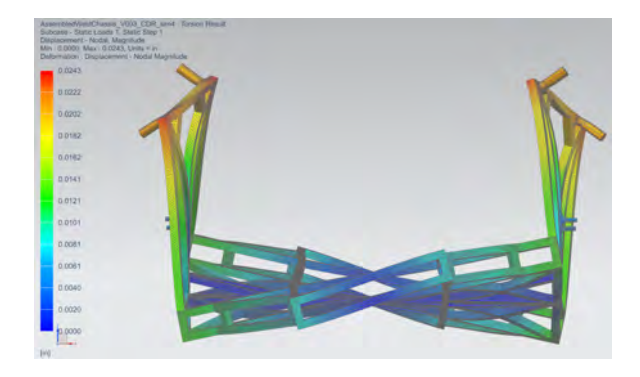


Figure 15. Finite Element Analysis example for chassis design

The chassis was designed to withstand three main contingencies: 1) front/rear impact, 2) corner rollover, and 3) bending and torsion resulting from uneven loading. Deformation areas were designed in the front and rear to allow for deformation in extreme cases for impact protection while being trivial to repair in such a case. The vertical protrusions on either side of the chassis provide attachment points for the linear actuators supporting the active pitch and roll system as well as all suspension components and future roll cage attachment points. A detachable suspension structure crossbar, as seen notionally in Figure 16, will turn the chassis structure into a full roll cage for astronaut protection, and will also serve as a mount for cameras, antennas, navigation sensors, and science instruments; incorporating it in the final design will increase the stiffness of the vertical chassis sections. For situations such as autonomous operations the roll cage may not be necessary, and a set of stiffening bars to support these areas while maintaining areas of useful enclosed volume is also under development as an alternative.

F. Energy Storage, Power Management, and Electronics

The flight version of VERTEX has a power system sized for a six-hour EVA of which 40% is spent driving at an average velocity of 2.5 m/sec. This gives a nominal traverse distance of 21.6 km, on a battery pack of 6.5 kWhrs. The required "keep-alive" power for quiescent periods is 90 W, so the rover can survive 72 hours of darkness. Longer dark periods will require a connection to an external power source.

The VERTEX prototype's electrical system is designed to leverage facilities commonly found on Earth, while remaining faithful to the capabilities of a flight system. However, for budgetary and development time reasons, several features of the rover have been removed or modified. The main requirement reductions were that self charging was removed due to cost and the Earth testbed nature not requiring it, and also the maximum



Figure 16. VERTEX chassis upper crossbar for sensor mounting and to complete full roll cage

range was reduced due to the infeasible weight and cost of batteries capable of meeting this requirement. The power system was then modeled after commercially available electric vehicles, which enables the use of commercial off-the shelf (COTS) parts, and allows for the usage of EV chargers. The usage of COTS parts keeps cost and development time low, and adds a considerable amount of safety to the system, as the lab does not have to design kilowatt-capable high voltage equipment. The main power source is a rechargeable LiFeMnPO4 battery with 100Ah at 100V nominal output, with a total energy storage capacity of 10 kWhrs.

System charging is possible via two methods: Fast 1-hour charging via a level 2 EV charger, and a backup 14-hour charge through a conventional 120V, 15A household receptacle. The ability of the system to fast charge at 10KW enables an accelerated test schedule, where morning and afternoon sorties are separated by a 1-2 hour "lunch" period where the rover and operators replenish their respective energy storage systems. If the system lacked the fast-charge capability, the 200lb battery would have to be removed and replaced with a fully charged battery during such a test schedule. The difficulty of performing this process in the field in unimproved terrain, the safety considerations of handling the 100V pack, and the budgetary considerations of acquiring a second pack made the battery replacement system an infeasible design choice.

G. Crew Interfaces

A design issue still in the preliminary phase is that of crew interfaces; that is, how the crew will ingress and egress, where and how they will be seated and secured, and what interfaces will be used to command the rover and to receive data back from it. One of the lessons learned from the Apollo LRV is that sitting down is not easy in a pressurized suit, even one like the A7L-B which was modified to facilitate it. For the Chariot rover prototype, NASA chose a standing position for the two EVA crew, but this is not feasible in a vehicle as small and lightweight as VERTEX. A number of innovative concepts have been put forward, such as semi-prone seating, which are planned to be investigated using suit simulators at lunar and Mars gravity in the UMd Neutral Buoyancy Research Facility, but the current default plan is to use a conventional seat with accommodations for the suit backpack located on the deck of the rover. The roll cage will provide mounting locations for ingress/egress aids, along with a pull-down restraint bar for securing the driver in the seat. Tests with the VERTEX prototype will investigate the feasibility of using the movable chassis to enable ingress and egress, or whether a deployable step would be preferable. Driving commands will be issued with a sidearm controller similar to that used for the LRV, capable of changing speeds, braking, and steering to both sides. Displays for vehicle status, driving parameters such as speed and direction, and navigational information will be presented to the driver via the head-mounted display⁸ in the MX-D spacesuit simulator.⁹

VI. Status and Future Plans

With the detailed design process nearly complete, the SSL team is moving into the fabrication and testing phase of VERTEX. Long-lead parts, such as motors and gearing for the wheel drives, are on order, and work will begin shortly on the fabrication of the chassis.

During this shift between mission phases, a parallel effort has been initiated to mitigate the risks for some of the

critical areas which were not unambiguously resolved during the design analysis, such as the correct values for wheel steering torque and how that is affected by castor and camber angles. SSL is beginning the design and construction of a single-wheel test track that will be used to verify drawbar pull projections from terramechanics studies, and to conduct research on how caster angle and camber angle affect steering forces. If these wheel angles are found to significantly affect the wheel's steering or traction, future plans include mechanizing the wheel-linkage joint for adjusting the wheel angle depending on slope or terrain. During the physical build activities for the VERTEX chassis, the electronics and power systems will be integrated onto RAVEN, an earlier SSL rover, for extensive testing. Autonomous control functions are being implemented on an RMP-440LE commercial four-wheel skid-steer mobility platform as a third parallel development testbed.

Recently, it has become clear that the crew mass estimates of requirements 6 and 8, based on Apollo and Shuttle EMUs, are far below the figures currently being used for Artemis, which allocates 187 kg for the mass on one xEMU.⁷ Combined with the 99 kg mass of a 95th percentile astronaut, the proper allocation for each suited crew would be 286 kg rather than 170. While these numbers are likely to change with further xEMU development and will not affect the design or operation of the analog field version of VERTEX, the team will investigate any redesign necessary to accommodate this much greater crew mass for the flight design.

With the completion of VERTEX, initial testing will occur locally to the University of Maryland for simplicity and access to any necessary test equipment or spares. This testing will be used to measure VERTEX performance against the design guidelines, and to ensure reliable functionality in all operating modes. Initial field testing of VERTEX is scheduled to occur in September, 2021, at the Lava Beds National Monument in California in conjunction with the GEODES SSERVI science team investigations. VERTEX is also scheduled to be outfitted with simulated EVA life support systems and robotic umbilical handling system for field tests of the SSL BioBot concept under the NASA Innovative Advanced Concepts (NIAC) Phase 2 project currently underway at the University of Maryland. This project is planned to culminate with a test/demonstration in the "Rockyard" facility at the NASA Johnson Space Center in 2022.

Acknowledgements

The authors would like to thank Lemuel Carpenter of NASA Langley (technical monitor) and Eirik Holbert and Sharon Wagler of NASA Kennedy (program monitors) for their support via the 2021 Moon-to-Mars eXploration Systems and Habitation (M2M X-Hab) program, as well as the NASA Innovative Advanced Concepts (NIAC) program which supports the BioBot program, which will be the first field use of VERTEX. We would also like to thank the other members of the Fall 2020 ENAE 788X class for their design efforts which contributed in a major way to this project: Pat Hoskins, Jaad Lepak, Joe Perrella, and Loy McGuire (Protogonus); Justin Albrecht, Brian Bock, Prateek Bhargava, and Sayani Roy (Courage); and Aalay Patel and James Winsley (ROCI).

References

- ¹Saverio F. Morea, "The Lunar Roving Vehicle Historical Perspective" *Second Conference on Lunar Bases and Space Activities of the 21st Century*, NASA Johnson Space Center, September 1992.
- ²Harry Litaker, Shelby Thompson, and Robert Howard, "A Comparison of the Unpressurized Rover and Small Pressurized Roer During a Desert Field Evaluation" *Human Factors and Ergonomics Society Conference*, January, 2009.
- ³Dale Arney and Alan Wilhite, "Rapid Cost Estimation for Space Exploration Systems" AIAA 2012-5183, AIAA Space 2012 Conference and Exposition, Pasadena, California, Sept. 2012.
 - ⁴-, accessed online 3/15/2021 at https://www.astrobotic.com/griffin
- ⁵Jessica R. Vos, Michael L. Gernhardt, and Lesley Lee, "The Walkback Test: A Study to Evaluate Suit and Life Support System Performance Requirements for a 10 Kilometer Lunar Traverse in a Planetary Suit" ICES 2007-01-3133, 37th International Conference on Environmental Systems, Chicago, IL, July 2007.
 - 6-, "LRV Operations Handbook, Appendix A (Performance Data)" NASA TM-X-66816, NASA Manned Spacecraft Center, April, 1971.
- ⁷-, "Human Landing System (HLS) Requirement Document" NASA HLS-RQMT-001, NASA Marshall Space Flight Center, September 27, 2019
- ⁸K. Fox, R. Karsalia, J. Kunze, C. Neisess, Z. Peters, R. Rao, B. Sack, M. Sieh, R. Skoletsky, S. Szanto, M. Wilkin, and D. L. Akin, "Development of a heads-up display for extravehicular activities" 49th International Conference on Environmental Systems, July 2019.
- ⁹D. L. Akin, "Technology development and systems tests of a next-generation suit simulator for analog field trials" 48th International Conference on Environmental Systems, July 2018.

Development and Testing of the BioBot EVA Support System

Charles Hanner¹, Nicolas Bolatto¹, Joshua Martin¹, Daniil Gribok ¹, and David Akin² *University Of Maryland, College Park, MD, 20742, USA*

Under the support of the NASA Innovative Advanced Concepts program, the University of Maryland Space Systems Laboratory has been developing the BioBot concept for initial Earth-analogue testing. One of the primary factors limiting EVA duration and astronaut fatigue is the weight of the portable life support system (PLSS) in the spacesuit backpack. Current plans for the xEMU suit for Artemis will more than double the mass of the Apollo PLSS, with concomitant impact on astronaut fatigue rates and ability to pursue science leads into difficult planetary terrains. The BioBot concept is an autonomous rover which follows the EVA crew carrying the primary life support system, relieving them of the physiological burden of carrying the weight of the PLSS in a lunar or Mars gravity field. The BioBot rover carries a robotic system for minding the umbilical that provides life support to the suit, ensuring the umbilical is free of all potential obstacles while allowing the EVA crew free range within a 5m radius of the rover. Adding the capability for the rover to autonomously follow the EVA crew presents the potential of unrestricted walking travel for EVA exploration activities without the carried weight of the full PLSS. The BioBot system consists of the rover, robotic umbilical handling system, the spacesuit modifications to accept umbilical-supplied consumables and en route recharge of the short-duration PLSS carried in the backpack, but this paper focuses on the central component which is the "linchpin" of the entire concept; the uniquely-capable rover and the design responses to the suite of requirements arising from both its role as an EVA support rover and the constraints placed on the design from the rest of the BioBot systems architecture.

Nomenclature

CLPS Commercial Lunar Payload Services

DOF Degree Of Freedom

DYMAFLEX DYnamics MAnipulator FLight EXperiment

EVA Extravehicular Activity
LRV Lunar Roving Vehicle

NIAC NASA Innovative Advanced Concepts

PLSS Portable Life Support System ROS Robot Operating System

RRT Rapidly-exploring Random Tree SSL Space Systems Laboratory

SST Stable Sparse RRT
UMd University of Maryland

VERTEX Vehicle for Extraterrestrial Research, Transportation, and Exploration

xEMU Exploration Extravehicular Mobility Unit

I. Introduction

With the resumption of human lunar exploration and plans for eventual Mars landings, extravehicular activities (EVAs) in gravitational environments will again become a primary focus of the human spaceflight program. Geological

¹Graduate Research Assistant, Space Systems Laboratory

²Director, Space Systems Laboratory. Professor, Department of Aerospace Engineering

exploration in early missions will require daily EVAs, rather than the roughly monthly sorties on International Space Station. Even in the reduced gravity of the Moon, EVA system weight on the crew will be the predominant factor in crew performance, fatigue, and safety; the largest single item contributing to this is the weight of the portable life support system. Under NASA NIAC sponsorship, the University of Maryland has been investigating the "BioBot" concept, using a highly capable rover to accompany each EVA crew, carrying their life support system and supplying necessary consumables via a robotically-tended umbilical.

Under the BioBot concept of operations, an astronaut at a lunar or Mars habitat would egress the airlock using a limited-duration backpack-mounted life support system, and, upon reaching the BioBot rover, the astronaut would attach to a rover-mounted umbilical. From that point on, the life support functions for the EVA would be supplied by the BioBot rover, including consumables such as oxygen, water, and power. The rover would also work as a communications relay, providing longer-range communications than would be practical in a suit-mounted system. Based on the results of trade studies on the size and capabilities of the support rover [1], the rover would be sized to allow the user to drive between exploration sites, reducing crew physiological workload and reducing consumables usage. Since EVA would only be performed in pairs, there would be a BioBot rover for each crew; the design was based on being able to predeploy two BioBot systems on a single Commercial Lunar Payload Services (CLPS) lander before the arrival of the crew. In the event of a systems failure, both EVA crew could ride on the functional BioBot and share life support during the return to the surface habitat, thus eliminating the "walk-back" criteria limiting EVA crew to traverse distances which allow them to walk back to the base within remaining life support capabilities. When the EVA crew leaves the rover for exploration, a robotic arm mounted on the rover will tend the umbilical, allowing the crew to move freely within a 5m radius of BioBot, on slopes up to 30° (Figure 1). As the crew approaches the limits of the work envelope, the rover will autonomously adjust position to allow essentially unrestricted access in trafficable terrain without direct input by the EVA crew. There will always be areas difficult for the rover to traverse which can be accessed by the EVA crew; these regions may be the most interesting scientifically, and for that reason the system will allow the astronaut to temporarily release their umbilical and proceed without the rover for a limited time by using their personal life support. Upcoming field tests will investigate the effect of independent time limits on science operations, which will allow a quantitative trade study between independent duration and backpack weight. At the end of the independent traverse, the EVA crew will once again hook up to the BioBot umbilical, and while attached the system will recharge the backpack life support consumables [2].

Under the support of the NASA Innovative Advanced Concepts (NIAC) program, the University of Maryland undertook the development of an Earth analogue BioBot system for field testing and assessment of the concept. Under the original schedule, this paper would be reporting on initial systems testing of the completed vehicle. However, due to the "double whammy" of COVID-19 and supply chain failures, the system is still in final assembly and integration, and testing is slated to begin in the summer of 2022. This paper will therefore focus on the core critical system for a functional Earth-analogue BioBot system: the roving vehicle. As will be detailed below, the BioBot application mandates a number of capabilities outside the range of typical unpressurized rover concepts which our rover, the Vehicle for Extraterrestrial Research, Transportation, and Exploration (VERTEX) system, was designed to meet. This has resulted in a unique and highly capable



Figure 1. BioBot concept supporting EVA crew on 30° slope including VERTEX rover and umbilical tending robotic arm

roving vehicle that serves as the mobility platform for BioBot concept testing. Other papers are presenting the details of the ancillary BioBot systems, such as the autonomous umbilical tending robot [3], a BioBot-compatible spacesuit simulator for Earth analogue testing and discussion of BioBot implications for flight spacesuits [4], and crew interfaces (controls, displays, and restraints) for the BioBot operator [5].

A. Lunar Design and BioBot Concept Requirements

The following are an applicable subset of rover performance-related requirements used to design the initial lunar rover concepts, all of which informed the Earth-analogue rover design discussed in this paper:

- Rover shall have a maximum operating speed of at least 4 m/sec on level, flat terrain This corresponds to 14.4 kph, based on the published LRV top speed of 13 kph, although the LRV Operations Handbook [6] states that the LRV is "uncontrollable" above 10 kph (2.8 m/sec).
- Rover shall be designed to accommodate a 0.3 m obstacle at minimal velocity This sets a minimum ground clearance of 30 cm, comparable to the 35 cm ground clearance for the LRV.
- Rover shall be designed to accommodate a 0.1 m obstacle at a velocity of 2.5 m/sec This was deemed a reasonable value for an obstacle which could be safely driven over at a nominal cruise speed.
- Rover shall be designed to safely accommodate a 20° slope in any direction at a speed of at least 1 m/sec and including the ability to start and stop The Lunar Exploration Science Working Group study of 1995 found that, for general access to anywhere on the moon, rovers should be capable of ascending and descending a 25° slope. This did not look at the dynamics of locomotion, including the interactions of slopes with turning and acceleration limits, or the increasing difficulty of specifying motors and gearing for peak slopes while accommodating desired maximum velocities. Since even younger craters with steeper wall slopes usually have one or more ingress/egress routes with more limited slopes, the decision was made to adopt 20° as the maximum slope including a worst-case turn and/or acceleration profile.
- The rover shall have a nominal sortie range of 54 km at an average speed of 2.5 m/sec This is six hours of constant driving on level terrain at 2.5 m/sec. On the basis of kinetic energy, it also equals 2.4 hours of driving at the peak speed of 4 m/sec, with a total traverse distance of 34 km. This provides a significant energy margin for sorties involving maximal slopes over extended distances.
- Rover shall be capable of carrying one 170 kg EVA crew and 80 kg of assorted payload in nominal conditions The nominal mass of the EVA crew was based on an 80 kg astronaut and a 90 kg spacesuit/life support system. The 80 kg of additional payload was allocated for tools, science instruments, and samples.
- Rover shall be capable of also carrying a second 170 kg EVA crew in a contingency situation. Payload may be jettisoned if design permits Required for the redundancy element of the twin-rover architecture. Jettisoning the nominal payload was left as an additional accommodation for the designers.
- A nominal sortie shall be at least eight hours long This is based on the fact that later Apollo surface EVAs were six hours or slightly more, and that the HLS requirement document [7] cites a standard EVA duration of "6±2" hours. The intent was to ensure that the rover would not be the critical item in allowable sortie duration.
- Two rovers must be launched on a single CLPS lander Fundamental to the concept, assuming that the additional capabilities of a more massive rover would not be sufficient to justify doubling the cost by delivering two rovers to the surface via individual CLPS missions.
- A single rover shall mass \leq 250 kg This was based on the understanding that the Astrobotics Griffin rover had a 500 kg payload limit, although no specific information was available at the time. Since the creation of these requirements Astrobotics has announced that the Griffin payload limit is 475 kg [8], so the actual mass limit should be 237 kg, or 166 kg to leave a 30% mass margin for this preliminary design.

Four initial concepts were designed in UMd's 2020 ENAE788X class, and the most notable features of each design were incorporated as an initial lunar rover to serve as foundation for the BioBot rover. The most notable features included over-wheel steering, independent suspension for each wheel, and the ability to actively control the vehicle's chassis in roll, pitch, and height [1].

B. Earth Analogue Translational Design Summary

The VERTEX vehicle produced by the SSL is not a proto-flight copy of what the lunar rover should be. The vehicle's main goal is not to be tested in high-fidelity lunar simulant in confined locations for minute rover characteristic studies. Rather, VERTEX is a research platform highly conducive for Earth-bound research with a vehicle with the same capabilities as the lunar design outlined in section A. This means, with a university-level budget, the mechanisms and systems designed and used are not flight-capable. Pneumatic tires, unsealed motors/gearboxes, unsealed linear actuators, pneumatic springs, and open coiled springs are not suggestions from this rover that should be included in a final Lunar design. In translating the lunar rover capabilities to an Earth system, significant mass increases were

seen (details in Table 1), and various consumer-available products needed to be used within budgetary and resource constraints. The inclusion of these Earth-restricted systems were focused on creating a rover capable of the same performance with the exception of sortie distance and vehicle duration. It is not expected that the testing phases of the rover be directly integrated with a long-duration testing program such as HI-SEAS in the near future but rather support shorter duration mobility experiments. If longer duration experiments are determined necessary by the planned short-duration testing, the next iteration of VERTEX could be modified to accommodate increased range.

C. VERTEX as a Unique Platform for BioBot

VERTEX is an Earth-analogue support platform for testing human factors and EVA umbilical tending of an unpressurized lunar roving vehicle. The purpose of building and testing an Earth-analogue to a lunar rover is to evaluate the effectiveness of the rover's unique capabilities in research-friendly testing environments. VERTEX is a student-focused research platform for the Space Systems Laboratory's (SSL) BioBot concept; creating a rover development program that achieves competitive performance to desired lunar capabilities in local simulation environments will significantly bolster research efforts for a comparatively low cost.

The rover is designed to be controlled by a single astronaut, allowing the paired astro-



Figure 2. VERTEX rover in a kneeling configuration

naut to either sit and manually control or walk with the rover autonomously tracking and following, discussed further in section II.C. The walkback contingency criterion is effectively eliminated as VERTEX is capable of carrying two astronauts in a contingency scenario, with each EVA crew member provided a rover for nominal exploration. As detailed in a prior publication [1], the lunar versions of Biobot were designed such that two systems, including the rovers, could be launched on a single Commercial Lunar Payload Services (CLPS) landers for pre-emplacement prior to arrival of an Artemis surface crew.

VERTEX offers unique platform capabilities to support EVA activities, including providing a stable platform for a robotic umbilical management system [3] through automated chassis leveling. This also allows VERTEX additional support capability for accommodating the limited flexibility of spacesuits by kneeling during ingress or egress as seen in Figure 2. A set of series-elastic linear actuators allow VERTEX to individually adjust drive wheel position and, by extension, chassis pitch and roll angles. Designed for pitch and roll compensation of 30° and 40° respectively, this capability allows the rover to remain robustly stable during steep slope climbing and compensate for angular displacement of the astronaut's bodies. A small group of test subjects reported discomfort levels beginning at $\approx 12^{\circ}$ pitch and $\approx 10^{\circ}$ roll when experiencing pure angular displacements in the SSL laboratory. This suggests the importance of angle compensation for this Earth-analogue platform, but it should be noted that astronauts in reduced gravitation environments may perceive these adjustments to a lesser extent [9].

D. Earth-Analogue vs. Lunar

The design effort in transitioning from a notional lunar rover design is outlined in a previous publication [1]. When making the Earth analogue, considerable effort was placed in preserving lunar-design capabilities at the expense of mass and power in every subsystem. The focus of the rover is not to accurately represent the lunar design requirements like launch configurations, CLPS landing mass, or lunar environment compatible mechanisms (e.g., no extensive drive motor/gearbox sealing, pneumatic tires, gas struts, non-sealed linear actuators, etc.) but rather focus on the rover's expected performance capabilities in slope climbing, steering, and mechanical proportions for human factors testing. Field testing of the Earth analogue will be used to evaluate the effectiveness of VERTEX's unique features and thus inform the design of future extreme-terrain lunar rovers.

The effects of Earth's greater gravity caused a positive feedback loop (spiral engineering) where rover mass had to increase continuously to achieve equal capabilities to the lunar case. Beginning with payload, the rover must carry samples, tools, the BioBot umbilical handling arm, and up to 2 EVA astronauts in a contingency. With all of these being 6 times heavier in 1g, the drive system and deck-leveling must increase in mass and power to compensate. With



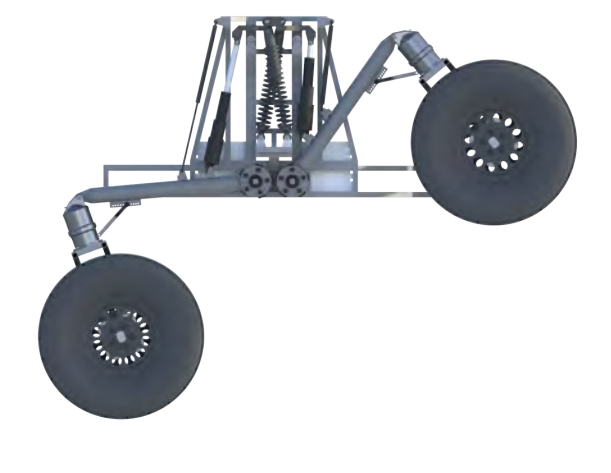


Figure 3. 40° Cross slope capability

Figure 4. 30 ° Up slope capability

the increase in power comes an increase in battery, motor driver, wiring, and thermal management mass. To carry all of the above, the structure must increase in strength and mass. Of course, the propagation comes full circle when the need for equal traverse capabilities requires the drive system to be stronger once again.

The resulting mass of the current VERTEX design is shown in table 1 compared to the original lunar design, with the masses split by subsystem. Of special note is the extreme difference in motor/gearbox mass. The lunar version used a heritage actuator design to the SSL's DYMAFLEX (DYnamic MAnipulator FLight Experiment) robotic manipulator, which was designed as a small 4-degree-of-freedom satellite servicing robot using a frameless brushless DC motor and harmonic drive system, outputting up to 93 Nm for hill-climbing on the moon at ≈100 W. The Earth drive motors were especially subject to the spiral engineering mentioned above, in specific the rising ratios of structural mass to required torque. A framed brushless DC motor and 1:33 planetary gearset were ultimately selected producing 278 Nm of continuous torque capability at each wheel. This results in an increase of 298% of torque at a cost of 1,690% increase in mass over the lunar specifications. One significant cause for such the large increase in mass relates to the difference in use between a frameless motor and housing-less gearbox for the lunar design. The framed motor and housed gearbox add a large amount to the Earth subtotals, and the actual housings were considered structural mass in the lunar design phases. Similarly, the "Steering" category has been summed separately because the original lunar design employed skid-steering rather than the 360° independent steering that is seen on VERTEX due to large loads. The lunar version will be revised to include independent steering, and a more similar segmentation of hub motor structure mass to VERTEX for a more complete comparison in the future. Overall, it is interesting that this preliminary comparison shows a ≈6:4 ratio rather than a 1:1 ratio between increasing gravity and increasing overall rover mass from a preliminary design.

This 6:4 ratio likely stems from two main factors. The first is likely from the lunar design following an idealized focus using a traditional frameless brushless DC motor and Harmonic Drive combination in a lightweight aluminum housing. The final Earth drive system for VERTEX using a consumer-available housed brushless motor with integrated dynamic brake and encoder, with a large planetary gearset from Harmonic Drive was the only way to achieve the torque required for positive drawbar pull in a cost-efficient way (including significant sponsorships from manufacturers). None of these systems are optimized for mass, but rather maximize available torque for price in systems available commercially at our level that matched the required speed. This resulted in an increase of 1,690% in mass of the drive system alone, contributing significantly to the \approx 6:4 ratio. Secondary, the system core structures were ultimately decided to be manufactured from mild steel rather than the aluminum selection from the lunar design. This was done mostly for ease of manufacturing, repair, and accessibility to the student researchers building the rover. For example, the core chassis is a welded square tube structure made of steel, which is significantly easier to weld at an entry-level than aluminum, and it also allows for easy future modifications with welding or repair at higher yield stresses. This structure increase had an additional primary driving constraint to support the much more powerful suspension in large planes on either side of the operator seat. The original notional lunar chassis was a welded aluminum frame, at \approx 17% the structural mass of the produced Earth chassis.

Comparison	Lunar Earth		rth	Earth Percent	
Category	lbm Subtotal	kg Subtotal	lbm Subtotal	kg Subtotal	Mass of Lunar
Wheels	96.8	44	168	76	174%
Motors	12.4	5.6	160	73	1290%
Gearbox	9.7	4.4	211	96	2180%
Suspension	52.8	24	112	51	212%
Structure	110	50	634	288	576%
Batteries	143	65	221	100	154%
Avionics	30.8	14	120	55	390%
Steering	-	_	120	55	N/A
Total w/o Steering	455	207	1630	739	357%
Total w/ Steering	455	207	1750	793	383%

Table 1. Mass summary table comparing the current VERTEX Earth-analogue design to the lunar design. Note: Motor/Gearbox describe the drive components exclusively. Deck-level actuators fall under Suspension. Batteries do not have equal storage.

II. Mobility Systems Design

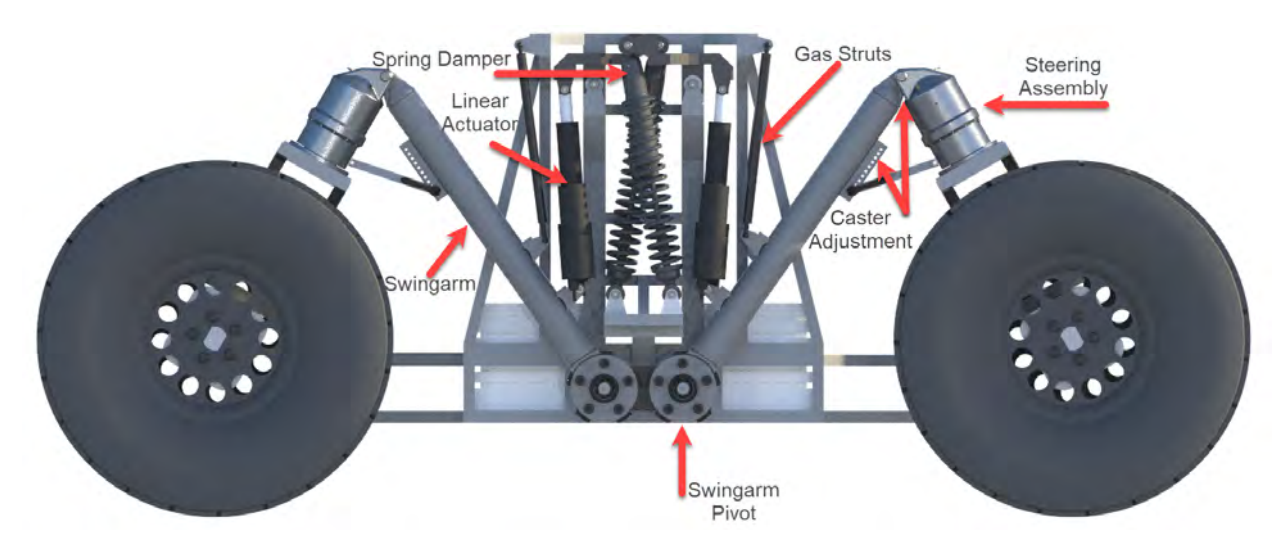


Figure 5. VERTEX mobility system diagram

A. Manual Steering and Suspension Control

As the BioBot rover system must be able to navigate its environment both autonomously and when being piloted by an astronaut, a variety of steering and control modes are required for the astronaut to make the most of the system's many degrees of freedom. As VERTEX is designed as a test platform to, in part, evaluate how an astronaut would drive such a high-degree-of-freedom vehicle, three different qualities of the suspension/steering system must be commanded either independently or cooperatively depending on the manual control mode: the wheel steering, the deck angle, and the deck height.

Multiple steering modes are being investigated for field testing and will each be selectable by the rover driver during operation. Traditional Ackermann steering, which will be familiar to most test operators or astronauts, will be the primary means of steering-only control, with double-Ackermann steering (with the back wheels also rotating to enable turning) also selectable as a control mode. BioBot's unique configuration also offers other means of steering and driving control, including a turn-in-place option (or, indeed, selectable turning point selection via a joystick and

graphical user interface for visualization) and "crab steering", with the wheels rotating to all turn in a given direction to allow the rover to drive independent of chassis orientation. All these steering options will be able to be run in conjunction with either autonomous suspension control or manual deck positioning, discussed below.

Simultaneously with the steering of the rover, the deck angle must be controlled in order to ensure proper rover operation. In most scenarios, especially those utilizing chassis-dependent payloads like the umbilical tending arm, it will be desired to keep the deck level relative to the local gravity vector. As such, the primary control mode for deck angle will autonomously zero the deck pitch and roll as different obstacles are encountered using an inverse kinematics solver and treating the rover suspension as a parallel manipulator. For more direct manual control, a joystick will also be available to control the deck pitch and roll in both velocity control mode, in which releasing the joystick will reset the suspension to a "neutral" position relative to the wheels instead of the gravity vector. All of these will be oriented using multiple inertial measurement units (IMU's) onboard the rover chassis itself.

Lastly, the height of the deck relative to the wheels can also be modified: multiple possible limb orientations can be selected to yield a given deck angle, each corresponding to a different deck height above the ground. By default, the system will choose a height to enable maximum flexibility to adjust the suspension up or down in order to better deal with obstacles and slopes. Like deck angle, there will also be position- and velocity-based control modes for the user to specify deck heights during operations, which may be useful for adjusting to certain obstacles or manually lowering the rover's center of gravity. Further discussion of the complex driver-interfaces necessitated by this high-DOF rover can be found in a concurrent publication [5].

B. Deck-Angle Actuators

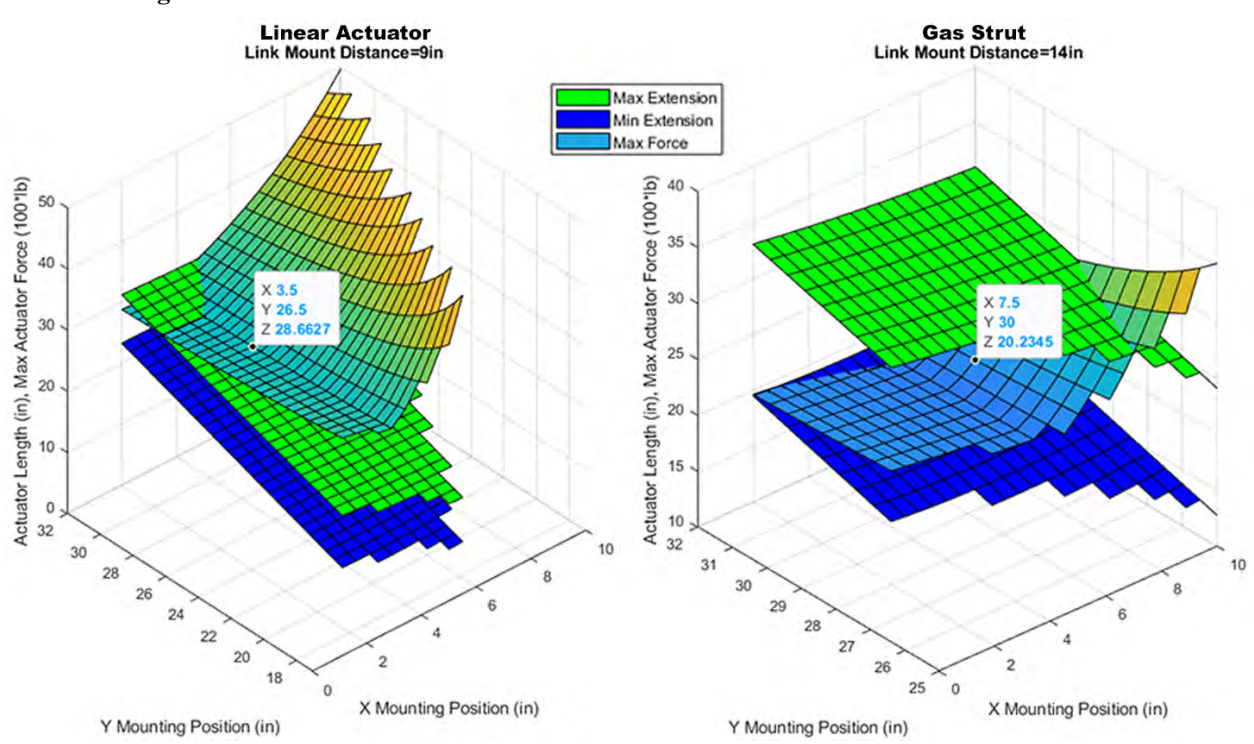


Figure 6. Surfaces and point generated for the final placement of the actuator and struts. Max/Min Extension surfaces cannot be approximated as planes since they are slightly concave and not parallel. The difference between the two defines minimum stroke length, and the Max Force surface describes a two-point wheel contact scenario.

One of the features that makes VERTEX unique is its ability to individually position its wheels with respect to the rover deck. This is accomplished by mounting the swingarm structure that supports the wheels onto a central pivot whose angle is controlled by an electric linear actuator (see Fig. 5). A total of 60° of motion is required from each of the swingarms to allow the deck to remain horizontal while climbing up 30° slopes since each swingarm is roughly half the total length of the rover. Because VERTEX is smaller in width than length, designing for the up-slope capability resulted in superior cross-slope capability of 40° (Fig. 3). The overall system is called the "active suspension" because it allows the rover to actively respond to the terrain in order to improve stability in addition to the passenger's ride.

In designing the active suspension system, there were several factors that had to be balanced: the (X,Y) mounting position of the actuator in the swingarm plane and the mounting distance of its connection along the swingarm itself. These variables affected the force the actuator needed to counteract the vehicle's weight as well as the minimum/maximum extension of the actuator across the -5° to 55° rotation range of the swingarm (Fig. 7). Ideally the actuator position would be chosen to maximize its leverage over the swingarm and minimize its load. However, except for telescopic systems that are prone to deflection, the stroke of linear actuators is typically less than 40% of the system's fully extended length. Thus, the surfaces are cut-off where this stroke parameter is exceeded in the plots generated for each mounting possibility in Fig. 6. To make matters more difficult, off-loading of the actuator via compression gas struts was required to maximize actuation speed. Two 250 lb gas struts were mounted in parallel, outboard of the linear actuator to take advantage of their larger stroke-to-length ratio and leverage. Once potentially feasible commercial-off-the-shelf (COTS) parts were found, their measurements were imported into another MATLAB tool to show their relative positioning throughout the swingarm sweep and to reject combinations that caused collisions (Fig. 7).

The final design uses a 2000 lb electric linear actuator combined with 500 lb of compression gas strut on each of the 4 swingarms to regulate VERTEX's deck-angle. Due to the assembly's geometry throughout a swing, the actuator's linear extension speed of 0.27 in/s converts into an exponential angular speed curve for the swingarm with a low of 1.8°/s at full extension, high of 9.6°/s at full retraction. This trend can be used to maximize ride comfort and response when travelling at high speeds with the rover deck and center of gravity low, whereas the extended pose reserved for hill-climbing or clearing large obstacles can be taken more slowly. With safety as a top priority, actuators with an ACME screw mechanism were selected so that, even in the event of a power failure, the actuators would not backdrive and collapse the vehicle. The static holding force of the actuators is also over 2-times higher than required with a full payload, and additional gas struts could be added for larger payloads.

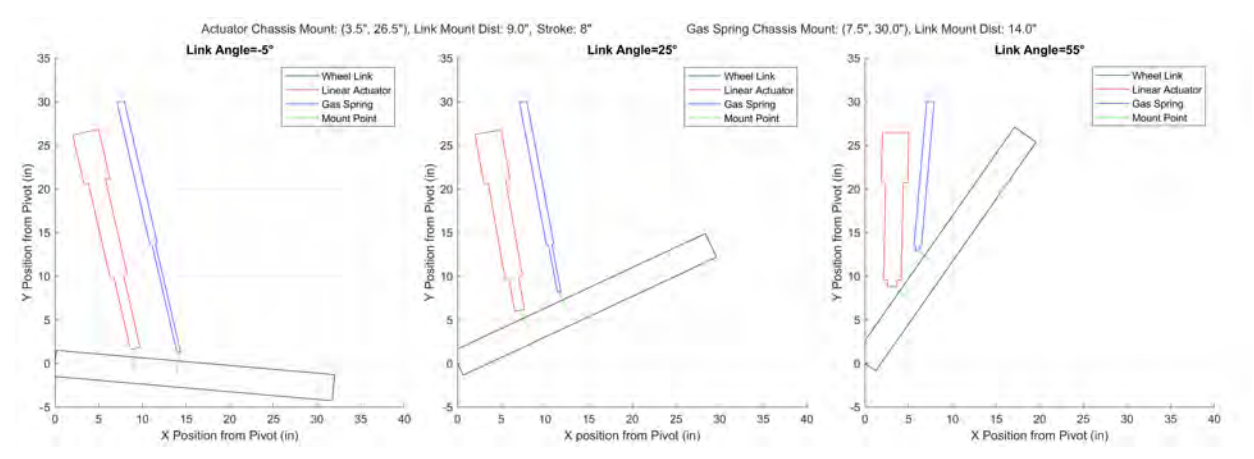


Figure 7. Tool for checking actuator and gas strut collisions across the swingarm's 60° range of motion. Manufacturer-provided measurements served as the input for drawing the devices to scale at their mounting positions.

C. Suspension Integration

The deck-angle actuators were designed to accommodate a 700kg lifting payload (with 100% margin for 2 point contact scenarios) to accommodate sprung rover mass, astronaut with xEMU, umbilical arm, and additional payload. The line of demarcation between sprung and unsprung mass is a difficult segmentation to precisely define in all scenarios. A simplifying assumption leaning to the heavier side of sprung mass was made to place the dividing line on the rover swingarms after all suspension component attachment points as shown in figure 10. This results in almost exactly 250 kg of sprung rover mass, leaving nominally 450 kg for any chassis bound payloads needed, and 1150 kg including margin. Subtracting the umbilical-tending manipulator to be attached (85kg), and including 183.6 kg for xEMU architecture [10] leaves \approx 180 kg pre-margin for a test subject and additional payload.

The high-density of suspension components in a small area presented challenges with integration. The combined length of any spring damper system with the full extension of the linear actuators was too long for any direct in-line system proposed (doubled the rover height), so a pivot system was designed. The spring dampers selected has a compression force of 575 lbs and a stroke of 8.35", which needed to be balanced proportionally with the forces seen in the linear actuators in expected driving loads. It was decided to focus the suspension around the nominal payload case of 700 kg as opposed to tuning for the 100% margin scenario. Ensuring the 700kg scenario would not compress the

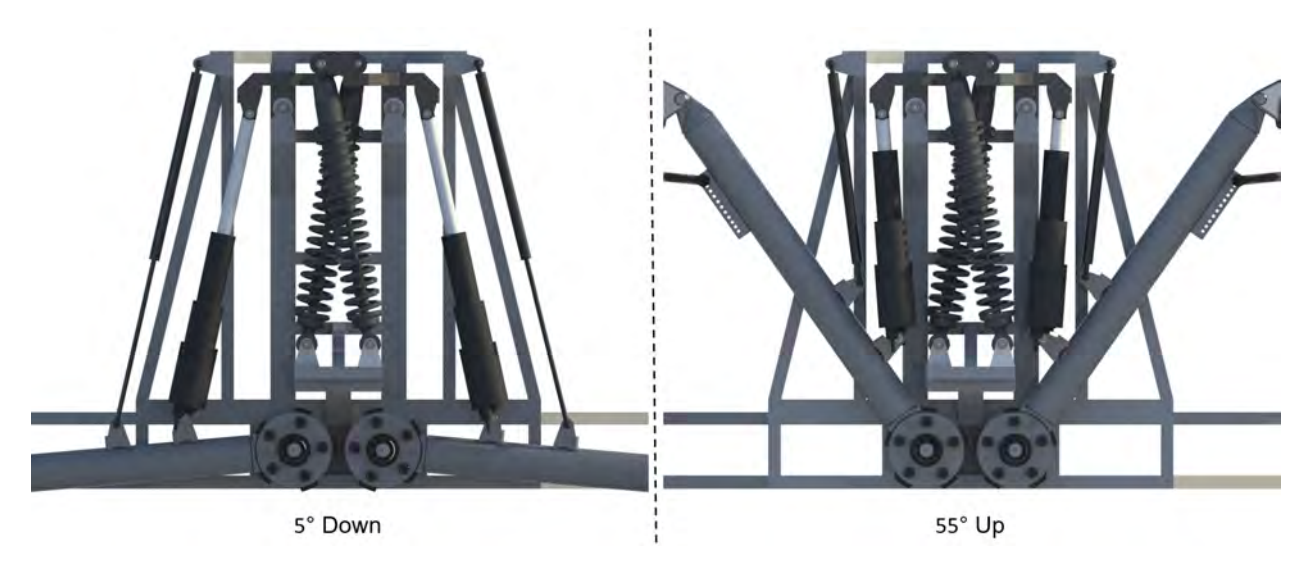


Figure 8. Suspension range of motion

spring dampers statically, \approx 1300 lbs of linear actuator force was desired to start this compression of the series-elastic component. A pivot point was designed to reduce overall volume of the system, with a lever ratio of 2.625 in and 5.75 in for the linear actuator and spring damper respectively. The design maximized the volume allotted in the chassis while being very close to the goal force in easy fractional numbers for manufacturing. The spring damper is expected to begin compress when 1,260 lbs seen in the linear actuator. One notable benefit of the pivot design is in allowing other pivots to be designed and easily swapped with the originals to change these ratios as the rover's design begins to be tested and improved upon.

D. Caster & Camber Angle Adjustment

As the swingarms rotate through their full range of motion, the angle between the steering axis and the ground plane diverges from 90°. When the wheels are pointing parallel to the longitudonal axis of the vehidle, this effect translates directly to the caster-angle (ϕ), and a 90° steering angle will translate this angle to be purely a camberangle (γ). Intermediate angles combine these angles, and will contribute to significant kinematic in-efficiencies as ϕ , γ increase [11], and an accommodating mechanism needed to be designed to reduce these effects. A triangle was created between the swingarm and steering assembly using an adjustable pin and bar mechanism for manual angle control as well as increasing out-of-plane rigidity.

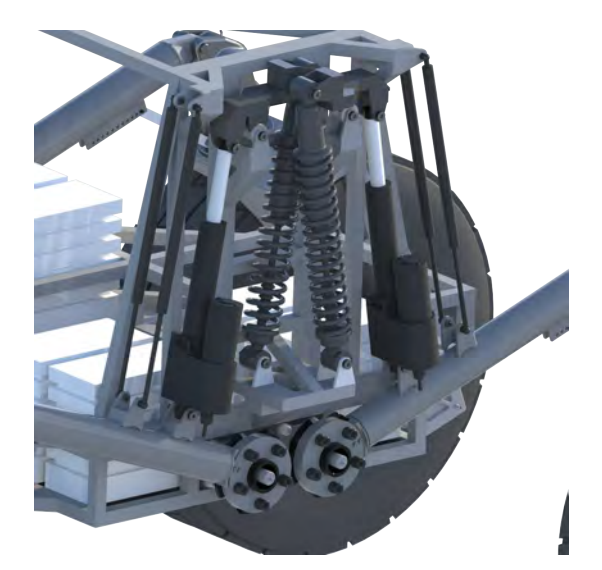


Figure 9. Suspension design isometric view

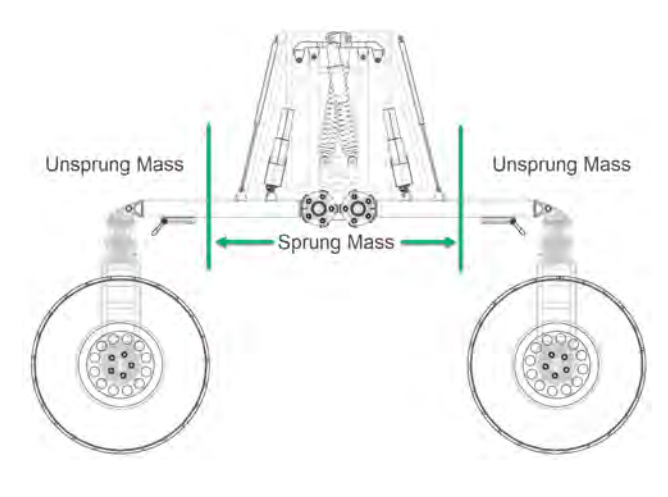


Figure 10. Lines of demarcation between sprung and unsprung mass

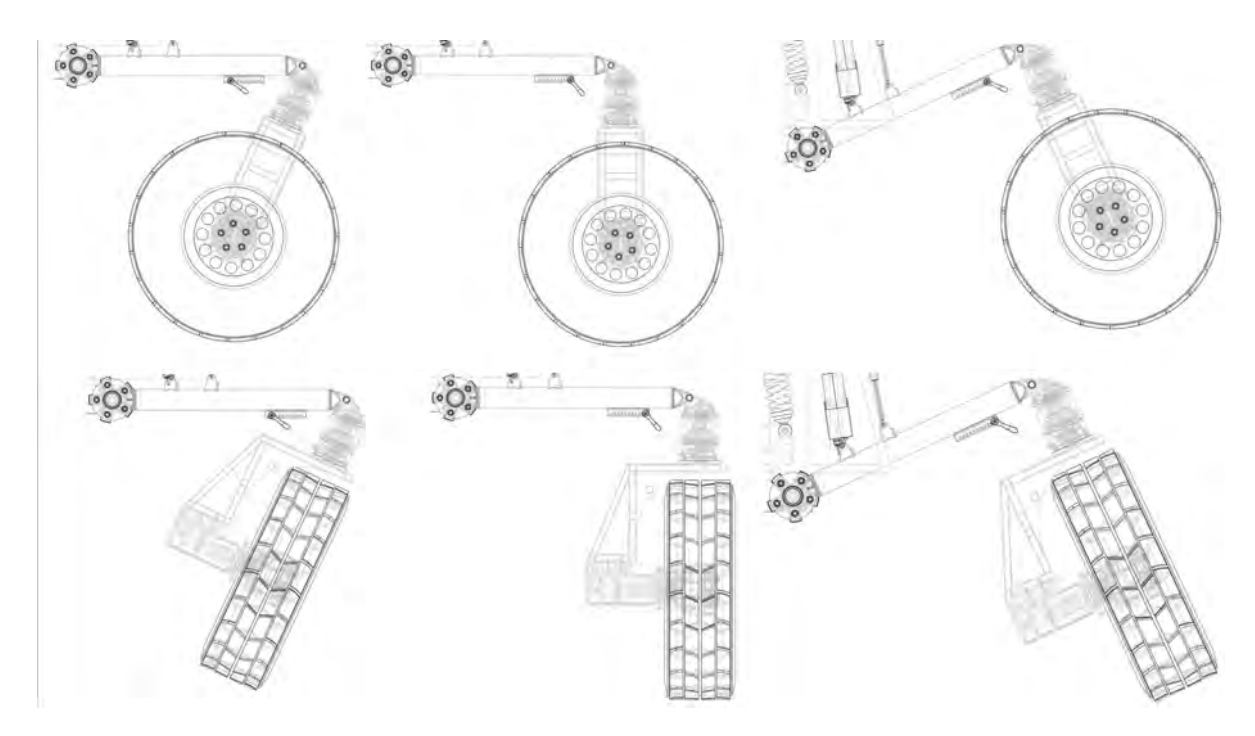


Figure 11. Caster (top) and camber (bottom) adjustments

E. Steering Design

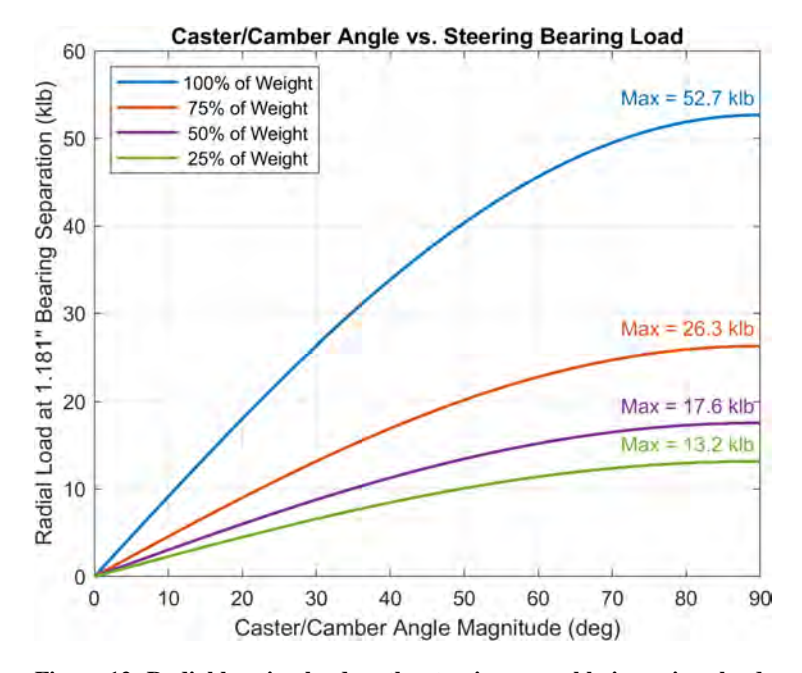
Full 360° independent steering was chosen for VERTEX to maximize the rover's agility in following astronauts, especially with the expected payload of a large umbilical handling robot [3]. Prior SSL studies [1] outline the formulas used to arrive at a required steering torque of 300 Nm, which has been accomplished using a brushless DC motor and 60:1 Harmonic Drive combination (Fig. 13).

While the over-wheel design was chosen to minimize necessary steering torque, immense loads must nevertheless be reacted by the steering actuator because of the lever arm created between it and the wheel contact patch - especially at large caster angles. As shown in Fig. 12, the combination of caster/camber angle with over-wheel steering on such large wheels requires extreme bearing strength to sustain full vehicle roll-overs. In nominal driving cases the caster/camber angle can still be in the 0° - 40° range, where the rover will still regularly enter 2 or 3 contact-point states that generate $\approx 10,000$ lb bearing loads. Simple oil-lubricated composite bushings surrounding the harmonic flexspline cup were selected over larger cylindrical or needle bearings to minimize the overall assembly size, which is over 5.5" in diameter and 8.5" tall. These radial bushings can be seen as thin gray parts between the purple housing and the red geared output in Figure 13.

The structural arch that unites the over-wheel steering assembly to the wheel drive motors (most easily seen in the bottom row of Fig. 11), is designed to crumple into the wheel with 1700 lb of combined loading. This corresponds to a single-wheel tip-over of the vehicle. Requiring this arch structure and the caster-adjustment structure to fail earlier than more critical systems helps prevent damage to the more expensive steering and drive motor assemblies.

F. Electrical Design

The VERTEX electrical system underwent several descopes and modification since the previous publication. Notably, a removal of battery fast charging, and a restructuring of the power delivery system. VERTEX was originally designed to be able to complete two full battery charge/discharge cycles in a single day. However, upon review it was found that a two-sortie test day was not plausible. The required time for setup, test, evaluation, and cleanup did not leave sufficient room for a second sortie during the same day. Furthermore, quick charging introduces additional logistical complexities, such as the acquisition of a 10KW power source, and any necessary permits/authorization to operate one. For example, many state/national parks restrict the usage of gas generators, and/or require permits to operate one. For these reasons, and to reduce the complexity of the initial version of VERTEX, fast charging was



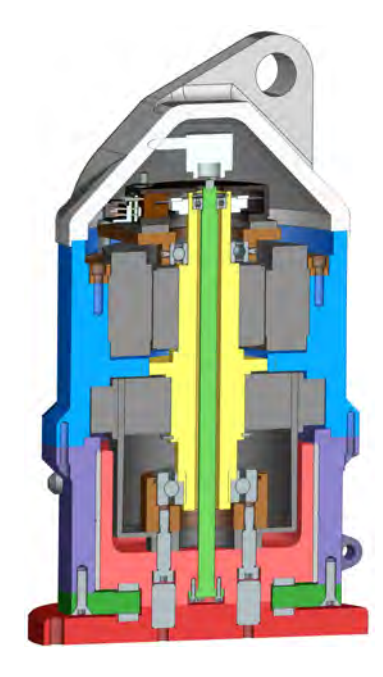


Figure 12. Radial bearing load on the steering assembly in various loading cases. Full weight at 90° would indicate a complete rollover onto one wheel. The 50%-25% load cases at angles of 0° - 40° show nominal loads in 2-4 point contact scenarios.

Figure 13. Cross-section of the steering actuator assembly. Dark gray = motor & harmonic, white/blue/purple = stationary housings, light/dark red = load-bearing output.

dropped. Should the need arise for fast charging, it can be retrofitted to the system with minimal modification to the existing circuitry.

VERTEX is powered by a 32-cell Lithium Iron Phosphate battery, running at a nominal voltage of 96 V, and capacity of $10\,\mathrm{kW}\,h$. The system tops out at $300\,\mathrm{A}$ sustained current output, but is capable of surging to $1000\,\mathrm{A}$ for $30\,\mathrm{s}$. Figure 14 details the primary consumers of power. Note that the power handling electronics immediately after the battery are only protection and interconnect circuits - there is no power conversion between the battery and wheel motor drivers. This is due to the high power consumption of the wheel motors, which at full speed draw $17\,\mathrm{kW}$ when on flat terrain, and up to $34\,\mathrm{kW}$ at full speed hill climb. The remaining actuator systems will draw approximately $6\,\mathrm{kW}$ at full load. Assuming $\approx 20\,\mathrm{kW}$ of continuous draw traveling continuously at near full speed across mildly varying terrain, we expect $\approx 7\,\mathrm{km}$ of range from the vehicle. However, it is not expected that the vehicle travel at full speed continuously for such distances in completing experiments and gathering testing data, and power consumption will be highly dependent on steering and suspension mode selection as well as terrain conditions.

This system is not designed to be a perfect analogue of lunar drive capabilities in all aspects. Budgetary and safety restrictions limited battery technology purchase, and the Earth drive motors requiring $\approx 288x$ more power than the lunar design significantly reduces expected range from similar sized battery packs. As a research vehicle, in-field recharging during break times or slow overnight charging are accessible options.

The rover utilizes a split control scheme, where multiple independent control boards are used to control certain sets of axes. A Galil DMC-4143 4 Axis controller is connected to 4 Advanced Motion Controls AB100C200 motor drivers for the traction motors. A separate DMC-4183 controller connects to a set of 8 AB50A100 motor drives to control both steering and suspension motors. A second DMC-4183 is connected to a set of 6 AB50A100 drivers to control the arm. The DMC controllers close the servo loop at the hardware level, but do not execute any kind of high-level control. Instead, a ruggedized vehicle PC mounted on the chassis performs all high-level tasks and sends motor commands to the DMC controllers. The closure of the servo loop at the DMC controller allows for the performance requirements of the onboard PC to be greatly relaxed, as it does not have to run 16 real-time servo controllers. The entire system communicates over a standard fast Ethernet network, using COTS hardware. This allows for easy interconnect, and simple debugging. The network also connects to a Galil RIO-47300 I/O card, which provides the system with sufficient I/O pins to drive the operator interface.

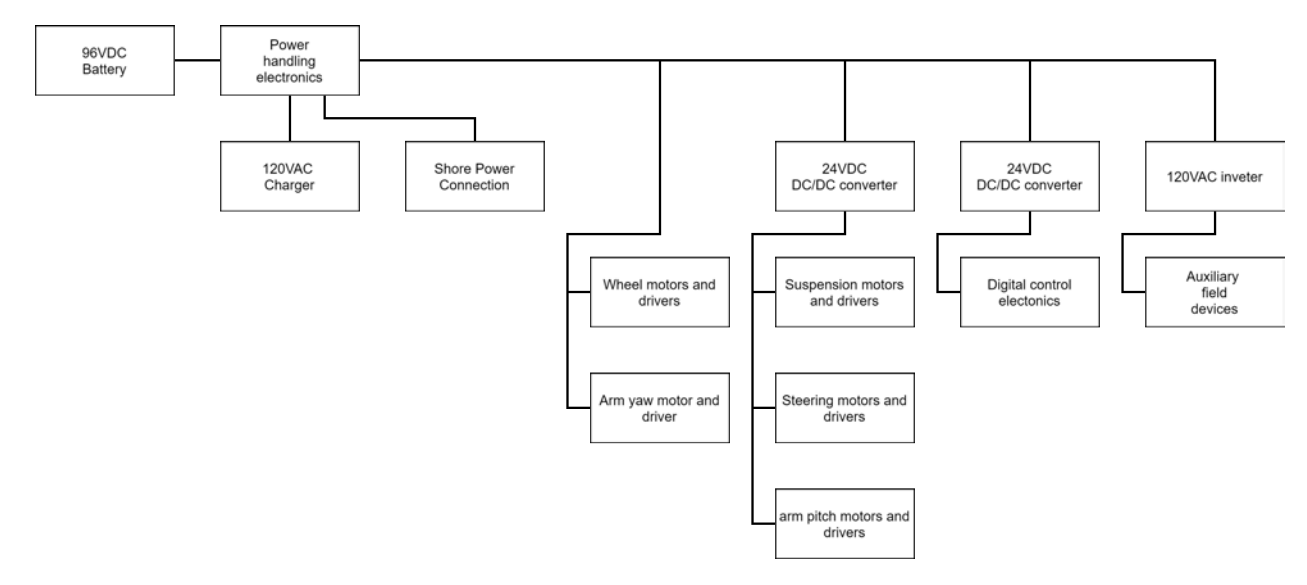


Figure 14. Major power distribution in the VERTEX system

III. Rover Autonomy and Control

A. Software Architecture

In order to mediate the BioBot system's autonomy, the rover's software will utilize the open-source Robot Operating System (ROS) as the primary control system [14]. The SSL has developed robot-agnostic software architecture using ROS for its serial manipulators, with much of the overall architecture being immediately applicable to rovers and parallel robotic systems such as VERTEX without significant modification. Additionally, ROS enables the design of a modular software architecture: as the software needs to run. A simplified physics model of the robot is able to interface with the physics simulator Gazebo through ROS as well, allowing for the testing of the same software run on the physical VERTEX rover itself with simulated actuators and sensors before final hardware implementation [15]. Figure 15 provides an overview of the VERTEX rover software architecture, detailing relevant ROS packages and software processes.

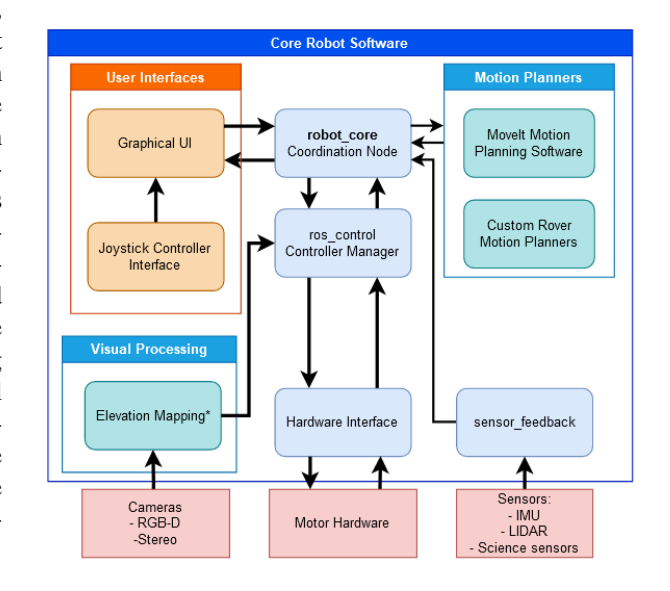
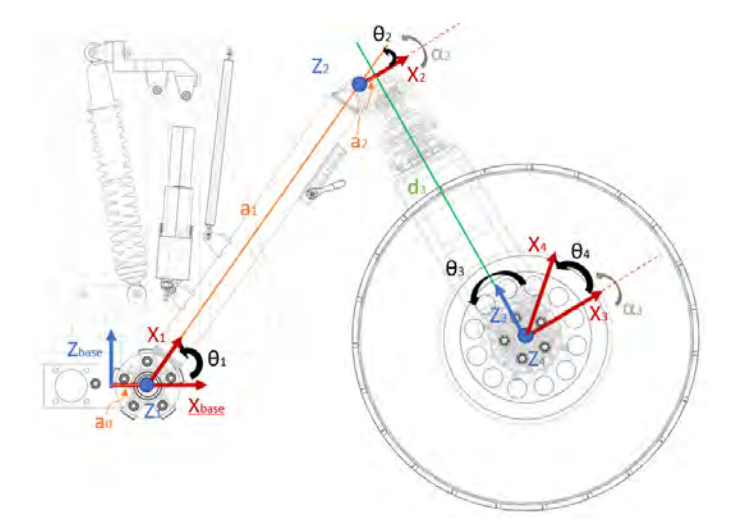


Figure 15. Overview of the SSL robot-agnostic software architecture and open source mapping package used [12] [13].

B. VERTEX Suspension Limb Kinematics

As discussed above, the suspension of VERTEX consists of four limbs connecting the steering assemblies to the chassis, each of which is positioned by a linear actuator and supported by a spring-damper system that serves as passive suspension. In the control software, simple nodes convert linear actuator positions and velocities to rotational velocities of the limbs about their respective joint axes. Note that, as discussed above, camber angle adjustment of joint 2 is positioned manually ahead of time. Figure 16 and Table 2 overview the kinematics of each limb in more detail.



Joint i	α_{i-1}	a_{i-1} (m)	d_i (m)	θ_i
1	0	0.051	0	θ_1
2	0	0.806	0	θ_2 *
3	-90°	0.051	-0.686	θ_3
4	90°	0	0	θ_4

Table 2. DH parameters of the front right leg. Each joint is revolute, but θ_2 is not actuated and is set manually. The table follows the modified DH format described in Criag (2005) [16].

Figure 16. DH parameters of the front right leg. Other leg frames and axes are similarly aligned.

C. Autonomous Motion Planning

1. Astronaut Tracking

Critical to the BioBot's capabilities is the ability to track its paired astronaut autonomously and generate trajectories around obstacles to follow them as the astronaut conducts surface operations. To ensure that the rover knows both the position and orientation of the astronaut, the vision system onboard the rover tracks AprilTag fiducial markers printed on the astronaut's spacesuit [17]. As these fiducial markers would often be obscured by glare, dust, or astronaut orientation, however, other methods of astronaut tracking using more complicated vision processing tools that are more robust to such obstacles are currently being investigated. The topic of astronaut tracking covered in considerably more detail in a corresponding paper on the BioBot architecture's autonomous umbilical handling capabilities, as the same software is used for both positioning the BioBot umbilical arm and orienting the rover towards its paired astronaut independently of the umbilical system [3].

2. Mapping

The BioBot system's need to follow an astronaut autonomously over rough terrain is a difficult problem to tackle, requiring the rover to not only be aware of the astronaut's position and the rover's own internal odometry, but also be knowledgeable about the surrounding terrain's slopes and potential obstacles. The fact that a human may be agile to overcome certain obstacles that the rover cannot only compounds the complexity of this issue: if a human can step over a large rock or pit, having the rover be intelligent enough not to blindly drive after the astronaut and encounter the environmental hazard, instead planning a safer and more efficient path.

The rover will use a suite of sensors connected to the core ROS software to perceive and map its environment. Primary terrain mapping is accomplished via the use of an array of Intel RealSense D435i cameras, RGB-D sensors capable of providing both camera images and depth feedback to identify obstacles. The D435i also possesses integrated IMU's which will be used by the mapping software to generate accurate robot-relative terrain maps. Testing is being conducted in simulation to determine the optimal positioning of these sensors on the rover, but placing one camera at the front and one on each of the left and right sides of the chassis has worked to help generate a detailed terrain map. As each rover's dimensions vary wildly, the positioning of these sensors will be determined experimentally through both simulation and field testing to ensure accurate environmental measurements are achieved.

Mapping the terrain for motion planning also poses unique challenges: the unstructured terrain and potential large slopes that the BioBot system must navigate are not conducive to simple motion planning. Indeed, the core open-source navigation and mapping packages for ROS are not designed for planning in any environment more complicated than a flat plane, necessitating more comprehensive methods of motion planning and mapping are required. To map the environment, the BioBot system will utilize the Robot-Centric Elevation Mapping ROS package developed by ANYbotics, which uses RGB-D, stereo, and/or LIDAR images to create and categorize terrain maps of surrounding

environments for mobile robots like BioBot [12] [13]. The resultant slope maps will be used to generate a costmap of the environment and of potential trajectories for BioBot to take when following an astronaut or autonomously travelling to a miscellaneous objective.

3. Trajectory Planning

The BioBot system's motion planning challenges are unique among planetary rover concepts. In addition to the challenge of path planning in difficult terrain as described above, the system must calculate and complete these plans in a manner that is helpful to and predictable by the astronauts that BioBot is paired with. The trajectories generated must be fast enough to keep up with an astronaut conducting surface operations in order to both keep the astronaut in sight and keep the majority of the weight of the umbilical borne by the BioBot mobile manipulator system instead of putting that burdern on the astronaut. These different challenges create conflicting requirements for both solution speed and optimality that must be balanced for a successful motion planning solution. Two methods of motion planning are being explored for this application simultaneously: grid-based paths followed by a trajectory controller on the rover; and more detailed trajectories directly taking rover dynamics into account using random sampling.

For grid based planning, the Field D* algorithm is a flight-proven method of generating organic trajectories to a goal in a grid-based map [18]. Field D* has the distinct advantage of producing organic trajectories in a 2D grid: instead of stepping between square grid segments in an angular and inefficient means, the rover linearly interpolates between nodes of similar costs, allowing for much more organic and efficient paths. This capability is especially important due to the rover's close interaction with human astronauts, as the paired astronaut should be able to approximately predict the rover's path over terrain for safety and efficiency purposes. The map generated by the Elevation Mapping package is converted into a costmap for the rover that takes the slope of the terrain and presence of obstacles into account, allowing for the rover to generate trajectories through a grid and replan as new obstacles are discovered. There are complications to this algorithm, however: the fact that both the rover position and the astronaut position will change over time means that the plan must often be recompiled from scratch at each step, which will inevitably increase the processing time of the problem. This will be mitigated by changing the rover's goal position only when the astronaut moves out of the arm's reach of the previous goal point instead of planning to the astronaut's location continuously.

Grid based planning via Field D*, however, has limited resolution in true rough terrain and does not directly consider the dynamics of the rover, leaving such concerns to the costmap and a trajectory-following controller instead. As such, random sampling that directly considers the rover's overall trajectory is also being investigated. SST—the stable spare RRT algorithm—and its asymptotically optimal variant SST* offer fast solutions to motion planning problems on dynamically complex vehicles [19]. Unlike commonly used random sampling algorithms like RRT* and RRT#, SST* offers the additional advantage of not requiring a closed-form solution to the vehicle's dynamics, instead propagating the dynamics forward between samples and optimizing motion with whatever time is left for planning. This non-reliance on closed-form kinodynamic solutions is especially helpful in a high degree of freedom system such as VERTEX, and the anytime nature of SST* allows for paths to be improved over time but for generated trajectories to be followed prior to perfect optimization. In the event that this algorithm does not reliably find and optimize a solution quickly enough on onboard hardware, alternate random sampling methods will be investigated, including biasing the SST algorithm with an RRT* solution generated using a simplified model of the rover dynamics. These algorithms will enable the VERTEX rover and overall BioBot system to generate trajectories in unexplored environments during surface operations and maintain life support connection to its paired astronaut.

IV. Looking Forward

A. Hardware Assembly

The rover is nearing the end-stages of completion, and is expected to have its first driving tests performed in early summer. Figure 17 shows the current completion of the rover chassis, with full integration of linear actuators, gas struts, and spring dampers. Figure 18 shows a wheel, gearbox, and drive motor assembly during a test fit. Interfacing and support hardware for the wheels is in the final fit and integration stages with small adjustments to guarantee proper alignment and documentation efforts.





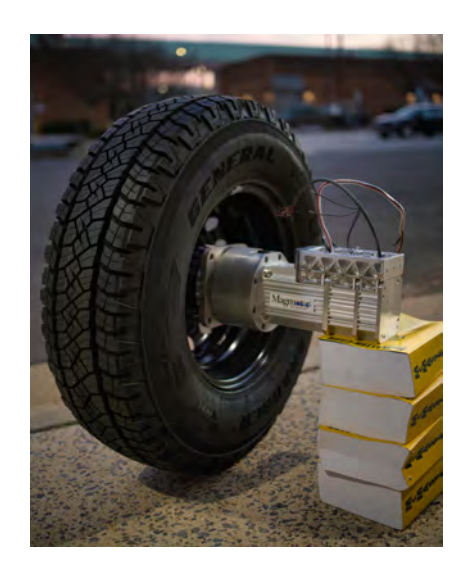


Figure 18. Wheel Assembly Test Fit

B. Planned Testing

A few locations are currently under negotiation for testing use including Maryland Department of Natural Resources off-road vehicle (ORV) trails, a private ORV complex, a disused rock quarry, and an outdoor facility at the Aberdeen Proving grounds. A few different phases of testing are currently being planned including: 1) Human control interface testing, 2) Autonomous astronaut tracking/following, and 3) Rover capability verification.

1. Human Interface Testing

Local on-site testing across the university is expected to encompass a majority of the control testing to allow both a large-variety of personnel available and close proximity to the SSL machine shop for rapid iterations. Urban environment obstacles such as staircases, curbs, steep grassy hills, and parking lots will allow inexperienced operators to safely operate VERTEX in safe yet semi-challenging environments and provide feedback for design improvements.

2. Autonomous Feature Testing

Rover autonomy will be tested in gradual phases. Local testing in various lighting conditions will be used to test the validity and quantify the performance of tracking strategies such as AprilTags. Control strategies in managing the active umbilical management arm and the rover mobility in collaboration with eachother will need to be refined based on human activity and interaction.

3. Rover Capability Verification

Challenging terrain will be required to push VERTEX into the verification zone including 30° slopes with loose soils, cratered areas, and large rock formations. Off-site locations will be used as a pseudo-lunar environment, and the testing will thoroughly test systems such as the automated chassis-leveling, astronaut boarding/deboarding, robotic umbilical tending feasibility, and multi-astronaut emergency transport capabilities.

Acknowledgments

The authors would like to thank the NASA Innovative Advanced Concepts (NIAC) program as well as the 2021 Moon-to-Mars eXploration Systems and Habitation (M2M X-Hab) program as supporters of the BioBot program over the last two years of development. The authors would also like to thank Chandler Sheatzley for his contributions to the design of the over-wheel steering arch and caster-angle support structure, as well as Nicholas Limparis for his patience during design reviews and critical input to the design of the mechanical and electrical systems.

References

- [1] David Akin, Charles Hanner, Nicolas Bolatto, Daniil Gribok, and Zachary Lachance. 'Design and Development of an EVA Assistance Roving Vehicle for Artemis and Beyond'. In: 50th International Conference on Environmental Systems (ICES). 2021. URL: https://hdl.handle.net/2346/87097.
- [2] David Akin. Biobot: Innovative offloading of astronauts. Mar. 2018. URL: https://www.nasa.gov/directorates/spacetech/niac/2018_Phase_I_Phase_II/Biobot_Innovative_Offloading_of_Astronauts/.
- [3] David Akin, Nicolas Bolatto, Robert Fink IV, Joshua Martin, Zachary Lachance, and Rahul Vishnoi. 'Development of an Autonomous Umbilical Tending System for Rover-Supported Surface EVAs'. In: *51st International Conference on Environmental Systems*. ICES-2022-361. July 2022.
- [4] David Akin. 'Development of a Next-Generation Suit Simulator System for Neutral Buoyancy and Field Testing'. In: 51st International Conference on Environmental Systems. ICES-2022-362. July 2022.
- [5] David Akin, Nicolas Bolatto, Daniil Gribok, and Charles Hanner. 'Controls, Displays, and Restraint Concepts for Highly Capable Crewed Planetary Rovers'. In: *51st International Conference on Environmental Systems*. ICES-2022-363, July 2022.
- [6] NASA TM-X-66816. 'LRV Operations Handbook, Appendix A (Performance Data)'. In: NASA Manned Spacecraft Center. Apr. 1971.
- [7] NASA HLS-RQMT-001. 'Human Landing System (HLS) Requirement Document'. In: NASA Marshall Space Flight Center. Sept. 2019.
- [8] David Akin. Astrobotic Griffin Lander. Mar. 2021. URL: https://www.astrobotic.com/griffin.
- [9] Raquel C. Galvan-Garza, Torin K. Clark, David Sherwood, Ana Diaz-Artiles, Marissa Rosenberg, Alan Natapoff, Faisal Karmali, Charles M. Oman, and Laurence R. Young. 'Human perception of whole body roll-tilt orientation in a hypogravity analog: underestimation and adaptation'. In: *Journal of Neurophysiology* 120.6 (Dec. 2018), pp. 3110–3121. DOI: 10.1152/jn.00140.2018.
- [10] Office of Auits. NASA'S DEVELOPMENT OF NEXT-GENERATION SPACESUITS. 2021. URL: https://oig.nasa.gov/docs/IG-21-025.pdf.
- [11] Dai Vo, Hormoz Marzbani, Mohammad Fard, and Reza Jazar. 'Caster–Camber Relationship in Vehicles'. In: May 2016, pp. 63–89. ISBN: 978-3-319-27053-1. DOI: 10.1007/978-3-319-27055-5_2.
- [12] Péter Fankhauser, Michael Bloesch, and Marco Hutter. 'Probabilistic Terrain Mapping for Mobile Robots with Uncertain Localization'. In: *IEEE Robotics and Automation Letters (RA-L)* 3.4 (2018), pp. 3019–3026. DOI: 10.1109/LRA.2018.2849506.
- [13] Péter Fankhauser, Michael Bloesch, Christian Gehring, Marco Hutter, and Roland Siegwart. 'Robot-Centric Elevation Mapping with Uncertainty Estimates'. In: *International Conference on Climbing and Walking Robots* (CLAWAR). 2014.
- [14] Morgan Quigley, Ken Conley, Brian Gerkey, Josh Faust, Tully Foote, Jeremy Leibs, Rob Wheeler, Andrew Y Ng, et al. 'ROS: an open-source Robot Operating System'. In: *ICRA workshop on open source software*. Vol. 3. 3.2. Kobe, Japan. 2009, p. 5.
- [15] Nathan Koenig and Andrew Howard. 'Design and use paradigms for gazebo, an open-source multi-robot simulator'. In: 2004 IEEE/RSJ International Conference on Intelligent Robots and Systems (IROS)(IEEE Cat. No. 04CH37566). Vol. 3. IEEE. 2004, pp. 2149–2154.
- [16] John J Craig. Introduction to Robotics: Mechanics and Control. Pearson Education, 2005.
- [17] John Wang and Edwin Olson. 'AprilTag 2: Efficient and robust fiducial detection'. In: 2016 IEEE/RSJ International Conference on Intelligent Robots and Systems (IROS). IEEE. 2016, pp. 4193–4198.
- [18] Dave Ferguson and Anthony Stentz. 'Field D*: An interpolation-based path planner and replanner'. In: *Robotics research*. Springer, 2007, pp. 239–253.
- [19] Yanbo Li, Zakary Littlefield, and Kostas E Bekris. 'Asymptotically optimal sampling-based kinodynamic planning'. In: *The International Journal of Robotics Research* 35.5 (2016), pp. 528–564.

Development of an Autonomous Umbilical Tending System for Rover-Supported Surface EVAs

Nicolas Bolatto¹, Robert Fink IV², Joshua Martin¹, Zachary Lachance¹, Rahul Vishnoi², and David Akin³ *University Of Maryland, College Park, MD, 20742, USA*

For surface extravehicular activities, no other parameter is more impactful on the design of spacesuits than the "weight on the back," or the weight of the suit system that must be supported by the astronaut under gravity. The portable life support system (PLSS) alone has nearly doubled the weight of the astronaut historically, significantly increasing the exertion required to conduct manned surface activities and drastically curtailing the range of motion of the astronaut due to the movement of the center of mass rearwards and upwards. Both of these negatively affect EVA performance of astronauts; as a result, the capability to offload an astronaut's PLSS would be of great benefit to future EVA operations. The University of Maryland Space Systems Laboratory has been investigating one potential solution to this via its "BioBot" concept, supported by the NASA NIAC program. The overall concept is of a rover carrying the life support system for the EVA crew and supplying consumables via umbilicals. This paper focuses on the critical technology to make this approach viable: the umbilical-handling robot and its associated rover-mounted life support hardware. The robotic manipulator must support both its own weight and that of the umbilical, while keeping close enough to the EVA crew to eliminate the need for additional slack which could snag the umbilical on surface features. This paper details the design of the umbilical-handling robot, which must function as an Earth analogue system for human factors testing, and the designs of the umbilical, suit disconnect, and Earth analogue life support system. Additionally, this paper describes the sensors and algorithms for smoothly blended motion between the manipulator and the rover, as well as the design implications for the astronaut-following rover itself. Future design modifications are also discussed.

Nomenclature

ARMLiSS Active Rover Mounted Life Support System
D-FLEAS Desert Field Lessons in Engineering And Science

DH (modified) Denavit–Hartenberg

DOF Degree Of Freedom
EVA Extravehicular Activity
J0, J1, ..., J4 Joint 0, Joint 1, ..., Joint 4

NIAC NASA Innovative Advanced Concepts

PLSS Portable Life Support System
ROS Robot Operating System
SSL Space Systems Laboratory
UMd University of Maryland

VERTEX Vehicle for Extraterrestrial Research, Transportation, and Exploration

xEMU Exploration Extravehicular Mobility Unit

¹Graduate Research Assistant, Space Systems Laboratory

²Undergraduate Research Assistant, Space Systems Laboratory

³Director, Space Systems Laboratory. Associate Professor, Department of Aerospace Engineering

I. Introduction

For extravehicular activity (EVA) on a planetary surface, such as the Moon or Mars, one of the most significant limitations to astronaut capability is the weight of the suit system that they must support. The A7L-B suits worn on the later Apollo missions had a mass of 96 kg, a 130% increase to a 75 kg astronaut. Of this mass, 61 kg was for the portable life support system (PLSS), with the remainder of the mass being the pressure garment assembly itself. This additional mass results in significant increases to wearer exertion, especially due to the upward and rearward shift in center of gravity and resulting decrease in stability, which becomes a limitation to the duration of EVA operations, walking distance, and productivity. In the Artemis missions, the xEMU EVA system mass is expected to double from 96 kg for Apollo to 187 kg due to the addition of a hard upper torso and other weight increases. This will result in an Artemis astronaut increasing their mass by a factor of 3.5 during EVAs, resulting in an apparent weight on the Moon 60% that of the crew on Earth. On Mars, the astronaut's apparent weight during EVAs will be the same as in shirtsleeves on Earth, notwithstanding losses in muscle tone during 9-12 months of microgravity on the way to Mars. Thus, the "weight on the back" of astronauts will be an even greater concern in the coming human exploration missions.

Earlier missions, such as those of the Gemini program, utilized umbilical systems to provide the necessary life support equipment during microgravity EVAs. While it was necessary to control and manage the umbilical in this design, it allowed for greater ease of motion of the crew due to the reduction in bulk and mass of the overall system. In surface missions, umbilicals were dismissed due to the limitation of needing to remain in close proximity to the lander system. An umbilical system for life support during astronaut surface operations that did not have the limitations of umbilical management and range restriction would allow for greater surface EVA capability and reduced astronaut exertion without limitation. This is the goal of the University of Maryland BioBot system: a mobile, astronaut tracking platform that utilizes a robotic arm to tender an umbilical for astronaut life support offloading, shown conceptually in Figure 1.



Figure 1. Artist's concept of the original BioBot reference configuration.

This paper details the umbilical tending Earth-analogue design of the BioBot system: the Active Rover Mounted Life Support System (ARMLiSS). This 5-degree-of-freedom robotic manipulator supports the umbilical above any potential obstacles prevent snagging, removes the umbilical weight from the astronaut, and manages the umbilical positioning utilizing astronaut tracking and following software. The arm can be mounted in a static position for localized EVAs, such as on a lander or on a separate support stand, or it can be mounted on a rover system for long-distance capability. Details of a rover specifically designed as the basis for a BioBot system, with specifics regarding suspension and active payload roll and pitch control, can be found in a concurrent paper [1].

II. Concept Development

Initial testing of the BioBot umbilical tending system focused on three preliminary designs: a passive single lifting point catenary design, a passive pantograph-type kinematic chain, and an actively-controlled manipulator with passive yaw control. These three designs can be seen in Figure 2.

In this testing, the single point catenary design was deemed to be overly difficult for EVA crew to manage, as the astronaut was required to support half of the umbilical weight which resulted in a downward and backward force applied to the attachment point. There were also concerns about the lateral swinging of the umbilical catenary, which was demonstrated to induce cyclical side loading. Both of these effects had negative impacts to motion and comfort for the test subjects. Thus, the other two designs were developed to reduce the physical and cognitive loads of the system on the user.

While the conclusion from the phase 1 study was that both the active and pantograph designs performed sufficiently and were recommended for development for phase 2, the phase 1 team preferred the pantograph design. It was







Figure 2. Phase 1 preliminary designs: (L-R) single point catenary design, pantograph-type kinematic chain design, and actively-controlled manipulator[2].

determined that this design was significantly simpler, as the active system introduced much greater control and power requirements. However, the pantograph system was cited as having insufficient torsional stiffness and experienced an over-center "latching" effect, as well as being "kinematically complex" [2].

All of these systems were meant to function in a proof-of-concept role; thus, materials such as plywood were utilized which are unsuitable for the final design. Furthermore, the use-case of the arm being positioned on a slope was not considered by the phase 1 study, with all testing being done on relatively level terrain. Thus, upon development for the phase 2 design, it was determined that the drastic increase in weight necessary to meet the functionality requirements while simultaneously minimizing the overall impact of the umbilical to the astronaut ruled out the passive design. On slopes of 10 degrees for an Earth analogue system, the yaw torque increases substantially to over 400 Nm (see Section V-2). This is sufficient to pull an astronaut over if not actively controlled, especially in a lunar environment, and also risks tearing the umbilical. As a result, the passive design was ruled out and the actively controlled system was selected for further development.

III. Umbilical Design

In order to offload as much equipment from the astronaut as possible while maintaining the highest EVA performance and comfort possible, the umbilical was designed with five separate components contained within one overall structure. These consist of two tubes for the air loop, two tubes for the cooling fluid loop, and communications/avionics electrical connections. Air and cooling fluid are cycled through the system via pumps located on the rover or stand. All of these connections are passed through an umbilical connection hard-point on the astronaut's suit to integrate with the suit-based loops and electronics (the cooling and airflow systems on the suit side remain unchanged from current suit designs other than interfacing with the umbilical itself instead of a backpack PLSS).

The concept of operations for BioBot includes the ability for the user to release the umbilical and perform certain operations using a short-duration portable life support system (PLSS) on the suit backpack. One of the major objectives of the current BioBot research is to perform analogue field tests to better understand the operational environment and safety implications of short-term untethered operations, then recharge the backpack consumables when the user is attached to the umbilical again. This testing, which has not yet been conducted and will be detailed in a future paper, will be used to determine the efficacy of this short-duration PLSS and to determine the optimal concept of operations surrounding its use in relation to tethered operations. The process of being able to unhook and reengage the umbilical puts design constraints on both the interfaces and on the operation of the ARMLiSS system. Since the EVA crew will require a highly reliable means of performing the umbilical interactions, the umbilical will mate to the chest area of the spacesuit to be within the dual-hand working envelope. The details of the umbilical interface are presented in a separate paper [3]; however it is worth noting here that engaging the umbilical interface is a one-handed motion, but releasing it requires independent coordinated motion of both hands to ensure prevention of inadvertent release.

Since the umbilical will mate on the chest of the spacesuit, the end of the umbilical will be a rigid external structure that goes under the helmet, over the left shoulder, and upwards to mate with the rest of the umbilical. In this way, the end of the umbilical cannot intrude on the user's vision, or present a snag hazard to the EVA crew's arms or hands. The rest of the umbilical will be conventional, consisting of separate tubing for both oxygen and cooling water inlet and exhaust, as well as wiring for suit power, communications, and data. For design purposes, the umbilical will match studies of conceptual Artemis umbilicals, with an outer diameter of 5 cm, a mass of 1.25 kg/m, and a minimum bend

IV. Umbilical Arm: Purpose and Requirements

The purpose of the umbilical arm design presented in the following sections is to demonstrate the BioBot concept's capabilities here on Earth, where field testing can show the merits of the unique system before implementation on the Moon or Mars. In other words, the goal is to show the effectiveness of an umbilical handling arm that can offload the life support equipment for an EVA astronaut up to 5 m away and on 30° slopes. This design however cannot be directly compared to what a true "flight" version of the umbilical tending system would be in terms of mass, power, and volume. Designing an Earth-analogue robot with the same capabilities as a lunar version comes at a significant cost to structural and actuator mass due to gravity being approximately 6 times greater as shown in the design of the VERTEX rover. This additional mass does not necessarily scale at the same rate as the change in gravity environment due to compounding factors (such as increases in structural mass driving increases in actuator mass and power which drive further increases in structural mass) [1]. This relationship also is expected to hold for the martian gravity case, albeit to a lesser degree due to the gravity levels of the Earth and Mars being closer than that of the Earth and Moon. As a result of these factors and limitations, the design of ARMLiSS is expected to be less capable in extension speed and more massive than a flight equivalent because of the actuator gearing required for Earth gravity. As such, if this concept is shown to improve EVA performance and comfort through field testing compared to a traditional PLSS, a flight equivalent (without the limitations of weight and speed) is thought to be only more effective. A future goal of this study is to design a version to lunar specifications and compare the lunar and Earth-analogue designs.

With the intention of creating a design that is as conducive to implementation on the Moon or Mars as possible, the ability to compactly package the arm was key. Keeping within the VERTEX rover's footprint so that both could be easily transported for field testing, the maximum permissible footprint for the packed arm was 2m long by 1.5m wide. Furthermore, to be suitable for use atop a mobile platform, the umbilical arm should be able to retract while driving for greater stability while still maintaining a connection to the astronaut. These requirements originally removed telescopic-boom-style arms from consideration, and SSL's NIAC Phase 1 study showed that a pantograph design would be costly in terms of mass and volume to scale upwards in length. A tension-cable design like NASA's Lightweight Surface Manipulation System could be more mass-efficient, although it would be difficult to modify for stowage and would require significant on-site assembly by astronauts. To truly benefit surface operations, the umbilical arm must be operationally transparent to astronauts and easy to set up for use.

The SSL has conducted significant field testing on the impacts of using rovers to aid in suit-simulated EVA as part of Desert Field Lessons in Engineering And Science (D-FLEAS) with suited geologists traveling and collecting samples with and without a transportation rover [5]. These studies demonstrated that subjects would often be interested in locations that were accessible on foot but not for a wheeled rover: "Test subjects routinely traversed slopes of up to 30° in the approach to the vertical faces of the test sites, and climbed slopes in excess of 60° in cases where the footing was acceptable." [6] To enable the exploration of difficult terrain that may be beyond the rover's capabilities, such as rocky areas, crater rims, and other steep faces, the arm's workspace was maximized. At the same time, the um-

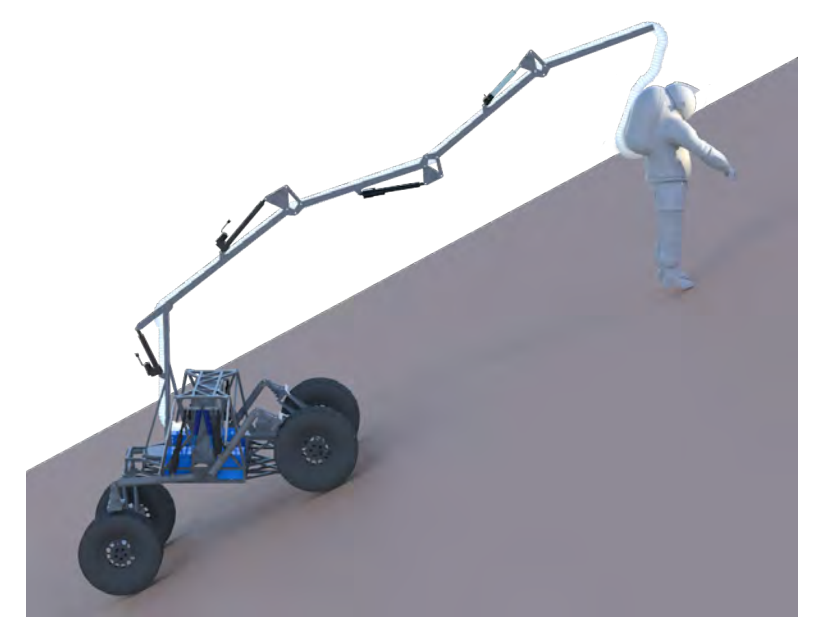


Figure 3. Rover-mounted arm providing umbilical tending on up to 30° slopes while the VERTEX rover maintains a level deck for stability.

bilical arm must retract far enough for an astronaut to drive in the front seat of the rover or to access the rover exterior where scientific payloads may be stored. This way, the number of umbilical disconnect and reconnect operations and potential for dust impingement is minimized.

The umbilical arm's principal use case is mounted on a mobile rover platform where a combination of the rover's motion and arm extension would be used to keep a tended astronaut within the arm's workspace. However, there are cases where the arm must match astronaut walking speeds by itself without the assistance of the rover, such as when an astronaut returns to the rover to drive elsewhere, deposit samples, or deploy instruments. To accomplish this without requiring an astronaut to slow down, the arm's retraction speed would have to surpass the ≈ 0.6 m/s average walking speeds of Apollo astronauts on J-missions [7]. Although new-generation suits will increase the mobility of astronauts and possibly increase their average walking speed, it is also expected that a lunar version of the arm would be faster because of its reduced weight. Thus, the current Earth-analogue design focused mainly on meeting the workspace and packing requirements while making the 0.6 m/s extension speed a soft goal.

Initial feasibility studies indicated that a 5m-long umbilical arm was possible while remaining within the aforementioned footprint requirements by using a 5-link over-actuated arm design. Such a design requires more resources in terms of power, computation, and sensing; however, these costs are necessary to achieve the desired performance while keeping the arm relatively transparent to the astronaut, as will be described in the following sections.

V. Mechanical Design

The umbilical arm is designed to position the flexible portion of the astronaut's umbilical slightly above and behind the astronaut's head, with enough umbilical "slack" to connect to the suit without restricting high-frequency motions such as bobbing while walking. Therefore the arm must be capable of supporting the weight of the extra umbilical and quick-disconnect at the tip, in addition to the arm's own structural and actuator weight, while simultaneously keeping up with an exploring astronaut.

A. Joint Design and Torque Analysis

1. Pitch Joints

A parametric model of the arm was created in MAT-LAB, containing the measurements and mass of each link bar, joint lever assembly, and linear actuator. The additional mass of the umbilical itself was modelled as a 2 kg/m linear density across the full length of the arm, with a further 1.5 m of umbilical leading from the tip of the arm to the astronaut. Margin for the mass of an umbilical quick-disconnect at the tip was also factored in. By inputting a trajectory of joint angles from the stowed configuration to full extension, an accurate model of the torques experienced by each joint was created (Fig. 5). The maximum torques required for each joint are summarized in Table 1.

Joints 2 through 4 of the arm need to to actuate about 160 degrees and also require a large amount of torque. Due to the high torque requirements, the joints were designed to take advantage of a lever arm, rather then generating the torque at the pivot with a direct drive solution. Initial design inspiration was taken from concrete pump trucks. They have long arms which fold compactly onto the back of a truck. In many ways, this is similar to ARMLiSS, except it supplies water, power, and data as opposed to concrete. Initial designs of the arm considered two types of joints driven by linear motion, ones driven from the outside and ones driven from the inside. By alternating these two types, the folded volume can be minimized. However, as design efforts progressed, the interior style joints were abandoned. This design deci-



Figure 4. Diagram of arm joint locations, corresponding to torques in Fig. 5. Structural links are numbered by their proximal joint, with the vertical mast being link 0 and the tip being link 4.

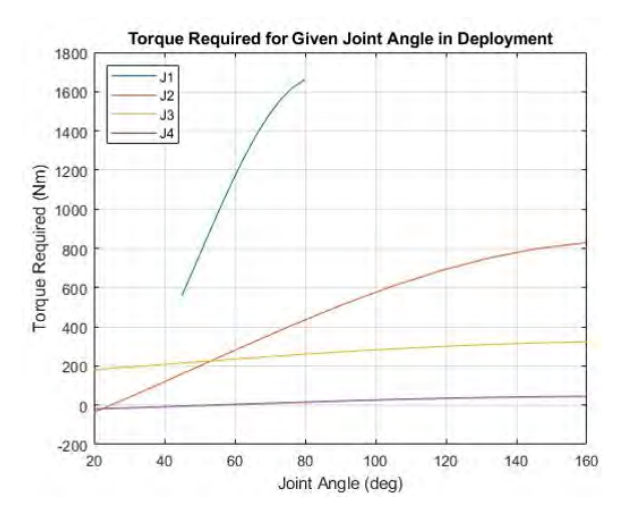


Figure 5. Torque required for each joint from the stowed configuration to full extension, color-coded to Fig. 4.

sion cost a few inches of vertical space when the arm is folded, but cut development time in half by discarding the need for an additional lever design. For this Earth-analogue system, the trade-off was considered acceptable as there

is more interest in the overall concept than the detailed design of the arm itself. Following this decision, extensive optimization of a generic design was carried out for joints 2 through 4.

Using MATLAB to create surface plots, the distances between each pivot point were optimized to produce the required torque. An example plot can be seen in Fig. 6. At the same time, the design also tried to minimize the lever arm to keep the speed up and volume and mass minimal. The optimized dimensions were then verified for a safety factor of at least 1.6 and optimally 2. As iterations were made, the CAD models were updated and verified with FEA, and various linear actuators were considered. This produced more accurate mass estimations, allowing for further refinement of the parameters.

Joint 1 differs from the other joints in that it is a simpler first-class lever. It serves mostly to keep the arm clear of the astronaut's head and contributes very little to extending the arm and folding compactly, unlike the other joints. Because of this, joint 1 does not need the range of motion that the other joints do and is not as space constrained. Like the other joints, the design was optimized for torque and speed, and it was analyzed to ensure that it could actuate sufficiently throughout its entire range.

2. Yaw Joint

As described in Section II, testing of a passive yaw arm in Phase 1 indicated that, for a lightweight wooden test arm structure on flat terrain, passive control was a feasible option. However, the significant increase in arm weight (which in the current design is approx. 85 kg) compared to that initial design has the potential to pull astronauts backwards and sideways, especially on upward and cross slopes which were not investigated in the original testing. This increase is due in large part to the speed requirements of the linear actuators to achieve the desired astronaut tracking rates. The result is much higher forces and torques that the subject would need to contend with in a passive system on slopes. Indeed, the risk for the umbilical pulling an astronaut over and down slope or severing the umbilical due to tension failure would be catastrophic to the objectives of the umbilical tending concept. As such, passive control of the umbilical arm yaw was deemed to be impractical, thus necessitating either active control through driving the joint or locking the joint and steering the rover to maintain a fixed orientation to the subject. However, the desire to traverse through rough terrain that would be of highest geological interest for lunar and Martian EVA applications makes yaw control through steering the rover while simultaneously requiring the rover to follow the astronaut within a certain distance (to avoid tension on the umbilical) impractical. Thus, the choice was made to actively control the yaw joint.

The joint will be subjected to extremely high compression forces, lateral forces, and bending moments due to the weight of the arm and the location of the center of gravity at full extension. On flat terrain, compression forces are expected to be approximately 1.6 kN and bending moments of up to 3.75 kNm are possible, while on slopes the worst case lateral force is approximately 0.8 kN (all reported with a safety factor of 2 included). To accommodate these high loads, a 9.5 in (24.1 cm) slewing bearing with external gearing was chosen due to the ability to resist all of the various loading configurations and to be easily integrated with the required active yaw control system.

Actuating the yaw joint proved to be the most demanding actuation on this arm. In the worst case, the yaw joint will need $452\,\mathrm{N}\,\mathrm{m}$ at $12\,\mathrm{RPM}$ to account for a

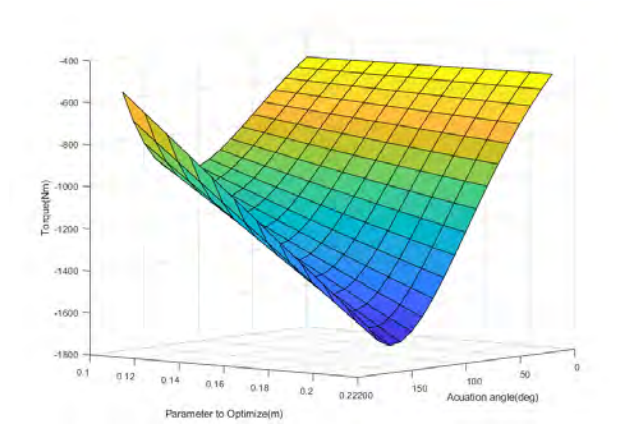


Figure 6. Example of plots used to optimize torque output.

tip speed of 1 m/s on 10° cross slopes. The torque requirements are so high because of how far the arm's COM is from the base. To achieve the required torque, a spur gear and a speed reducer will be utilized, creating an effective gear ratio of 159:1. This system is then driven by a 0.55 kW motor. This does result in a angular velocity of only 11 RPM, but that is for the highest load case on the motor. Top speed is required when the arm tip is near the base. In that case, loading on the motor is lower and it can operate at higher RPMs. If the astronaut intends to drive the rover on cross slopes where the deck angle will exceed 10° from horizontal, then the yaw joint will need to be manually locked out with a pin. This design decision was made because adding a system to either control the yaw joint or automatically lock it out with a brake at angles over 10° would have significant mass and footprint costs. Additionally since the rover can actively control its deck angle, it is highly unlikely that it will deviate more the 10° from horizontal in normal operation and therefore additional capability would likely be unused.

3. Arm Speed and Position Determination

The target tip speed was at least 0.6 m/s, the average walking speed of the later Apollo missions [7]. Tips speeds of up to 2 m/s, the average walking speed on Earth, were considered but quickly found to be impractical and the objective was set to 1 m/s at most. Additionally there were safety concerns about having the arm tip move at significant speeds near the astronaut's head. In the event that the astronaut outruns the arm, there will be slack in the umbilical and the rover can translate to make it up. In the final design, to reach the desired tip speed most of the linear actuators selected are overrated for the application as they move faster at lower loads. Additionally, for joint 2, two linear actuators were put in series to double the actuation speed. This came at the cost of double the mass, but increasing the torque produced at joint 1 to account for the added mass was trivial compared to increasing the speed of joint 2 in other ways such as decreasing the lever arm and sourcing a higher-powered linear actuator.

All of the joints are directly instrumented with 12-bit absolute encoders. Using these encoders, the arm will be able to report its tip position within a few inches at max extension. Higher bit count encoders were considered, but the added resolution would have little benefit as the tip deflection at full extension would have been greater than the pointing accuracy, rendering the additional accuracy useless without extensive and complicated control software that could account for arm deflection based on pose. Such advanced software may prove useful for a lunar model, but for demonstrating the concept on Earth, this capability is outside the scope of the project. Additionally given the decision to place an astronaut tracking camera on the arm tip that was made later in the design process, the pointing accuracy will depend very little on mechanical deflection and accumulated pointing errors from the encoders as the relative position of the arm tip with respect to the astronaut will be well known.

Joint	Torque Required (Nm)	Linear Force Required (N)	Actuator Capability
0	452	N/A	484 Nm
1	1650	4400	5338 N
2	830	6600	8896 N
3	320	3520	5338 N
4	45	660	890 N

Table 1. Joint summary table. Joint 0 is actuated by a revolute motor, joints 1-4 use a linear actuator and lever arm.

B. Arm Capabilities

The final arm design when mounted on VERTEX is capable of umbilical tending on 30° slopes. The umbilical line reaches up to 4 m above the base of the arm or up to 1 m below - in either case the arm can reach up to 4.4 m away or up to 5.08 m when the arm is not at an angle. The umbilical reaches 0.5m from the arm base at minimum extension with the arm fully above the rover seat. This leaves enough space to service an astronaut while entering the rover seat, driving, or walking anywhere around the rover (Fig. 9). The arm's yaw joint pivots a full 360° , providing a total service area of 80 m^2 around the rover (Fig. 7). Taking into account only linear tip extension $\pm 30^{\circ}$ from the base, the umbilical arm's workspace is $\approx 270 \text{ m}^3$. Although it would require a sophisticated tracking system, it is mechanically possible for the arm to reach much higher or lower if it operates joints unevenly to increase its workspace. For example, the arm in Fig. 4 could halve the angle of J3 in order to raise J4 and the tip directly overhead.

1. Center of Mass

The total prototype mass is 85 kg, with the yaw joint and related structure at the base of the arm accounting for 19 kg. The rest of the arm totals 66 kg, and at full extension the center of mass of this portion is 2.0m away from the base. As explained in Section IV, the mass of the arm is largely tied to the gravitational forces it must support, and as such, it is helpful to place the arm in context of its mounted rover. Acting as an Earth-analogue to an equally capable 250 kg lunar design, the total mass of the VERTEX rover is at least 690 kg [1]. Mounted on VERTEX, the umbilical arm only shifts the total center of mass location by 0.175 m at full extension. The arm also shifts the total center of mass upwards by about the same amount, but this is necessary to loft the arm high over the astronaut's head to prevent injuries.

2. Extension Speed

In order to maintain ample clearance as the astronaut dismounts from the driver's seat, the arm will be programmed to pitch the first joint upwards 30° from its stowed position (Fig. 9). The second joint will then be used to follow the astronaut as they step off of the seat and onto the ground in front of the rover. From there, the arm is free to actuate joints 2-4 to extend at maximum velocity while joint 1 exclusively adjusts for extension angle, and the yaw joint rotates the arm with respect to the rover. The arm generates a tip speed of 0.55 m/s while joints 1-4 actuate together in this fashion after the astronaut dismounts.

3. Stowed Volume

In its "packed for flight" configuration with joint 1 detached, the arm takes up a volume of 1.0 $x 2.0 \times 0.25 \text{ m}$, or 0.5 m^3 , as shown in Fig. 8. Transported this way, on-site assembly would only consist of connecting the pivot between link 1 and the joint 1 actuator output and the pivot between link 1 and the vertical link 0 (see Fig. 4 for numbering definition). The umbilical system, pre-mounted to the arm, would also need to be attached to the life support equipment on the rover. Otherwise, in the arm's fully assembled but retracted or "stowed" configuration, it occupies 2.0 m in height by 2.2 m in width. In this retracted pose, the arm tip (carrying the umbilical) lies 0.5 m from the arm base, or just over the driver's head when mounted to the VERTEX rover (Fig. 9). The seat design shown is tentative as it is still being designed at the SSL, but it does accommodate the largest PLSS that is planned for testing [8].

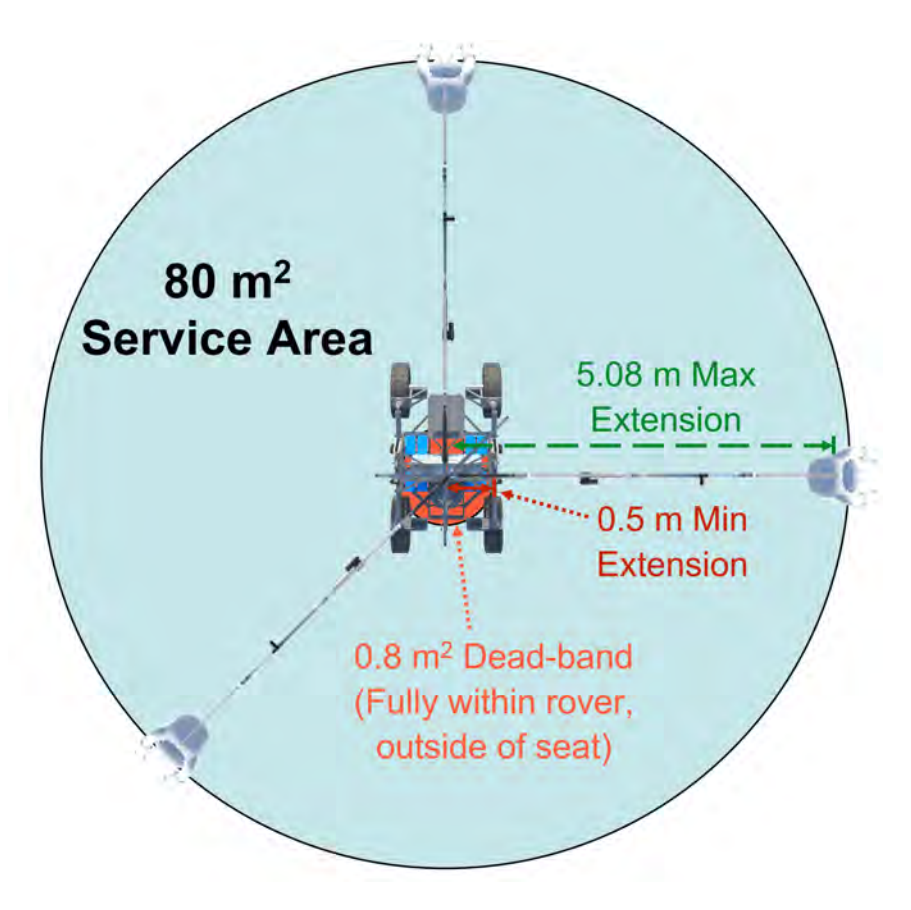


Figure 7. The umbilical tending arm's work area when mounted on a rover.

VI. Safety and Contingency Considerations

With BioBot being a human system, there were several design choices made for increasing the safety of the user. The rover base itself, VERTEX, was designed around having the large umbilical arm as a possible payload. The rover is able to actively control the vertical position of all wheels in order to maintain the chassis horizontal on slopes up to 30°. This has been shown to increase stability on slopes, especially when the combined center of gravity of the vehicle is raised by large robotic arm payloads [9]. The rover design also increases dynamic stability by pitching into the local gravity vector tracked by onboard accelerometers, which is also expected to provide stabilizing responses to forces on the umbilical arm. All of these capabilities reduce the probability of vehicle rollover while umbilical tending.

Despite the benefits provided by mounting the umbilical arm to VERTEX, additional safeguards are of course necessary in the design of both the umbilical and the arm. Further discussed in Section VII, an autonomous astronaut tracking system will be used to maintain the umbilical arm close enough to the astronaut to prevent any pulling by the umbilical while still maintaining a safe position above and behind the astronaut at all times. Umbilical slack between the arm tip and astronaut will also be provided to account for motions of higher bandwidth than the arm's response, the

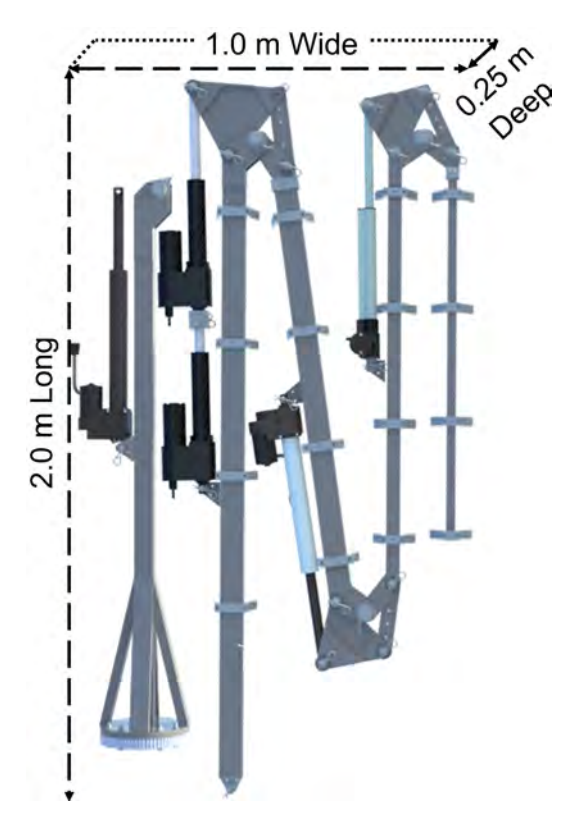


Figure 8. Umbilical arm disconnected and packed for flight for minimum arrival assembly, occupying a total of 0.5 m³ that the umbilical itself can also be packed into.



Figure 9. Umbilical arm in its retracted "stowed" pose, mounted on a cross-section of the VERTEX rover and ready for astronaut driving.

necessary length of which will be determined through field testing. The effects of umbilical torsion on the astronaut are unknown but will likewise be analyzed during testing. Sufficient slack in the umbilical combined with arm and rover control schemes should prevent pulling on the astronaut in nominal-use cases, but low breakaway-force mounting points between the arm and umbilical as well as a breakaway disconnect analogue in the umbilical itself will protect the astronaut from being significantly affected in off-nominal situations.

In all cases, emergency stops will be present on the rover, on the test subject, and on testing observers to halt all robot motions. The arm actuators were chosen such that, even in the event of a power loss, the arm would seize but not collapse. The selected linear actuators operate with an ACME screw and nut rather than a ball screw, providing superior backdriving resistance. The weight of the arm is not sufficient to backdrive any of the joints by over 50%. In the event of a power loss or motor failure that renders the arm motionless, the astronaut would simply disconnect from the umbilical arm, walk back to the rover, and reconnect at the rover-mounted supply. One of two short auxiliary umbilicals would provide life support to the seated driver for the duration of the drive back to base. The interface for the two auxiliary connections would be on opposite sides of the rover, so that one is always available in the (improbable) case of vehicle rollover and damage to the arm.

On the umbilical arm itself, no two motors can fail in a way that would leave the arm in a seized position that interferes with the VERTEX rover's operations, even on slopes, because of the arm's link lengths and height. However, if for whatever reason the seized arm is prohibitive to the astronaut, the flight arm should be completely disconnectable from its mounting at the base to be cast aside for emergency return to base. Because of the Earth analogue's prohibitive weight, this capability will only be simulated in field tests with an equivalent lunar weight - removing the Earth analogue arm is straightforward but would require 1-2 people to hold up the arm while its 8 connecting bolts are removed.

Since the BioBot rovers work in pairs to eliminate the need for NASA's walk-back criteria [9], a secondary rear seat is being designed for accommodating the driver of the second rover. This will be located behind the umbilical arm mounting location. If either of the rovers fail, both astronauts can connect to the working rover's life support and return to base. In the case of one of the two BioBot rovers failing at the same time as an umbilical arm failure on the working rover, two of the shortened auxiliary umbilicals are necessary to provide life support to both astronauts

during the return to base. The second auxiliary also provides an alternative if one fails to make a connection due to dust impingement.

VII. Autonomy and Control

A. Astronaut Tracking

Key to the BioBot's functionality is the ability of the system to accurately identify the position of an astronaut relative to the rover chassis. If the arm lags too far behind the astronaut during surface operations, tension in the umbilical cable will cause significant and noticeable impairment to the astronaut's motion. As such, fast and reliable positioning of the arm throughout EVA is critical. Additionally, the rover must be able to track an astronaut's position even while the umbilical cable is not connected to the astronaut's spacesuit—while the tracking need not be as precise as is required for umbilical handling, whatever solution used for astronaut tracking must achieve some degree of accuracy without the use of the arm to facilitate astronaut exploration using a short-duration PLSS.

To ensure the rover knows the relative position of the astronaut, an array of cameras onboard track fiducial markers on the astronaut's spacesuit (Fig. 10). AprilTags, a fiducial marker architecture integrated with open-source robotics software, is used for this applications as a calibrated camera can use a single AprilTag to identify both the relevant position and orientation of the tag and, in this case, the astronaut by extension [10]. While the optimal positioning of the AprilTags on the spacesuit is currently being experimentally investigated, they are being positioned with larger tags in high-visibility, low-mobility areas like the spacesuit chest, back, and helmet. Multiple AprilTags will also be made visible simultaneously regardless of astronaut orientation so that the camera system has multiple measurements to compare, enabling the system to better reject some noise, inaccuracies in the system, or obfuscation of one or more fiducial markers.



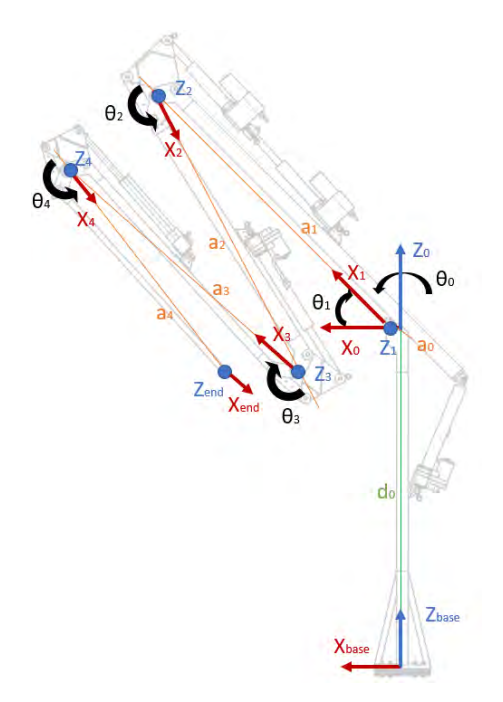
Figure 10. AprilTags on a simulated astronaut.

AprilTags present several limitations when it comes to usability in the field: glare and dust will obfuscate them, and the vision algorithm that identifies them as-written is not tolerant to such noise. Alternative means of tracking astronauts are discussed in greater detail in the discussion of future work in Section VIII to provide supplemental—but perhaps less accurate—means of identifying an astronaut's precise pose. However, for testing of the overall mobile manipulator control system, AprilTags provide a convenient and comprehensive method of identifying astronaut position and pose. As any alternate solution will similarly yield the position and orientation of the astronaut with respect to the rover chassis, AprilTags can easily be replaced by any alternate method of astronaut position identification without further modifying the control software due to the software's modular architecture.

Two camera systems are used for tracking the astronaut: a turret-mounted camera onboard the rover follows the astronaut at all times, and a secondary camera mounted at the end of the manipulator arm always looks straight down and ensures that the astronaut is always in view when the arm is positioning the umbilical. The first camera is always in use, following the astronaut's movements and reporting the position of the astronaut's body as a position goal to the rover and umbilical handling manipulator. Whenever the astronaut's position would be obscured by part of the rover, the system coordinates with the autonomous astronaut following capabilities of the rover and shifts the rover chassis and manipulator to keep the astronaut within the rover's field of view. However, AprilTags have limitations: at long distances, their position readings tend to become less accurate in practice (even for well-calibrated cameras), as was determined by an investigation by a University of Maryland freshmen team affiliated with the SSL. To compensate for this lack of accuracy at distance, the second camera onboard the arm will provide position data at a much shorter range. Combined with the encoders present in the arm, the camera will report the position of the astronaut relevant to the rover base, allowing the arm to be positioned above the astronaut at all times. For nominal operations, this camera system will look for an AprilTag at the top of the astronaut's helmet; however, it can similarly use any AprilTag on the spacesuit in the event of the astronaut being in an unexpected angle or orientation.

B. Arm Kinematics, Positioning, and Control

Being a 5-degree-of-freedom serial manipulator, the arm possesses simple kinematics that can be solved onboard the robot to yield desired joint behavior during control of the system. The manipulator has the following modified Denavit-Hartenberg (DH) parameters described in Fig. 11 and Table 2 below.



Joint i	α_{i-1} (deg)	a_{i-1} (m)	d_i (m)	θ_i (deg)	θ_{stow} (deg)
0	0	0	1.512	θ_0	0
1	-90	0.048	0	θ_1	-44.85
2	0	1.433	0	θ_2	161.77
3	0	1.344	0	θ_3	-158.19
4	0	1.326	0	θ_4	169.43
End	0	1.126	0	4.075	4.075

Table 2. DH parameters of the umbilical handling manipulator, as well as joint angles in the stowed position. Each joint is revolute. The table follows the modified DH format described in Criag (2005) [11].

Figure 11. DH parameters of the umbilical handling manipulator, shown in stowed position.

Key to the control of the arm is making sure it is positioned above and behind the astronaut at all times, ensuring astronaut safety and minimal interference from the umbilical cable during surface operations. As discussed above, the astronaut tracking system produces a transform from the astronaut's position to the camera frame in the robot's description and, therefore, the astronaut's position and orientation with respect to the rover and arm. As the arm is limited in its degrees of freedom and by the presence of the umbilical cable, it is commanded only to position the end of its final link and, therefore, the umbilical above the astronaut with respect to the local gravity vector (reported by IMU's onboard the rover), without preference for the angular position of the end of the manipulator relevant to the astronaut.

The SSL has significant experience in developing Cartesian controllers for robot manipulators and, as such, is able to leverage existing control software to command the arm to a desired position. The unique DH parameters of the arm, as well as the more general link-joint description, are used to determine the desired joint positions based on a manipulator kinematics solver written using Orocos-KDL [12]. These desired joint positions and velocities are then forwarded to individual joint controllers via Robot Operating System (ROS)-based control software and the ros_control package for tracking on the joint level [13]. All of the SSL's robot manipulators operate at the velocity control level when commanding individual joints, enabling accurate tracking of astronaut position over time.

The Cartesian position controller the arm runs on is separate from that of the ground motion of the rover upon which it is mounted: the rover itself follows an astronaut autonomously over rough terrain with the goal of remaining within the reach of the arm, while the arm controller continuously solves the inverse kinematics needed to position itself above the astronaut. For more details into the overall software architecture and the SSL's extensive software, see the full overview of the BioBot rover architecture [1].

Before hardware testing is conducted, the software will be run in a simulated environment to ensure it behaves as expected independent of hardware. The use of ROS and ros_control enables simulation of the system via several means and the testing of software in sim before hardware integration: both SSL's own kinematics simulator and the Gazebo physics simulation environment allow for the system software's effectiveness to be explored prior to hardware completion [14]. Critically, Gazebo also enables the simulation of camera inputs and targets, allowing for AprilTags given movement commands by the simulator to be read by camera systems on the rover and be tracked by the arm, all purely within simulation.

Implementing the control software on physical hardware does lead to several changes from the idealized simulation model. The fact that the true dynamics of the arm links and joints will be different from that in simulations means that individual PID gains on each joint must be tuned differently on hardware for accurate control. More significantly, the

simulation idealizes the joints as simple revolute joints driven by rotary actuators, while the physical manipulator's joints are instead driven by linear actuators. While the joints are equipped with rotary encoders to measure joint position directly, the software must convert desired joint positions and velocities to linear actuator positions and velocities when running on the physical hardware. This occurs between the motor command and hardware interface software levels using the same simple algorithm utilized for the rover suspension system itself [1].

VIII. Future Work

Presently, the manipulator and rover function using simultaneous but independent control processes: an astronaut-following controller and motion planner for the rover that tries to remain within manipulator-reach of the paired astronaut, and the manipulator controller discussed in this paper. While this serves as a functional solution for ensuring the manipulator's position, closer coordination between the two systems may be beneficial by reducing total system energy usage, increasing system robustness, and better tracking the astronaut as both human and rover move in rough terrain. In the future, a full-body mobile manipulator controller for the rover-manipulator system may be desirable and will be investigated as a means of improving the system.

The exclusive use of AprilTags for vision could also be supplemented to make the system more robust. While fiducial markers function well in a pristine laboratory environment, an investigation by SSL-affiliated students showed that they are not robust to environmental changes or obfuscation by dust or glare common in lunar environments: as little as 5% noise (digitally added to AprilTag images to mimic the effects of environmental factors) rendered the algorithm unable to detect the tags at all ranges. As such, poor camera calibration or obfuscation of AprilTags may make AprilTag-based detection alone difficult or inaccurate. To combat this, future work will involve the use of alternate software tools and image preprocessing to ensure the astronaut's position is properly tracked at all times. Common tools like OpenCV will enable tracking of patterns on the astronaut's suit that are more robust to noise than AprilTags [15]. For more complex and robust tracking, more developed algorithms like YOLO can be used to find the contours of the astronaut's silhouette, a method that will be more robust than looking for specific patterns that can be more easily blocked or obscured [16]. The presence of high lighting contrasts and glare still present technical challenges for any vision system, so methods like using radio beacons on the suit or other means of locating the astronaut (less accurately but more robustly than vision methods) are also being investigated as alternatives for when accuracy is not as critical, such as navigating the rover base to the astronaut independent of the manipulator system itself.

Lastly, testing to compare the performance and ease-of-use of the umbilical handling arm will be conducted in the coming months at several locations. Testing of the arm on a stationary stand will be done at UMD to see how effective the system is without being mounted on a mobile platform, serving as an analogue for umbilical tending around a lander or lunar habitat. The rover-mounted umbilical arm will also be tested as part of D-FLEAS or GEODES to collect human factors data with test subjects wearing suit simulators, much like previous SSL field-testing [6]. Additionally, this testing will be used to drive the design parameters for future modifications and revisions of the system. Also as a part of this testing, investigation will be conducted into the best operational mode for the BioBot system: remaining tethered throughout the EVA or utilizing the system to refill a smaller PLSS while driving and disconnecting when walking around an area. While the latter would be significantly easier from the standpoint of BioBot, it is currently theorized that the time required to recharge the life support system that the astronauts carry will be longer than the time that is spent driving. Thus, this would necessitate remaining connected throughout the majority of the EVA as opposed to just when seated on the rover; however, future testing will be required to be able to make any conclusions about the best methodology to utilize the system.

Acknowledgments

The authors would like to thank the NASA Innovative Advanced Concepts (NIAC) program as well as the 2021 Moon-to-Mars eXploration Systems and Habitation (M2M X-Hab) program as supporters of the BioBot program over the last two years of development. The authors would also like to thank fellow SSL researchers Nicholas Limparis and Charlie Hanner for their participation in design reviews and manufacturing expertise. Furthermore, the authors would like to thank the members of the "Astronaut Tracking for BioBot" freshman project for the ENAE100: Aerospace Engineering Profession course— Connor Blevins, Eli Brennan, Ege Korkmaz, Samir Rathore, and Francesca Sciarretta— who worked to investigate how the AprilTag algorithm and fiducial markers performed in simulated field environments.

References

- [1] David Akin, Charles Hanner, Nicolas Bolatto, Joshua Martin, and Daniil Gribok. "Development and Testing of the BioBot EVA Support System". In: 51st International Conference on Environmental Systems. July 2022.
- [2] David Akin, Kate Melone, Brady Sack, and Jeffrey Zhu. "BioBot: Investigating an Alternative Paradigm for Planetary EVA". In: 49th International Conference on Environmental Systems. 2019.
- [3] David Akin. "Development of a Next-Generation Suit Simulator System for Neutral Buoyancy and Field Testing". In: 51st International Conference on Environmental Systems. ICES-2022-362. ICES. 2022.
- [4] Jud Hedgecock, Chris Dyer, Dominick Mancuso, Richard Patten, Richard Patten, John McKeon, Brian Battisti, Jacob Dang, and Nicole Jordan. "IVA/EVA Life Support Umbilical System". In: 2004 IEEE/RSJ International Conference on Intelligent Robots and Systems (IROS)(IEEE Cat. No. 04CH37566). Vol. 116. SAE. 2007, pp. 445–465.
- [5] David L. Akin, Srikanth Saripalli, Kip Hodges, Kelsey Young, and Kevin P. Davis. "Desert FLEAS IV: Results from Field Tests of EVA/Robotic Collaborative Planetary Geological Exploration". In: 43rd International Conference on Environmental Systems. American Institute of Aeronautics and Astronautics, July 2013. DOI: 10.2514/6.2013-3429.
- [6] David Akin, Srikanth Saripalli, Kip Hodges, Kelsey Young, Massamiliano Di Capua, Kevin Davis, and Nicholas D'Amore. "Results from Desert FLEAS III: Field Tests of EVA/Robotic Collaboration for Planetary Exploration". In: 42nd International Conference on Environmental Systems. American Institute of Aeronautics and Astronautics, July 2012. DOI: 10.2514/6.2012-3464.
- [7] M. Eric Jones and Ken Glover. *Lunar Gaits*. 2001. URL: https://www.hq.nasa.gov/alsj/a11/a11.gaits.html.
- [8] David Akin, Nicolas Bolatto, Daniil Gribok, and Charles Hanner. "Controls, Displays, and Restraint Concepts for Highly Capable Crewed Planetary Rovers". In: 51st International Conference on Environmental Systems. July 2022.
- [9] David Akin, Charles Hanner, Nicolas Bolatto, Daniil Gribok, and Zachary Lachance. "Design and Development of an EVA Assistance Roving Vehicle for Artemis and Beyond". In: 50th International Conference on Environmental Systems (ICES). 2021. URL: https://hdl.handle.net/2346/87097.
- [10] John Wang and Edwin Olson. "AprilTag 2: Efficient and robust fiducial detection". In: 2016 IEEE/RSJ International Conference on Intelligent Robots and Systems (IROS). IEEE. 2016, pp. 4193–4198.
- [11] John J Craig. Introduction to Robotics: Mechanics and Control. Pearson Educacion, 2005.
- [12] Herman Bruyninckx. "Open robot control software: the OROCOS project". In: *Proceedings 2001 ICRA. IEEE international conference on robotics and automation (Cat. No. 01CH37164).* Vol. 3. IEEE. 2001, pp. 2523–2528.
- [13] Takashi Yamamoto, Koji Terada, Akiyoshi Ochiai, Fuminori Saito, Yoshiaki Asahara, and Kazuto Murase. "Development of human support robot as the research platform of a domestic mobile manipulator". In: *ROBOMECH journal* 6.1 (2019), pp. 1–15.
- [14] Nathan Koenig and Andrew Howard. "Design and use paradigms for gazebo, an open-source multi-robot simulator". In: 2004 IEEE/RSJ International Conference on Intelligent Robots and Systems (IROS)(IEEE Cat. No. 04CH37566). Vol. 3. IEEE. 2004, pp. 2149–2154.
- [15] Gary Bradski. "The openCV library." In: *Dr. Dobb's Journal: Software Tools for the Professional Programmer* 25.11 (2000), pp. 120–123.
- [16] Joseph Redmon, Santosh Divvala, Ross Girshick, and Ali Farhadi. "You only look once: Unified, real-time object detection". In: *Proceedings of the IEEE conference on computer vision and pattern recognition*. 2016, pp. 779–788.

Development and Testing of Crew Interfaces for an Advanced Unpressurized Exploration Rover

Charles Hanner¹, Nicolas Bolatto ¹, Daniil Gribok ¹, Spencer Quizon ², Rowan Quintero ², Ian Welfeld ², and David L. Akin³

University Of Maryland, College Park, MD, 20742, USA

Although revolutionary in its impact on lunar exploration, the Apollo Lunar Roving Vehicle (LRV) had only rudimentary navigation capabilities, and crew controls were essentially limited to go/stop and turn right/turn left. After more than five decades, rovers supporting the Artemis program will have vastly increased capabilities, and a corresponding need for more detailed and complex crew interfaces. The VERTEX rover has been developed at the University of Maryland as a field test analogue of concepts such as the Lunar Terrain Vehicle, and incorporates advanced capabilities such as active suspension, variable deck height and angle, reconfigurable payload interfaces with multipurpose electronic interfaces, and advanced control modes including teleoperation and autonomous driving. This paper details the development and human factors evaluation of controls, displays, and driver restraint systems for the VERTEX rover, based on both laboratory and field testing. While advanced robotic systems are often controlled from graphical user interfaces including touch screens, the extremes of lighting on the lunar surface and effects of regolith on pressure suit gloves drive designers to greater use of discrete and dedicated control interfaces and single-function displays easy to read in both bright sunshine and darkness. Extensive human factors testing was performed to examine potential layouts for the comparatively large number of discrete displays and controls, without impacting rover ingress/egress in spacesuits. Display and control layouts are also inherently impacted by crew seating and restraints, and a focused effort was made to move beyond the unsatisfactory simple seat belts of the Apollo LRV to restraint systems which are easier to engage and release in a spacesuit. The seat design itself is strongly driven by the portable life support system, and the VERTEX seat system was optimized to accommodate a number of different backpack designs and sizes to support external test objectives.

Nomenclature

BMS	Battery 1	Management	System
-----	-----------	------------	--------

CG Center of Gravity
EVA Extravehicular Activity
HLS Human Landing System
PLSS Portable Life Support System

RAVEN Robotic Assist Vehicle for Extraterrestrial Navigation

ROS Robot Operating System
SSL Space Systems Laboratory
TLX [NASA] Task Load Index
UMd University of Maryland

VERTEX Vehicle for Extraterrestrial Research, Transportation, and Exploration

xEMU Exploration Extravehicular Mobility Unit

¹Graduate Research Assistant, Space Systems Laboratory

²Undergraduate Student, University of Maryland

³Director, Space Systems Laboratory. Professor, Department of Aerospace Engineering

I. Introduction

One major lesson from the Apollo program was that the range and extent of scientific exploration was greatly enhanced on the last three missions by the presence of the Apollo Lunar Roving Vehicle (LRV). The lightweight four-wheel vehicle increased the traverse distances by an order of magnitude, reduced fatigue by transporting the astronauts, tools, and samples, and provided a base for continual transmission of images back to Earth [1]. Recognizing this fact, NASA has already begun commercial development of the Lunar Terrain Vehicle (LTV), another unpressurized two-person vehicle for use in the Artemis program.

NASA believes that the Artemis LTV should be a crewed combination of Mars 2020-style exploration rovers and the Apollo LRV in order to enhance the program's scientific capabilities alongside or independently of astronauts [2]. If that is the case, it is important to consider that some of the lessons learned from Apollo were that the LRV was not a perfect vehicle in terms of human interfacing. The A7L pressure garments had to be significantly redesigned into the A7L-B to allow the wearer to sit in the LRV seat; even with those revisions, the seated posture was not completely comfortable. The traditional flexible seat belts were extremely hard to work in pressurized gloves, and did not easily latch around a pressurized suit torso. The control device was a simple two degree-of-freedom control stick, limited to driving the vehicle in Ackermann steering mode while controlling forward speed.

It also needs to be considered that a lunar rover of the 2020's will certainly have extensive improvements in capabilities over one from the 1960's. A current state-of-the-art mobility chassis may well have the ability to change clearance height, deck angle in pitch or roll, or wheel configurations. It may have all-wheel steering, allowing standing turns about a point or driving in a different direction than the central axis of the chassis. Additional degrees of freedom require additional control devices, or at least mode-switching in a primary controller. A modern lunar rover will have much more capable electronics than the Apollo era vehicle, providing additional capabilities, but also requiring much more detailed controls and displays. Critical information such as navigation data needs to be displayed graphically to the driver, reflecting the change from the Apollo-era "this is the direction to the Lunar Module" to autonomous route and path planning with updates from orbital navigation and imaging assets in real time.

Based on all of this discussion, a critical aspect of the design and development of a next-generation lunar roving vehicle for human exploration must be a systematic research program into the three critical areas of rover/human interaction: controls, displays, and safety restraints. An initial start on this research and preliminary integration efforts are the focus of this paper.

To experimentally investigate how a human subject interacts with a highly capable rover system, the first requirement is an available testbed vehicle which includes many of the augmentations under consideration for LTV and future planetary surface vehicles. To that end, the University of Maryland (UMd) Space Systems Laboratory (SSL) is entering the final stages of development of the Vehicle for Extraterrestrial Research, Transportation, and Exploration (VERTEX), an Earth-analogue lunar astronaut-assistance vehicle intended to investigate mission capabilities relevant to NASA's upcoming Artemis program (Figure 1). VERTEX will nominally be capable of transporting an astronaut in an Exploration Extravehicular Mobility Unit (xEMU), in addition to geological sampling tools and other scientific equipment.

The flight version of VERTEX was designed to allow a pair of vehicles to be launched to the moon on a single Commercial Lunar Payload Services (CLPS) lander, to support early Artemis missions without presuming sufficient cargo capacity existing on the human landing sys-



Figure 1. BioBot concept system render with VERTEX rover, umbilical tending arm, and astronaut walking up-slope

tem (HLS) vehicle. Such single-person rovers would allow two-astronaut EVAs to double their effective exploration as each conducts their own science stops while remaining within short walking distances of each other in case of a failure. If a failure does occur, a second astronaut can be driven back to base in a jumpseat at the rear of the vehicle. The capability of returning both astronauts to safety can extend the allowable excursion range far beyond NASA's current walkback criteria by introducing an additional fault tolerance.

When the Earth analogue version of VERTEX is used in support of the ongoing BioBot concept testing under NASA Innovative Advanced Concepts (NIAC) support, it will also carry an umbilical-tending robotic manipulator and

life support system, providing rover-based life support to offload the astronaut from having to carry a full portable life support system (PLSS). The umbilical tending manipulator will primarily be used alongside VERTEX's autonomous functions, capable of tracking and following an astronaut for exploration of the lunar surface on foot [3]. However, the astronaut may always choose to ride on the vehicle and drive using manual controls between sites.





Figure 2. VERTEX rover presently in development, in a standing pose

Figure 3. Pre-VERTEX development RAVEN rover

Details regarding the design process and functionality of the rover can be found in a previously published paper [4], but in summary VERTEX is a compact rover platform (\approx 1.5 m wide, \approx 2 m long) that uses a custom series-elastic linear actuator configuration to achieve active chassis pitch (25°), roll (40°), and height control (1 meter range) in a fully electrically-driven package. The Earth analogue rover uses 32 inch tires paired with a brushless DC motor and 33:1 planetary gearset capable of climbing 30° slopes with \pm 180° independent steering on each wheel. The rover itself has a total of 12 actuators to continuously control, both in autonomous and manual modes, leading to some unique challenges for any human/rover interfaces.

This complexity is exacerbated by the fact that VERTEX is an unpressurized rover, meaning there are difficulties in keeping all controls both accessible and easy to operate despite a pressurized suit's lack of dexterity and limited range of motion. Considerations for these accessibility issues are discussed later in this paper regarding component selection of the control panel, but this is still an active area of research for the vehicle for items like joysticks. Additional concerns such as dust mitigation are not considered in this investigation, as the rovers for development in question are Earth-analogues more focused on the applicability of the system concepts to EVA and general operations.

The Earth analogue version of VERTEX nearing the end of production as of summer 2023. The main structure and assembly of subsystems is complete with the exception of steering, expected to be integrated by June 2023. However, even if the hardware were complete, the first drive of the rover could not be completed without a semi-comprehensive set of controls and an appropriate astronaut accommodation system. The integration, testing and planning of these control surfaces is occurring concurrently with the VERTEX build, and progress to date in this effort is described later in the paper.

II. Control Panel Functionality

A few basic concepts of operations for the rover have been short-listed as the hardware design evolved, breaking down into low-level operational procedures and higher-level control capabilities.

A. Startup

Low-level operational control items such as items for the startup sequence, battery protection, and computer booting systems are considered to be baseline functions. Protection for not only the user, but also technicians, other students, and people in the area is paramount since this vehicle has a 96V/300A capable power system, has > 1,000 ft-lbs of torque, and weighs 1,750 lbs. A *Master Enable* switch is activated by key to allow a push button *Master On* to be activated. The emergency stops (E-stops) must be released (more details in section III), and there are several different E-stops including two untethered remote E-stops. VERTEX will also be equipped with lighting systems including forward facing, rearward facing, under-chassis, and hazcam illumination in the near-future. Adjusting the intensity alongside the state of each of the lighting systems individually through a series of toggle switches is expected of the controls system. Each drive wheel on VERTEX is equipped with a normally-on brake that is disengaged when

the rover is in a drive-ready state. Additionally, a battery management system (BMS) interface is integrated for monitoring the health (voltage, capacity, etc.) of the battery system alongside debugging and external power storage uses. A driver-focused panel can be alternatively included with only top-level charge information if the standard interface is deemed too complicated. Lastly, two joysticks with a total of 5 degrees-of-freedom (DOFs) will be needed for controlling all 12 of VERTEX's actuators: 4 for driving the wheels, 4 for steering, and 4 for adjusting the rover's pitch, roll, and height (separated in up/down directions). These are yet to be integrated to the final rover as through the integration process the team has been using sets of inexpensive and small joysticks for electronics development, which not suitable for use with EVA gloves. A second iterative step of testing and trade studies will need to be completed before a pair of final joysticks are selected.

B. Control Modes

Manually controlling each of the vehicle's DOFs in driving conditions is challenging without integrating underlying levels of autonomy. One example of this is the rover having a faster-response in chassis roll authority than pitch authority due to the suspension dynamics. Subdividing each of the three actuated rover subsystems into a set number of operator-friendly control modes will greatly simplify both the mental task load and the number of required control interfaces.

1. Chassis Control

Active control of the chassis (also referred to as the *deck*) state is a fundamental capability of the VERTEX vision. The original design feature focused on leveling the chassis on all slopes to increase the stability margins of the rover, even in heavily loaded cases. This quickly extended to potentially influencing the center of gravity beyond maintaining level, in order to maintain stability margins if a large off-hanging payload shifts the overall center of gravity (CG). A series of suspension autonomy modes were defined based on the expected desires of operators in rock- or slope-climbing conditions:

- Auto Zero maintains a deck angle perpendicular to the gravity vector using inertial measurement units (IMUs) housed onboard.
- Auto Hold maintains a specified deck angle relative to the gravity vector in a specified direction.
 For example, if auto hold is activated with the chassis pitched up 5°, and rolled left 7° on level ground, then as the rover begins to climb an obstacle the linear actuators will servo to maintain these



Figure 4. VERTEX suspension with series-elastic linear actuators

deltas from the gravity vector, and will likely help when the rover CG is significantly displaced from its nominal position at all times.

- Proportional control will allow some manual input to adjust pitch and roll proportionally to the joystick inclination, but the rover will revert to Auto Zero when there is no manual input. This would allow a driver to roll the vehicle into expected turns, or momentarily pitch the rover towards the ground for a better view of a geological feature. In the future, the autonomous control of the rover's angles based on sensed rover accelerations will be implemented in this mode to maintain greater stability, regardless of driver input. This way, if the rover enters a left turn the chassis would be able to dynamically lean left to increase cornering stability, or lower itself to increase rollover margins while braking.
- Manual control will rely purely on operator input across on a 3-DOF joystick. Two axes of the hand-controller
 will manage chassis pitch and roll angle control, and a third (whether out-of-plane or twist) control axis will
 adjust the chassis height. Rover height will be possible to adjust manually in all the chassis control schemes
 since raising the structure for obstacle avoidance should always have a manual override option. However, a

system for sensing and automatically regulating the rover's ground clearance will also be implemented in the future for additional stability.

- The Lock function will hold the linear actuators at their present extensions.
- The last autonomous function is *Kneel*, which will prepare the rover to "kneel" by first pitching forwards and then lowering itself to present an easier opportunity for an astronaut to board and deboard (Figure 2).

The driver may also need to be able to independently control the angle of each corner of the rover for precise rock-scaling, which will be accomplished through a series of momentary rocker switches.

2. Steering

Each VERTEX drive wheel has an over-wheel steering system that can rotate each drive assembly \pm 180° as seen in Figure 5. Six independent steering modes will be available for the astronaut to select from. For safety, the steering modes, unlike the suspension modes, will not be able to be adjusted while the rover is moving, at least for the foreseeable future.

• Ackermann steering is expected to be the most commonly selected configuration as it is most similar to a normal car. When selected, the progressive steering system will turn the front left and right wheels as to align to the same turning point that is in-line with the set of steering-locked rear wheels.



Figure 5. VERTEX turning in place

- *RWS* (Rear Wheel Steering) switches the roles of the front and back wheels of *Ackermann* to provide maneuverability more similar to that of a forklift.
- *Double Ackermann* will adjust both the front and the rear wheels to align on a common central radii to decrease the turning radius further than the previous settings.
- *Crab* steering mode will align all wheels at the same angle to allow the rover to travel diagonally or sideways without turning the driver, as seen on NASA's Modular Robotic Vehicle (MRV) and Chariot.
- *In Place* will also be able to align the wheels to turn around the geometric center point of the rover so it can turn in place.

3. Drive Control

The rover speed and steering angle (for the dynamically changing steering schemes) are planned to both be controlled with velocity control. Previous laboratory experience with an acceleration-based rover speed controller on a Segway RMP-440LE led to imprecise and jerky control motions from operators, and is not likely to be comfortable or precise as a main control type for the drive and steering motors. A two-axis drive controller with the drive motor velocity axis in-line with the chassis lengthwise, and steering axis aligned either perpendicularly (L/R) or in a yaw axis motion is expected to be included as the final drive controllers.

III. Emergency Stops and Operational Safety

Multiple E-stops will be placed near the operator controls in easily accessible locations for on-board vehicle halting. Initially one will be placed directly next to the driving joystick, since it is likely one of the astronaut's hands will be there in an emergency situation. The other, to be installed after initial evaluations of an integrated panel, will be accessible to both of the astronaut's hands in a central location on the control panel. Additionally, since this is an autonomous vehicle, wireless remote E-stops will be used to halt the vehicle by other operators from a distance. This would ideally be a pair of remote E-stops, one on the test subject's person and another on an outside testing observer keeping a close watch.

The design of the E-stop procedure must be strategic, because VERTEX's E-stops cannot simply cut all power from each subsystem for a few reasons. First, each drive wheel contains a normally-on brake (similar to many commercial

hauling vehicles) that is disengages by the control system at times when the motor is spinning. If the E-Stop is pressed and power is immediately cut from the drive system, this brake will engage and may lead to a dangerous situation at any significant speed or when stability margins are decreased. Full system testing of the suspension in different configurations is to happen to evaluate stability under significant and sudden deceleration. Under an E-stop condition the elastic linear actuator system that actively controls wheel position is not expected to see any decrement in performance as the unpowered holding force of the actuator is twice the operating force. However, the steering motors present possibly the largest uncertainty in E-stop conditions.

A stability issue arises as the effective caster angle of the wheels change due to swingarm angle as shown in Figure 6. If the caster angle is negative (e.g., opposite of the front forks of a bicycle), the wheels will not self-align with the direction of motion when unpowered, especially since the brushless DC motor/Harmonic Drive actuators are backdriveable when unpowered. Excessive off-axis torques may be seen in the steering actuators if the wheels turn sideways and collide into rocks at speed, whereas an aligned wheel could tackle the obstacle in combination with the suspension. The current plan to remedy this is to simultaneously cut battery power from the actuators while connecting a large power resistor across the motors. As the motors spin freely, the resistor causes mechanical resistance by loading the circuit, braking the system. Since the entire rover's kinetic energy is being converted into heat by the resistor, high heat-capacity resistors and heatsinks will have to be used to avoid damage. This modified system eliminates the safety issues of not having the E-stop cut all power while also helping keep the rover more stable during a shut-off at speed.

Many controls need input-limiters in software to stop sudden extreme inputs from the astronaut from various sources including rough terrain and accidental motions. These limits will be implemented in software through scaling the maximum input magnitude and shaping of the central dead-zone area. Software also must limit the driver's manual control of deck-angle adjustment to assure that the vehicle is never in danger of rolling. After the initial inertial property testing, the center of gravity placement of the rover should be known within approximately 10%, and a spherical expansion of that point will be made to appropriately encapsu-

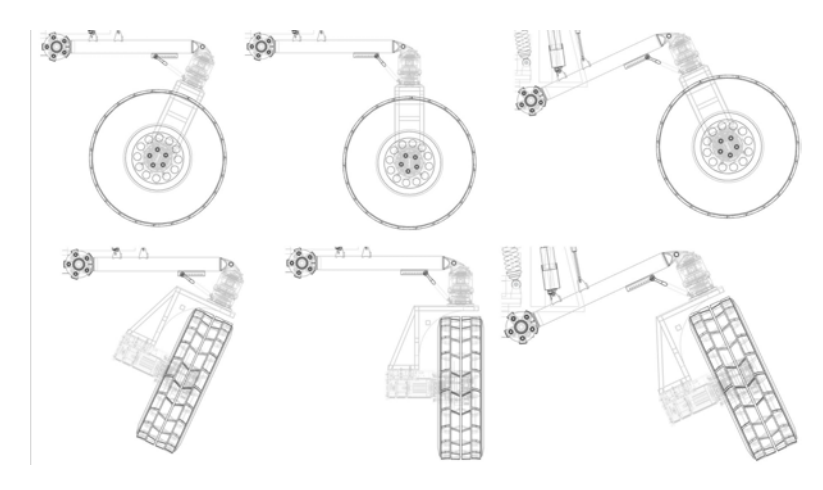


Figure 6. VERTEX Caster and Camber Swing

late how any payload for a given mission could change the CG during the testing.

Finally, for safety of the VERTEX team, a "Development Mode" is intended to be activated via a switch for running basic testing and diagnostics inside the laboratory. This mode will reduce both the maximum input values and the maximum speed of the rover to avoid the rover moving unsafely if the controls are accidentally bumped into.

IV. Control Panel Design Considerations

Some initial design considerations have been outlined to guide a few rounds of experimental iteration detailed in the following sections.

A. Joystick/Drive Controller Design

VERTEX will likely finalize with two multi-degree-of-freedom tactile input devices (joysticks), one for each hand, for controlling the suspension and drive functionality as described in section II. B. Each joystick will likely have an extended hand-rest similar to the Lunar Roving Vehicle (LRV) to reduce required gripping hand pose and reduce exertion. The astronaut will be able to rest their hand on a flat surface, instead of pinning or rigidly attaching the glove in any restrictive way. An initial setup was manufactured in adapting a 3-axis shuttle-style translational hand controller to an LRV configuration as seen in Figure 7. These controllers will not be used in the final VERTEX panel due to their high cost and age. Final selection of a suitable replacement has not yet been sourced.



Figure 7. Closeup of conceptual hand controllers for VERTEX



Figure 8. RAVEN rover outfitted with conceptual controllers for initial position and accessibility tests

B. Displays

VERTEX requires a system to display relevant data to the operator. This data varies from self-evident values such as vehicle speed, to exotic parameters such as deck angle and per-cell voltages of the battery. These numbers also vary significantly in update rate requirement - vehicle speed should be updated several times per second, while remaining battery charge can be updated once every few seconds with no adverse effects. A potential solution that accommodates all these needs is a multifunction display. However, due to limited development resources, a fully-featured multifunction display interface was deemed infeasible for the first generation of VERTEX. Instead, the concept was simplified to use fixed display interfaces, and rely on dedicated buttons to control rover features which may prove better-suited for gloved operators.

Selection of appropriate display devices considered both outdoor readability and adaptability to data update rates. While traditional color panel displays such as LCD, TFT, LED, and plasma suffer from poor sunlight readability their update rates are significantly faster than highly-readable e-ink displays. A combination of both IPS monitors, e-ink displays, and 7-segment LED display modules are included in the first integrated control panel for teams to transfer different metrics between and iterate and develop final screen interfaces and layouts. The details of these panels is described further in section VII.

C. Layout

Logical systems placement is obviously a key to successful operation of VERTEX, and a few assumptions have been made in the course of panel placement. Firstly, a right-hand operation for driving controls and left-hand operation of the chassis suspension controls was selected. Both systems require joysticks to function and the right hand driving controls of RAVEN proved to be natural for operators. The goal of the autonomous vehicle control systems is to allow for infrequent use of the deck-angle controls, which would free the left hand to operate switches and buttons operable while driving such as lights or communications. Throughout testing so far, no operators have complained about these arrangements, though it should be noted that this could change in the future.

Visibility through and around the control panel is a concern, especially considering the large number of controls needed. Firstly, the controls will be placed lower than in most vehicles to reduce forward ground-visibility conflicts. Second, the control panel is made up of a left and right half that do not join in the center. This central gap grants extra visibility for watching the rover's clearance, since it reduces the central blind spot down to the driver's own knees. Another idea to increase visibility under consideration is the use of abrasion-resistant polycarbonate sheeting as a transparent medium to mount the controls and minimize blind-spots in front of the wheels, although this view may become impeded by wiring and electronics boxes.

A few different button styles were tested and selected to be compatible with mockup suit gloves. Large toggles, both momentary and two position, will appear in numerous places along the control panel including lights and independent suspension controls. Buttons were found to be useful as long as some form of a visual confirmation can be made that the button was pressed, since small tactile bumps of most commercial buttons were nearly imperceptible through gloves. Small buttons are also difficult to operate while gloved, especially while the rover is in motion. The

rover's integrated panel utilizes mostly large diameter momentary buttons with LED indicators and large multi-position switches as discussed in section VII.

V. Early Control Panel Testing

A. Control Panel Mockup

As a first attempt, low-fidelity mockups were created as an initial test setup, with representative controls and displays layouts affixed to RAVEN to facilitate testing with various undergraduate volunteer groups. Initial test plans focused on subjects rating and operating controls and displays layouts without operating the vehicle. These have consisted of timed reaction tests where a conductor announces actions the operator must perform, after which the subject moves from a neutral driving position to activate the correct button. Such tests are timed and were used to initially informing placement of rarely used but critical interfaces such as the emergency stops and warning lights. These types of tests were used to generate inferences about basic layout structure, but provided little detail on specific operational applicability in the long term. Later tests focused (and continue to focus) on this and are discussed in later sections of this paper.



Figure 9. RAVEN left side controls mockup

The realization of the sheer number of controls and displays that are needed to operate VERTEX's many DOFs in the varying control schemes led to the development of the first full-size mockups seen in figures 9 and 10. These mockups were mounted to RAVEN in a similar configuration to that of VERTEX, focused around a central seating position as seen in Figure 11. The development team created 2 different control panel layouts to test (referred to as panels A and B) and varied the panel height relative to the seat in *tall* (T) and *short* (S) configurations.

RAVEN's 2-motor skid-steer drive system was disengaged on the rear wheels, and turned into a front wheel drive vehicle with the rear wheels mounted onto casters in order to more closely represent the free-steering style of VERTEX. This improved mobility and ease of control on payement, at the expense of rear-wheel obstacle



Figure 10. RAVEN right side controls mockup



Figure 11. RAVEN with the control panel and seat mockups

climbing and a detriment to off-road performance. As such, initial driving tests with RAVEN took place on closed courses over pavement only. As the VERTEX vehicle's status is brought up to operational, similar tests will take place with the first integrated control system of VERTEX to simulate scenarios in low-risk conditions and gather interable feedback.

B. Testing Procedure

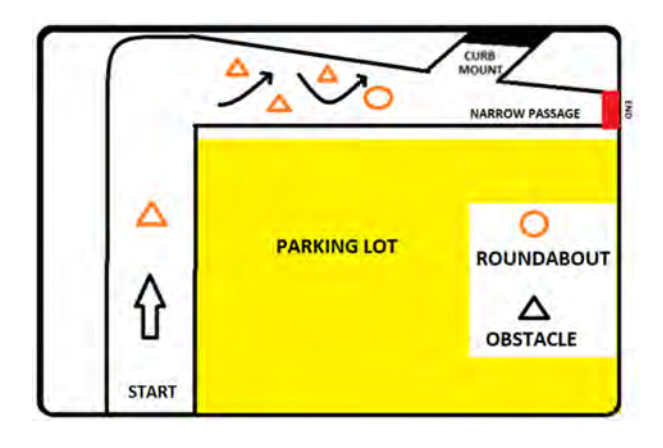




Figure 13. Early preferability results of the four panels

Figure 12. Overhead illustration of the testing path

This initial testing was conducted on a course defined by cones as shown in Figure 12. The goal was to drive RAVEN through the course while avoiding obstacles, perform a curb-mount, and finish by driving RAVEN through a narrow passage. The undergraduate team leading these tests believed this would provide an appropriate variety of tasks while not straining available resources during COVID or mobility in RAVEN. During each trial, the test subject was commanded by a test conductor to perform varying startup procedures and then to proceed through a test course consisting of an initial straightaway, several alternating obstacles, and a full rotation around a tight roundabout before driving to a curb mount. Evaluation of an operator's precision in the mobility included counting number of cones displaced, and measuring how far outside the rover was from a goal bounding box in certain areas such as the curb mount.

C. Early Testing Results

At the end of the trial, subjects were prompted with qualitative questions rating 1-5 regarding subjective comfort from the undergraduate team. Questions were of a more qualitative nature than NASA TLX or Cooper-Harper because of the preliminary stage of the control panel design and contents, but subsequent testing more closely aligned with those standards. The average total ratings were 22, 20.3, 24, and 24.3 for the TA, TB, SA, and SB control panels respectively. The high ratings from both SB and SC appear to initially indicate a preference for control panels mounted lower to increase forward visibility. Multiple test subjects noted the course was significantly easier in these lower configurations as it granted a better visual contact with the front wheels. Driver visibility was elevated to a high priority in future iterations as a result of this testing and is the most significant result from these early tests.

VI. Enhanced Control Panel Testing using an RTRS

A. Real-Time Rover Simulation

To build upon the early testing efforts and more-informatively design and optimize the first integrated control panel, a Real-Time Rover Simulation (RTRS) was designed, created, and implemented. The RTRS, shown in use in Figure 14, is a stationary testing apparatus designed to acquire quantitative data from the operator, without the need of an operational vehicle and large navigation course as VERTEX is being assembled in parallel with the control system. RTRS is designed to acquire four categories of data: reaction time, navigation error, visibility, and task load. Each subject wore an SSL-developed space suit analogue (MX-C) and gloves. They were then strapped into the experimental seat restraint to limit mobility similarly to expected on-rover conditions. The RTRS architecture is comprised of the following 5 sections of elements.

1. Modular Testing Panels

The two main variables that will drive the design of VERTEX's control panel are the type of interfacing component, i.e., buttons or dials and the placement of components and displays. Interfacing with the display will be difficult when operating while strapped in and wearing a space suit, so minimizing the amount of time the astronaut spends with hands off-stick is important. Gaining a better understanding of the benefits and limitations buttons or dials will allow more specific component selection and create a more efficient panel layout that has an easy interface with VERTEX'S wide variety of systems including suspension and drive modes.

To easily iterate between layout and components, a modular control panel architecture was designed with three possible



Figure 14. Real-Time Rover Simulation testing

configurations to start with a focus on controlling suspension and steering modes. Configuration 1 (Figure 15) utilizes dials with a display on the far right panel. Configuration 2 (Figure 16) utilizes exclusively buttons. Finally, configuration 3 consists of dials in mirrored position of configuration 1 and a display on the center right panel (Figure 17). Configurations 1 and 2 are designed to provide insights on component selection between systems, and configurations 1 and 3 are designed to provide insights on component and display placement.







Figure 15. Control panel configuration 1

Figure 16. Control panel configuration 2

Figure 17. Control panel configuration 3

2. Interactive Component Timing

To understand the performance benefit of various component positions, the time required to carry out each task within a simulation was measured. To accurately measure this time data, the control panel's buttons, lights, dials, and displays were wired to an Arduino Mega tracking each display and command input over the time per trial. The Arduino commands the operator to complete a simple task using the LCD display, recording time between command display and task completion. Time averages will be recorded for two primary operation tasks. The first is steering, which is used to toggle between different drive modes. The second is suspension mode, which is used to manipulate VERTEX'S deck height and angle.

3. Driving Emulator

To emulate the focused effort required in operating a rover, a simulation was developed in Unity simulating simple obstacle avoidance. The obstacle game is displayed on a large screen in front of the rigidly mounted control panel, as seen in Figure 18. The operator can control the red cube via the right joystick of the control panel. The simulation requires test subjects to maneuver the rover away from obstacles (grey) while the rover moves at a continuous speed forward. The simulation records primarily obstacle collision data for post processing alignment with the recorded Arduino data to rank different control panels relative to each other and improve before the next iteration is integrated to the VERTEX rover.

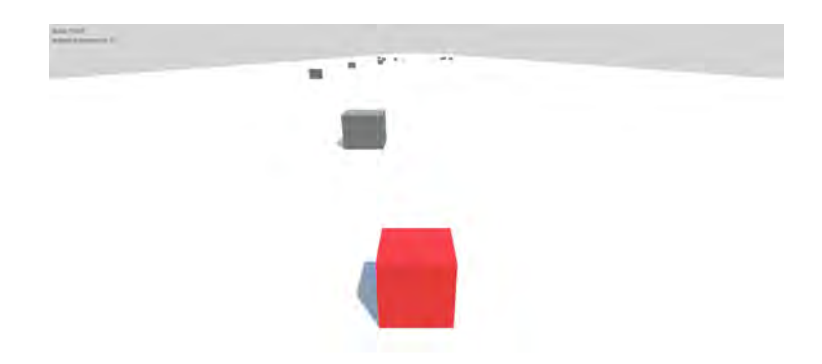




Figure 18. Unity driving simulator with generated obstacles

Figure 19. Operator with Tobii 2 Pro tracking glasses

4. Eye Tracking Glasses

A pair of Tobii Pro Glasses 2 eye-tracking glasses were used during each of the tests, alongside the Tobii Pro Lab software suite to help better understand which information media the test subjects refer to the most. Two metrics can be used with this system to justify design. First is the visualization of the precision and accuracy of eye fixations on the panels using generated heat maps looking at the width of the nodal areas in a fixation-count type heat map as shown in Figures 21, 22, and 23. Second is showing the duration of visits where the eyes spend the most time fixating in a specific area with a fixation-duration heat map. By evaluating these items separately, the panels can likely be improved by identifying areas high or low visibility and changing the panel layout accordingly with respect to importance and urgency of each of the panel's components.

B. Results

The RTRS ran 3 times per panel, with a new subject per test. Each test had a duration of three minutes, measuring the operators reaction times, navigation error, visibility, and task load.

1. Task Reaction Times

Using the system to measure the operator's time to completion for each task, the average total task time was found for suspension and steering selection tasks. These time averages across all three subjects for each task type and overall averages were plotted for comparison in Figure 20. There is a significant difference in completion times between configuration 2 (button components) and configurations 1 and 3 (dial components). Faster times for configuration 2 reveal the value in the simplicity of button operations. The button press proved to be significantly faster than clicking through each dial to reach the desired setting.

Configuration 1 had longer steering and suspension mode task times than in configuration 3. This is likely due to the placement of the rightmost steering dial on configuration 1 requiring a farther reach with the left

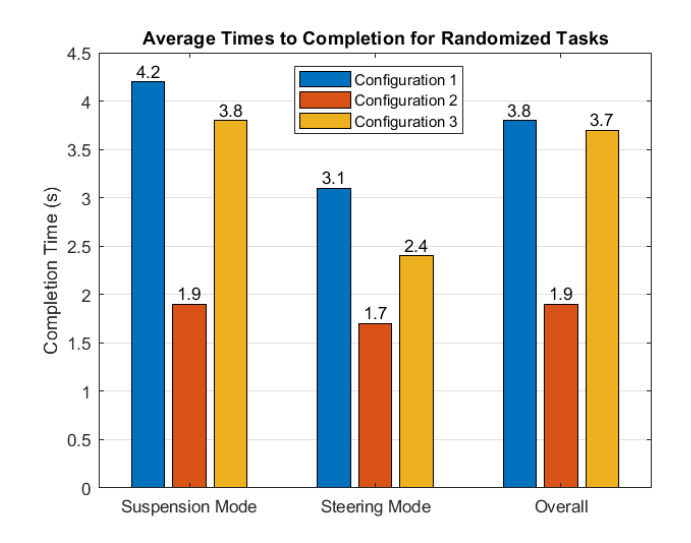


Figure 20. Clustered bar graph of reaction times

hand. Since the operator will be driving with their right hand, operators will take longer to reach the rightmost panel with their left hand. However, differentiation placement of components between the center left and center right panels

may not be as significant as the steering mode column shows configuration 3 with a faster completion time than configuration 1. This result is more likely due to a compounding effect of the display reading and processing times before switch actuation.

2. Average Navigation Errors

Each time an operator contacted an obstacle in the driving emulator, an error was recorded. Errors are used to partially quantify the level of distraction each configuration induces on the operator. After averaging and rounding across each test, configuration 1 had the most errors at 26, while configuration 2 had the least with 12. Configuration 3 saw an average of 17 collisions, suggesting component or display placement has a significant impact when compared with configuration 1. Configuration 2's low errors point to another advantage in the simplicity of buttons. It should be noted that the individuals who performed this test had extensive experience with the RTRS system before collecting this data, but no learning curve was quantified during these tests and may have been a small factor.

3. Visibility

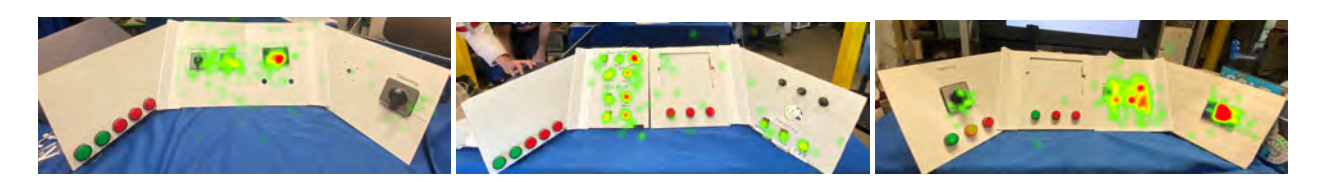


Figure 21. Configuration 1 heat map with fix-Figure 22. Configuration 2 heat map with fix-Figure 23. Configuration 3 heat map with fixation count ation count

Using the Tobii 2 Eye Tracking Glasses and Tobii's Pro Lab software, heat maps were generated using assisted mapping. As aforementioned, both duration and fixation count heat maps were generated for each configuration across the test subjects. In each of the figures 21 through 25, red represents areas of high-count, and green represents lower-count in each map style. The fixation count maps (Figures 21, 22, 23) show a stronger concentration of fixation on configuration 3's far left dial when compared to configuration 1's far right dial. These figures also show a high concentration of fixations on the far right display on configuration 3 when compared to the center right display on configuration 1, a result also mirrored in the fixation-duration heatmaps of Figures 24 and 25. This high visual demand of the center right panel of configuration 1 may suggest the far right panel as more desirable as it required less duration for transmission of similar information.

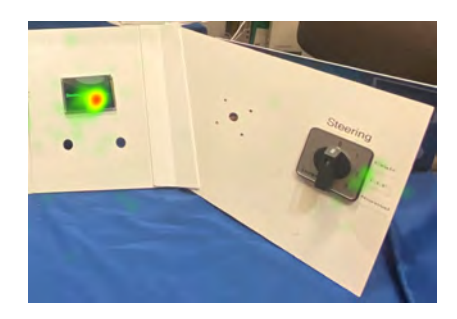


Figure 24. Configuration 1 heat map with fixation duration

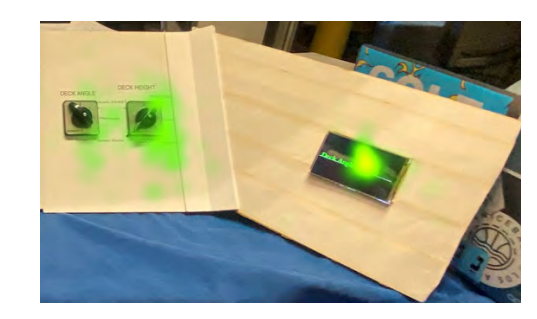


Figure 25. Configuration 3 heat map with fixation duration

Duration of each eye fixation within areas of each interface were also recorded and averaged to understand what dial placement demanded more attention (Figure 26). Configuration 1 demanded the longest fixations for steering, while configuration 3 demanded the least. This may be attributed to the longer time to task completion for a dial on the far right vs. a dial on the far left. Configuration 2 had the longest average duration time for suspension modes. The issue can be attributed to the large number of distributed buttons. A consolidated button layout or a dial could offer faster navigation than a panel with multiple spread-out buttons.

4. Task Load

To understand the operator's perspective towards the control panel configurations, the NASA-TLX was assessed immediately following each test. The results show that configuration 1 had the highest rounded task load score of 76 and configuration 2 had the lowest rounded score of 53. Configuration 1 likely had the highest score because of the right most dial causing far reaches. Configurations 1 and 3 displayed higher physical demands likely due to more precise operation required of a dial versus a button.

Operators were also asked to write down aspects of each configuration that worked well and did not work well. A common note was that while strapped into the seat and wearing gloves, using a dial becomes significantly more difficult than pressing a button. Another note said the small button size made it difficult to accurately press in bulky gloves. Lastly, the larger steering of

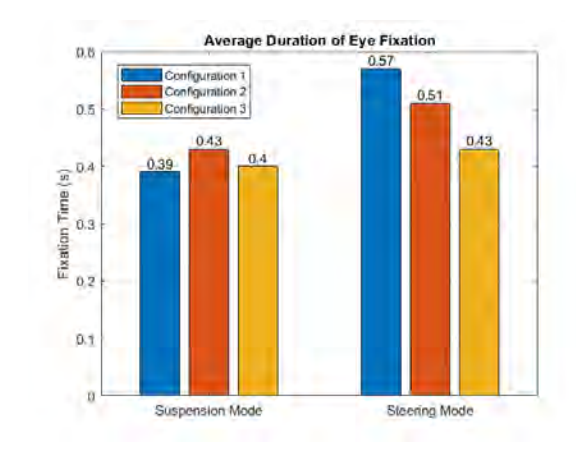


Figure 26. Average eye tracking fixation duration for each configuration $% \left(1\right) =\left(1\right) \left(1\right) \left$

rately press in bulky gloves. Lastly, the larger steering dial was easier to operate than the smaller suspension mode dials.

C. Design Conclusions

The RTRS tests provided valuable information regarding component selection and placement for VERTEX'S control panel. With the constraints of a spacesuit, the operation of buttons can be fast and smooth, although possibly requiring additional attention to locate the desired component. Dial operation proved to be more difficult and time costly in comparison and should be left to more time insensitive tasks.

As for button and dial placement, the most costly panel was found to be the far right panel because the operator must reach across the panel with their left hand while operating the rover. The operator will benefit from having most, if not all, interfacing components on the left half of the control panel (barring emergency stop buttons). However, it should be noted displays showed greater visibility and easier fixation when positioned on the far right panel.

It is apparent that there is no clear overall choice for interface components. While buttons work well for smooth operation, dials work better for consolidation and panel simplicity and the integrated panel reflects this.

VII. Control Panel Design and Implementation



Figure 27. Integrated control panel in open position



Figure 28. Integrated control panel in closed position

The first integrated design utilizes both buttons for steering modes and dials for suspension modes to maximize each of their benefits. Steering modes are expected to be changed frequently depending on terrain, thus lending advantage to buttons and have been simplified to a 4 button layout. Suspension modes utilize dials which reduces panel clutter and is not expected to be changed from auto-leveling often. The panel has displays featured on the right

side of the control panel, with all interfacing components and a battery management screen positioned on the left half. The panels can be found in Figures 27 and 28 integrated to the rover.

Moving from left to right across the panels, the far left segment contains an E-stop next the the more accessible hand of the astronaut and the battery management system screen. The center left panel has the four buttons for steering and one multi-position rotary switch for suspension control. The four buttons will each activate the Ackermann, Rear Wheel Steering, Crab, and In Place steering modes. To activate Double Ackermann, the astronaut will press both Ackermann and Rear Wheel Steering, preventing additional clutter. Each button is accommodated by an LED indicator. The center right panel contains one IPS screen for driving data, two switches for auxiliary accessories like lights, a two-position key start, and a button for vehicle startup. The two-position key start allows for the rover to activate non-driving electronics or all electronics depending on the selection, similar to a typical car ignition switch. The far right panel contains an array of indicator lights for monitoring the status of simple systems, an additional IPS screen for less driving-focused data, and an e-ink display for low-refresh rate but highly-critical data. The right panel only has informational components because it is the least accessible, yet most visible panel.

Final selection of data placement on specific panels has yet to occur, and will likely change continuously throughout the first few months of driving the rover. Items such as a hazcam display could be put on whichever display is most preferable, aiding in any blind-spot compensation.



Figure 29. Integrated control panel in open position with test subject $% \left(1\right) =\left(1\right) \left(1\right) \left($



Figure 30. Integrated control panel in closed position with test subject

As the first iteration of VERTEX'S control panel, the design will reinforce previous findings and identify areas of improvement. In the next phase, conducting additional tests on specific features will further tailor the panel to fit VERTEX'S needs. Applying the early testing and the Real-Time Rover Simulation has provided strong, objective insights into the selection and placement of components, which establishes a sturdy foundation for further design and enhancement.

VIII. Seating and Restraints

A new Portable Life Support System (PLSS) series is under development at the SSL for the purpose of evaluating the BioBot concept's astronaut-assistance focused architecture. Each astronaut will carry a minimum functional life-support backpack to house solid-state cooling and ventilation, which will carry mounts for a series of volumetric and mass simulators for untethered EVA activity shown in table 1.

Unit	Duration (min)	Size (cm)	Lunar weight (kg)
Cooling and Ventilation	N/A	30x15x8	TBD
Short	20-40	50x22x22	3
Medium	240	50x50x22	10
Long	480	50x74x22	17

Table 1. Suit simulator portable life support system sizing

Due to VERTEX's unpressurized nature, it must be compatible with the various PLSS sizes in the SSL's upcoming



Figure 31. Bent sheet steel and welded seat chassis concept

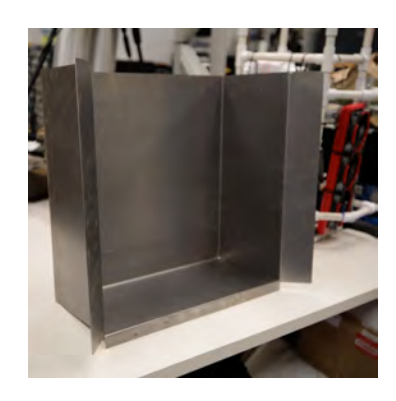


Figure 32. Bent sheet metal seat back - will be installed in a welded structure

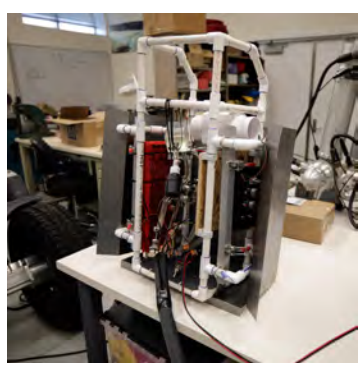


Figure 33. Bent sheet metal seat back with prototype suit backpack installed

lineup. A rectangular, semi-form-fitting cavity has been designed into the EVA seat to provide room for each backpack, as seen in Figures 31, 32, and 33. Unlike the upcoming Artemis suit architecture, the new MX-D suits being developed in-house are not Hard Upper Torso (HUT) style but rather are fabric suits with high-fidelity mobility restrictions. This is one scenario where the use of the upcoming hard upper torsos in the xEVAS suit may provide benefit, potentially allowing for a direct and semi-rigid connection using this hard structure between the astronaut and seat without the astronaut engaging any restraints. The EVA seat fabricated in Figures 32 and 33 is focused on the Medium size to create a smaller seatback to maintain clearance for other systems like the umbilical tending robotic arm, and it is expected that test subjects will not percieve a large difference in a 14cm shorter seat than if it were to conform to the Long size.

To reduce fatigue generated by flexing joints in a pressurized suit, armrests will be adjusted to conform as much as possible to a relaxed body posture used when driving and will be integrated with the final control panel. The armrests will support the astronaut's arm both vertically and laterally to prevent the astronaut's elbows from naturally splaying out further than the joystick operation pose due to suit pressurization. A similar strategy may need to be implemented with the subject's knees, all of which are intended to increase stability and with the astronaut subconsciously perceiving their stability.

The main restraint systems are a source of continual conflict between appropriately securing the astronaut, and restraining them to a point of safety concern. In the event of a rollover or significant anomaly, simple latch mechanisms need to be both easy to release (ideally with one hand) but 2-fault tolerant so as to not unlatch accidentally. Furthermore, restraints need to be accessible within easy working space of the astronaut hands for both reaching and buckling. Restraints must also respect "keep out" zones for any VERTEX peripheral payloads like the umbilical tending manipulator, any wheel zones, or any overhead roll-cage effectively eliminating overhead bound restraints. A first iteration of restraints that may satisfy these conditions is shown in Figure 34. A four-point commercial webbing harness was purchased and integrated with an early-prototype seat and found to be somewhat difficult to secure but was easy to remove while wearing gloves. The next iteration will likely include 3D printed grip-aids to help astronauts affix the belts without full hand dexterity.



Figure 34. Initial testing of a seat concept by volunteer ENAE100 team

Acknowledgments

The authors would like to thank the NASA Innovative Advanced Concepts (NIAC) program as well as the 2021 Moon-to-Mars eXploration Systems and Habitation (M2M X-Hab) program as supporters of VERTEX over the last three years of development. Additionally, the authors would like to thank the following volunteers for their work and contribution in concepts and prototyping as a part of ENAE100: Chris Kingsley (mentor), Joshua Sambrano, Bence Szego, Dira De Andrade, Sathya Gopalakrishnan, Sam Ondrusek, Chethin Gamage, Daniel Mehreteab, Jesus Quintana, Benjamin Kraft, Sravanthi Papolu, and Mathew Scholl.

References

- [1] Earl Swift. Across the Airless Wilds: The Lunar Rover and the Triumph of the Final Moon Landings. Custom House/Harper Collins, July 2021.
- [2] NASA. LTV Industry Day Aug 2022 Presentation.pptx. Online. Accessed: 2022-28-10. URL: https://sam.gov/opp/16c5e42788c4406d8687cb22ec5d3a70/view.
- [3] Nicolas Bolatto, Robert Fink IV, Joshua Martin, Zachary Lachance, Rahul Vishnoi, and David Akin. "Development of an Autonomous Umbilical Tending System for Rover-Supported Surface EVAs". In: *51st International Conference on Environmental Systems*. ICES-2022-361. July 2022.
- [4] Charles Hanner, Nicolas Bolatto, Joshua Martin, Daniil Gribok, and David Akin. "Development and Testing of the BioBot EVA Support System". In: *51st International Conference on Environmental Systems*. July 2022.

Earth-Analogue Roving System Development and Testing for Lunar Surface Exploration

Charles P. Hanner, Nicolas U. Bolatto *, David L. Akin[†], and Nicholas M. Limparis* *University of Maryland, College Park, Maryland, 20742*

Simplify, and add lightness. From Antoine de Saint-Exupéry to Colin Chapman, this mantra has direct application to improving astronaut experiences on the moon. Simplify the EVA experience and reduce on-suit mass to create a lighter system. Enabling lunar endeavors to travel greater distances, at a faster rate, with a greater payload all while reducing required effort is a substantial component in best enabling the greatest exploratory opportunity in the last fifty years - the Artemis mission series. Solving this engineering challenge begins on the ground, and through NASA's Innovative Advanced Concepts (NIAC) division the University of Maryland's Space Systems Laboratory is investigating a system titled "The BioBot Concept" consisting of a highly-mobile roving vehicle, life support system offloading via an umbilical-tending robotic arm, and a lighter, customizable-duration, on-suit life support system. The translation of a roving vehicle concept designed for lunar conditions to an Earth-analogue vehicle with equivalent capabilities in slope climbing, wheel articulation, and payload capacity underneath a university-level budget and a low barrier for entry among students of various experience has been a significant challenge with rewarding results. This paper provides an overview of progress to date on the to-date design, assembly, subsystem, and integrated testing of this multi-part lunar roving concept development.

Nomenclature

CLPS = Commercial Lunar Payload Services

COTS = Commercial Off The Shelf
DOF = Degree Of Freedom
EVA = Extravehicular Activity

LCG = Liquid Cooling Garment
 LRV = Lunar Roving Vehicle
 PLSS = Portable Life Support System
 SSL = Space Systems Laboratory
 UMD = University of Maryland

VERTEX = Vehicle for Extraterrestrial Research, Transportation, and EXploration

I. Introduction

For those old enough to remember the Apollo program first-hand, there have been a number of abortive attempts to return to human exploration of the Moon and/or Mars. However, it appears that at last Artemis is a program with enough support from both the legislature and the public to finally return humans to the Moon. Much of the Artemis architecture takes advantage of a half-century of technological advancement, as well as programmatic changes such as the reliance on commercial partnerships. However, some aspects seem to be still rooted in the Apollo paradigm, such as the planned Lunar Terrain Vehicle (LTV), which is functionally the Apollo Lunar Roving Vehicle (LRV) with remote and autonomous control modes proposed in the 1960's but rejected at that time due to schedule constraints.

The University of Maryland (UMD) Space Systems Laboratory (SSL) has for more than three decades focused on how to expand human and robotic capabilities in space, with particular emphasis on possibilities for direct human/robot collaboration. The central focus of the SSL has been to develop and test advanced technologies for space exploration and

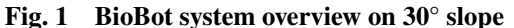
^{*}Doctoral Student, Department of Aerospace Engineering.

[†]Space Systems Laboratory Director and Professor of Aerospace Engineering. Associate Fellow, AIAA.

industrialization, but also to consider innovative concepts and architectures and evaluate their effectiveness in realistic simulation environments, including neutral buoyancy and analogue field testing.

In the context of Artemis and human planetary exploration, the SSL is focusing currrent efforts on developing and testing an Earth-analogue lunar roving system designed around enabling Artemis astronauts to travel farther across the lunar surface with more tools, increased cargo capacities, and less fatigue. The Apollo LRV revolutionized lunar surface exploration fifty years ago, but had some significant operational limitations such as the restricting exploration to a walkable distance from the lander in case of breakdowns, known as the "walk-back" limit. The SSL's concept for improvement is the "BioBot", consisting of three main parts: an extreme-access roving vehicle, an umbilical tending robotic arm, and a new approach to portable life support systems (PLSS). The roving vehicle, named VERTEX (Vehicle for Extraterrestrial Research, Transportation, and EXploration), aims to extend an astronaut's capabilities by offsetting a majority of their life-support to a rover-mounted system with an actively tended umbilical providing air, water, and power. The vehicle is additionally capable of autonomously following an astronaut on foot or being manually controlled if onboard, and minimizes the need for a formal walkback criteria by being small enough to provide a dedicated rover to each astronaut on EVA. The design requirement for VERTEX was to launch two rovers on a single CLPS (Commercial Lunar Payload Services) lander. A render of the concept is found in Figure 1; thanks to support from NASA's Innovative Advanced Concepts (NIAC) program, an Earth-analogue version is presently finishing development and beginning testing as the NIAC Phase 2 cycle comes to a close.





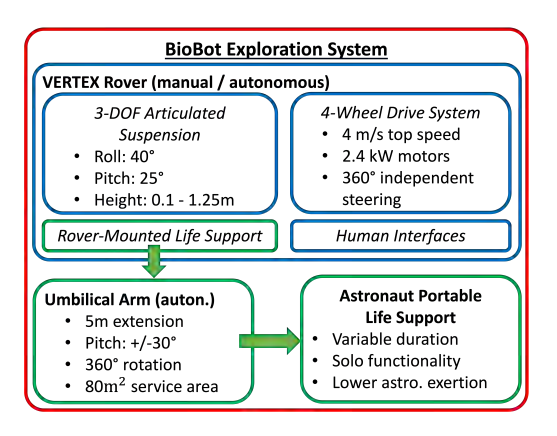


Fig. 2 Chart overview of the BioBot system

This rover development started with a risk analysis showing crew safety would be enhanced by baselining two single-person vehicles, either of which could transport both crew following a vehicle failure, thus minimizing or eliminating the walkback criteria. Enhancing the design to provide access to areas of high slopes (more than 20 ° for extreme access), rocky terrain, and cratered regions further enhances surface exploration possibilities compared to Apollo. The first design trade was to perform a detailed design of multiple lunar roving vehicles, building specifically to meet requirements under CLPS guidelines. The final design had a mass including margin of 220 kg, allowing two vehicles to land on an Astrobotics Griffin lander preparatory to an Artemis human landing.

An adaptation from the lunar design trade study to a system capable of being built, maintained, and operated by university students without compromising system capability then occurred. The main areas of focus for VERTEX in operational requirements included 30° slope climbing, chassis leveling on these extreme slopes, independent wheel steering, and a high payload limit capable of carrying multiple astronauts and life support systems in a contingency. Leveling the rover chassis (sometimes referred to as "the deck"), as seen in action in Figure 1, gives the rover significantly greater stability margins when climbing or crossing slopes. Design of this system required multiple iterations, resulting in an electrically actuated adjustment system to individually control wheel height without sacrificing passive dampened suspension. Climbing these high-grade slopes will facilitate sample return by removing the necessity of astronauts hand-carrying samples and tools to and from the roving vehicle, and enables exploration of difficult terrain such as crater interiors. A full conversion of the lunar design to a capability-matched Earth design was undertaken, prioritizing terrain capabilities over attempting to match the mass and structures of the original [1, 2]. The result is VERTEX, a roving vehicle with a 5-meter umbilical tending robot arm, independently-steered wheels, independently articulated elastic linear actuator suspension with over 1 meter of wheel travel, and over 460 Nm of sustained drive torque per wheel.

The ability to independently steer each wheel, up to $\pm 180^{\circ}$ in each direction, will be most useful when the rover







Fig. 4 VERTEX lowered and arm retracted

autonomously follows the astronaut as they walk across the lunar surface, ideally without perceptible limitation. Natural motions such as sidestepping or a sharp turn then step would be difficult for a rover with only traditional Ackermann steering, so VERTEX was designed to have as capable of a steering system as possible for following arbitrary astronaut motions in any direction. The steering system includes sets of brushless DC motors, harmonic drives, bushings, and both absolute and incremental encoders. To further improve the ideally imperceptible motions of the system behind an astronaut, the umbilical tending arm acts as an intermediary buffer for rover motion. The arm will extend and retract autonomously based on an active vision-based tracking architecture. The arm can be free to rotate at its base yaw joint, ideally helping to both lower the bandwidth required for rover motions and increasing the feeling of an unrestricted workspace for the astronaut.

Emphasizing manufacturability in the design significantly accelerated the rover's development time, even when plagued with COVID related delays and supply-chain issues. The chassis was converted from an aluminum structure to square steel tubes to allow for easy welding of structures by relatively inexperienced individuals. $80/20^{\text{TM}}$ compatible design frameworks were used by undergraduate students to develop the first seat and control panel prototypes, which have been integrated with the vehicle for initial testing and allow for easy adjustments to meet operator preferences. Student interface with electronics was made easier with the integration of a set of GalilTM motion controllers providing GPIO interface support to the more hazardous high-voltage drive system and related components. With the main system batteries capable of providing 300 amps of current at 96 volts continuously, significant safety considerations have been included to separate and create a multistep process before accessing these systems. Lower-power systems, such as the control panel and umbilical arm, are easier for students to iterate with and make improvements for the future.

II. Vehicle Overview

VERTEX was designed to provide the ability to climb and compensate the chassis on slopes of approximately 30° for enabling extreme access [3] while nominally carrying one astronaut and all required EVA tools including the umbilical arm, and a second astronaut in a contingency. Chassis compensation evolved into an independently articulated system for both roll and pitch active control as opposed to a semi-independent system or traditional rocker-bogie system. The independently articulated suspension created greater stability at the rover velocity goal of 4 m/s than other suspension systems could have provided. Rocker-bogie systems have significant stability issues at these higher speeds [4] and the added kinematic advantage of independent wheel adjustment can guarantee wheel contact. Independently articulated suspensions are a growing area of interest at NASA, as shown by the development of the VIPER rover, where the increased complexity of the articulation system was an acceptable risk in the trade for exploring more uncertain terrain [5]. Figures 5 and 6 show the slope compensation capabilities of the VERTEX rover with the newest suspension design totaling 40° roll and 28.5° in pitch. The evolution of the suspension design to version 2, discussed later in section III.A, decreased the pitch compensation ability from 30° for an increase in payload capacity and adjustability via setting preloads.

Each wheel is independently steerable to facilitate the ability to traverse in any direction to accommodate surface activities of an exploring astronaut such as with dual Ackermann (front/rear), crab, and turn-in-place steering modes. The independent steering is performed by a brushless DC motor and 100:1 harmonic drive; further details about the

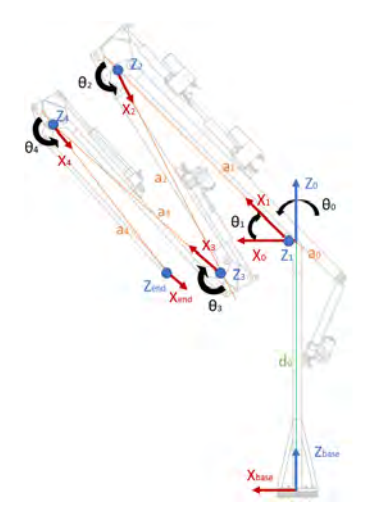


Fig. 5 VERTEX pitch compensation



Fig. 6 VERTEX roll compensation

actuator system is provided in section III.B. Traction power is independently provided through a brushless DC motor and 33:1 planetary gearbox, and transferred via a set of 32" commercial pneumatic tires, of which all components were sized by terramechanics analysis of the system under Earth conditions. The design evolution for the rover, along with these analyses, can be found in previous publications at the International Conference on Environmental Systems (ICES) [1] [2].



tion for the BioBot umbilical arm

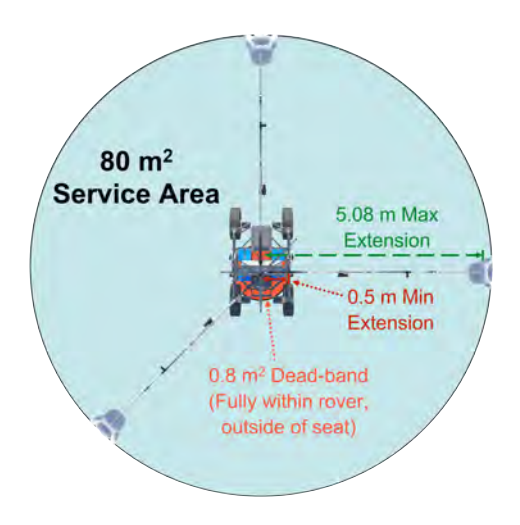


Fig. 7 Joint and Denavit-Hartenberg parameter defini- Fig. 8 Workspace of the BioBot umbilical arm with respect to the VERTEX rover

A. BioBot Arm overview

The umbilical tending arm, referred to as the "BioBot Arm", is a 5 link planar arm designed to extend and retract as an astronaut explores the surface on foot. The arm, shown in Figures 7 and 8, uses linear actuators and a series of offset multibar linkages to achieve the desired range of motion, similar to that of a concrete pumper truck's boom arm. The original design goal was an arm of length 10 meters, but in Earth gravity the overall system requirements became impractical, requiring significantly more expensive actuators and carbon fiber links to maintain the reach and strength within mass goals. The arm length was therefore descoped to a 5 meter length, achievable with commercially available thin-walled structural tubing, consumer-grade linear actuators, and extensive use of simple fabrication techniques wherever possible. The arm features absolute encoders on each joint for motion planning and tracking. Just like all

main structural members of VERTEX, the arm links are made of mild steel, and the interface plates for mounting joint pins, encoders, and actuators are waterjet-cut steel plates welded together. The resulting assembly has a weight of approximately 100 kg and can achieve a consistent tip extension speed of 1 m/s. Further details about the arms design process and optimization schemes can be found in a previous publication at ICES [6]. The passive yaw joint uses a slew bearing featuring a ring gear on the periphery to allow for motorization or damping to be easily added in the future; the assembly that holds the bearing has a series of holes to allow the arm to be pinned in various angular orientations for testing or stowage needs.

B. Suit LSS Concept Overview

The Space Systems Laboratory has a long history of developing and operating spacesuit simulators in support of analogue field testing of extravehicular activities associated with exploration, including long-term support of the NASA HI-SEAS isolation studies in Hawaii[7] (Figure 9. To fully test the BioBot concept, the suit simulators worn by the test subjects must be compatible with the BioBot concept offloading some of the portable life support system (PLSS) functions and consumables onto the roving vehicle, as seen in an early concept in Figure 10. Under the developed concept, the astronaut can choose to disconnect from the rover-supplied life support to reach objectives beyond the capacity of the rover and reach of the umbilical. Studies identified a set of potential durations for on-back life support in this case[8]; the plan is to test three different durations, evidenced by three unique sizes of backpacks as shown in Table 1, dependent on a mission's desired "off-tether" duration. For Earth analogue testing, these characteristics will be represented by volumetric and mass accurate modules able to be interchanged the MX-D series of spacesuit simulators, currently in final development. The test subjects will be able to disconnect and reconnect to the umbilical via a mating plate mounted to the chest area of the suit, but will always have a cooling and ventilation unit attached to the suit simulator, the prototype of which is presented in Figure 11. This features a solid state Peltier cooling system for the liquid cooling garments (LCGs) worn under the suit simulator and the main fan for suit ventilation. The prototype PVC structure featured in Figure 11 is sized to a long duration PLSS unit; the crew seat in VERTEX was sized to this largest backpack and fabricated out of sheet metal for ease of manufacture. The plan is that the operational version of the analogue PLSS will be integrated to the smallest backpack size in Table 1, with properly sized and ballasted outer shells interchanged for testing of each PLSS concept.



Fig. 9 MX-C spacesuit simulators at HI-SEAS



Fig. 10 Early field testing of BioBot concept

III. Design

A. Suspension Evolution

In the course of the design of the rover, the suspension has seen two integrated iterations of designs. The suspension had to not only articulate for active wheel placement, but also have elements of compression and rebound for a smoother ride in comparison to the rigid suspension systems of previous SSL rovers. The challenge posed was to balance maximum articulation range with minimum cost, a nontrivial optimization problem compounded by limitations in

Unit	Duration (min)	Size (cm)	Lunar weight (kg)
Cooling and Ventilation	N/A	30x15x8	TBD
Short	20-40	50x22x22	3
Medium	240	50x50x22	10
Long	480	50x74x22	17

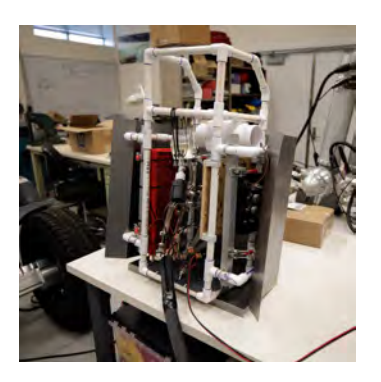


Table 1 Suit simulator PLSS sizing

Fig. 11 Solid state cooling system prototype

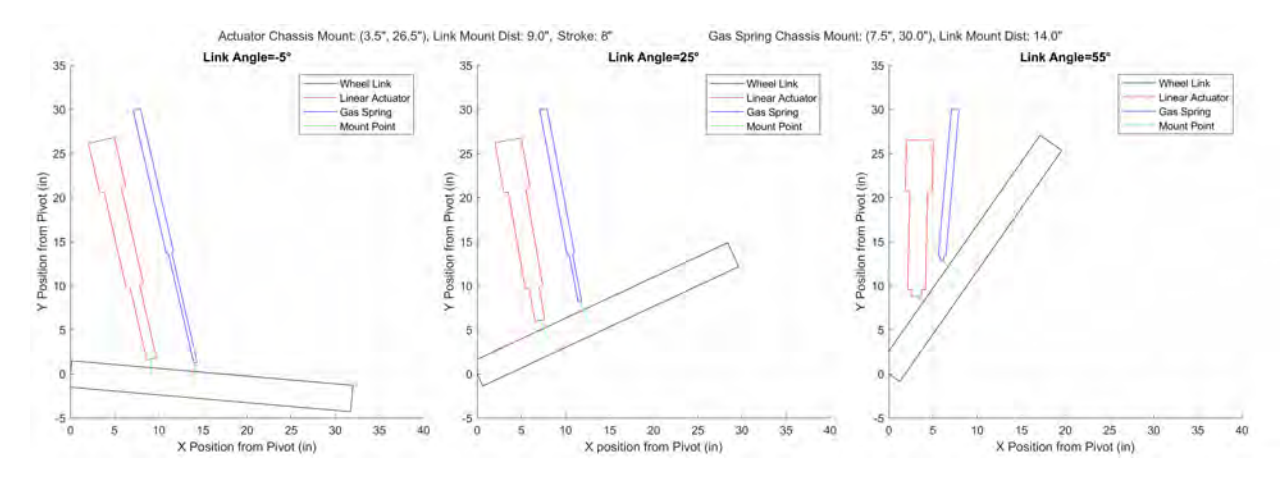


Fig. 12 Suspension design 1 positioning overview

component availability due to COVID supply shortages. A trade study was performed comparing varying actuation methods at the scale of the VERTEX rover, and linear actuators were chosen in providing a sufficiently large actuation length at the approximately one tonne forces required under an optimized placement at an appropriate cost. Force requirements for the actuation methods relied heavily on actuator placement and stroke to achieve a desired 60° actuation range on the limbs the steering and wheel actuators are attached to, referred to as "swingarms". This placement analysis, as shown in Figure 12, used initial estimates for rover mass segmented via sprung and unsprung mass, and ultimately a pair of 250 lb gas springs were used to offset additional weight. After finalizing the design and integrating to the rover, the system was successfully able to actuate and demonstrate the rover's slope compensating capabilities with each swingarm able to raise 55° above level with the chassis and 5° below. The initial testing can be seen in the video linked here: https://youtu.be/d75GtesbtNo. However, the placement of the actuators was performed under the assumption that the chassis-side mount for the actuator was a point with high stability, and the integrated system used a pivot with an attached spring damper to create a series-elastic linear actuator to satisfy the compression and rebound requirements. While the spring damper selected was cost effective and statically stable, under added payloads above 200lbs and at high swingarm angles when the mechanical advantage of the system is lowered, the rover suspension began to lose its ability to rebound. This discovery in testing required a new system to be retrofitted to a nearly complete chassis at a low cost.

The second suspension design began by modeling the rover in a way that was more true to the final design, an advantage only presented to us because of how far along the entire project had evolved. With better estimates for the final masses of various components, and a more intuitive understanding of where the sprung and unsprung masses lie new models were created inclusive of the existing pivot points. These were verified by modeling the existing system and confirming estimates to when the system would lose ability to rebound under varying loads and configurations. Minimization of component replacement and large system changes was key as the suspension area is already as compact

as possible and modifications to the chassis take significant amounts of time within an already compressed deadline. The code was designed to analyze replacement of either the series-elastic actuator spring dampers or the gas springs, but not both in an attempt to minimize total modification effort. The new design effort also aimed to decrease risk in the system by allowing the linear actuators to extend fully; this was not possible in the previous design due to a length limitation of the gas springs which were not tolerant to any extension forces via manufacturer guidelines, resulting in a software limitation requirement in the actuator extension. The new analysis code also introduced an element of domain randomization by slightly adjusting the sprung, unsprung, and a wide range of payload masses in varying combinations to increase the robustness and sim2real applicability of the data since these values are not precisely known or are variable depending on mission and EVA goals. The data analysis focused on maximization of stability margins across the varying mechanical advantage regions of the swingarm range of motion to guarantee rebound of the system in any configuration. Ultimately the solution found to reduce added structural mass and increase stability margins was to replace the gas springs with a set of two-stage spring coilovers with an overall length of 32" and a stroke of 14" as seen in Figure 14. These spring dampers are common in offroad racing trophy trucks and use standardized 2.5" springs allowing for stronger or lighter springs to be swapped in/out depending on how the rover evolves in the next few years. This system most notably allows for the quality of ride to be tuned depending on rover sprung mass and desired performance. For example, when the umbilical-tending robot arm gets mounted to the rover the sprung mass increases by approximately 30% over the empty weight and as a result the rover suspension remains stable with rebound capabilities but responds significantly more sluggishly to commanded suspension motions. The new suspension allows for tuning of the performance by not only allowing the preload of the springs to be increased by adjusting a threaded ring and compressing the dual springs more, but also allows for a customizable breakover point between utilizing both springs and transitioning to only compressing the lower spring. The spring rates chosen for integration are 150 lb/in upper, and 200 lb/in lower, resulting in a combined spring rate of 86 lb/in in the first region and then 200 lb/in when the transition ring becomes engaged. This preload adjustment only occurs when heavy payloads like the robot arm, boxes of tools, and batteries are installed and is tuned with an astronaut's weight to provide acceptable performance in both crewed and uncrewed states.

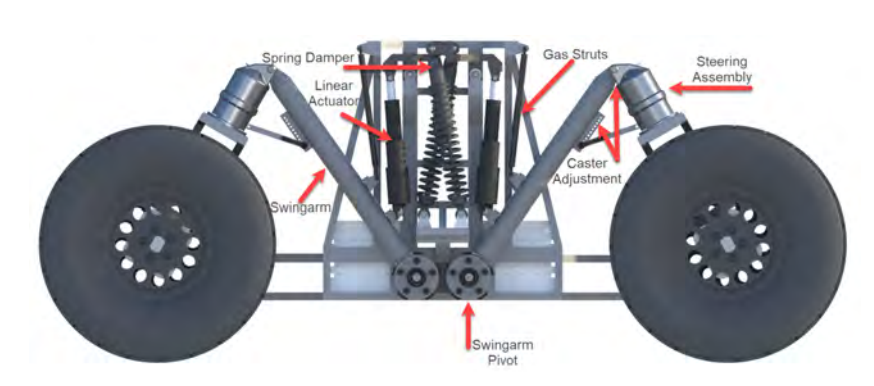




Fig. 13 VERTEX suspension 1 overview diagram

Fig. 14 VERTEX suspension 2

To close the control loop on the swingarms, magnetic absolute encoders are mounted at the chassis-mounted pivot points and wire directly to the GalilTM controllers. These encoders complete the suspension setup as a servomechanism, allowing the high-level control system to adjust the linear actuators to achieve a desired swingarm angle. The closed loop system has been tested to be fully functional, and tuning of the integrated system is underway.

B. Steering and Traction Actuators

Independent 360° steering of each wheel on an articulated rover creates significant challenges for design and operational procedures. Designing the actuators to be able to produce "adequate" torque at an "acceptable" speed involves two parameters that are very difficult to quantify. Definition of a required torque value would require a model considering wheel friction on varying surfaces (pavement, hard pack, loose soils, etc.) at varying caster angles which are not initially known. To minimize the effect of scrubbing friction during steering, the steering axis is directly over the drive wheels. Still, caster is a prominent issue with the articulated suspension found on VERTEX because it continuously varies with swingarm position and the particular terrain geometry. Caster measures the intersection between the

steering axis, as shown in green in Figure 16, and the contact patch which shifts as the swingarm raises and lowers. Coincidentally, when the wheels are turned 90° this angle becomes known as camber and the result of any angular inefficiency places force on the sidewall of the wheels. Both conditions will significantly increase torque requirements for steering when above 0° ; to reduce this a manually adjustable system is present on the rover as seen in Figure 17.

This system will be set to produce an approximately 0° caster and camber angle in a nominal driving configuration, and that angle will remain close to zero when compensating both along and across slopes. However, as terrain geometry or chassis ground-clearance varies throughout a traverse, these angles will increase and affect steering performance. Reducing steering motions in these compromising situations may become an operational requirement in field testing.

Caster angle also creates a challenge for the structural design of the steering system by generating significant off-axis torque proportional to the weight on the wheel. As such, a custom steering actuator was designed with bushings rather than ball-bearings to save both mass and costs. A detailed cross-section of the steering actuator is shown in Figure 15. Parts in this picture are colored to represent source and function as follows: all gray/white/brown parts are COTS while the rest are custom-made, and all similarly-colored parts rotate together. The blue outer housings remain stationary as they connect to the swingarms through the two pivots at the top and left of the cross-section. A Kollmorgen RBE-02110 brushless DC motor drives the red hollow driveshaft into a harmonic drive HDC-32 wave generator through an interstitial Oldham coupling. After the 100:1 gear reduction, the green output parts direct motion down to steer the wheels. The red driveshaft is hollow to allow absolute encoding of the central green shaft in the conical cap. An incremental encoder is also attached to the red driveshaft. Power and data wires for the motor and all sensors are directed out of the conical cap to wiring conduit up the swingarm.

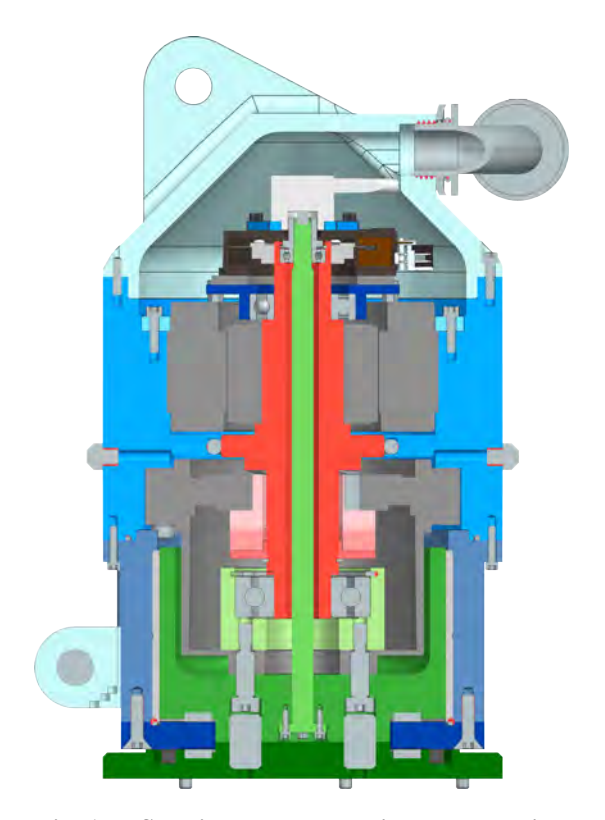


Fig. 15 Steering actuator design cross-section

Note that in Figure 15, the green output is supported against the blue housing by two double sets of bushings to prevent damage to the actuator from axial loads, side loads and off-axis torque. Composite bushings were implemented due to the prohibitive cost of bearings at this actuator diameter and loading. The wheel diameter and over-wheel steering design amounts to a large lever arm for ground-contact forces to generate torque. A tipping rover or transient ground-contact would require the steering bushings to react tens of thousands of pounds [2]. With the combined presence of greased gearing and bushings, the bottom half of the actuator is sealed to prevent leaks and dust ingress.

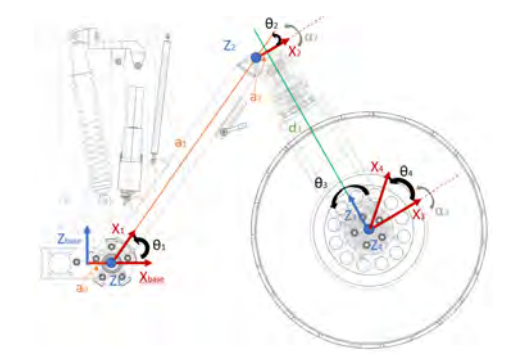


Fig. 16 VERTEX Swingarm DH Diagram

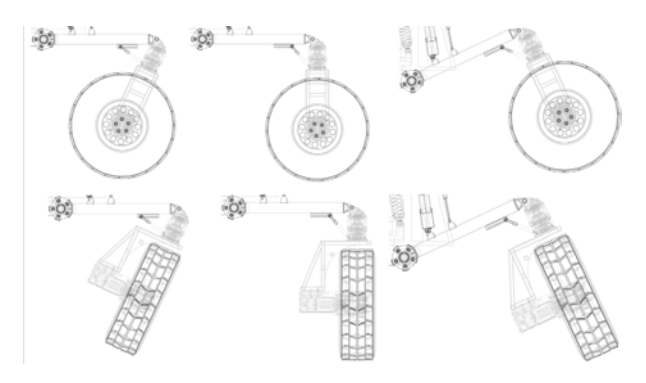


Fig. 17 Caster and Camber Diagram





Fig. 18 IVA seat on rover

Fig. 19 EVA seat on rover

C. EVA and Shirt Sleeve Vehicle Interfaces

Testing of the full BioBot system is expected to progress in phases, starting with either remote control or shirt-sleeved test subjects driving the rover and becoming comfortable with vehicle performance. This allows both the engineering teams and the vehicle to debug, fix, and become acquainted with full operations; having an ability to operate the rover without the spacesuit will be crucial logistically in transport and preparations for testing. To this effect, an "IVA Seat", shown in Figure 18, was procured from the farming and construction industries featuring commercial seat belts and a tunable under-seat suspension to help dampen shock loads. An EVA-compatible seat has been designed, as seen in Figure 19, and features an adjustable angle backrest, hard points for mounting restraints, and an appropriately sized recess for a portable life support system mockup. In the BioBot concept, all astronauts are equipped with a cooling and ventilation backpack equipped with mounts for volumetric and mass simulators of multiple-duration life support add-ons with durations of 40, 240, and 480 minutes. All astronauts participating in EVA testing will be given one of these three durations to allow them to disconnect from the rover for various amounts of time and then reconnect to replenish any used resources. The EVA seat is able to accommodate all three sizes of backpack, and would ideally use a rigid restraint system clipping to these life support system frames and reducing astronaut time and frustration with alternate methods. However, the space suit simulators to be used in testing BioBot are descendants of the soft suit simulators the SSL developed for the Desert RATS and Desert FLEAS field testing, and a traditional 4-point harness will be used initially, allowing for quick disconnecting at the expense of possible difficulty for clipping in.

Both the seats and the controls and displays are mounted via structures attached to a steel plate featuring standardized 80/20TM hole spacing. This allows for not only 15-series structures to be created, modified, and assembled directly on the rover by students of all skill ranges, but also allows for steel welded tube structures such as the EVA seat to be fitted to the rover with simple laser- or waterjet-cut brackets. Additional threaded holes are provided for mounting the shirt sleeve seat, and the entire plate is mounted on a set of manually adjustable seat rails similar to that of an automobile to allow test subjects to not only customize their seating position within the rover chassis, but to also allow full access to electronics boxes mounted in the footwell and in the chassis section immediately behind the seat.

The rover control system presented in Figures 20 and 21 is the last non-functioning prototype to exist on the rover platform. The controls and displays present on the rover have taken a multi-year evolutionary cycle evolving from prototypes on smaller, less capable rovers to eye-tracking of subjects controlling simulations to assess various layouts; these figures show the final check mockups before manufacturing the functional system with final modifications. These design efforts and the decisions and trades behind the control choices can be found in another paper from ICES published this year [9].

IV. Subsystem Testing

A. Suspension Testing

As the rover chassis has transitioned from a completed base vehicle to an outfitting phase, significant mass has been added to the vehicle as features are incorporated. Items such as the control panels, seats, batteries, and robotic arms add approximately 250 kg to the total mass, changing the overall response of the suspension at the original tuning.





Fig. 20 Test subject suited up on VERTEX

Fig. 21 Final control system mockup

By adjusting the preload in the new coilover suspension members, the rover can accommodate large adjustments in permanent or semi-permanent payload and maintain similar levels of dynamic response. The preload can be set and fine tuned to provide very similar responses when lighter loads like an astronaut move on and off the rover. Adjusting the preload is a manual process, requiring threaded rings to be spun via a wrench to compress both stacked springs. This is not a process that test subjects will adjust on the fly during EVAs, as these values are set before testing may begin and different values could be used back to front if an abnormally heavy payload is present at one end of the vehicle. The suspension was initially set to accommodate an empty rover as well as a person or two in street clothes stepping onto the chassis. The peripheral equipment was then added and preload was not changed, resulting in a notably slower system response. As the linear actuators exerted more force onto the swingarms to raise the chassis higher, the connected spring would have to significantly compress before reaching equilibrium. If the swingarms were then moving such that the actuators were more perpendicular to the swingarms (i.e. had the greatest amount of mechanical advantage in the range of motion) this could result in the springs uncompressing and the system overshooting the desired swingarm angle. Increasing the preload significantly improved this response, as did the inclusion of encoders on the swingarm pivot axis to close this servo loop. Servo loop control is highly dependent upon an appropriate preload being set. Quantification of the improvements and the creation of a preload curve based on added vehicle payload will occur by measuring suspension response between both inertial measurement units and the encoders.

B. BioBot Arm Testing

The BioBot arm is easily able to extend and retract itself from a multitude of different poses and configurations. While the system has only been tested under manual control of each joint via an analog controller, the arm operates as expected in both joint speed and rotational precision seen via the absolute encoders on each joint. Final wiring is presently underway for closed loop control through a GalilTM motion controller. However, the response characteristics of the arm so far are not ideal for robot control purposes. The primary issue lies in a low frequency resonance frequency under the deployment of the arm, measured at ≈ 1 Hz measured via video timing. This characteristic is likely due to two different factors. First and most obvious, the arm is attached to the rover via a 3/16" steel plate and a series of 10, 1/4-20 studs welded



Fig. 22 Deflection in BioBot arm mounting plate

to the chassis. The plate was originally intended to be welded to the chassis along all 4 sides, but it was later decided after manufacturing that welding the arm to the rover produced greater issues in both limiting available storage space on the rover, and increasing difficulty with more steps required to remove the arm both in both the field and laboratory. While welding the plate would have reduced the deflections as seen in Figure 22, it would not have eliminated them; development of a new mounting structure is underway to reduce these deflections as they are observed to be a significant

factor in the low resonance frequency. Secondly, the tubes and joints themselves are very likely contributing somewhat to this response, with each link being several feet in length and made of thin wall steel. An upgrade to the present mounting plate is underway; it will either be replaced with a thicker plate, or will have steel tubes welded to the plate to increase resistance to bending in the primary direction. After the upgrade is complete, characterization of the final resonance frequency is planned via motion capture for the design of the final arm control system. This frequency is not seen in the absolute encoders at each joint pivot and therefore the Robotic Operating System (ROS) controller will not have true system state knowledge, but the motions will be perceived in the camera located at the tip of the arm, seen in Figure 3, intended to track the astronaut as they move around the rover. Depending on the results, dampers could be added to the system to reduce bending near the joints, but deflections of the tubes themselves may prove difficult to eliminate.

C. Steering Motor Testing







Fig. 23 Steered wheel to the right

Fig. 24 Straight wheel

Fig. 25 Steered wheel to the left

Steering motors have been installed and tested at the front of the vehicle. Testing of the steering system is progressing through four phases including testing under no load with the vehicle suspended from a crane, steering under load at 0° caster, motion at small caster angles, and motion at extreme caster angles. All testing so far has occurred with the vehicle suspended off the ground by the crane or small amounts of load placed on the wheels. The team is now very confident that the wheels will successfully steer at very low caster angles on both asphalt and loose surfaces. However, at caster angles more than a few degrees from vertical, significant wheel scrubbing and adjustment to the contact patch position is seen as shown in Figures 23, 24, and 25. As a result, steering at higher caster may become operationally limited to loose soils, which means the vehicle should not steer more than a few degrees when the chassis is in extreme high or low positions on flat ground once the caster is set to be $\approx 0^{\circ}$ at a nominal driving chassis height, likely around 0.5m.

D. Seat, Controls, and Displays Testing

In testing the final control and display mockups, the team has decided to take a progressive step towards a final integrated design by 3D printing the electronics enclosures and using 15-series 80/20TM members for a reconfigurable test setup. At the expense of a delay in producing a finalized system including weatherproofing, this solution allows the team to adjust display angles, component positions, and overall placement of the displays without requiring repurchasing of any boxes and remanufacturing of any steel support structures, both of which will cost considerable time, money, and effort. Additionally, to reduce integration time and risk with custom interfaces with existing laboratory joysticks, a commercial unit and button panel has been purchased to be integrated with the rover. This combination will be integrated on the left hand side of the control panel, and a primary joystick (either commercially-sourced or custom) will be placed on the right. Right side controls will be the main driving interface, and left side controls will be for suspension and chassis compensation control.

E. Traction Motor Testing

The first powered motion for the rover was a single-wheel test drive. Wiring a single front wheel motor to a set of three 12V batteries and the traction motor driver allowed the team to do a first test drive of the rover using an analog joystick. While the voltage and current were significantly reduced in comparison to the final power delivery system, the rover was able to drive at a brisk walking pace, and was capable of climbing roadway curbs with relatively little trouble. Tuning the traction drivers is a challenging process as there are configurations for transitions between various states such as power forward, power rearward, and free-wheeling, and integration with the purchased drivers with the

overarching Galil™ control architecture has yet to be performed. Based on preliminary results to date, the team is confident that the traction drive system in general will be sufficiently powerful for intended field testing.

V. Planned Future Work

A. Testing Plans

Testing of the fully integrated BioBot system will take place in three phases: 1) locally on the UMD campus, 2) in regionally-accessible quarries or off-road areas, and 3) at demonstration events such as at NASA Johnson's "Rockyard" testing facilities or extended analogue field tests similar to Desert RATS in known test sites. Testing at UMD is a progressive effort, seeing incremental upgrades in system assembly as subsystems complete their initial development paths. This is the phase that the most tweaking and repairs are expected, such as steering at progressively higher caster angles. Testing at UMD will also help best inform the team of any spare parts, tooling, and other support structure that will be required or beneficial in subsequent testing. Testing phase 2 is aimed at evaluating integrated systems functionality, and identifying changes to the system CONOPS differentiating the BioBot system from traditional EVAs. Finding adequate testing locations near to the UMD campus such that a full testing cycle can occur within a single day has been challenging. Internal deadlines for this testing are slated for late October of this year while favorable weather conditions are still likely. Additional testing in Phase 3 requiring travel to sites such as NASA test facilities or established analogue sites such as the San Francisco Lava Fields (SFLF) in northern Arizona will likely have to be deferred due to the impending completion of the NIAC Phase 2 grant, and will require additional funding sources; it is hoped that phases 1 and 2 will show a substantial benefit to further testing of the BioBot concept and/or the component technologies such as VERTEX. Extended analogue field trials would be ideal for fully examining the BioBot concept, and would leverage extensive UMD experience, particularly a standing series of trials at SFVF.

B. System Improvements

The two main focuses of immediate improvement for the BioBot system include the system's control panels and the spacesuit simulator cooling systems. The present rover control system, as seen in Figure 21, is a final verification mockup based on many semesters of research regarding overall design, component placement, and comfort. However, since the roving vehicle system as a whole has 16 actuated DOFs and 5 manually operated payload DOFs, vehicle control methods will very likely have to evolve as the vehicle is driven over the first few tests. At the moment five steering modes (Ackermann, rear Ackermann, double Ackermann, turn in place, and crab steering) and 6 suspension control modes (auto zero, auto hold, proportional, manual, lock, and kneel) are available for a driver to choose from, and separated driver inputs for the suspension and steering/traction system are required. Varying joystick configurations are being integrated at the moment, ranging from COTS simulation-grade equipment to repurposed robotics workstation translational hand controllers to find the most appropriate combination between cost, ease of integration, and maximum comfort and controllability. To reduce iteration cycle time, 3D printing is being used to prototype the chosen configurations for components such as buttons, dials, and displays. 3D printing these boxes will aid in preventing dust intrusion by enclosing panel wiring, and will ideally provide the lowest effort path to a finalized system such as laser-cut impact-rated commercial boxes for the components to rest in.

Second, a solid-state cooling system is being developed in parallel with the vehicle for a low-mass, high-efficiency, electrically-powered comfort device for individuals wearing spacesuit simulators. Staying true to the BioBot concept, reducing crew fatigue on Earth during testing is also important; minimizing the core backpack size to include a solid-state Peltier cooling system in lieu of a water-ice cooler reduces both mass and size of the field testing PLSS on a test subject's back. As mentioned before, this system is presently being reduced to a more appropriate volume, and if necessary testing can begin with the COTS ice bath cooler used in past SSL field tests and at HI-SEAS.

C. Extended Research Opportunities

The BioBot vehicle is both extremely capable and highly modular beyond the original concept, lending itself very well to additional research support after the conclusion of the NIAC BioBot study. Without the life support mission, the BioBot arm could transport cameras and sampling equipment for close investigation of regions out of reach of the vehicle or crew, such as fine exploration of vertical stratigraphy for better geological understanding of the local surface history. Apart from the BioBot architecture, VERTEX is a highly capable mobility chassis, which includes the capacity to transport payloads of more than 500 kg in Earth gravity without substantial modifications. VERTEX can

be outfitted with equipment for purely robotic exploration, including dexterous manipulators for sample collection or drilling hardware for deep core samples. It can be outfitted with blades or other equipment for regolith manipulation to explore techniques for site preparation at a lunar base, such as for landing pads or habitat location. It is well suited to investigation of lunar logistics, both in transport and transfer of payloads from a CLPS lander or taking advantage of the adaptive suspension to position and berth pressurized logistics modules to a surface habitat.

One unique concept which leverages the capabilities and algorithms from the BioBot research is to utilize the vehicle as a portable gravity offload system, as shown in Figures 26 and 27. Inspired by systems like NASA Johnson's ARGOS (Active Response Gravity Offload System), VERTEX could host a steel framed structure with gravity offset mechanisms for a suited subject, which could be either passive (counterweights and pulleys) or powered actuators. A two-dimensional track system overhead would allow local motion of the test subject, while the astronaut-following sensor and control system would allow VERTEX to track the gross motions of the subject over the terrain. Such a system would bring the functionality of ARGOS into the field, allowing extended simulations of surface activities with suit simulators or actual pressure suits with the appropriate weight for the Moon or Mars.

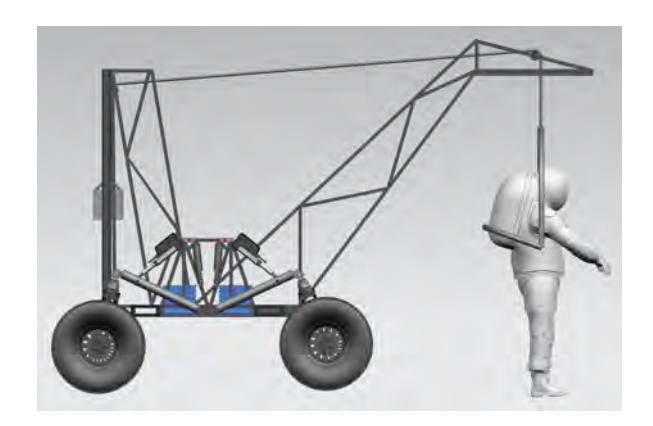




Fig. 26 Side view of astronaut mass offset concept

Fig. 27 Corner view of astronaut mass offset concept

VI. Conclusions

BioBot, if successful, represents a new paradigm for human planetary exploration with lower metabolic costs due to lighter weight carried by the astronaut, and the potential for substantially farther and longer surface sorties without the need to adhere to strict walkback criteria. However, each of the constituent systems of BioBot provide their own new capabilities and potentials for surface exploration and development. The VERTEX roving vehicle provides not only a comfortable and extremely capable foundation for the 5-meter umbilical tending robot, but is a highly adaptable mobility system for both research and student projects. The BioBot arm is one of the first attempts at robotic umbilical tending, which has applications beyond BioBot itself; it also has sufficient reach to position instrument packages in sites not otherwise reachable. The spacesuit simulators and solid state cooling systems allow full-duration analog field sorties with total weight on the subject similar to that on the Moon or Mars, while the tailoring and design of the suit replicates some of the bulk and restrictions of a pressurized suit. The SSL team is excited about taking all of these component systems into final development and testing, and looks forward to reporting on test results and new applications in the coming years.

VII. Acknowledgements

The authors would like to thank the many volunteers and research groups that worked on various parts of the BioBot concept including Chandler Sheatzley for his contribution to varying parts of the rover structure, Spencer Quizon, Rowan Quintero, Ian Welfeld for their invaluable work with the control panel system, and Chris Kingsley for his aid in multiple areas.

This project was supported by the NASA Innovative Advanced Concepts (NIAC) program, with additional support for VERTEX development from the NASA Moon-to-Mars Exploration Systems and Habitat (M2M X-Hab) Academic Innovation Challenge. The support of these programs and their technical monitors is gratefully appreciated.

References

- [1] Akin, D., Hanner, C., Bolatto, N., Gribok, D., and Lachance, Z., "Design and Development of an EVA Assistance Roving Vehicle for Artemis and Beyond," 50th International Conference on Environmental Systems, 2021, p. 12. URL https://ttu-ir.tdl.org/handle/2346/87097, accepted: 2021-06-23T23:02:42Z Publisher: 50th International Conference on Environmental Systems.
- [2] Hanner, C., Bolatto, N., Martin, J., Gribok, D., and Akin, D., "Development and Testing of the BioBot EVA Support System," 51st International Conference on Environmental Systems, 2022, p. 16. URL https://ttu-ir.tdl.org/handle/2346/89836, accepted: 2022-06-21T13:56:19Z Publisher: 51st International Conference on Environmental Systems.
- [3] Dunbar, B., and Hall, L., "Lunar Surface Innovation Initiative nasa.gov," https://www.nasa.gov/directorates/spacetech/Lunar_Surface_Innovation_Initiative, 2020. [Accessed 29-08-2023].
- [4] Wang, S., and Li, Y., "Dynamic Rocker-Bogie: Kinematical Analysis in a High-Speed Traversal Stability Enhancement," International Journal of Aerospace Engineering, Vol. 2016, 2016, pp. 1–8. https://doi.org/10.1155/2016/5181097, URL https://www.hindawi.com/journals/ijae/2016/5181097/.
- [5] Cao, C., Rogg, A., and Tardy, A., "Actuated Suspension Tuning Characterization of the VIPER Lunar Rover," 2023 IEEE Aerospace Conference, 2023, pp. 1–11. https://doi.org/10.1109/AERO55745.2023.10115796, iSSN: 1095-323X.
- [6] Bolatto, N., Fink, R., Martin, J., Lachance, Z., Vishnoi, R., and Akin, D., "Development of an Autonomous Umbilical Tending System for Rover-Supported Surface EVAs," 51st International Conference on Environmental Systems, 2022. URL https://ttuir.tdl.org/handle/2346/89837, accepted: 2022-06-21T13:57:26Z Publisher: 51st International Conference on Environmental Systems.
- [7] Swarmer, T., Akin, D. L., and Davis, K. P., "Suit Simulators for Analog Sites: Lessons Learned from HI-SEAS Testing," *45th International Conference on Environmental Systems*, 2015. URL http://hdl.handle.net/2346/64536, the 45th International Conference on Environmental Systems was held in Bellevue, Washington, USA on 12 July 2015 through 16 July 2015.
- [8] Akin, D. L., Melone, K., Sack, B., and Zhu, J., "Biobot: Investigating an Alternative Paradigm for Planetary EVA," 49th International Conference on Environmental Systems, 2019. URL https://hdl.handle.net/2346/84449.
- [9] Hanner, C., Bolatto, N., Gribok, D., Quizon, S., Quintero, R., Welfeld, I., and Akin, D., "Development and Testing of Crew Interfaces for an Advanced Unpressurized Exploration Rover," 52nd International Conference on Environmental Systems, 2023. URL https://ttu-ir.tdl.org/handle/2346/94805, accepted: 2023-06-21T14:21:28Z Publisher: 2023 International Conference on Environmental Systems.

Initial Testing and Evaluation of the BioBot EVA Support System

Charles Hanner¹, Nicolas Bolatto², and David L. Akin³ *University Of Maryland, College Park, MD, 20742, USA*

Current concepts for the Artemis personal life support system (PLSS) for lunar exploration are trending towards twice the weight as that used during Apollo. While the Artemis PLSS will be superior in many respects, the additional weight on the astronaut's back will hamper the widespread use of EVA required to make the Artemis program a success in terms of both science and public engagement. Under the NASA Innovative Advanced Concepts (NIAC) program, the University of Maryland (UMD) is developing and field testing the "BioBot" concept for extended EVA support. In this paradigm, a highly capable rover accompanies each EVA crew, carrying the bulk of their life support on the rover and supplying consumables to the astronaut via an umbilical tended by an autonomous manipulator system. This scenario places a number of technical demands on the individual BioBot components, such as rover trafficability comparable to the suited crew walking, autonomous crew tracking and umbilical manipulation, and limited on-back life support systems for independent mobility at will with simple and highly reliable mate/demate of the umbilical from the suit in the field. The baseline of two single-person rovers allows dedicated support of each crew, but also allows both crew to return on the functional vehicle following a rover failure, thus alleviating the onerous "walkback" criteria of a single two-person rover. BioBot was designed for deployment of both rovers on a single CLPS (Commercial Lunar Payload Services) lander during the early phases of Artemis, with each rover having a 10meter umbilical-tending manipulator. The prototype system developed at the UMD Space Systems Laboratory is limited to a 5-meter arm due to the requirement for analogue field testing in Earth gravity.

This paper details the development and field-testing of BioBot, from localized testing on the UMD campus to full system simulated geologically-focused EVA activity in analogue field sites.

Nomenclature

ARMLiS	SS Active Rover Mounted Life Support	LTV	Lunar Terrain Vehicle
	System	MIG	Metal Inert Gas
CG	Center of Gravity	MUREP	University Research and Education Project
CLPS	Commercial Lunar Payload Services	NIAC	NASA Innovative Advanced Concepts
DOF	Degree Of Freedom	PLSS	Portable Life Support System
EVA	Extravehicular Activity	ROS	Robot Operating System
FDM	Fused Deposition Modeling	SSERVI	Solar System Exploration Research
GEODI	ES Geophysical Exploration of the Dynamics		Virtual Institute
	and Evolution of the Solar System	SSL	Space Systems Laboratory
IMU	Inertial Measurement Unit	UMD	University of Maryland
IK	Inverse Kinematics	UMES	University of Maryland Eastern Shore
LCG	Liquid Cooling Garment	VERTEX	Vehicle for Extraterrestrial Research,
LRV	Lunar Roving Vehicle		Transportation, and EXploration
		xEMU	Exploration Extravehicular Mobility Unit

¹Doctoral Candidate, Space Systems Laboratory

²Doctoral Student, Space Systems Laboratory

³Director, Space Systems Laboratory. Professor, Department of Aerospace Engineering

I. Introduction

The world is mobilizing for a return to human lunar exploration via the Artemis program and independent efforts in countries like India and China. It has been more than half a century since Apollo 17 returned from the Moon, but the legacy of Apollo is still the only experience base available for planning and executing human lunar missions.

The J-class Apollo missions demonstrated the massive utility of the lunar roving vehicle (LRV) for lunar exploration. Apollo 14, the last of the pre-LRV missions, had the crew accomplish a total traverse of about 4 km, resulting in high levels of exhaustion for both walking up slopes and manipulating a handheld cart for tools and samples. The three LRV-assisted Apollo missions, on the other hand, averaged 30 km per mission in surface traverses at reduced physiological workload levels. It seems reasonable to assume that the early Artemis lunar missions will be at least as capable as the last Apollo missions, and will provide an unpressurized roving vehicle for the astronauts to use.

But after five decades of technological development, what other differences will emerge between Apollo and Artemis extravehicular activities? At the time this project started in 2018, additional features and redundant systems added to the Artemis spacesuit designs led to an estimated mass of 84 kg for the pressure garment and 103 kg for the portable life support system (PLSS)[1]. Comparing this to the equivalent Apollo suit system masses of 35 and 61 kg, respectively, it appeared that Artemis astronauts would have even higher physiological demands than in Apollo, with even greater need for rover support.

This dramatic growth in the mass of the lunar spacesuit system led to the development of the BioBot concept: augmenting the rover capabilities to allow it to carry the bulk of the astronaut's life support system, using an autonomous robotic manipulator to tend the umbilical directing life support consumables to the suit, and providing additional sensors and autonomy to allow the rover to safely and robustly follow the EVA crew through almost all terrains accessible on foot.

A Phase 1 grant under the NASA Innovative Advanced Concepts (NIAC) program was established in 2018. During the nine-month duration of this effort, the University of Maryland team developed a concept of operations for BioBot, examined six possible configurations ranging from a small dedicated rover only for life support to a dual system hosted from a pressurized rover, and performed trade studies on eight different backpack configurations providing anywhere from 30 minutes to 8 hours of independent activities in addition to the rover-mounted life support system. Critical decisions made during this effort included the decision to focus on single-person unpressurized rovers as the basic configuration for BioBot. Risk analysis showed that such an architecture would be more robust than a single two-person rover, and the presence of a second rover provided a high likelihood of being able to drive both crew back to the habitat/lander following the failure of one rover. [2]

In 2020, the UMD team started further development of the BioBot concept under a NIAC Phase 2 grant. This effort, which was beset by the COVID 19 pandemic, supply chain problems, and rising inflation, focused on the development and testing of an integrated BioBot prototype system designed for Earth analogue field testing. At the beginning of the study, a set of 17 Level 1 requirements were developed for the BioBot system, including most notably traversing 30° slopes and 0.3 m obstacles. Based on these requirements, four independent design teams developed conceptual designs for the rover element of BioBot. Each of the subsequent designs were analyzed, and the best features of each were identified and brought together into a final lunar design. This design followed the chosen design paradigm of the first phase, with two identical single-person rovers each capable of carrying two EVA crew in case of contingency. Each rover system was projected to have a mass of 200 kg with margin, allowing both rovers to be pre-emplaced prior to crew arrival using an Astrobotic Griffin-class commercial lunar payload services (CLPS) lander.[2]

The UMD team then went into the detailed design phase on a version of BioBot designed for analogue field testing on Earth, with groups working in parallel on the constituent systems of BioBot: the rover[3], the umbilical-tending manipulator[4], and the spacesuit simulator garments with accommodations for umbilical-supplied life support. All of these were strongly driven by gravity issues; in particular, the accommodation of all terrain and speed requirements for the Moon in an Earth analogue vehicle drive a substantial increase in mass. Similarly, the umbilical tending manipulator length was restricted to 5 m on Earth as compared to 10 m on the Moon, due to gravitational loads on actuators. Operational details also had to be designed and developed, such as crew interfaces for control of the system, both remote and onboard [5]. Improvements to these EVA-facilitating details such as handrails, steps, and monitors are benefiting greatly from the rapid feedback cycle of the field trial process.

After approximately three years of design, manufacture, assembly, and iteration, the BioBot system was fully assembled for the first time as shown in Figure 1.



Figure 1. BioBot complete during testing

II. BioBot Overview

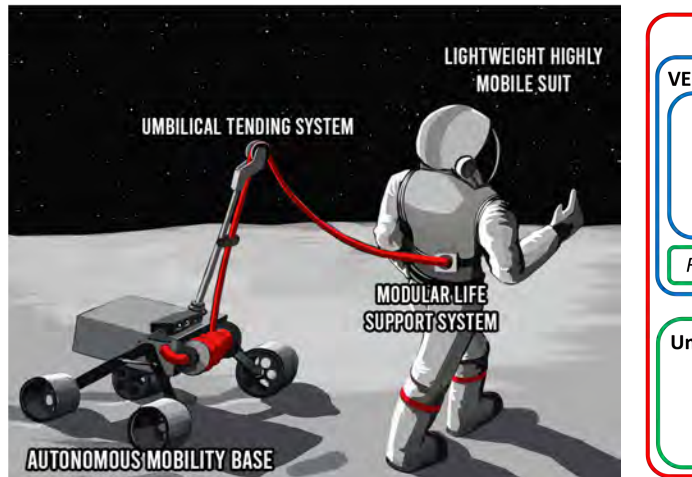
The BioBot system is primarily comprised of three parts: a spacesuit with a customizable-duration PLSS, a highly-capable autonomous mobility base, and an umbilical-tending robotic manipulator. An illustration of the original system concept is shown in Figure 2, and served as the original point of inspiration behind the project. Figure 3 overviews the capabilities and high-level details and flow through each subsystem.

The Earth-analogue design process ultimately led to a *capability-matched* system on Earth, prioritizing matching the EVA experience for a test subject or astronaut operating the vehicle in lieu of preserving lunar-specific details such as mass, deployment, or dust seals. This approach does not produce a vehicle capable of studying terramechanics of a lunar vehicle on Earth or preserve the center of gravity (CG) for stability studies, but does allow a test subject to board BioBot and operate in very similar ways to that of an actual lunar EVA. Manufacturability was another key advantage of this design approach; MIG (Metal Inert Gas) welding a mild steel chassis, milling structural parts from aluminum and steel, and FDM (Fused Deposition Modeling) 3D printing presented a lower barrier to entry and cost for production.

A. VERTEX

The Vehicle for Extraterrestrial Research, Transportation, and EXploration (VERTEX), as shown in Figure 4, is the highly-capable autonomous mobility base. VERTEX features independently-driven traction motors, $\pm 360^{\circ}$ over-wheel steering on each wheel, and independently articulated suspension for active chassis height, pitch, and roll control. In late 2020, a series of lunar rover designs were completed for the BioBot concept taking into account regolith terramechanics and reduced gravity. To evaluate the BioBot concept with analogue field trials, VERTEX was then designed to provide the same slope climbing, chassis leveling, and steering capabilities but in Earth conditions at the expense of added mass and complexity.

This design effort in spiral engineering saw the vehicle total mass increase from the original lunar-case 250 kg (estimated) to a 1000 kg vehicle as a consequence of the more powerful motors, batteries, and stronger structures



BioBot Exploration System VERTEX Rover (manual / autonomous) 3-DOF Articulated 4-Wheel Drive System 4 m/s top speed Suspension Roll: 40° 2.4 kW motors Pitch: 25° 360° independent Clearance: 0.1 - 1.25m steering Rover-Mounted Life Support **Human Interfaces Umbilical Arm (auton.) Astronaut Portable** Life Support 5m extension Variable duration Pitch: +/-30° Solo functionality 360° rotation 80m² service area Lower astro. exertion

Figure 2. Artistic render of the BioBot concept.

Figure 3. Overview flow chart of the BioBot system capabilities



Figure 4. The Vehicle for Extraterrestrial Research, Transportation, and EXploration

needed to climb slopes in 1G. As VERTEX was nearly entirely manufactured in-house, accommodations for simpler manufacturing methods such as the square-tube, MIG welded mild-steel chassis with a mixture of aluminum and steel (mild and stainless) components also contributed to the mass increase.

The main interfaces for the test subject including the seat, control panels, and joysticks have followed a modular and easily-reconfigurable approach. Figure 5 shows the control panel as used in the first sets of field trials. It features a battery management screen, emergency stop, key start, status lights, brake enable switch, a terminal screen, and two peripheral units with joysticks. The joystick and button combination peripheral on the right is the main interface method between the astronaut and the rover control software. The buttons command all driver-required functions from command authority and motion enabling to a debug mode and incremental control of the suspension and steering. The joystick on the right peripheral is mode-locked to either suspension or steering depending on the color of a status LED built into the joystick (blue = steering, red = suspension). The joystick on the left peripheral is repurposed from an early suspension control box and only the analog joystick is connected. The traction motor drivers are initially controlled via a throttle interface built into the traction motor drivers. This control method bypasses the ROS (Robot Operating System) architecture for the robot software, sending the same potentiometer-driven voltage to each driver and using torque-mode to drive each wheel independently as a temporary measure while electronics refinement is underway. The validation of the interface circuits between the high-level controllers and motor drivers is taking extra



Figure 5. Control panel and joystick setup for first field trial

time as the traction motors are the most dangerous actuator system on the vehicle. Unintentional accelerations of individual or all wheels, which have nearly 600 ft-lbs of continuous torque available each, could result in significant damage to the vehicle and persons around the vehicle and additional safety precautions and validation efforts need to be taken. The analogue control system has less risk in signal transmission since commands are physically limited via potentiometers on a 0-5V signal. The joysticks present are not EVA-glove compatible, but as the software and electronics progress further larger rotational and translational hand controllers are to be implemented.

B. ARMLiSS

ARMLiSS (Active Rover Mounted Life Support System), shown in Figure 6, is the umbilical-tending manipulator that sits atop of the VERTEX vehicle. The arm has an extension length of 5 meters, descoped from the original concept's 10 meter length due to challenges and cost in Earth gravity, weighs approximately 110 kg and uses linear actuators at each joint. A particular challenge in the design process was to create a kinematic chain which allows the arm to fully stow overhead in the rover, and extend outwards as the user egresses the vehicle and starts to walk around the periphery, without contacting the subject or allowing the umbilical to touch the ground. A camera system was designed and prototyping is underway to provide information to the autonomous control system on the relative location of the suited subject. When disconnected, the ARMLiSS system keeps the suit interface approximately 1.5 m above the surface, in easy reach of the suited subject for reconnection but as far as practical above the surface to minimize dust intrusion.

C. MX-C+ Spacesuit Simulator

In order to test the interaction with EVA crew, the BioBot system requires a suited test subject. For this purpose, we have adapted the MX-C spacesuit simulator, originally designed for analogue field testing in conjunction with the NASA HI-SEAS Mars mission simulations in Hawaii. As part of the adaptation, the MX-C suits have also been modified with features under development for the MX-D next generation suit simulators, such as scye shoulder bearings and new body seal closures. More details on the MX-D development progress are available in a co-published paper [6].

BioBot-specific modifications include a chest plate interface for the umbilical, which initially is a mechanical interface only, with the suit continuing to supply ventilation and cooling for field testing. Two versions of the chest connection have so far been tested, the first of which can be seen in Figure 7. Upgrades between the first and second



Figure 6. ARMLiSS deployed on VERTEX with the BioBot team for scale

field trails, as shown in Figure 8, included a magnetically-actauted mechanical connection, umbilical port, and a power connector for batteries. The electrical connector distributes power to the ventilation and LCG (Liquid Cooling Garment) system and provides an easy, field-replaceable battery for field trials. Ultimately, a higher fidelity umbilical cable carrying water, power, and air lines will be included but for the moment the umbilical provides a mechanical representation of the concept and the suit provides these operations.





Figure 7. Closeup of MX-C+ suit with umbilical attachment and FDM printed Figure 8. Version 2 MX-C+ umbilical interface device bearing arm

The other primary BioBot modification is in the reconfigurable PLSS mockup. One of the major test objectives of BioBot is the better understand the operational implications of the umbilical-supplied primary life support system, supplemented with a smaller backpack-based portable system to allow the crew to release the umbilical for surface operations incompatible with the umbilical and/or accompanying rover. These operations could include transition from the habitat to the vehicle, activities on slopes or ledges, or emergencies in transitioning life support to the second rover on EVA. The size and mass of backpack required is directly proportional to the allowable disconnect time; the new backpack consists of a small base module incorporating a UMD-developed solid state cooling system

and suit-mounted ventilation fans, along with the ability to attach different sized PLSS outer mold lines to represent longer-duration suit life support systems. Figures 9 and 10 show the cooling and ventilation in the lower unit, with a small unit added atop that represents a 20-30 minute life support duration. Larger volumetric modules with appropriate ballast are presently being created to allow for in-field adjustment of PLSS duration. Field tests with experienced field geologist test subjects will examine the role of untethered intervals on data collection, with the aim of obtaining a better understanding of the trade-offs between umbilical and onboard life support systems. BioBot aims to optimize for minimum PLSS mass, and therefore untethered duration, without interfering with the exploration desires of field geologists and test subjects.



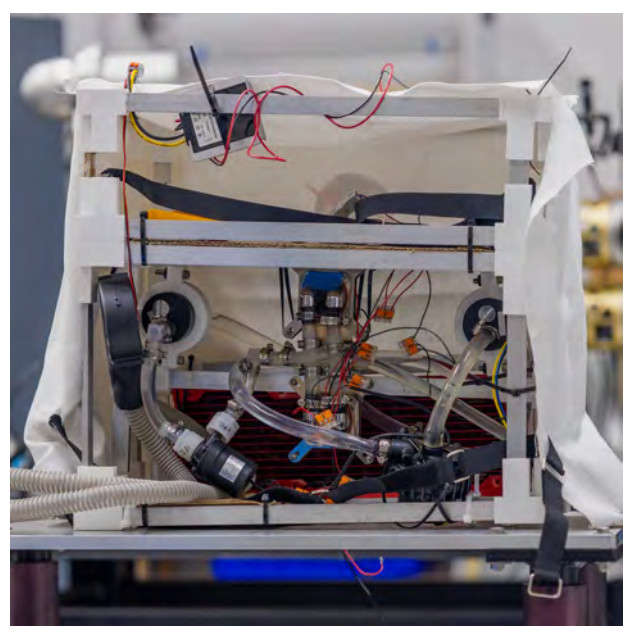


Figure 9. Reconfigurable PLSS with outer protective fabric covering

Figure 10. Reconfigurable PLSS internal structure

While the BioBot field test system will eventually be integrated to the MX-D suits, which will feature a wider range of allowable test subjects and ease of operations, all near-term BioBot tests will be based on the modified MX-C suits. To reflect the extensive changes to these suits, they have been designated MX-C+ variants.

III. Pre-Field Trial Full System Checkouts

The four main subsystems of BioBot were broken into the electrically related categories of suspension, steering, traction, and ARMLiSS for independent testing prior to rolling the vehicle out for full system checkouts. The suspension and steering systems performed nominally throughout these tests and were very quickly signed off as ready for field trials. The traction motor drivers, purchased from Kelly Controls, had poor documentation and did not perform as desired out of the box. The most notable issue faced was a tendency for any one of the four wheels to accelerate to full speed and then halt within a fraction of a second when the joystick was pushed forwards or backwards from a standstill. This resulted in whichever wheel was affected losing traction and jolting up off the ground, shaking the vehicle and making a very concerning noise; it was ultimately remedied by disabling a hill-start function. Similar settings had to be experimentally tested to understand their function, most of which were disabled. The current traction drive is only planned for use in initial testing; ultimately, traction motor control will be integrated digitally via the rover's onboard Galil multi-axis motion controller. The development of a custom interface card between the traction drivers and this system will allow for full closed-loop control of the wheel drives in position, velocity, or effort control modes. At the moment, operators use the effort control scheme via the analog drive system and does not have compensation for rolling back. As such, testing on hills requires very fine control of the joystick that software will be able to ultimately automate in the near future.

All of the VERTEX subsystems were tested thoroughly with each other outside the laboratory environment before bolting the arm on top. Delays in power electronics integration and overall high-backlash in the distal joints of ARMLiSS has prevented effective inverse-kinematics (IK) control of the manipulator before the first field trials. In

keeping costs as low as possible by using welded and pinned fabrication techniques, the pinned joints of the arm have an amount of backlash that is easily excitable by the control software. Efforts to reduce this backlash before continued field trials are underway, and backlash-compliant control methods are also being examined. The arm was operated in joint-space for the initial field trials, and afterwards inverse kinematics was prioritized in the software development and validation process.

With each system performing at or above the minimum requirements for a full system test, ARMLiSS was mounted to VERTEX's chassis and all systems were tested simultaneously. This began with testing the steering, suspension, and arm within the lab environment; traction tests were limited to only inching forwards or backwards within the high-bay space in the SSL's advanced robotics development facility before venturing outside.

Figure 11 shows the first full test of the BioBot system climbing a 21° hill just outside the SSL's electronics integration facility. In a majority of the full system tests, the chassis was automatically compensating for the slope, keeping the vehicle chassis horizontal and the operator's body in line with the gravity vector. This mode is called "autozero suspension" and uses the inertial measurement unit (IMU) mounted inside one of the electronics boxes to servo the four suspension linear actuators and achieve a set level point. This suspension mode was used most commonly for the tests, as there were only very few instances where a different, manually adjustable, suspension configuration was desired. The auto-level mode allows commands from yaw-rotation of the right-hand joystick to adjust chassis height in accordance with right-hand rule; interestingly, For the purposes of these field tests, either this or the "locked" suspension modes were used, where locked attempts to freeze the current suspension setting and minimizes linear actuator movement, effectively reducing it to purely passive spring-damper suspension. Other suspension modes such as kneel, focused on astronaut boarding and egress, are available but are not effectively managed through a combined steering and suspension joystick. As was seen in Figure 6 earlier, controlling 18 independent degrees of freedom with complex hierarchies of steering, suspension, and traction control modes while monitoring system functions requires a highly complex control station; altering input devices and control modalities throughout testing is bringing to light the most important aspects of each control mode and improvements are a continually ongoing effort.

In these early tests each steering mode, except for turn-in-place, was validated to point the wheels and turn the rover as expected. Turn-in-place mode was unable to be fully validated in initial tests as the interim traction motor setup does not allow for the required differential drive of the wheels. Front Ackermann (the steering mode most cars use), rear Ackermann (similar to forklift steering), double Ackermann (combined mode for tighter turns), and crab steering were all tested and used in varying situations, but the most popular choice was front Ackermann. While all four modes have individual advantages, test operations utilizing vehicle dynamics familiar to those with driver's licenses kept the tests running smoothly.

In early testing, one additional factor that affected the selected steering mode was a tendency for whichever wheels were steering to gain varying amounts of positive and negative camber, as shown by the differential wheel cambers with wheels steered straight in Figure 12. The two points where the steering actuators are connected to the suspension swingarms are under great amounts of stress when driving; this is exacerbated when the wheel camber angle is not 0° . The undesired wheel camber is partially the result of the resolution of the 12-bit absolute encoders within the steering actuators, resulting in $\approx 0.08^{\circ}$ of resolution per increment. The closed-loop control scheme is only able to point each wheel reliably to within 1-3 counts due to the high friction/stiction forces at each wheel. Since the first steering tests were performed mostly on asphalt on the road outside the laboratory, the rubber tires gripped very well and any amount of steering in or out caused the camber to follow. There were points where the camber would "settle out" and maintain a set angle outwards or inwards when the play in the connection matched the preload; the vehicle behaved acceptably at slow speeds in that condition. From these early fully integrated tests, the root cause was investigated, and it was found that the tests had worn the bushings and bushing holes to become ovular and cracked a set of bushings on each corner. A weldable clevis was designed to better react the lateral forces and link the steering and tire assembly more rigidly in the lateral plane to suppress this camber flexibility and was integrated into the vehicle between the first and second field tests.

VERTEX also handles differently with ARMLiSS affixed to the rear payload mounting structure. The rear suspension on the vehicle already carried an extra inch of preload to help compensate for the added weight in the first field trial, but the added weight still makes the suspension respond slightly more slugglishly than without the arm. ARMLiSS is approximately 10% of the weight of VERTEX, not enough even at full extension to significantly change the vehicle stability margins, but it is enough to slightly compress the passive suspension on whichever side, left or right, the arm is leaning over. Thanks to the nominal VERTEX operating mode of autonomously keeping the chassis level, ARMLiSS was designed with a passive shoulder yaw joint, allowing the test subject to easily rotate the arm around the vehicle with little effort while working in the area. The shoulder yaw joint has holes available for pinning and fixing the direction of the arm, preventing it from an uncontrolled swing left or right, but it unfortunately had a large amount





Figure 11. Full BioBot system climbing a hill for the first integrated test

Figure 12. Wheel camber issue demonstration

of play, $\approx 10^\circ$ of yaw. When pinned as close to the centerline as possible, this caused the CG to oscillate between the left and right sides of the vehicle, compressing the suspension on the respective side a small amount, causing a small harmonic between the auto-zero suspension control attempting to continually level and the arm oscillating left to right as a result. While the suspension adjustments are only $\approx 2^\circ$ or so in each direction, the motion made test subjects feel as if they were rocking on a boat and reduced their confidence in driving the vehicle. A secondary yaw restraint method of clamps were used as a stopgap measure for the initial tests and upgrades to both the suspension spring rates and the ARMLiSS mounting plate were made between the first and second field trials.

IV. Field Test 1 - UMD Campus



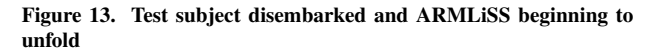




Figure 14. Test subject with deployed umbilical arm

The first field trial of the complete BioBot Earth analogue system occurred on the University of Maryland campus on January 24^{th} 2024, aiming to minimize travel distance in the event any form of vehicle recovery and repair was needed. The site chosen was relatively narrow and made of grass and dirt that began flat and became wider and hilly further down the track with slopes approaching 40° .

A. Testing Overview

As the inverse kinematics control system was not functional for ARMLiSS at the time, this test progressed in evaluation phases. Each phase had the vehicle drive to a test location, then the suited test subject would disembark while ARMLiSS was deployed manually. They would explore the area around the rover, and then reverse the process to ingress the rover and move to a different testing site. While this test did not demonstrate the full user-transparent experience that BioBot should be, it did validate the lighter-weight tethered EVA experience in the key areas of vehicle operation and sample collection. Two test subjects were the suit simulator and tested the system concept.





Figure 15. Test subject manually moving umbilical arm around VERTEX

Figure 16. Subject accessing VERTEX panel displays while standing

For the first disembarkation the rover was on flat ground and the arm at a medium extension length as Figures 13 and 14 show. The test subject found the arm overall easy to rotate around the base (Figure 15) and unobtrusive when picking up rocks or interfacing with the rover displays while standing (Figure 16. The baseplate that interfaces between ARMLiSS and VERTEX was found to still have too much deflection with the arm at extension, even with additional stiffening structure added; a new arm mounting plate was designed and implemented before the second field trial.





Figure 17. Slope testing with ARMLiSS fully extended

Figure 18. Additional angle of slope testing with arm fully extended

The next site aimed to test deployment with slope compensation. At the first hill in the test area the rover was driven up the beginning of the incline and the deployment procedures were repeated. The test subject was now able to traverse above the vehicle on the hill to reach a higher point with the arm raised above the nominal level (Figures 17 and 18). Once the test subject was finished working around the rover, VERTEX then climbed the hill with ARMLiSS deployed, shown in Figures 19 and 20, and automatically leveled the chassis. ARMLiSS was pinned to point in the uphill direction and the test subject temporarily disconnected from the umbilical while the vehicle was in motion for safety in these initial tests.

The third and final deployment test of the day aimed to position BioBot higher than the astronaut on the hill,







Figure 20. Additional angle of BioBot with ARMLiSS fully extended on slope

simulating the test subject investigating a small crater or depression on the surface. Figure 21 shows the system with test subject at the top of the hill and Figure 22 has the test subject descended into the depression. The slope of the hill at this point was approximately 40°, and ARMLiSS's height articulation allowed the test subject to descend into the depression with the vehicle stable along the rim.



Figure 21. Second test subject disembarking from VERTEX



Figure 22. Astronaut investigating within a depression with VER-TEX above the area rim

B. Lessons Learned and Improvements from UMD Field Tests

The UMD team was quite pleased with the outcome of the first daylong field test on campus. Even with some of the operational bugs VERTEX and ARMLiSS proved to be a highly functional pairing with great promise. The rover was operated at relatively low speeds, and wattage required for climbing hills up to 20° was in the 6kW range; since the batteries are capable of 30kW sustained output, there is still a lot of margin left for tackling much more challenging terrain.

Three specific improvements of the hardware needed to occur before the tests at NASA Goddard in field trial 2. First, a new, thicker connection plate between ARMLiSS and VERTEX needed to be designed, manufactured, and integrated that reduces both bending deflections from the large cantilevered load and allowed the arm to be pinned straight along the vehicle. Secondly, the suspension needed to be stiffened to increase articulation capability with heavy payloads and was achieved with a higher-rate spring. Third the connection between the steering actuators and the main suspension members needed to be stiffened to reduce camber effects and was achieved by welding a milled stiffening part to the rover structure. Additionally, an ingress improvement was made after this test by adding a physical step to the structure the traction motors mount to.

V. Field Test 2 - NASA Goddard Campus

NASA Goddard was selected as a second field trial location due to both its 4 kilometer gravel track that spans the perimeter of the facility and it being within 15 minutes of the University of Maryland.

A. Testing Overview

Testing at NASA Goddard spanned two days, April 18^{th} and 19^{th} 2024, with differing goals between the two days. Due to advanced badging and inspection requirements these test dates were confirmed in mid-March and initially provided a window of flexibility if April showers arrived. Luckily both test days were relatively rain-free (beyond a few hours on day 2) and two separate test goals were set for each day.





Figure 23. VERTEX transportation method

Figure 24. EVA with test subject, VERTEX, no umbilical arm

Day 2 was viewed as the main testing day as that day more personnel were traveling to Goddard, and day 1 was then largely intended as a logistical and operational checkout of the vehicle to allow any repairs or upgrades to happen overnight. Day 1 was also being used as a secondary datapoint without ARMLiSS mounted, as this both simplified transportation logistics for the first venture outside of UMD and allowed the VERTEX suspension and dynamics to be assessed without an extra 110 kg payload of the arm.





Figure 25. Test subject operating vehicle

Figure 26. VERTEX capability checkouts

After working through some logistical issues in the transportation of VERTEX, the vehicle and team arrived at Goddard early-afternoon on the 18th. As multiple components in the electronics, software, and suit simulators were still in preparatory phases for more rigorous testing on day 2, tests on day 1 were brief, covering approximately one kilometer in total distance before returning to UMD. Figure 23 shows VERTEX in its transportation configuration to field trials, and Figure 24 shows a test subject operating the vehicle along the gravel track. Even though the analog traction control system was still implemented, the motor drivers were capped at 25% of full speed, approximately 3 m/s, which successfully reduced oversensitivity to hand controller inputs.

Figure 25 shows a test subject operating VERTEX without a helmet visor as the ventilation system was undergoing repairs. The test subject additionally did not wear the MX-C+ gloves as the joysticks were too small to effectively control with covered hands. Beyond having the test subject operating the vehicle, members of the team also drove VERTEX in different modalities including an extended reversing operation as shown in Figure 26. Overall, the upgrades to the suspension and camber system had provided a much more stable and confident-feeling system. Camber was significantly reduced and was more steady during driving operations, even at varying caster angles.





Figure 27. Day 2 test subject after vehicle ingress

Figure 28. Test subject operating vehicle with ARMLiSS stowed above

Testing on day 2 was shorter than anticipated due to a combination of intermittent rain and in-situ code upgrades, but still provided very valuable experience for not only the SSL BioBot team but also students from the University of Maryland Eastern Shore (UMES). Electrical and software challenges minimized the use of ARMLiSS throughout the testing, so day 2 testing focused on taking advantage of the loose gravel surface and evaluating VERTEX performance in driving, turning, and climbing hills. Figure 27 shows a test subject post-ingress attached to the umbilical system with the upgraded interface connection plate and Figure 28 shows the test subject operating the vehicle while in motion.

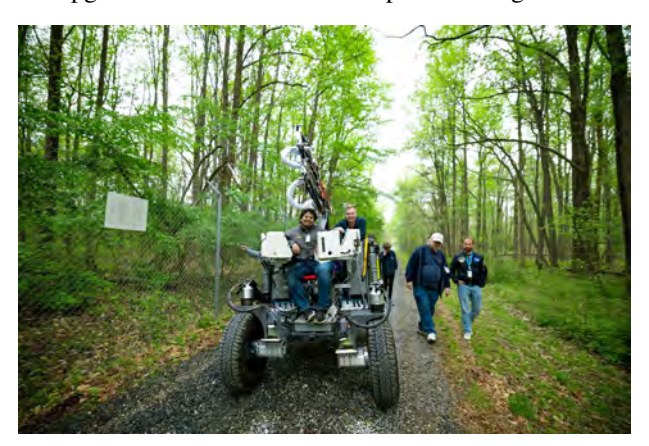




Figure 29. Day 2 team operations/evaluations

Figure 30. Day 2 team operations/evaluations

During a drizzly hour the team protected the vehicle with a tarp, and after the skies cleared only an hour of time remained before we needed to leave Goddard. Figures 29 and 30 show the team operating the vehicle post-rain shower with one individual driving the rover, and the other standing on the back as a secondary astronaut might when returning to base during an anomaly. In this configuration, the rover climbed an extended 15°, actively leveling the chassis through the duration of the climb. The power draw from the rover increased from approximately 2.5 kW to 5

kW during the climb, a small fraction of the 30 kW available via the batteries, and did not appear to have any struggle or hesitation carrying approximately 325 kg of payload up the slope.

B. Lessons Learned

One of the earliest lessons learned in the Goddard tests was that the line of sight to the rear wheels is blocked by the large electronics boxes. When driving in reverse, even if the VERTEX operator is not wearing a spacesuit simulator and can rotate their torso to view backwards, the rear wheels cannot be seen which makes positioning the vehicle along a track or when nearing obstacles more difficult. If an MX-C+ suit is donned, it is presently unsafe for the operator to reverse the vehicle without external people guiding the direction of the vehicle. A high information bandwidth via an appropriate selection of sensors and cameras is going to be required to allow unaided reversing. Secondly, the new steps that were attached to the traction motor structure require too great of a bend in the hips and knees to comfortably step onto from the ground. However, at the operating height of the chassis it does provide a nice step to the rover chassis, indicating that a possible solution could be adding a second intermediate step. When the umbilical is attached to the MX-C+ suit and the test subject is sitting in the VERTEX seat, the umbilical presently restricts some line of sight to the left and may be more comfortable in a slightly altered orientation. While the control panels provide good line of sight to the front wheels and the road ahead, the current suspension and steering mode indicators available on the terminal screen are are too small alongside the joysticks. However, the updated suspension springs provided a highly stable and more controllable articulation system, and the new thicker baseplate that mounts ARMLiSS to VERTEX significantly increased the system stiffness.

VI. Field Test 3 - UMES

The UMD Space Systems Laboratory is currently working with the University of Maryland Eastern Shore on a NASA Minority University Research and Education Project (MUREP) focused on lunar robotics. The centerpiece of the UMD portion of the collaboration is to test BioBot in proximity to UMES in collaboration with their surface robotics systems. The Eastern Shore is much less populated than the DC region, and UMES is currently scouting for locations to perform BioBot field testing in their vicinity in summer and fall of 2024.

A. Testing Plan

Once one or more appropriate testing locations have been found, additional test objectives beyond the NASA Goddard trials will likely be a focus on greater rover autonomy and mobility performance in soft sands. While it is difficult to predict the path of the autonomy integration, continued field trials are expected to highlight trouble areas. Iterative and incremental improvements to the system autonomy will ultimately provide the full BioBot experience to the test subject.

VII. Additional Field Testing Possibilities

As the system becomes capable of more complex and realistic test environments, the challenge expands from hardware and software to operations and logistics. It would be ideal to identify a number of equivalent sites in the mid-Atlantic region, hopefully within 1-2 hour drive of the UMD campus. However, this region is devoid of desert areas, and almost all potential sites are heavily covered with vegetation, affecting both the visual fidelity and (more important) the accurate simulation of terrain trafficability. Rocky conditions, sand, and quarries with finer grains may provide an environment more closely representing the lunar surface.

The search for mid-Atlantic field sites is ongoing. Active quarries would be ideal, since vegetation is not able to grow due to the excavation, and a wide variety of slopes and soils are accessible; however, issues with liability and safety have proved to be difficult to surmount. Talks are underway to allow testing at the Army Robotics Research Collaborative Campus (R2C2) at Graces Quarters, Maryland, but issues with photography and students without U.S. citizenship are challenging at such DoD facilities. The team has identified some near-term test sites, however, and planning is underway for the next several series of field tests.

Private off-road trails in Maryland do exist, and the SSL is presently trying to get access to a few different trails. The SSL is also a part of the GEODES (Geophysical Exploration of the Dynamics and Evolution of the Solar System) SSERVI (Solar System Exploration Research Virtual Institute) and has a standing invitation to participate in their annual field tests at the San Francisco Lava Fields in northern Arizona. This would be ideal, as the site is a scientifically

interesting analogue site to the Moon and Mars, experienced field geologists would be available as test subjects, and the GEODES team has already established all of the necessary permits to test in the area, but BioBot participation would require independent funding sources. As the system reaches maturity, there is a strong desire to demonstrate it in the Rockyard at the NASA Johnson Space Center, as well as at other NASA sites which might be interested in a demonstration of the concept.

VIII. Considerations and of the BioBot Concept

While the BioBot concept may prove to lighten the energetic burden on astronauts during EVA, there is a level of added system complexity that cannot be overlooked. The presence of a large robotic manipulator sitting atop the rover, while not infeasible, may prove to be costly and sensitive to regolith abrasion over extended trials. The independently articulated suspension system with as long of an actuator stroke as required to level the VERTEX chassis may also prove to have regolith-sensitivity challenges. Similarly, requiring the astronauts to cycle an umbilical connection in an unpressurized environment on the moon will likely subject these connectors to regolith intrusion, especially with dirty gloves. These considerations would need to be investigated for the lunar case, but provide little overhead or issue in Earth testing.

From the field trials, BioBot is an engaging vehicle to drive with great capabilities that our field locations have yet to truly stress to its limits. While individual component upgrades may be needed as testing continues, the actuators, chassis, and form factor have proven to perform very well and be appropriate for the testing as expected. The ability to manually change caster angle has been especially tricky to work with, as any amount of backlash in the connection between the steering actuator and the suspension system allowed the wheels to camber in and out. This adds unnecessary stresses to the steering actuators and suspension system, and improvements for this connection are underway. One very helpful approach in the creation of the Earth-analogue was designing for modularity. Around the vehicle various mounting patterns can be found including 1/4-20 threaded studs, 80/20 TMcompatible hole patterns, and a pair of 2" trailer hitch receivers that have allowed the integration of camera mounts, lights, steps, and more without modifications to existing structures. This significantly lowered the barrier to entry for rapid system iteration.

IX. Conclusions

Even without world-wide problems such as the pandemic and associated supply chain problems, in hindsight a fully working BioBot analogue system was an ambitious goal within the time and cost limitations of the NIAC program. Results to date have provided real assurance that the concept of providing life support to EVA crew on the Moon or Mars from an advanced rover is both viable and potentially valuable. The VERTEX rover suspension, steering, and drive systems have shown their basic functionality, and appear to deliver on the design requirement to be capable of traversing any terrain safely walkable by a spacesuited human. The ARMLiSS umbilical handling system has demonstrated basic functionality, and is nearing feasibility of autonomous operations in response to crew motion around the vehicle. The prototype hardware for crew-operated umbilical disconnect/reconnect is functional and ready to be used in simulated EVA operations to quantify the interaction between rover-mounted and suit-mounted life support requirements.

Much work needs to be done in extended field testing to move from the anecdotal results presented by necessity in this paper to the quantified and verifiable results which remain the goal of the team, but results to date are promising.

Acknowledgements

The authors would like to thank the NASA Innovative Advanced Concepts (NIAC) program for the funding for BioBot, and the NASA MUREP program and the University of Maryland Eastern Shore for support with continuation of the testing operations. We would also like to sincerely thank all of the students who have participated in BioBot design, fabrication, assembly, and testing over the past five years.

References

- [1] NASA Marshall Space Flight Center. Human Landing System Requirements Document. Sept. 2019.
- [2] David Akin, Kate Melone, Brady Sack, and Jeffrey Zhu. "BioBot: Investigating an Alternative Paradigm for Planetary Surface EVA". In: *International Conference on Environmental Systems (ICES)*. July 2019.
- [3] Charles Hanner, Nicolas Bolatto, Joshua Martin, Daniil Gribok, and David Akin. "Development and Testing of the BioBot EVA Support System". In: 51st International Conference on Environmental Systems. July 2022.
- [4] Nicolas Bolatto, Robert Fink IV, Joshua Martin, Zachary Lachance, Rahul Vishnoi, and David Akin. "Development of an Autonomous Umbilical Tending System for Rover-Supported Surface EVAs". In: 51st International Conference on Environmental Systems. ICES-2022-361. July 2022.
- [5] Charles Hanner, Nicolas Bolatto, Daniil Gribok, Spencer Quizon, Rowan Quintero, Ian Welfeld, and David L. Akin. "Development and Testing of Crew Interfaces for an Advanced Unpressurized Exploration Rover". In: *International Conference on Environmental Systems (ICES)*. July 2023.
- [6] Meredith Embrey and David Akin. "Design, Fabrication, and Evaluation of the MX-D Spacesuit Simulator". In: *International Conference on Environmental Systems (ICES)*. July 2024.